

Division of Biopharmaceutics and Pharmacokinetics
Faculty of Pharmacy
University of Helsinki
Finland

MODIFICATIONS AND CARRIERS FOR IMPROVED
OLIGONUCLEOTIDE DELIVERY: SYNTHESIS, ANALYSIS
AND BIOLOGICAL TESTING

Unni Tengvall

ACADEMIC DISSERTATION

To be presented, with the permission of the Faculty of Pharmacy of
the University of Helsinki, for public examination in Auditorium 1041 at Viikki
Biocenter 2, Viikinkaari 5E, on 7th June 2013, at 12 noon.

Helsinki 2013

Supervisors: Prof., Ph.D. Marjo Yliperttula
Division of Biopharmaceutics and Pharmacokinetics,
Faculty of Pharmacy
University of Helsinki
Helsinki, Finland

Prof., Ph.D. Alex Azhayev
School of Pharmacy, Faculty of Health Sciences
University of Eastern Finland
Kuopio, Finland

Prof., Ph.D.(Pharm.) Seppo Auriola
School of Pharmacy, Faculty of Health Sciences
University of Eastern Finland
Kuopio, Finland

Ph.D. Maxim Antopolsky
Centre for Drug Research, Faculty of Pharmacy
University of Helsinki
Helsinki, Finland

Reviewers: Prof., Ph.D.(Pharm.) Pia Vuorela
Pharmaceutical Sciences, Department of Biosciences
Åbo Akademi University
Turku, Finland

Ph.D.(Pharm.) Marika Ruponen
School of Pharmacy, Faculty of Health Sciences
University of Eastern Finland
Kuopio, Finland

Opponent: Prof., Ph.D. Mikko Oivanen
Department of Chemistry, Faculty of Science
University of Helsinki
Helsinki, Finland

© Unni Tengvall 2013

ISBN 978-952-10-8915-2 (paperback)

ISBN 978-952-10-8916-9 (PDF, <http://ethesis.helsinki.fi>)

*Helsinki University Print
Helsinki 2013, Finland*

To Valtteri

ABSTRACT

Several serious diseases remain without non-toxic curative treatments. To fill this void, one of the promising groups of medicines is that of oligonucleotides, encompassing aptamers, transcription factor decoys, and antisense therapeutics such as short interfering RNA and splice-correcting oligonucleotides. These short strands of DNA or RNA can bind to specific cellular nucleic acids or proteins and thereby inhibit or correct the function of disease-causing molecules. Extensive enzymatic degradation and poor cellular uptake are the most important obstacles for systemic oligonucleotide therapy. Numerous chemical modifications have been introduced to improve enzymatic stability, but they must be carefully optimized to avoid toxicity and to maintain target affinity. One solution is to design topological modifications, such as looped or circular oligonucleotides, which conserve the natural phosphodiester backbone but cannot be attacked by exonucleases.

Cellular uptake has proven to be even more challenging. Oligonucleotides are internalized into cells by endocytosis, after which they often remain trapped in endosomes. Therefore, it would be advantageous to develop delivery vectors capable of bypassing endocytic routes of uptake or enhancing endosomal escape. Cell-penetrating peptides, for example, exploit several mechanisms of uptake, some of which lead to rapid entry without endosomal localization. In addition, encouraging results have been achieved using liposomes, gold nanoparticles, and other nanocarriers, which also shield the oligonucleotide from degrading enzymes.

The aim of this work was to improve the *in vitro* delivery of oligonucleotides by employing chemical modifications and nanoparticle carriers. The synthesis of the compounds, their characterization by various analytical methods, and the evaluation of biological effects are described. First, we covalently conjugated several cell-penetrating peptides to unmodified and phosphorothioate oligonucleotides *via* disulfide linkages by convergent conjugation of separately synthesized and purified compounds. Confocal microscopy of conjugate-treated cells revealed endosomal entrapment, explaining the observed lack of antisense activity in cells.

In another study we used similar disulfide linkages to circularize phosphodiester oligonucleotides, resulting in significantly improved enzymatic stability in serum and cellular extracts and enhanced selectivity to complementary targets.

Altogether 44 compounds, including the above mentioned constructs, a peptide–ribozyme conjugate, and several additional peptide–oligonucleotide conjugates prepared by stepwise solid-phase synthesis without intermediate purifications, were analyzed by negative ion electrospray ionization mass spectrometry or liquid chromatography–mass spectrometry with a maximum mass error of 0.05%.

Finally, we synthesized cationic gold nanoparticles modified with a Tat-related cell-penetrating peptide, and characterized them with various methods. The gold particles did not affect cell viability and effectively delivered short interfering RNA into cells as non-covalent complex. In addition, the gold nanoparticles seemed to stimulate cellular proliferation compared to untreated cells.

ACKNOWLEDGEMENTS

This study was carried out in two different universities and two different disciplines. The first part, encompassing the first three publications, was done at the Department of Pharmaceutical Chemistry, Faculty of Pharmacy, University of Kuopio (nowadays known as School of Pharmacy, Faculty of Health Sciences, University of Eastern Finland), during the years 1998–2002, under the skillful supervision of professors Alex Azhayev and Seppo Auriola. I wish to sincerely thank them for introducing me the fascinating worlds of oligonucleotides and mass spectrometry, respectively, and for offering me a chance to pursue a scientific career. I would also like to thank my colleagues from Kuopio, especially Tuula, Elena and Piia, for creating a friendly and supportive working atmosphere.

The second part of this study took place at the Division of Biopharmaceutics and Pharmacokinetics, Faculty of Pharmacy, University of Helsinki, during the years 2008–2013. I wish to express my deepest gratitude to professors Marjo Yliperttula and Arto Urtti for enabling me to finish my doctoral studies and to deepen my understanding of biopharmaceutics and pharmacokinetics, and also for welcoming me to the wonderful group of DDN (Drug Delivery and Nanotechnology). Thanks to you I found the link between community pharmacy work and biopharmaceutics, the intriguing world of cell biology and nanotechnology, and many wonderful friends. I am also very grateful to my second supervisor in Helsinki, Ph.D. Maxim Antopolsky, for his skilled guidance in oligonucleotide and peptide chemistry. M.Sc.(Pharm.) Tatiana Elizarova deserves enormous credit for performing a large part of the gold nanoparticle study and also for nice lunchtable conversations.

I wish to thank all my colleagues in the DDN group for contributing to an informal and encouraging working atmosphere. Special thanks go to Alma, Astrid, Erja, Hanna, Leena P, Melina, Patrick and Voula for many nice conversations, help in the lab, advice in preparing and printing my thesis, and collaboration in teaching issues. The company and cooperation of Carmen, Gloria, Heidi, Huamin, Lauri, Leena K, Leo, Madhu, Marco, Mari H, Mari R, Mecki, Niko, Otto, Polina, Sanjay, Tapani, Timo, Vincenzo and Yan-Ru are also greatly acknowledged, without forgetting former co-workers Chang-Fang, Jonna, Kati-Sisko, Manuela, Marikki and Yuuki, or those currently on family leaves, Julia and Martina. Staff from other divisions and the faculty office are also warmly acknowledged.

I am deeply grateful to my family members for their love and support: my mother Anu, my father Pekka, our Kuopio family Ulla, Aki, Jeremy, Jaakko and Juhana, and my other siblings Petteri, Anna and Petra. Especially I would like to thank my 90-year-old grandmothers Aila and Kaija for their love and presence in my life. I also wish to thank Enrique for being my best friend.

And Valtteri, my son: we did it together.

Espoo, May 2013

Unni Tengvall

Contents

ABSTRACT	5
ACKNOWLEDGEMENTS	7
LIST OF ORIGINAL PUBLICATIONS	10
ABBREVIATIONS	11
1 INTRODUCTION	13
2 REVIEW OF THE LITERATURE	16
2.1 Chemical modifications of oligonucleotides	16
2.1.1 Changing the chemistry of natural oligonucleotides.....	16
2.1.2 Modifications to the phosphate linkage	17
2.1.3 Carbohydrate 2'-modifications	18
2.1.4 Conformational restriction and backbone replacement.....	20
2.1.5 Topological modifications	22
2.2 Cell-penetrating peptides as vectors of oligonucleotide delivery	23
2.2.1 Pharmacokinetics and delivery of oligonucleotides	23
2.2.2 Cell-penetrating peptides in oligonucleotide delivery.....	26
2.2.3 Classes and efficacies of cell-penetrating peptides.....	27
2.2.4 Mechanisms of cellular uptake	31
2.2.5 Combining cell-penetrating peptides to other modifications	32
2.3 Analysis of modified oligonucleotides by mass spectrometry	35
2.3.1 Mass spectrometry of oligonucleotides	35
2.3.2 Liquid chromatography–mass spectrometry of oligonucleotides	38
2.3.3 Mass spectrometry of peptide–oligonucleotide conjugates	38
3 AIMS OF THE STUDY	39
4 SUMMARY OF THE METHODS	40
5 PEPTIDE–OLIGONUCLEOTIDE PHOSPHOROTHIOATE CONJUGATES WITH MEMBRANE TRANSLOCATION AND NUCLEAR LOCALIZATION PROPERTIES*	41
6 CHARACTERIZATION OF ANTISENSE OLIGONUCLEOTIDE–PEPTIDE CONJUGATES WITH NEGATIVE IONIZATION ELECTROSPRAY MASS SPECTROMETRY*	51
7 SELECTIVE CIRCULAR OLIGONUCLEOTIDE PROBES IMPROVE DETECTION OF POINT MUTATIONS IN DNA*	62
7.1 Introduction	63
7.2 Materials and methods	64
7.2.1 Oligonucleotide synthesis	64
7.2.2 Labeling of oligonucleotides	64
7.2.3 Characterization.....	65

7.2.4	Stability of circular oligonucleotides.....	65
7.2.5	Melting experiments	66
7.2.6	Preparation of oligonucleotide-coated microparticles.....	66
7.2.7	Hybridization assays	67
7.3	Results and discussion.....	67
7.3.1	Synthesis and characterization of circular oligonucleotides.....	67
7.3.2	Stability of circular oligonucleotides.....	74
7.3.3	Binding of circular oligonucleotides to complementary targets.....	77
7.3.4	Mixed-phase hybridization experiments	79
7.4	Conclusions	83
7.5	References	84
8	ONE-STEP PRODUCTION OF PEPTIDE-MODIFIED GOLD NANOPARTICLES FOR SIRNA DELIVERY*.....	86
8.1	Introduction.....	87
8.2	Materials and methods	88
8.2.1	Peptide synthesis.....	88
8.2.2	Oligonucleotide synthesis	89
8.2.3	Synthesis of cell-penetrating peptide-modified gold nanoparticles.....	89
8.2.4	Preparation of siRNA/gold nanoparticle complexes.....	90
8.2.5	Characterization of gold nanoparticles and siRNA/gold nanoparticle complexes	90
8.2.6	Engineering of stable ARPE-19 cell lines expressing secreted alkaline phosphatase.....	91
8.2.7	Cell culture and transfection.....	91
8.2.8	Cell viability assay	92
8.2.9	SEAP expression assay.....	92
8.3	Results and discussion.....	93
8.3.1	Synthesis and characterization.....	93
8.3.2	Complex formation with siRNA	94
8.3.3	Cell viability	95
8.3.4	Effect of gold nanoparticles on SEAP secretion	98
8.3.5	Gene silencing.....	99
8.4	Conclusions	101
8.5	References	101
9	GENERAL DISCUSSION AND FUTURE PERSPECTIVES.....	105
10	CONCLUSIONS	112
11	REFERENCES.....	113

LIST OF ORIGINAL PUBLICATIONS

This thesis is based on the following publications:

- I Antopolsky M, Azhayeva E, **Tengvall U**, Auriola S, Jääskeläinen I, Rönkkö S, Honkakoski P, Urtti A, Lönnberg H, Azhayev A. 1999. Peptide–oligonucleotide phosphorothioate conjugates with membrane translocation and nuclear localization properties. *Bioconjugate Chem.* 10(4): 598–606.
- II **Tengvall U**, Auriola S, Antopolsky M, Azhayev A, Biegelman L. 2003. Characterization of antisense oligonucleotide–peptide conjugates with negative ionization electrospray mass spectrometry. *J Pharm Biomed Anal.* 32(4–5): 581–590.
- III Tennilä T, Ketomäki K, Penttinen P, **Tengvall U**, Azhayeva E, Auriola S, Lönnberg H, Azhayev A. 2004. Selective circular oligonucleotide probes improve detection of point mutations in DNA. *Chem Biodivers.* 1(4): 609–625.
- IV **Tengvall U**, Elizarova T, Takashima Y, Pietilä L, Reinisalo M, Laurén P, Urtti A, Antopolsky M, Yliperttula M. One-step production of peptide-modified gold nanoparticles for siRNA delivery. (In revision.)

The publications are referred to in the text by their roman numerals.

Previously unpublished data is also presented.

ABBREVIATIONS

AMD	age-related macular degeneration
ANA	D-arabinonucleic acid
Antp	Antennapedia
CeNA	cyclohexene nucleic acid
CGE	capillary gel electrophoresis
CID	collision-induced dissociation
CMV	cytomegalovirus
CPP	cell-penetrating peptide
DMD	Duchenne muscular dystrophy
ENA	ethylene nucleic acid
EPR	enhanced permeability and retention effect
ESI	electrospray ionization
FAB	fast atom bombardment
FANA	2'-deoxy-2'-fluoro-D-arabinonucleic acid
GAG	glycosaminoglycan
GNP	gold nanoparticle
gp41	glycoprotein 41
HFIP	1,1,1,3,3,3-hexafluoro-2-propanol
HNA	hexitol nucleic acid
HNF1	hepatocyte nuclear factor 1
HPLC	high pressure/performance liquid chromatography
HRP	histidine-rich peptide
K-FGF	Kaposi fibroblast growth factor
LC/MS	liquid chromatography–mass spectrometry
LNA	locked nucleic acid
LSC	liquid scintillation counting
LTR	long terminal repeat
MALDI	matrix-assisted laser desorption/ionization
MAP	model amphipathic peptide
MEND	multifunctional envelope-type nano device
miRNA	microRNA
2'-MOE	2'-O-(2-methoxyethyl)
MP	methylphosphonate
MPEG	methoxy poly(ethylene glycol)
MPM	membrane permeable motif
MPP	membrane permeable peptide
MPS	mononuclear phagocyte system
MS	mass spectrometry
MS ⁿ	tandem mass spectrometry
MTS	membrane translocating sequence
<i>m/z</i>	mass-to-charge ratio
NF-κB	nuclear factor-kappaB

ABBREVIATIONS

NIR	near-infrared
NLS	nuclear localization signal
NP	N3'→P5' phosphoramidate
NPS	N3'→P5' <i>thio</i> -phosphoramidate
2'-OMe	2'- <i>O</i> -methyl
ON	oligonucleotide
PA	phosphoramidate
PAGE	polyacrylamide gel electrophoresis
PCL	poly(ϵ -caprolactone)
PEG	poly(ethylene glycol)
PEI	poly(ethylene imine)
PLL	poly(L-lysine)
PMO	phosphordiamidate morpholino oligomer
PNA	peptide nucleic acid
PO	phosphodiester
POC	peptide–oligonucleotide conjugate
PS	phosphorothioate
PTD	protein transduction domain
RNAi	RNA interference
RNase H	ribonuclease H
SEAP	secreted alkaline phosphatase
SELEX	systematic evolution of ligands by exponential enrichment
siRNA	short/small interfering RNA
SNALP	stable nucleic acid lipid particle
SPE	solid-phase extraction
SV40	Simian virus 40
Tat	<i>trans</i> -activator of transcription
TEA	triethylamine
TEM	transmission electron microscopy
TF	transferrin
TP10	transportan 10
TPA	tripropylamine
UNA	unlocked nucleic acid
VP22	virus protein 22

1 INTRODUCTION

Diseases are frequently caused by malfunctioning proteins and, therefore, conventional drug development strives to find small molecules which affect at the protein level. As small-molecule drugs are often non-specific and thereby somewhat toxic, research has been directed towards the earlier phases of protein synthesis, according to the ‘central dogma of molecular biology’ known since 1958 (Crick 1970): DNA makes RNA makes protein. In theory, pharmacotherapy can be rendered more specific by inhibiting the translation of disease-causing proteins at the RNA level. An especially high selectivity of RNA targeting can be achieved by employing short strands of complementary nucleic acids. These strands, known as oligonucleotides (ONs), are now widely used as tools in molecular biology and investigated as potential gene-based therapeutics for *e.g.* cancer, genetic diseases and viral infections. Moreover, it has recently been found that besides coding for harmful proteins, RNA can have a disease-causing function *per se* (O’Rourke and Swanson 2009; Bennett and Swayze 2010), highlighting the demand for RNA-targeting medicines.

Therapeutic ONs display a wide variety of pharmacodynamic mechanisms, the most advanced one being the antisense approach (**Figure 1**). Bennett and Swayze (2010) define antisense ONs as “ONs of 8 to 50 nucleotides in length which affect the function of a specific target RNA upon binding by Watson-Crick base pairing”. The two primary modes of antisense effect are (1) degradation of the target RNA and (2) modulation of its function by non-degrading mechanisms. The cleavage of the target can be achieved *via* various routes: activation of the cellular enzyme ribonuclease H (RNase H) by ‘classical’ antisense ONs (Zamecnik and Stephenson 1978), the intrinsic catalytic activity of ribozymes (RNA enzymes) (Cech et al. 1981) and deoxyribozymes (DNAzymes) (Breaker and Joyce 1994), harnessing the natural gene silencing pathway of RNA interference (RNAi) by short interfering RNAs (siRNAs) (Fire et al. 1998), or inhibition of polyadenylation by U1 adaptors (Goraczniak et al. 2009).

Steric block antisense ONs, in contrast, do not activate any terminating events and exert their effect by stoichiometric binding to target RNA. They can be used as splice-correcting ONs which correct aberrant splicing of pre-mRNA (Sierakowska et al. 1996), as antagomirs, *i.e.* anti-miRNA ONs, which antagonize the gene regulating effects of microRNA (miRNA) (Krützfeldt et al. 2005), to block the translation of disease-causing proteins such as mutant huntingtin by binding to expanded triplet repeats in mRNA (Hu et al. 2009), or as competitive inhibitors of the cancer-related reverse transcriptase enzyme called telomerase (Norton et al. 1996). There are also non-antisense ONs, which do not target RNA but bind to specific proteins in the case of aptamers (Tuerk and Gold 1990) and transcription factor decoys (Bielinska et al. 1990), or to DNA in the case of triple helix-forming ONs, *i.e.* antigene ONs (Moser and Dervan 1987).

Currently, RNA interference and splicing correction are the ON strategies undergoing the most extensive research, including clinical studies. The traditional RNase H-recruiting antisense approach is also still very much alive and widely represented in ongoing clinical studies. Two local ON treatments have so far reached the market as ocular injections for ophthalmic diseases: the RNase H-activating antisense ON fomivirsen (de Smet et al. 1999) and the RNA aptamer pegaptanib (Ng et al. 2006). Very recently, the FDA approved the first systemic ON drug mipomersen (Crooke and Geary 2012), a subcutaneously administered RNase H-competent antisense ON against homozygous familial hypercholesterolemia. However, the EMA refused to grant marketing authorization to mipomersen due to its serious adverse effects (EMA 2012), and even in the US it can only be prescribed and sold by specially trained personnel (Genzyme 2013). The progress of ONs as systemic therapeutics remains, therefore, in its beginning phase. Apart from toxicity issues, this progress has been delayed by the poor pharmacokinetic properties of ONs. Firstly, ONs are rapidly degraded in serum by nuclease enzymes if they are administered as unmodified natural nucleic acids. The enzymatic stability has been enhanced by introducing numerous chemical modifications, which need to be carefully optimized in order to maintain or increase the efficacy and specificity of ONs. Even more importantly, the main limitation of ONs is their inefficient cellular delivery, preventing them from reaching the site of action. Nanocarriers are promising ON vehicles which combine shielding against degradation with enhanced cellular uptake and/or endosomal escape.

This thesis is focused on improving the enzymatic stability and cellular uptake of antisense ONs and siRNAs, comprising synthetic methods to produce the ONs and their carriers, analytical methods to characterize them, and biological methods to test their effect. In the literature review, strategies for the chemical modification of ONs and for the use of cell-penetrating peptide (CPP)-based carriers for ON delivery are discussed, followed by methods for the mass spectrometric characterization of modified ONs. The experimental part describes the modification of phosphodiester ONs by circularization, covalent conjugation of phosphorothioate ONs to CPPs, the characterization of the products by various analytical methods, and testing the biological properties of the modified ONs such as enzymatic stability, hybridization selectivity, cellular uptake, and antisense activity *in vitro*. The synthesis and characterization of positively charged CPP-modified gold nanoparticles and their complexes with siRNA is also reported, followed by the evaluation of their effect on gene silencing and cell viability *in vitro*.

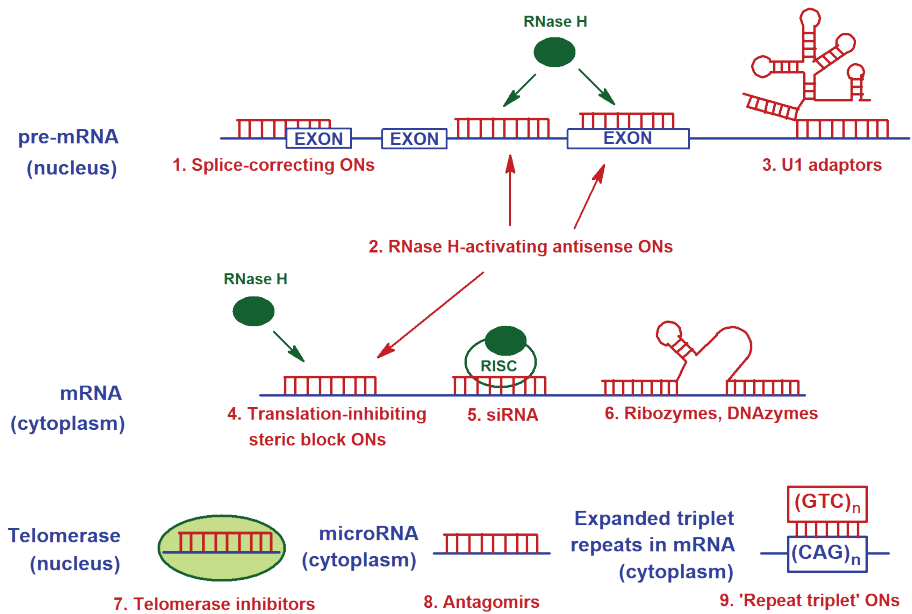


Figure 1 Mechanisms of action of antisense oligonucleotides (ONs). Blue, target RNA (principal site of action for the target); red, ON class; green, proteins/enzymes. Effects: (1) Correction of aberrant splicing. (2) Cleavage of target (pre-)mRNA by RNase H. (3) Inhibition of polyadenylation. (4) Steric inhibition of translation. (5) Cleavage of target mRNA via RNA interference. (6) Cleavage of target mRNA by catalytic nucleic acids. (7) Competitive inhibition of telomerase action. (8) Inhibition of microRNA-mediated gene regulation. (9) Selective steric blocking of the translation of mutant proteins.

2 REVIEW OF THE LITERATURE

2.1 Chemical modifications of oligonucleotides

2.1.1 Changing the chemistry of natural oligonucleotides

ONs with the natural phosphodiester backbone (PO-ONs) (**Figure 2**) have a half-life of only about 5 minutes in human serum (Akhtar et al. 1991). The enzymatic stability can be enhanced by altering the carbohydrate ring or the phosphate internucleotide linkage, by replacing the entire backbone with an isostere, or by changing the topology of the oligonucleotide by e.g. cyclization (reviewed in Milligan et al. 1993; Kool 1996b; Kurreck 2003; Shukla et al. 2010). The heterocyclic bases can also be modified, but that is beyond the scope of this review. **Table 1** shows examples on how the most promising ON chemistries affect biological properties. As classification according to generations is rather arbitrary, the following chapters will discuss modifications according to their site in the ON structure.

Table 1. Characteristics of different oligonucleotide chemistries.

Chemistry	Nuclease stability ¹	Target affinity ¹	Special characteristics and applications
First generation			
Phosphodiester (PO) ²	±	±	Natural DNA or RNA structure
Phosphorothioate (PS) ^{2,4}	+++	–	Protein binding, toxicity; is combined with 2'-O-alkyl
Second generation			
2'-O-Methyl (2'-OMe) ^{3,4}	+	+	Oral antisense formulation, splicing correction
2'-O-(2-Methoxyethyl) (2'-MOE) ⁴	+++	+	Antisense
2'-Deoxy-2'-fluoro (2'-F) ^{3,4}	±	+++	Fixed C3'-endo conformation
Third generation			
2'-Deoxy-2'-fluoro- D-arabino-nucleic acid (FANA) ^{2,4}	+	+	Ribose is replaced by its 2'-epimer, D-arabinose
N3'→P5' thio-phosphoramidate (NPS)	++	++	Competitive inhibitors of telomerase, RNA decoys
Locked nucleic acid (LNA) ^{3,4}	++	+++	Fixed C3'-endo conformation
Unlocked nucleic acid (UNA)	+	–	Acyclic; specificity modifier
Cyclohexene nucleic acid (CeNA) ^{2,4}	+	+	Six-membered ring analog
Peptide nucleic acid (PNA)	+++	+++	Non-ionic peptide backbone
Phosphorodiamidate morpholino oligomer (PMO)	+++	+	Six-membered ring; non-ionic; splicing correction
4'-Thio-RNA ^{3,4}	+	+	Annular oxygen replaced by sulfur; aptamers, siRNA

¹ Compared to natural DNA/RNA. ² RNase H-competent. ³ Aptamer-compatible. ⁴ siRNA-compatible.

2.1.2 Modifications to the phosphate linkage

The most common alterations of the phosphate linkage, representing the first and third generations of ON modifications, are shown in **Figure 2**. All of these modifications significantly improve the enzymatic stability of ONs (Letsinger et al. 1986; Akhtar et al. 1991; Gryaznov et al. 1996).

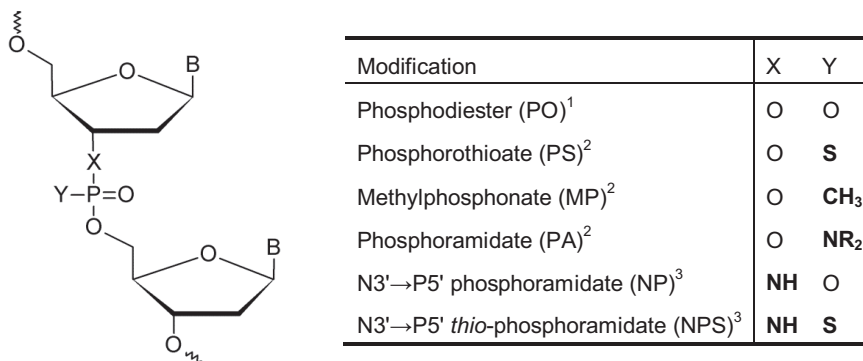


Figure 2 Chemical modifications to the phosphate linkage of oligonucleotides. (B = any of the nucleobases A, G, C, or T. ¹ Natural 2'-deoxyribonucleotide. ² First generation modifications. ³ Third generation modifications. Modified from Milligan et al. 1993, Gryaznov 2010.)

Phosphorothioates. The most successful analogs up to date are the phosphorothioates (PS-ONs), in which the non-bridging oxygen in the phosphodiester linkage is replaced by sulfur (reviewed in Agrawal 1999). Fomivirsen, a PS-ON used in cytomegalovirus (CMV) retinitis as intravitreal injections (de Smet et al. 1999), was the first antisense drug approved by the FDA in 1998, though it soon became redundant due to efficient anti-HIV treatments which rendered active AIDS uncommon. A uniformly modified PS-ON has a half-life of about 9 hours in human serum (Campbell et al. 1990). Although PS-ONs exhibit a somewhat lowered affinity to target RNA (Morvan et al. 1993), they are the only phosphate bond modified ONs that activate RNase H (Agrawal 1999). However, in addition to sequence-specific antisense activity, they display multiple mechanisms of action, including sequence-specific non-antisense and non-sequence-specific effects (Matsukura et al. 1987; Agrawal et al. 1988). Moreover, PS-ONs cause toxicity in the form of immune stimulation (Schechter and Martin 1998). The non-antisense and immune stimulating effects may arise from the extremely polyanionic nature that makes PS-ONs especially prone to bind proteins (Agrawal 1997). Mipomersen, the first systemic ON drug approved by the FDA in 2013 to treat hypercholesterolemia, contains uniform PS linkages combined with other modifications (Genzyme 2013). Mipomersen suffers from adverse effects such as flu symptoms and liver toxicity which severely limit its use.

Methylphosphonates and phosphoramidates. Another early analog, the methylphosphonate (MP) (Jayaraman et al. 1981), failed to enhance cellular uptake despite of its non-ionic structure (Bennett and Swayze 2010). More importantly, MP-ONs form significantly weaker hybrids with target RNA than PO-ONs do (Morvan et al. 1993). Replacing the non-bridging oxygen with an amino group in phosphoramidates (PA) (Letsinger et al. 1986) resulted in even weaker hybridization to RNA than with MP-ONs (Froehler et al. 1988). In the more promising third generation variants, N3'→P5' phosphoramidates (NP) (Gryaznov and Chen 1994) and N3'→P5' *thio*-phosphoramidates (NPS) (Pongracz and Gryaznov 1999), the nitrogen replaces the bridging 3'-oxygen. These compounds exhibit a remarkable affinity to target RNA, forming RNA-resembling A-form double helices due to the favored N-type (*i.e.* C3'-*endo*) conformation of the sugar (Gryaznov et al. 1995). This shift in the equilibrium from the S-type (*i.e.* C2'-*endo*) sugar puckering, typical for 2'-deoxy PO-ONs (**Figure 3**), towards the N-type, favored by ribonucleotides, arises from the substitution of O3' with the less electronegative nitrogen, allowing the anomeric nucleobase effect to prevail over the sugar 3'-*gauche* effect (Thibaudeau et al. 1994). NPs and NPSs are being investigated in various antisense, antigene and RNA mimic applications (reviewed in Gryaznov 2010) and as telomerase inhibitors (Herbert et al. 2002).

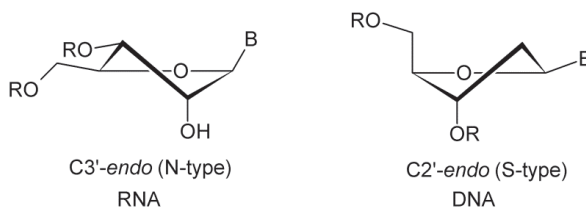


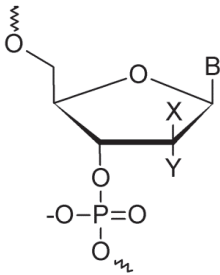
Figure 3 Sugar conformations in nucleic acids. In RNA, the favored ribose conformation is C3'-*endo*; in DNA, 2'-deoxyribose predominantly adopts the C2'-*endo* form. (Modified from Noronha and Damha 1998, Manoharan 1999.)

2.1.3 Carbohydrate 2'-modifications

Modifications to the 2'-position of the carbohydrate ring of ONs, depicted in **Figure 4**, are usually called second generation modifications (reviewed in Manoharan 1999). They exhibit altered pharmacokinetic properties *in vivo* and a significantly increased binding affinity to target RNA because of the more electronegative substituent at the 2'-position, which turns the sugar puckering equilibrium towards the N-type (C3'-*endo*) conformation. An extremely high binding affinity is thus achieved with the 2'-deoxy-2'-fluoro (2'-F) modification, which locks the sugar ring almost completely in the N conformation but does not protect against nucleases (Kawasaki et al. 1993, cited in Manoharan 1999).

2'-O-alkyl modifications. The most extensively studied 2'-modifications are 2'-O-alkyl derivatives such as 2'-O-methyl (2'-OMe) ONs, which exhibit increased affinity to target RNA (Inoue et al. 1987) and a somewhat improved resistance to nucleases (Sproat et al. 1989). Increasing the alkyl chain length decreases the

binding affinity and enhances the enzymatic stability *in vitro* (Cummins et al. 1995). *In vivo*, however, 2'-propoxy ONs showed substantial degradation after injection to mice (Crooke et al. 1996). Therefore, a complete or partial PS backbone is usually combined to 2'-O-alkyl modifications. 2'-OMe ONs have been studied extensively for splice correction applications (Sierakowska et al. 1996; Williams et al. 2009) and also as anti-miRNA ONs (Krütfeldt et al. 2005), U1 adaptors (Goracznik et al. 2009), and telomerase inhibitors (Beisner et al. 2010). An even more promising 2'-O-alkyl modification, the 2'-O-(2-methoxyethyl) (2'-MOE), confers both good binding affinity (Freier and Altmann 1997) and a nuclease resistance comparable to that of PS-ONs (reviewed in Manoharan 1999).



Modification	X	Y
RNA ¹	H	OH
2'-O-Methyl (2'-OMe) ²	H	O-CH ₃
2'-O-Propyl (2'-propoxy) ²	H	O-(CH ₂) ₂ -CH ₃
2'-O-(2-Methoxyethyl) (2'-MOE) ²	H	O-(CH ₂) ₂ -O-CH ₃
2'-Deoxy-2'-fluoro (2'-F) ²	H	F
D-Arabinonucleic acid (ANA) ³	OH	H
2'-Deoxy-2'-fluoro-ANA (FANA) ³	F	H

Figure 4 Chemical modifications to the 2'-position of the sugar ring of oligonucleotides. (B = any of the nucleobases A, G, C, or T/U. ¹ Natural ribonucleotides. ² Second generation modifications. ³ Third generation modifications. Modified from Manoharan 1999.)

Chimeric 'gapmer' oligonucleotides. Due to the inability of 2'-modified ONs to activate RNase H, second generation antisense ONs are usually designed as 'gapmers', chimeric ONs with a central 2'-deoxy-PS gap for RNase H recruitment and 2'-O-alkyl-PS wings at both ends (Manoharan 1999). These gapmers, also known as end-modified mixed-backbone ONs, exhibit fewer polyanionic-related side effects and a highly improved nuclease stability *in vivo*, allowing oral administration in some cases (Agrawal 1999). Mipomersen, a chimeric 2'-MOE/PS antisense ON against apolipoprotein B (Crooke and Geary 2012), has been approved by the FDA for the treatment of hypercholesterolemia.

Arabinonucleic acid derivatives. To overcome the limitation that 2'-O-modified ONs cannot activate RNase H, researchers have also designed compounds such as the D-arabinonucleic acid (ANA) derivatives, 2'-stereoisomers of RNA, which have been found to activate RNase H (Damha et al. 1998, cited in Manoharan 1999). The target affinity of 2'-OH-ANA is quite low but is enhanced in 2'-deoxy-2'-fluoro-D-ANA (FANA). The nuclease stability of both compounds is between that of PO-ONs and PS-ONs.

2.1.4 Conformational restriction and backbone replacement

In many of the advanced third generation modifications, the ribose conformation has been restricted or the ON backbone completely replaced (**Figure 5**).

Locked nucleic acids. The sugar pucker is fixed at the N-type ($C3'$ -endo) conformation in locked nucleic acids (LNAs), bicyclic ribonucleotide analogs bearing a 2'-O,4'-C-methylene bridge in the ribose ring (Obika et al. 1997; Koshkin et al. 1998; reviewed in Veedu and Wengel 2010). LNAs exhibit a substantially increased target affinity (Obika et al. 1998) and high nuclease stability but do not activate RNase H as uniformly modified ONs (Kurreck et al. 2002). Promising results have been achieved with LNA-modified AS-ONs and DNAzymes (Jakobsen et al. 2007), siRNA (Mook et al. 2007), aptamers (Lebars et al. 2007), anti-miRNA ONs (Elmen et al. 2008), and U1 adaptors (Goracznik et al. 2009).

Ethylene-bridged, unlocked, and 4'-thio nucleic acids. A further variation of the bicyclic ribose structure, 2'-O,4'-C-ethylene-bridged nucleic acid (ENA) (Morita et al. 2002a; reviewed in Koizumi 2004), retains the high binding affinity of LNA and shows a remarkable stability towards nucleases. ENAs have shown potential as antisense (Morita et al. 2002b), antigene (Koizumi et al. 2003), and splice correcting ONs (Yagi et al. 2004). In contrast to these rigid structures, unlocked nucleic acid (UNA; 2,3-seco-RNA) (Nielsen et al. 1995; reviewed in Pasternak and Wengel 2011) is an acyclic ribose derivative with increased flexibility and decreased target affinity. Depending on the site of modification, UNA monomers can either decrease or increase the specificity of target binding, making them versatile tools for ON optimization. Another alteration of the sugar moiety is the 4'-thio-RNA (Bellon et al. 1993), where the annular oxygen has been replaced by sulfur. 4'-Thio-RNA has shown enhanced nuclease resistance and hybridization affinity compared to natural RNA, and has been successfully used to modify aptamers (Hoshika et al. 2004) and siRNAs (Dande et al. 2006).

Phosphorodiamidate morpholinos. Several modifications have replaced the entire ribose ring with another heterocycle, as is the case in phosphorodiamidate morpholino oligomers (PMOs) (Stirchak et al. 1989; reviewed in Amantana and Iversen 2005). PMOs are extremely resistant to nucleases (Hudziak et al. 1996), and, in spite of their inability to activate RNase H, have proven efficient enough to progress to clinical trials in antisense (Kipshidze et al. 2007) as well as splice correction applications (Cirak et al. 2011). Due to their non-ionic backbone, PMOs should also be able to avoid the non-specific effects typical for PS-ONs.

Hexitol, cyclohexene, and peptide nucleic acids. Other examples of a six-membered ring in the ON structure (reviewed in Herdewijn 2010) are the hexitol nucleic acids (HNAs) (Verheggen et al. 1993), which have shown antisense activity as HNA-PS-HNA gapmers (Kang et al. 2004), and the cyclohexene nucleic acids (CeNAs) (Wang et al. 2000), flexible analogs that are able to activate RNase H, albeit weakly (Verbeure et al. 2001). The sugar-phosphate backbone is completely replaced with a polyamide chain in peptide nucleic acids (PNAs) (Nielsen et al. 1991; reviewed in Nielsen 2010). PNAs form very stable duplexes with complementary nucleic acids and bind double-stranded DNA *via* strand displacement. They have shown effective splice-correcting (Yin et al. 2008) and antibacterial (Tan et al.

2005) activity *in vivo* as well as antiviral (Tripathi et al. 2007) and targeted gene repair (Lonkar et al. 2009) activity *in vitro*.

Modifications tolerated in aptamers and siRNAs. Some groups of ONs only allow certain modifications due to restrictions caused by the mechanism of action or the method of drug discovery. Since aptamer ONs are enzymatically enriched from a random library *via* a procedure called systematic evolution of ligands by exponential enrichment (SELEX) (Tuerk and Gold 1990), only modifications recognized by the enzymes can be used (Ng et al. 2006). 2'-F substitutions to pyrimidines and 2'-OMe substitutions to purines meet this requirement, and they are used for example in pegaptanib, the only approved RNA aptamer against wet age-related macular degeneration (AMD) (Ng et al. 2006; Eyetech 2008). LNA modifications can be introduced to aptamers post-enrichment (Veedu and Wengel 2010). On the other hand, siRNAs need to be incorporated into the RNAi machinery, and the antisense (*i.e.* 'guide') strand then guides the degrading enzyme to the target sequence (*i.e.* 'passenger') strand (Hornung et al. 2006; Behlke 2008). Modifications such as 2'-MOE, FANA and LNA are thus better tolerated in the sense (*i.e.* 'passenger') strand (Hornung et al. 2005; Prakash et al. 2005). In contrast, PS, 2'-OMe, 2'-F, CeNA, and 4'-thio-RNA residues can be placed in either strand, resulting in slightly reduced, unaffected or even improved RNAi activity (Prakash et al. 2005; Dande et al. 2006; Muhonen et al. 2007; Nauwelaerts et al. 2007). Some modifications have, in addition, been able to reduce the non-specific immune stimulation (Hornung et al. 2005; Judge et al. 2006) and off-target effects (Jackson et al. 2006) often caused by siRNA.

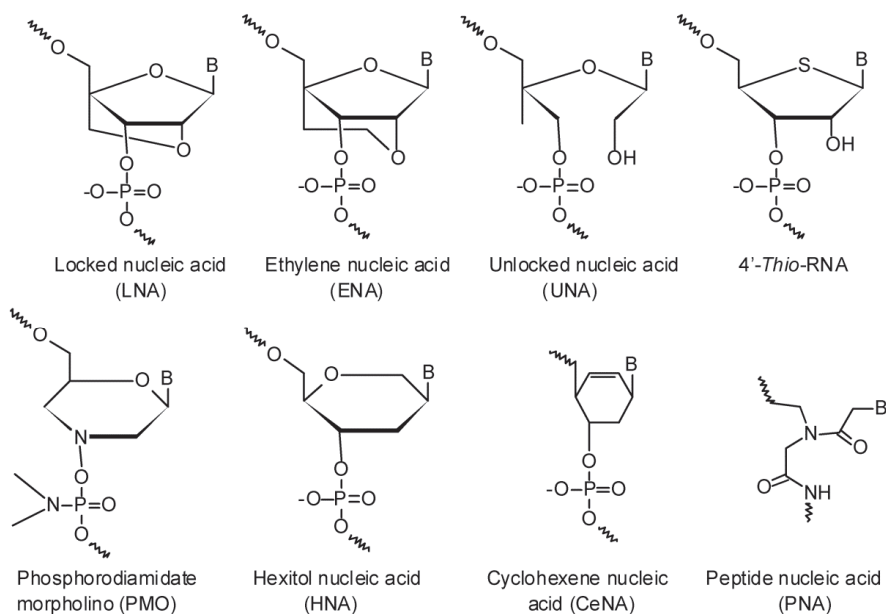


Figure 5 Third generation chemical modifications of oligonucleotides. (B = any of the nucleobases A, G, C, or T/U. Modified from Morita et al. 2002, Kurreck 2003, Hoshika et al. 2004, Herdewijn 2010, Pasternak and Wengel 2011.)

2.1.5 Topological modifications

The main source of degradation in serum have been found to be the 3'-exonucleases, and ONs containing modified residues at the 3'-end have been shown to exhibit relatively good stability in serum (Shaw et al. 1991; Tamsamani et al. 1992; Gilar et al. 1998). In RNAi, it is standard procedure to protect the siRNA strands with 3'-dTdT overhangs (Elbashir et al. 2001). Topological modifications (**Figure 6**) such as hairpin loops and especially circularization (reviewed in Kool 1996a) render the ON resistant to exonucleases due to the absence of free termini (Chu and Orgel 1992). In cells, however, endonucleolytic activity has also been detected (Fisher et al. 1993; Crooke et al. 2000), and only modestly improved stability was found for end-blocked PO-ONs in mice (Sands et al. 1995). Nevertheless, topologically modified ONs exhibit several favorable characteristics and are being investigated in various applications.

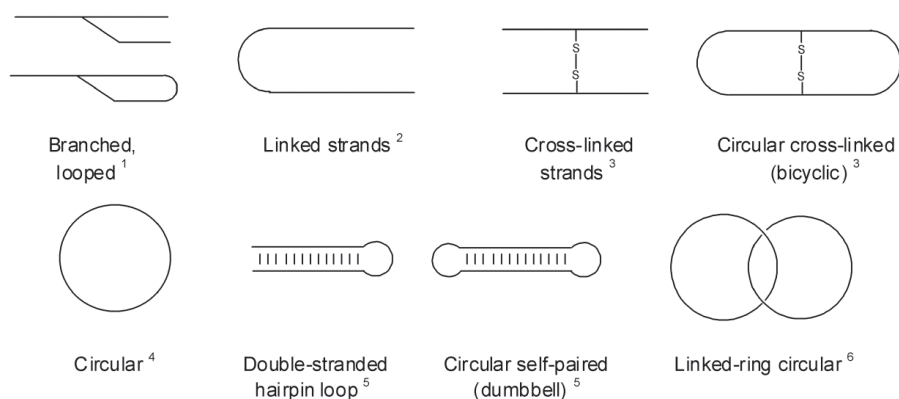


Figure 6 Topological modifications of oligonucleotides. (Partially modified from Kool 1996a. Modifications introduced in: ¹ Azhayeva et al. 1995, ² Giovannangeli et al. 1991, ³ Chaudhuri and Kool 1995, ⁴ Kool 1991, ⁵ Chu and Orgel 1991, and ⁶ Billen and Li 2004.)

Looped, branched, and circular ONs. Triple helix-forming antigene ONs pre-organized by a circular (Kool 1991), hairpin loop (Giovannangeli et al. 1991), or cross-linked (Chaudhuri and Kool 1995) structure have shown enhanced binding affinity and sequence selectivity. Looped ONs capable of forming stable hybrid complexes, *i.e.* adjacent double and triple helices (Azhayeva et al. 1995), and double helix-forming circular ONs (Azhayeva et al. 1997) have also been synthesized and tested *in vitro*. Branched ONs can inhibit splicing by mimicking lariat intron branchpoint sequences (Carriero and Damha 2003). Circular deoxyribo ONs may also be used as vectors to express ribozymes (Daubendiek and Kool 1997) and miRNA mimics (Seidl and Ryan 2011) due to their ability to undergo rolling circle transcription by RNA polymerases (Daubendiek et al. 1995). Remarkably, Billen and Li (2004) were able to link together two ON circles to form 'linked-ring' circular

ONs in an effort to design more complex deoxyribozyme molecules. Recently, Tang et al. (2010) designed antisense ONs circularized *via* photolabile linkers, which can affect their targets only upon irradiation and subsequent linearization. These ‘caged’ light-activated ONs have been studied with different ON backbones, including unmodified phosphodiester (Tang et al. 2010), 2'-OMe/PS (Wu et al. 2012), and PMO (Wang et al. 2012).

Circular dumbbell oligonucleotides. Self-complementary dumbbell-shaped circular ONs have been of particular interest to researchers because of their stabilized double-helical structure, especially in the decoy approach, which employs double-stranded ONs mimicking transcription factor recognition sequences to influence gene expression (reviewed in Gambari 2004). The double-stranded DNA-mimicking structure should also stabilize the ON against nuclease degradation compared to unpaired circular ONs, as it is known that double-stranded nucleic acids are more nuclease-resistant than single-stranded ones (Chu and Orgel 1992). Circular dumbbell decoy ONs have shown inhibition of hepatocyte nuclear factor 1 (HNF1) *ex vivo* (Clusel et al. 1993) and of nuclear factor-kappaB (NF- κ B) *in vivo* (Kim et al. 2009; Kim et al. 2010). Another decoy-type application for circular dumbbell ONs is to use them as irreversible inhibitors of the cancer-related enzyme DNA topoisomerase I (Li et al. 2007). A prodrug-like circular dumbbell chimeric RNA/DNA antisense ON has also been introduced where the RNA strand is cleaved by RNase H, releasing the active antisense DNA strand to inhibit viral replication (Abe et al. 1998).

2.2 Cell-penetrating peptides as vectors of oligonucleotide delivery

2.2.1 Pharmacokinetics and delivery of oligonucleotides

Cellular uptake and intracellular pharmacokinetics. Free ONs have been shown to enter cells *via* endocytosis, after which they become partially entrapped in endosomal compartments (Beltinger et al. 1995). Release from endosomes thus represents one rate-limiting step in ON delivery, as suggested also by the enhancing effect *in vitro* of cationic polymers, fusogenic peptides and pH-sensitive agents (*vide infra*). In contrast, ONs microinjected into the cytoplasm rapidly enter the nucleus (Leonetti et al. 1991; Fisher et al. 1993). This seems promising especially for antigene and decoy ONs, splice-correcting steric block ONs, telomerase inhibitors, and U1 adaptors, which are expected to act in the nucleus. The intracellular site of action for other ONs depends on target mRNA localization. For RNase H-activating antisense ONs, the site of action can reside either in the nucleus or in the cytoplasm, while siRNA, ribozymes, and translation-inhibiting steric block ONs mainly bind to cytoplasmic mRNA. Furthermore, siRNA has been shown to spontaneously accumulate in the appropriate site (Berezhna et al. 2006).

***In vivo* pharmacokinetics.** Most of the research concerning the *in vivo* pharmacokinetics of ONs has been done using PS-ONs (Agrawal et al. 1991; Geary et al. 1997). PS-ONs are highly bound to plasma proteins and are excreted mainly in

the urine (Agrawal 1999; Juliano et al. 2009). Since PO-ONs exhibit much less plasma protein binding, they are excreted faster than PS-ONs (reviewed in Bennett and Swayze 2010). Displacement of protein-bound ONs due to saturation or competition leads to increased urinary elimination (Agrawal et al. 1991). The charge-neutral PMO analogs, in contrast, exhibit minimal protein binding but are still excreted much slower due to their efficient tissue accumulation (reviewed in Amantana and Iversen 2005). As larger entities such as nanocarrier-bound ONs are unable to undergo glomerular filtration, uptake by the mononuclear phagocyte system (MPS) forms an important route of elimination (Juliano et al. 2009). Kidney and liver are the main sites of ON uptake, which makes them ideal target sites for systemic ON treatment but increases the risk of renal or hepatic toxicity, as is seen in the case of mipomersen (*vide ultra*). Other target tissues may be difficult to reach, and many applications have employed local administration, *e.g.* intraocular injections (de Smet et al. 1999) or nasal spray (DeVincenzo et al. 2008), thus enhancing the bioavailability at the site of action and reducing adverse effects (reviewed in Whitehead et al. 2009).

Delivery vehicles. ON treatment is usually carried out with a delivery agent in order to (1) protect the ON from enzymatic degradation and (2) to enhance its cellular uptake. The most widely used vehicles are positively charged compounds, which spontaneously form non-covalent electrostatic complexes with the negatively charged ON. Excess cationic charge is usually created in the complex mixture, facilitating the interaction with negatively charged moieties on the cell surface such as glycosaminoglycans (GAGs). However, the cationic charge also renders the vehicle prone to protein binding, which causes non-specific toxicity and inactivation of the complex by serum proteins.

The delivery agents most commonly used for ONs *in vitro* are cationic lipids (reviewed in Li and Szoka 2007). Their ON complexes, *i.e.* lipoplexes, are internalized by endocytosis (Zelphati and Szoka 1996). Cationic lipids facilitate endosomal release when combined with neutral helper lipids or fusogenic peptides (Jääskeläinen et al. 2000). Most cationic lipids are, however, toxic at high concentrations and ineffective in the presence of serum (Felgner et al. 1987; Bennett et al. 1992; Spagnou et al. 2004). Cationic polymers have also been widely studied as delivery agents for ONs as complexes, *i.e.* polyplexes. Poly(ethylene imine) (PEI) effectively delivers PO-ONs (Dheur et al. 1999) and siRNA (Urban-Klein et al. 2005), and has been suggested to exert endosomal escape via a 'proton sponge' effect (Boussif et al. 1995). For PS-ONs complexed with PEI, however, activity *in vitro* has not been achieved despite the enhanced cellular uptake (Dheur et al. 1999; Jääskeläinen et al. 2000). In addition, PEI exhibits significant cytotoxicity (Fischer et al. 2003; Neu et al. 2005). More recently designed nanocarriers aim at efficient *in vivo* delivery causing minimal toxicity. Gold nanoparticles (GNPs), for example, have been used *in vitro* as covalently linked antisense ON carriers (Rosi et al. 2006) and as complexes, *i.e.* nanoplexes, with siRNA (Lee et al. 2008; Bonoiu et al. 2009). Numerous other nanoparticles based on *e.g.* biodegradable polymers, dendrimers, cyclodextrins, mesoporous silica, and cell-penetrating peptides (CPPs) have also been investigated. However, only few of them have been studied *in vivo* so far.

Three notable nanocarrier functions have been widely pursued to improve the *in vivo* delivery of ONs: (1) enhanced endosomal escape, (2) avoidance of phagocytes, and (3) active targeting. To facilitate endosomal release, researchers have developed pH-sensitive liposomes, which are destabilized at the acidic pH of the endosome (reviewed in Fattal et al. 2004). To reduce protein binding and MPS clearance, Papahadjopoulos et al. (1991) designed sterically stabilized liposomes coated with poly(ethylene glycol) (PEG). These PEGylated ‘stealth’ liposomes, termed stable nucleic acid lipid particles (SNALPs) by Jeffs et al. (2005), have proven efficient in siRNA delivery against *e.g.* Ebola virus *in vivo* (Geisbert et al. 2006). Cholesterol conjugation, which affords partial targeting to the liver, has long been known to enhance the cellular uptake of antisense ONs *in vitro* (Krieg et al. 1993) and was also successfully employed to deliver cholesterol-lowering siRNA to mice *in vivo* (Soutschek et al. 2004). Various ligands have aided to target siRNA specifically to tumors, which overexpress receptors such as transferrin (TF) (Heidel et al. 2007) and folate (Yoshizawa et al. 2008).

Clinical trials. As discussed in previous chapters, marketing authorizations have been granted to only three ONs, two of which are administered locally as intraocular injections. Various systemic ON formulations are, however, being investigated in clinical studies (reviewed in Bennett and Swayze 2010; Burnett and Rossi 2012). Examples of ONs undergoing clinical trials for systemic use are shown in **Table 2**. The target diseases range from *myasthenia gravis* to cancers and Duchenne muscular dystrophy (DMD). While modern applications such as siRNA, splicing correction, and telomerase inhibition are present, it is noteworthy that RNase H-activating antisense ONs are still among the most numerous and successful ones. The chemistry of choice seems to be the second generation 2'-O-alkyl, which is also studied as an orally administered compound. This major advance has been enabled by the remarkably high nuclease resistance afforded by the uniform combination of 2'-OMe with PS linkages.

As the chemical modification of siRNA structure is not as straightforward as for other antisense ONs (*vide ultra*), siRNAs are usually studied as unmodified or slightly modified compounds, which are highly susceptible to degradation and exhibit unfavorable delivery properties. Thus it is not surprising that most siRNAs currently in clinical trials are administered locally (*e.g.* eye drops, ocular injections, or inhalations) or *ex vivo* (reviewed in Burnett and Rossi 2012). While these routes allow the use of naked siRNA, systemic administration without a delivery vehicle would require very high doses, increasing the cost of therapy and the prevalence of non-specific effects. Therefore, most research on systemic siRNAs *in vivo* is concentrated on the use of nanoparticle carriers to achieve maximal protection from enzymes and accumulation in the site of action. As Burnett and Rossi point out in their review (2012), the indications of systemic siRNAs clearly reflect the pharmacokinetic consequences of each delivery method: naked siRNAs end up in the kidneys, warranting their use for renal diseases, while nanocarrier-bound ONs generally stay in the liver, making them useful against hepatic cancer. For targeted delivery agents, the destination depends on the ligand used. Tumor targeting, for instance, was achieved by TF in the multifunctional PEGylated cyclodextrin-based nanoparticles

used in the first clinical trial of systemically administered siRNA, which also provided the first evidence of systemic RNAi in humans (Davis et al. 2010).

Table 2. *Examples of systemic oligonucleotide drugs in clinical trials. (Modified from Bennett and Swayze 2010, Burnett and Rossi 2012.)*

Name	Indication	Mechanism	Chemistry / carrier	Reference
Mipomersen (KYNAMRO™) ¹	Familial hypercholesterolemia	RNase H	2'-MOE chimera	Crooke and Geary 2012
Monarsen (EN101) ²	<i>Myasthenia gravis</i>	RNase H	2'-OMe chimera	Sussman et al. 2008
Custirsen (OGX-011)	Cancer	RNase H	2'-MOE chimera	Zielinski and Chi 2012
Drisapersen (PRO-051)	DMD ³	Splicing correction	2'-OMe PS	Goemans et al. 2011
Eteplirsen (AVI-4658)	DMD ³	Splicing correction	PMO	Cirak et al. 2011
Imetelstat (GRN163L)	Cancer	Telomerase inhibitor	Lipid-conjugated NPS	Marian et al. 2010
I5NP (QPI-1002)	Renal injury, graft failure	siRNA	Naked	Thompson et al. 2012
ALN-VSP02	Hepatic cancer	siRNA	SNALP	Vaishnav et al. 2011
CALAA-01	Cancer	siRNA	PEG-coated TF-nanoparticles	Davis et al. 2010
Angiozyme ⁴ (RPI.4610)	Renal cancer	Ribozyme	PS, 2'-OMe, allyl, inverted	Kobayashi et al. 2005

¹ Approved by FDA. ² Oral formulation. ³ Duchenne muscular dystrophy. ⁴ Clinical studies suspended.

2.2.2 Cell-penetrating peptides in oligonucleotide delivery

Cell-penetrating peptides (CPPs), also referred to as protein transduction domains (PTDs) or membrane permeable peptides (MPPs), have been shown to enhance the cellular uptake of varying cargoes, especially therapeutic macromolecules such as peptides, proteins, DNA, ONs, and siRNA (reviewed in Lindgren et al. 2000; Fonseca et al. 2009; Coursindel et al. 2012). Several types of CPPs have been discovered displaying a wide range of structures, most of them being relatively small, less than 30 amino acids, and exhibiting either a net positive charge or amphipathicity (Patel et al. 2007). While the polycationic nature of various CPPs has been estimated a key factor in their success, many of the most promising CPPs, especially those deemed capable of non-endocytic uptake (*vide infra*), are amphipathic and display at least some hydrophobicity. **Table 3** shows amino acid sequences of the most well-known CPPs and some of their analogs.

Table 3. Sequences of cell-penetrating peptides.

Name	Amino acid sequence	Reference
Protein-derived		
Penetratin (Antp ₄₃₋₅₈)	RQIKIWFQNRRMKWKK	Derossi et al. 1994
EB1	LIRLWSHLIHWFQNRRLKWKKK	Lundberg et al. 2007
Tat ₄₈₋₆₀	GRKKRRQRRRPPQ	Vivès et al. 1997
Chimeric		
MPM _(K-FGF) -NLS _(NF-κB)	AAVALLPAVLLALLAPVQRKRQKLMPC	Lin et al. 1995
MPG	GALFLGWLGAAGSTMGAWSQPKKKRKV	Morris et al. 1997
MPG ^{ΔNLS}	GALFLGWLGAAGSTMGAWSQPKSKRKV	Simeoni et al. 2003
MPG α (P α)	GALFLAFLAAALSMLGWSQPKKKRKV	Deshayes et al. 2004c
MPG-8	β AAFLGWLGAWGTMGWSPKKKRK	Crombez et al. 2009
Transportan	GWTLNSAGYLLGKINLKALAALAKKIL	Pooga et al. 1998
TP10	AGYLLGKINLKALAALAKKIL	Soomets et al. 2000
Synthetic		
MAP	KLALKLALKALKAALKLA	Oehlke et al. 1998
Oligoarginine (R ₈ , R ₉)	RRRRRRRR, RRRRRRRR	Mitchell et al. 2000
Pep-1 (Chariot™)	KETWWETWTEWSQPKKKRKV	Morris et al. 2001
Pep-2	KETWFETWTEWSQPKKKRKV	Efimov et al. 2001
Pep-3	KWFETWTEWPKKRK	Morris et al. 2007

Covalent and non-covalent strategies. CPPs can be chemically coupled to ONs, forming covalent peptide–ON conjugates (POCs), or used as electrostatic complexes. Numerous synthetic methods have been introduced to conjugate CPPs to ONs and siRNAs (reviewed in Tung and Stein 2000; Meade and Dowdy 2007; Lebleu et al. 2008). The most frequently used bond types are disulfide, maleimide, thioether and amide. The bioreducible disulfide bridge has been reported to confer higher efficacy *in vitro* than a stable linker (Abes et al. 2007). The POCs with the most promising results are formed with neutral steric block ONs, frequently used for splicing correction, such as PNAs and PMOs (Lebleu et al. 2008). As non-ionic molecules they do not form electrostatic complexes with cationic compounds, and delivery vehicles can only be used as covalent conjugates, as complexes based on some other type of interaction (*e.g.* hydrophobic), or encapsulated inside the vehicle.

Negatively charged ONs, in contrast, have been complexed to cationic CPPs in various cases with good results (*vide infra*). Meade and Dowdy (2008) argue that non-covalent CPP/ON complexes might provide more efficient siRNA delivery, as the cationic charge in covalent conjugates could be neutralized by the anionic siRNA strands. Furthermore, they postulate that the enhanced siRNA delivery by unpurified CPPs observed in some studies (Chiu et al. 2004; Davidson et al. 2004; Muratovska and Eccles 2004) was not caused by the covalent CPP–siRNA conjugates but, in fact, by excess free peptide in solution acting as non-covalent

delivery vehicle. This hypothesis was supported by the failure of purified conjugates to assist in achieving significant gene silencing at usual siRNA concentrations (Moschos et al. 2007; Turner et al. 2007).

2.2.3 Classes and efficacies of cell-penetrating peptides

In the literature, CPPs have been classified by two different criteria: either according to the origin of the sequence or the structural characteristics of the peptide. The latter includes three categories: *i*) primary amphipathic CPPs with alternating hydrophilic and hydrophobic amino acids along the sequence, *ii*) secondary amphipathic CPPs, where the amphipathicity is revealed upon formation of secondary structures, and *iii*) non-amphipathic cationic CPPs (Madani et al. 2011). Here we will discuss the most important CPPs divided to three classes by their origin: *i*) CPPs derived from the membrane-translocating sequences of cellular proteins, *ii*) chimeric CPPs composed of two parts, one of which is usually a nuclear localization sequence (NLS) of natural origin, and *iii*) synthetic CPPs specifically designed for this purpose (Lindgren and Langel 2011). **Table 4** summarizes the impact of CPPs on ON delivery found in the literature, discussed in more detail in the following text. This table emphasizes the sequence-specific response in reporter-expressing or disease-relevant cell lines as a measure of enhanced delivery. This measure is more reliable than observed cellular uptake, because many uptake assays cannot distinguish membrane-bound from truly internalized ONs.

Protein-derived CPPs. Homeoproteins are transcription factors that bind to DNA *via* a specific 60-amino acid sequence called homeodomain (reviewed in Gehring 1987). In the early 1990s, it was found that the homeodomain of Antennapedia, a *Drosophila* homeoprotein, could enter nerve cells and accumulate in the nuclei (Joliot et al. 1991). Later a 16-amino acid secondary amphipathic peptide in the third helix of Antennapedia was specified as the sequence needed for cellular uptake (Derossi et al. 1994) and was termed as penetratin (Derossi et al. 1998). Penetratin covalently linked to a 2'-OMe PS-ON exhibited enhanced cellular uptake and sequence-specific splicing correction *in vitro* (Astria-Fisher et al. 2002) in HeLa-pLuc/705 cells, where the luciferase reporter gene is coupled to a thalassemic β -globin intron preventing luciferase expression unless splice-corrected (Kang et al. 1998). However, penetratin did not deliver the ON even nearly as efficiently as cationic lipids (Astria-Fisher et al. 2002). Better results were obtained with penetratin linked to the 5'-end of the sense strand of siRNA, showing an equal or better delivery than cationic lipids in various cell lines (Davidson et al. 2004; Muratovska and Eccles 2004).

Tat (*trans*-activator of transcription) is a protein involved in the replication of HIV-1 that activates gene expression from the HIV-1 long terminal repeat (LTR) (Sodroski et al. 1985). Tat was shown to readily enter cells *via* endocytosis and localize to the nucleus (Mann and Frankel 1991). It was discovered that cellular uptake depends on the basic domain extending from residues 48 to 60 (Vivés et al. 1997). The basic domain contains the NLS sequence GRKKR (Ruben et al. 1989), but the NLS alone is not sufficient to induce uptake without the rest of the basic

domain (Vivés et al. 1997). Similar to penetratin (*vide ultra*), covalently conjugated Tat_{48–60} only moderately enhanced the cellular uptake of a 2'-OMe PS-ON (Astrib-Fisher et al. 2002). In contrast, Tat_{47–57} conjugated to the 3'-end of the antisense strand of siRNA produced cellular uptake comparable to that mediated by cationic lipids and sequence-specific gene silencing in HeLa cells (Chiu et al. 2004).

Chimeric CPPs. Several CPPs have been designed combining NLSs to signal sequences, *i.e.* membrane translocating sequences (MTSSs), which guide translated proteins to different cellular organelles (Lindgren et al. 2000). The cationic NLS of the p50 subunit of NF- κ B was combined with a membrane permeable motif (MPM) comprising the hydrophobic region of the signal peptide of Kaposi fibroblast growth factor (K-FGF), known to interact with lipid bilayers (Lin et al. 1995). A conjugate composed of MPM and the homopolypeptide poly(L-lysine) complexed with PS-ONs was internalized in various cell lines, but no biological activity testing was performed on these complexes (Dokka et al. 1997). After the conjugation of the MPM to 2'-OMe/LNA mixmer steric block ONs, neither uptake nor inhibitory activity were observed in luciferase-expressing HeLa cells (Arzumanov et al. 2003).

Another CPP constructed this way is MPG (Morris et al. 1997), in which the hydrophobic domain is derived from the fusion sequence of HIV gp41 and the hydrophilic domain from the NLS of Simian virus 40 (SV40) large T antigen. As a non-covalent complex with PS-ONs, MPG promoted rapid nuclear uptake in human fibroblasts. Complexes with siRNA resulted in sequence-specific gene silencing comparable to Oligofectamine in various cell lines, which was further enhanced by a mutated NLS part impairing the nuclear localization in the MPG^{ANLS} analog (Simeoni et al. 2003). MPG also exhibited nuclear import and sequence-specific gene silencing in a study that, extraordinarily, showed transcriptional inhibition by siRNA in human cells (Morris et al. 2004a). Deshayes et al. (2004c) slightly modified the sequence of MPG and designed MPG α (P α), which has a higher helical content. MPG α exhibited ability for hydrophobic interactions with any phospholipid, while MPG seemed to favor anionic lipids. However, MPG α delivered siRNA 30-fold less efficiently than Lipofectamine 2000 *in vitro* (Veldhoen et al. 2006).

Langel et al. (1996) designed the primary amphipathic peptide galparan, which is a combination of the neuropeptide galanin and the wasp venom toxin amphiphilic peptide toxin mastoparan, the latter of which is known to increase membrane permeability. The [Lys¹³]galparan analog, transportan, demonstrated efficient uptake in Bowes' melanoma cells (Pooga et al. 1998). The transportan analog transportan 10 (TP10), with a truncated galanin part to reduce potential side-effects, also showed promising cellular uptake (Soomets et al. 2000). Covalent conjugation to TP10 failed to enhance the delivery of 2'-OMe/LNA mixmer steric block ONs (Arzumanov et al. 2003), whereas transportan–siRNA conjugates were efficiently delivered and exhibited RNAi (Muratovska and Eccles 2004). Coupling of transportan and TP10 to a PNA and subsequent hybridization of the conjugate with a partially complementary decoy ON was shown to confer NF- κ B binding activity in rat insulinoma cells (Fisher et al. 2004). A similar strategy incorporating an additional NLS to the TP10–PNA conjugate conferred good uptake and inhibition of the oncogene c-Myc in cancer cells (El-Andaloussi et al. 2005).

Table 4. Oligonucleotide delivery by cell-penetrating peptides in the literature.¹

Cell-penetrating peptide	Efficacy ²	Response	Cell line / <i>in vivo</i>	Complex/covalent	Oligonucleotide
Penetratin	(+)	SC	HeLa-pLuc/705	Covalent	2'-OMe/PS
	+	KD	Primary cells	Covalent	siRNA
	++	KD	COS-7,CHO,EOMA	Covalent	siRNA
Penetratin-R ₆	++	SC	HeLa-pLuc/705	Covalent	PNA
EB1	(+)/+	KD	HeLa, HepG2	Complex	siRNA
Tat ₄₈₋₆₀	(+)	SC	HeLa-pLuc/705	Covalent	2'-OMe/PS
	(+)	SC	HeLa-pLuc/705	Covalent	PNA
	(+)	KD	HeLa	Covalent	siRNA
MPM _(K-FGF) ³	-	AI	HeLa	Covalent	2'-OMe/LNA
MPG	+(+)	KD	HeLa, COS-7	Complex	siRNA
	++	KD ⁴	293FT	Complex	siRNA
MPG ^{ΔNLS}	+++	KD	HeLa, COS-7	Complex	siRNA
MPG α (P α)	(+)/+	KD	HTOL,ECV GL3	Complex	siRNA
Chol-MPG-8	+	KD	<i>In vivo</i> in mice	Complex	siRNA
Transportan	++	KD	COS-7,CHO,EOMA	Covalent	siRNA
Transportan-PNA	+	TFI	Rinm5F	Complex	decoy ON
TP10	-	AI	HeLa	Covalent	2'-OMe/LNA
TP10-PNA	+	TFI	Rinm5F	Complex	decoy ON
Stearyl-TP10	+	SC	HeLa-pLuc/705	Complex	2'-OMe/PS
PepFect6	++	KD	<i>In vivo</i> in mice	Complex	siRNA
Endo-Porter	+	KD	HeLa,Huh,Hek293T	Complex	siRNA
MAP	++	AI	Primary cells	Covalent	PNA
	++	SC	HeLa-pLuc/705	Covalent	PNA
Pep-1 (Chariot™)	+	KD	Primary cells	Complex	siRNA
Pep-2	++	AI	HS-68, 293, HeLa, MCF-7	Complex	PNA analog
	++	AI	HUVEC,Jurkat	Complex	PNA analog
Pep-3	++	AI	HUVEC,Jurkat	Complex	PNA analog
(RxR) ₄ ⁵	+	SC	HeLa-pLuc/705	Covalent	PNA
	+	SC	HeLa-pLuc/705	Covalent	PMO
	+	VRI	<i>In vivo</i> in mice	Covalent	PMO
Stearyl-(RxR) ₄	+	SC	HeLa-pLuc/705	Complex	2'-OMe/PS
Stearyl-R ₉	-	SC	HeLa-pLuc/705	Complex	2'-OMe/PS

¹ The corresponding references are given in the text. ² Compared to cationic lipids / evaluated otherwise: - no effect, (+) less effective / modest effect, + as effective / significant effect, ++ more effective / extensive effect. ³ MPM part only. ⁴ Transcriptional silencing. ⁵ x = 6-aminohexanoic acid. **Response types:** AI, antisense inhibition. KD, gene knockdown *via* RNA interference. SC, splicing correction. TFI, transcription factor inhibition. VRI, viral replication inhibition.

Synthetic CPPs. To overcome the need for unique protein-derived sequences, a model amphipathic peptide (MAP) was designed, the cellular uptake of which depended solely on its amphipathicity (Oehlke et al. 1998). Despite of its extensive cellular uptake in various cell lines without cargo, MAP exhibited poor delivery of PS-ONs conjugated *via* disulfide linkage or as non-covalent complexes (Oehlke et al. 2002). However, MAP stably linked to antisense PNA showed clearly enhanced cellular uptake and pharmacological effect in rat cardiomyocytes (Oehlke et al. 2004). MAP-conjugated PNA also exhibited enhanced splicing correction in HeLa-pLuc/705 cells, both disulfide and stable linkers working equally efficiently (Wolf et al. 2006). This might reflect cargo-dependence of the CPP carrier, as PNA is a DNA mimic with a peptide backbone. The CPP Pep-1 (Morris et al. 2001), which adopts an α -helical conformation in contact with phospholipids (Deshayes et al. 2004b), seems to be more versatile: it has been found effective in protein (Morris et al. 2001), PNA (Morris et al. 2004b), and siRNA delivery (Arita et al. 2005). In contrast, the helical MPG analog MPG α displayed a significantly weaker siRNA delivery than did the nonstructured/ β -sheet-forming parent compound (*vide infra*). The Pep-1 analogs Pep-2 (Morris et al. 2004b) and Pep-3 (Morris et al. 2007) also exhibited efficient PNA delivery *in vitro* and *in vivo*, respectively.

Polyarginines have been shown to be internalized by Jurkat cells more efficiently than other polycationic homopolypeptides (Mitchell et al. 2000). In a study by Abes et al. (2007), penetratin was coupled to an oligoarginine (R₆) stretch to improve the cellular delivery of PNA, and the compounds did indeed exhibit increased splicing correction activity in HeLa-pLuc/705 cells. Polyarginine derivatives have been investigated especially for the delivery of neutral steric block ONs, and significantly enhanced splicing correction in HeLa-pLuc/705 cells was obtained by using covalent conjugates of (RxR)₄, where x = 6-aminohexanoic acid, with PNA (Resina et al. 2007) and PMOs (Abes et al. 2008). Furthermore, (RxR)₄-PMO conjugates have shown high antiviral activity *in vivo* (Burrer et al. 2007; Deas et al. 2007).

2.2.4 Mechanisms of cellular uptake

Originally, for penetratin, Tat and transportan, the mechanism of internalization was believed to be non-endocytic since uptake was observed at 4°C as well as at 37°C (Derossi et al. 1994; Vivès et al. 1997; Pooga et al. 1998). However, it was later discovered that the nuclear import of another CPP, VP22 derived from herpes simplex virus protein, was an artifact arising from cell fixation (Lundberg and Johansson 2001). The same was demonstrated for Tat, R₉, and Tat-PNA conjugates (Richard et al. 2003). A study with penetratin-ON conjugates also suggested an energy-dependent pathway, as the uptake was found to be clearly temperature-dependent (Astriab-Fisher et al. 2002). Thus, as Madani et al. (2011) state in their review, the effect of surface-bound cationic CPPs must be eliminated by treating the cells with trypsin or by quenching surface-bound fluorophores, and methods such as live cell imaging, reporter assays, or target mRNA quantitation are to be preferred.

Console et al. (2003) recognized negatively charged glycosaminoglycans (GAGs) on the cell surface as essential mediators of the cellular uptake of penetratin and

Tat, and confirmed that the major route of uptake was endocytosis. Duchardt et al. (2007) found that penetratin, Tat, and R₉ employ three different endocytic pathways and, at higher concentrations, enter cells *via* a rapid endocytosis-independent, heparan sulfate-dependent mechanism. Moreover, a previous study had indicated that the uptake mechanism of Tat may depend on its cargo: smaller cargoes such as peptides displayed rapid translocation, while globular proteins were taken up by endocytosis (Tünnemann et al. 2006). The exact mechanism of this concentration- and cargo-dependent rapid uptake, assuming it was the same in both studies, remains to be investigated. Recently, the role of GAGs in CPP uptake was questioned by Subrizi et al. (2012), who unexpectedly found a higher Tat uptake in a GAG-deficient mutant cell line compared to wild-type CHO cells. Interestingly, they found the same amount of uptake for several structural analogs of Tat, suggesting that cationic charge rather than the exact amino acid sequence may be the main property governing the translocation of Tat-related CPPs.

According to a review by Madani et al. (2011), primary amphipathic CPPs (*e.g.* transportan, TP10, and MPG) are more likely to exhibit direct membrane penetration than cationic CPPs. A conformational study was performed on MPG to find the mechanism of the observed non-endocytic cellular internalization (Deshayes et al. 2004a). The results suggested the mechanism to be transient transmembrane pore formation (**Figure 7**; Deshayes et al. 2008) resulting from transition from non-structured to β -sheet conformation. A similar transition, but to an α -helix structure, was seen for Pep-1 (Deshayes et al. 2004b). In contrast, the MPG analog MPG α adopts a helical structure regardless of the presence or absence of lipids (Deshayes et al. 2004c), and has shown clear signs of endocytic uptake and endosomal entrapment as complex with siRNA (Veldhoen et al. 2006). Transportan, which is also mostly helical in various conditions, and penetratin, which shifts from helical to β -sheet conformation in contact with lipids (Magzoub et al. 2003), both exhibited endocytic uptake as covalent conjugates with splice-correcting PNA in HeLa-pLuc/705 cells in a comparative study by Lundin et al. (2008). Therefore, one might speculate that transition from non-structured to either helical or β structure favors direct transmembrane penetration. However, this mechanism remains unconfirmed and controversial, and more mechanistic studies are needed to fully elucidate its possibility and significance.

2.2.5 Combining cell-penetrating peptides to other modifications

Many known CPPs display promising but not ideal properties. For example, they may be trapped inside endosomes following their uptake by endocytosis, or high concentrations of CPP may be required for direct transmembrane penetration. These characteristics might be improved by modifications such as conjugation to adjuvant groups or the introduction of modified amino acids to the peptide sequence.

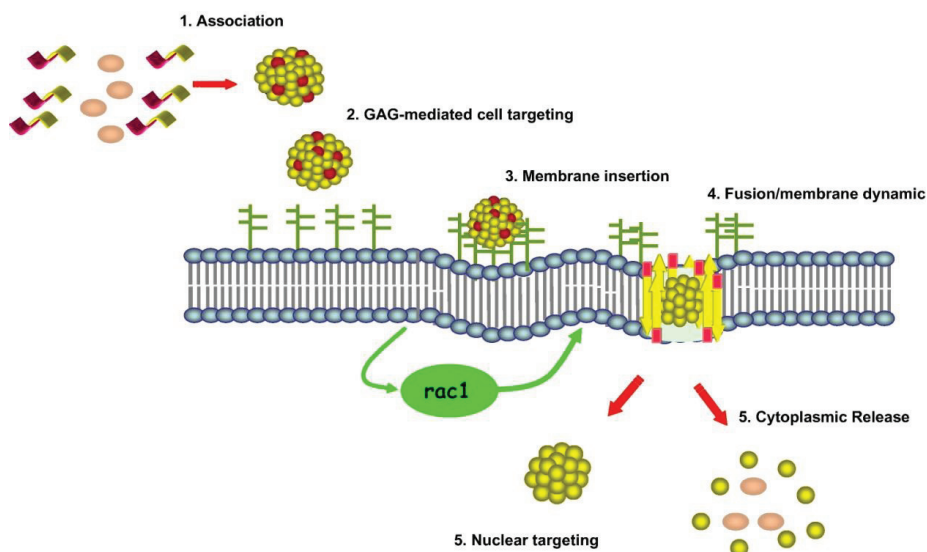


Figure 7 Proposed cell entry mechanism for the cell-penetrating peptides MPG and Pep-1. (1) Complex formation with the cargo. (2) Interaction with cell-surface glycosaminoglycans (GAGs). (3) Membrane insertion. (4) Transient transmembrane pore formation *via* rac1 activation. (5) Cytoplasmic release of the cargo. [Reprinted from Deshayes et al. 2008, p. 544, with permission from Elsevier.]

Promoting endosomal escape. One of the major limitations of CPP-mediated delivery, endosomal entrapment, may be avoided if the escape from endosomes is facilitated. This can be achieved by *e.g.* increasing the hydrophobicity of the CPP (Vivès et al. 2008). Systemic injection of siRNA as a complex with cholesterol-functionalized MPG-8, a tryptophan-rich MPG analog, resulted in highly efficient tumor growth inhibition *in vivo* (Crombez et al. 2009). Non-covalent packaging of 2'-OMe PS-ONs with stearylated TP10 (Mäe et al. 2009) and stearylated (RxR)₄ (Lehto et al. 2010) significantly enhanced the splice correction activity in HeLa-pLuc/705 cells. In contrast, unexpectedly, stearylation of R₉ failed to provide any enhancement (Lehto et al. 2010). Endosomal escape can also be promoted with the use of fusogenic (*i.e.* endosomolytic) peptides, which undergo conformational changes upon endosome acidification (Endoh and Ohtsuki 2009). Akita et al. (2010) used stearylated R₈ to package siRNA inside lipids to form a multifunctional envelope-type nanodevice (MEND), which was surface-modified with stearyl-R₈. When a pH-sensitive fusogenic peptide, GALA, was introduced among the lipids, the construct showed clear signs of enhanced endosomal escape and improved gene silencing effect in dendritic cells *ex vivo*, thus combining CPP-mediated uptake and pH-triggered endosomal release.

Histidine-rich peptides have been used as endosomolytic CPPs in various studies, as the weak base is protonated at acidic pH. A histidine-rich penetratin analog, EB1, enhanced gene silencing in HeLa and HepG2 cells compared to other CPPs (Lundberg et al. 2007). The authors propose a mechanism where EB1 forms an α -helix upon protonation in the acidic environment of endosomes, resulting in

membrane disruption and cargo release (**Figure 8**). In agreement with this mechanism, the commercial amphipathic histidine-rich peptide Endo-Porter displayed pH-dependent α -helix formation and endosomal release of siRNA, leading to RNAi effects in various cell lines (Bartz et al. 2011). Combining both the hydrophobic and pH-titratable endosomolytic properties, PepFect6, a stearylated TP10 analog bearing covalently linked proton-accepting trifluoromethylquinoline moieties, showed facilitated endosomal escape, remarkable siRNA delivery efficiency in various cell lines, and strong RNAi responses *in vivo* (El Andaloussi et al. 2011). While these peptides display favorable properties, it is noteworthy that endosomal release is still not 100%, and the majority of siRNA does enter lysosomes.

Even more high-tech approaches to enhance the endosomal escape used near-infrared (NIR) laser to release siRNA from Tat–lipid-coated gold nanoshells (Braun et al. 2009) and gold nanorods (Lee et al. 2009), achieving laser-activated gene silencing. Such triggered release strategies offer an attractive means of focusing the pharmacological effect at a restricted area, *e.g.* solid tumor, and thus avoiding adverse effects at other sites.

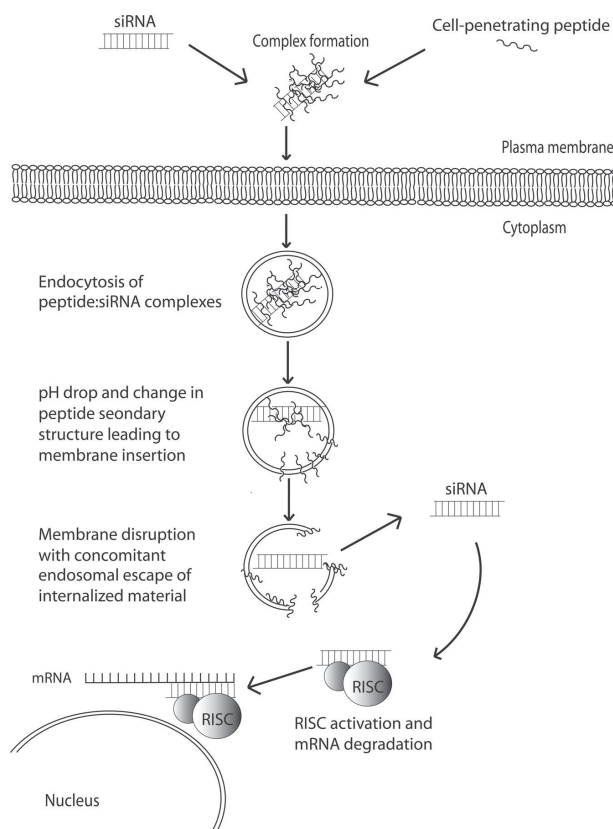


Figure 8 Proposed endosomal escape mechanism for the endosomolytic peptide EB1. [Reprinted from Lundberg et al. 2007, p. 2670, with permission from FASEB.]

Combining cell-penetrating peptides with nanoparticle vectors. Nanoparticle delivery vectors can also be modified with CPPs in order to enhance the cellular uptake of the vector. Tat peptide, especially, has been combined with numerous nanocarriers (reviewed in Torchilin 2008). Tat-liposomes have been found effective in intratumoral gene delivery *in vivo* (Torchilin et al. 2003), and siRNA delivery has been achieved with R_s-liposomes *in vitro* (Zhang et al. 2006) and with Tat peptide-modified methoxy poly(ethylene glycol)–poly(ϵ -caprolactone) (MPEG–PCL) nanomicelles *in vivo* (Kanazawa et al. 2012). Gold nanospheres have been studied extensively in siRNA delivery (reviewed in Lytton-Jean et al. 2011), employing for example PEI-coated GNPs (Lee et al. 2011b) or sandwich-type multilayer siRNA/GNP complexes (Lee et al. 2011a). However, few studies have examined CPP-modified GNPs for siRNA delivery, and GNPs have been conjugated to CPPs mainly for nuclear targeting experiments. 20-nm GNPs coated with BSA-conjugated SV40 large T antigen NLS showed cytoplasmic localization in HeLa, 3T3/NIH, and HepG2 cells (Tkachenko et al. 2004). The same NLS conjugated to gold nanorods, in contrast, was able to enter both the cytoplasm and the nucleus of HaCaT and HSC-3 cells (Oyelere et al. 2007). Tat enabled nuclear entry in immortalized primary human fibroblasts when conjugated to small but not to 35-nm GNPs; the latter entered the cytoplasm but showed no obvious advantage over PEG-coated GNPs (Berry et al. 2007). Sun et al. (2008) functionalized 35-nm GNPs with the octaarginine derivative CALNRR₈ and achieved efficient nuclear delivery in HeLa cells.

Combining cell-penetrating peptides with targeting moieties. According to Vivès et al. (2008), the main drawback of CPPs is their complete lack of cell specificity. They propose that CPPs be combined with cell-targeting peptides in order to achieve both tissue-specific targeting, allowing the CPP to accumulate in the correct tissue, and subsequent cellular internalization. Kale and Torchilin (2007) combined passive tumor targeting with CPPs in their ‘smart’ pH-sensitive PEGylated nanoparticles, where Tat peptide was masked under pH-sensitive PEG-lipids until the particles reached the more acidic intratumoral space. These particles were further augmented with tumor-specific monoclonal antibody to enhance doxorubicin delivery (Koren et al. 2012). Cell penetration and cell targeting were also combined in multifunctional siRNA-conjugated PEG–quantum dots, which displayed both RGD peptide, for brain tumor cell-specific delivery, and Tat peptide (Jung et al. 2010).

2.3 Analysis of modified oligonucleotides by mass spectrometry

2.3.1 Mass spectrometry of oligonucleotides

The major applications of mass spectrometry (MS) regarding ONs include the confirmation of the structure of synthesis products and the analysis of metabolites. The traditional methods, including liquid scintillation counting (LSC) and polyacrylamide gel electrophoresis (PAGE), used to study the pharmacokinetics of ONs,

require radioactive labels (Agrawal et al. 1991; Zhang et al. 1996). Somewhat more rapid and automatable techniques include high-pressure liquid chromatography (HPLC) (Bourque and Cohen 1993; Wallace et al. 1996) and capillary gel electrophoresis (CGE) (Leeds et al. 1996; Geary et al. 1997). Compared to these methods, MS has the advantage that the analysis is particularly specific and informative, in addition to being easy, rapid and reasonably sensitive. In MS, the mass-to-charge (m/z) ratio of the analyte is determined, precluding any ambiguities arising from the intrinsic nature of other methods, which detect *e.g.* radioactivity of the label or UV absorption. The main disadvantage is the requirement of appropriate pre-treatment of biological samples, especially in the case of electrospray ionization (ESI), to avoid damage to the instrument and excessive noise due to the matrix.

Ionization techniques. The MS analysis of ONs became possible when the soft ionization techniques, matrix-assisted laser desorption/ionization (MALDI) and ESI, were introduced in the 1990s (reviewed in Siuzdak 1994). In MALDI, the matrix-embedded sample is bombarded with a pulsed laser, and the spectra exhibit little or no fragmentation of the ON and singly charged ions as the major species. As MALDI produces uncomplicated spectra, it is frequently used for complex mixtures such as following enzymatic digestion (Gao et al. 2009) and for POCs synthesized by stepwise solid-phase synthesis (Grijalvo et al. 2010). In ESI, the analyte molecules are already ionized in solution, and they are brought to the gas phase by spraying the solution through a high-voltage capillary and facilitating the solvent evaporation with dry gas and/or heat, ultimately leading to the expulsion of the ions from the droplet (Siuzdak 1994). ESI is particularly suitable for the analysis of ONs, which are large, polar, thermally labile, and polyanionic in neutral to basic solutions because of the phosphate groups. As ESI is more straightforward and versatile for ON analysis than MALDI, this review mainly focuses on ESI applications.

Interpretation of electrospray ionization (ESI) spectra. The negative ion ESI spectra of ONs display a series of multiply deprotonated ions of the form $[M-nH]^{n-}$, the charge states typically ranging from 2 to 12 lost protons (Covey et al. 1988; Deroussent et al. 1995). An ESI-MS spectrum of a fluorescein-labeled PS-ON is shown in **Figure 9** as an illustrative example. The production of multiply charged ions enables the analysis of high-molecular-weight compounds with low mass range instruments; for example, an ion trap may have an upper m/z limit of only 2 kDa, which would preclude the analysis of usual size (15 to 25 bases) ONs if only singly charged ions were generated. The relative abundances of the charge states depend on the length of the ON but can be influenced by the choice of eluent; especially adding organic bases to the solution reduces the charge states (Muddiman et al. 1996; Griffey et al. 1997b). In addition, organic bases such as triethylamine (TEA), piperidine and imidazole reduce cation adduction by replacing the nonvolatile sodium or potassium ions with volatile adduct ions (Greig and Griffey 1995; Muddiman et al. 1996). Cation adduction can severely decrease the signal-to-noise ratio of ESI-MS spectra of ONs. Therefore, the preanalytical desalting of the sample is crucial, especially for PS-ONs which have a higher affinity for cations than unmodified ONs. Several strategies for the on-line desalting of ONs directly before

injecting to the ESI source have been proposed, *e.g.* microdialysis (Liu et al. 1996). The molecular weight (M) of the ON can be calculated with the formula

$$(1) \quad M = z \times (p + 1),$$

where z = the charge of the peak and p = the m/z ratio of the peak. Using two consecutive peaks in the spectrum, the charge of the second peak (z_2) can be calculated with the formula

$$(2) \quad Z_2 = \frac{p_1 + 1}{p_1 - p_2},$$

where p_1 = the m/z ratio of the first peak and p_2 = the m/z ratio of the second peak. The molecular weight can be reconstructed either manually or by deconvolution software. Mass accuracies of $\pm 0.01\%$ can be routinely achieved using ESI-MS (Siuzdak 1994).

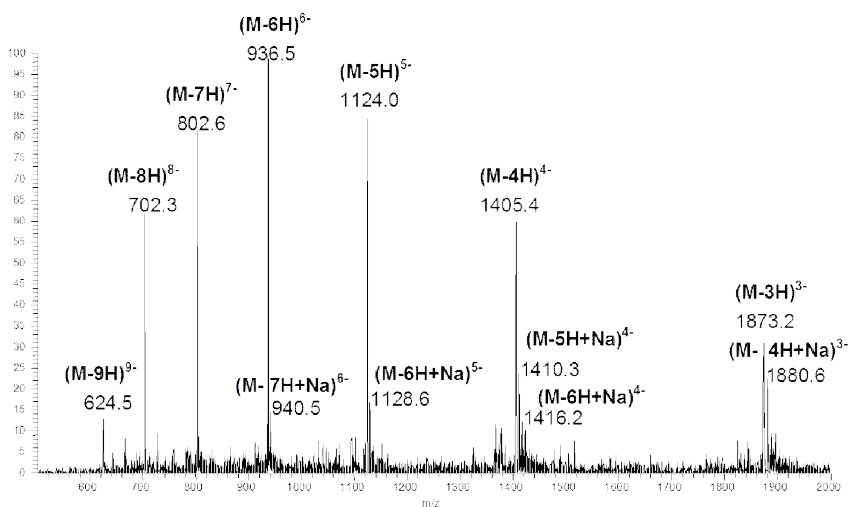


Figure 9 Negative ion ESI mass spectrum of a 5'-fluorescein-labeled phosphorothioate oligonucleotide (5'-TGG CGT CTT CCA TTT-3'; MW = 5624). Eluent: 25 mM triethylamine in 80% acetonitrile. [U. Tengvall, previously unpublished.]

Tandem MS. Apart from measuring the intact molecular ions, the ON sequence can be confirmed by tandem MS (MS^n ; n = the generation of the fragment ions). In MS^n , the molecular ion is fragmented due to collision-induced dissociation (CID), where a selected mother or precursor ion collides with a gas such as argon and dissociates into daughter or product ions (Siuzdak 1994). The MS^n of ONs produces a characteristic pattern of daughter ions, suitable for sequence confirmation (McLuckey and Habibi-Goudarzi 1993; Barry et al. 1995; Boschenok and Sheil 1996). The fragmentation pathways of modified ONs such as PS (Lotz et al. 1998), MP (Bartlett et al. 1996), and LNA ONs (Huang et al. 2010) have also been studied.

2.3.2 Liquid chromatography–mass spectrometry of oligonucleotides

The compatibility of ESI with aqueous solutions and relatively high flow rates has enabled the routine use of MS as a detector for HPLC (reviewed in Siuzdak 1994). Liquid chromatography–mass spectrometry (LC/MS) confers better sensitivity by reducing chemical background noise and facilitates the analysis of modified ONs (Bothner et al. 1995) or complex mixtures such as ON metabolites in biological samples (Gaus et al. 1997). The method of choice for ESI-LC/MS is ion-pair reversed-phase HPLC, employing an amphiphilic ion-pair reagent and a gradient of acetonitrile, methanol or 2-propanol. For ONs, the most commonly used ion-pair reagents are alkylamines such as TEA (Huber and Krajete 1999) or tripropylamine (TPA) (Gaus et al. 1997) with a suitable acid component, *e.g.* acetate (Graham et al. 2001) or bicarbonate (Huber and Krajete 1999). As an alternative ion-pair acid component, Apffel et al. (1997) introduced 1,1,1,3,3,3-hexafluoro-2-propanol (HFIP) adjusted to pH 7 with TEA, which proved to enhance both the chromatographic resolution and ESI sensitivity, one of which is usually compromised in LC/MS. HFIP was used successfully in the analysis of *in vivo* metabolites of PS-ONs (Griffey et al. 1997a). Beverly et al. (2005) used the HFIP-TEA ion-pairing buffer for the ESI-LC/MS of siRNA, and the intact duplex siRNA was preserved and separated from the single-stranded sense and antisense components. In contrast, in another study employing ESI-UPLC/MS with hexylamine acetate as ion-pairing reagent for the separation of siRNA from truncated duplexes, the siRNA duplexes did not fully survive the ionization process (McCarthy et al. 2009).

2.3.3 Mass spectrometry of peptide–oligonucleotide conjugates

In addition to the dominant method ESI, POCs can be characterized by negative ion MALDI-MS (Bruick et al. 1996; Zubin et al. 1999; Gogoi et al. 2007). In the early work, fast atom bombardment (FAB), the predecessor of MALDI, was used for the characterization of a small nucleopeptide (Robles et al. 1994). While FAB is limited to relatively small molecules, ESI enables the analysis of ONs more than 100 nucleotides long as well as of POCs (Potier et al. 1994; Robles et al. 1997). Soukchareun et al. (1995) used direct injection and LC/MS with ion spray to characterize PO-ONs coupled to HIV-1 gp41 fusion peptides. A more systematic study on the MS of POCs revealed that the behavior of the conjugates during MS is governed mainly by the ON part (Jensen et al. 1996). Comparing the two ionization methods, MALDI was found to be more sensitive and tolerant to sample impurities, while ESI exhibited better mass accuracy and resolution. ESI-MS and ESI-LC/MS were also used in our group to routinely characterize POCs (Antopolsky and Azhayevev 1999; Antopolsky et al. 1999; Antopolsky and Azhayevev 2000; Antopolsky et al. 2002). Recently, a method was developed for distinguishing peptide–ON cross-links from free peptides or ONs according to fractional mass differences by accurate mass LC/MSⁿ (Pourshahian and Limbach 2008).

3 AIMS OF THE STUDY

The general aim of the study was to improve the *in vitro* delivery of antisense oligonucleotides and siRNA with chemical modifications and nanocarriers. More specifically, the aims were:

- 1) to optimize various analytical methods for the characterization of oligonucleotides, including electrospray ionization mass spectrometry, liquid chromatography–mass spectrometry, pre-treatment for biological samples, and chromatographic separation of metabolites;
- 2) to enhance the enzymatic stability and target selectivity of oligonucleotide probes by circularization;
- 3) to enhance the cellular uptake and sequence-specific activity of antisense oligonucleotides by covalently conjugating them to cell-penetrating peptides;
- 4) to enhance the delivery and gene silencing effect of siRNA by complexing it with cationic cell-penetrating peptide-modified gold nanoparticles.

4 SUMMARY OF THE METHODS

The majority of the methods related to this thesis are of chemical nature. **Table 4** summarizes the methods, used in publications **I–IV**, related to this thesis. Briefly, the main methods were : *i*) the synthesis and purification of oligonucleotides (ONs), short interfering RNAs (siRNAs), and peptide-modified gold nanoparticles (GNPs); *ii*) the characterization of linear and circular ONs and peptide–ON conjugates by electrospray ionization mass spectrometry (ESI–MS) and liquid chromatography–mass spectrometry (LC/MS), and *iii*) of the GNPs by UV/VIS spectroscopy and transmission electron microscopy (TEM); *iv*) the enzymatic stability study; and *v*) effects of the GNPs on siRNA delivery and cell viability in SEAP-ARPE-19 cells.

Table 5. *Experimental and mathematical methods used in this thesis.*

Method	Target	Publ.
Synthesis		
Solid-phase DNA synthesis	Phosphodiester and phosphorothioate ONs	I–III
Disulfide cross-linking	Peptide–ON conjugates	I–II
	Circular ONs	III
Solid-phase RNA synthesis	Phosphodiester ribo ONs (siRNA)	IV
Reduction of gold salts	Peptide-modified GNPs	IV
Post-synthesis purification		
IE- and RP-HPLC, desalting	Phosphodiester and phosphorothioate ONs	I–III
by gel filtration or RP-SPE	Phosphodiester ribo ONs (siRNA)	IV
Dialysis	Peptide-modified GNPs	IV
Characterization		
UV/VIS spectroscopy	ONs (determination of concentration)	I–IV
	Peptide-modified GNPs	IV
ESI-MS, ESI-LC/MS	Various ONs and peptide–ON conjugates	I–III
TEM	Peptide-modified GNPs	IV
Stability study		
Sample pretreatment by IE- and RP-SPE, analysis by IE-HPLC	Metabolites of linear and circular phosphodiester and phosphorothioate ONs in biological media	III
Cell-culture methods		
SEAP production (SEAP assay)	Effect of peptide-modified GNPs on siRNA delivery	IV
Cell viability (MTT assay)	and cell viability in SEAP-ARPE-19 cells	IV
Mathematical methods		
ON concentration	Calculation of extinction coefficients of ONs	I–III
ON molecular weight (MW)	Calculation of accurate MWs of ONs for MS analysis	I–III
Spectra interpretation	Reconstruction of MW from the m/z ratios of MS peaks	I–III
Half-life ($t_{1/2}$)	Calculation of $t_{1/2}$ of ONs using semilogarithmic plots	III
GNP concentration	Calculation of the molar concentration of GNPs	IV

5 PEPTIDE–OLIGONUCLEOTIDE PHOSPHOROTHIOATE CONJUGATES WITH MEMBRANE TRANSLOCATION AND NUCLEAR LOCALIZATION PROPERTIES*

*Reprinted with permission from: Antopolsky M, Azhayeva E, Tengvall U, Auriola S, Jääskeläinen I, Rönkkö S, Honkakoski P, Urtti A, Lönnberg H, Azhayev A. 1999. Peptide–oligonucleotide phosphorothioate conjugates with membrane translocation and nuclear localization properties. *Bioconjugate Chem.* 10(4): 598–606. Copyright 1999 American Chemical Society.

Peptide-Oligonucleotide Phosphorothioate Conjugates with Membrane Translocation and Nuclear Localization Properties

Maxim Antopolsky,[†] Elena Azhayeveva,[†] Unni Tengvall,[†] Seppo Auriola,[†] Ilpo Jääskeläinen,[‡] Seppo Rönkkö,[‡] Paavo Honkakoski,[‡] Arto Urtti,[‡] Harri Lönnberg,[§] and Alex Azhayev*,[†]

Departments of Pharmaceutical Chemistry and Pharmaceutics, University of Kuopio, FIN-70211 Kuopio, Finland, and Department of Chemistry, University of Turku, FIN-20014 Turku, Finland. Received November 6, 1998; Revised Manuscript Received April 19, 1999

Eighteen peptide-oligonucleotide phosphorothioate conjugates were prepared in good yield and thoroughly characterized with electrospray ionization mass spectra. When applied to the living cells, conjugates exhibiting membrane translocation and nuclear localization properties displayed efficient intracellular penetration but failed to show any serious antisense effect. Studies on the intracellular distribution of the fluorescein-labeled conjugates revealed their trapping in endosomes.

INTRODUCTION

Synthetic peptides having membrane translocation properties and those possessing additionally nuclear localization properties have been found to be useful vectors for efficient internalization of oligonucleotides into living cells. These peptides and their polylysine derivatives have been shown to complex with oligonucleotides and hence serve as carriers for cytoplasmic or nuclear delivery (1, 2). Covalent oligonucleotide-peptide conjugates have also received considerable attention as new potential antisense agents exhibiting potentially enhanced cellular uptake (3-17). The preparation of such conjugates has been accomplished by various methodologies, based either on postsynthetic conjugation of oligonucleotides and peptides, both bearing appropriate reactive groups (3-8, 10, 11, 13, 14, 16, 17) or on solid-phase assembly (9, 12, 15). Most of these methods concern the synthesis of conjugates of natural phosphodiester oligonucleotides, and only few papers describe the preparation of oligonucleotide phosphorothioates linked to peptides. Lebleu and co-workers have synthesized a 25-mer peptide-oligo-dC phosphorothioate conjugate in a 53% coupling yield, assessed from the HPLC trace (8). However, neither the yield of the isolated product nor characterization of this conjugate were reported. Heitz et al. have recently reported on successful use of a carrier peptide-oligonucleotide phosphorothioate conjugate (POPC) in transfer of an antisense sequence into living cells (17). Unfortunately, no experimental details concerning the synthesis, isolation, and characterization of this interesting compound were given. Since most peptides used as carriers for oligonucleotides possess relatively long hydrophobic sequences, the properties of their conjugates (e.g. solubility, chromatographic behavior, etc.) appear to differ considerably from those of oligonucleotide phosphorothioates, which, in turn, possess some restrictions to the methods that may be applied to synthesis of POPCs. We believe that appropriate syn-

thetic procedures to obtain well-characterized POPCs are of considerable importance.

The present paper describes the synthesis of 18 POPCs. In these, the 3'-terminus of the oligonucleotide phosphorothioate is linked by a disulfide bond to the N- or C-terminus of either a 17-mer membrane permeable motif (MPM)—the hydrophobic region of signal peptide sequence of the Kaposi fibroblast growth factor, known to interact with lipid bilayers, or a 27-mer peptide (MPM-NLS), containing in addition to the above-mentioned MPM motif a nuclear localization sequence (NLS) of the transcription nuclear factor κ B (18). Furthermore, the cellular uptake and intracellular localization of fluorescein-labeled conjugates have been examined and inhibition of the luciferase gene expression in a cell-free model transcription-translation system and in living cells has been attempted.

EXPERIMENTAL PROCEDURES

Peptide Synthesis. Fmoc-L-amino acids for peptide synthesis were purchased from Bachem and Novabiochem. Peptides **P1** and **P2** were synthesized on Fmoc-rink amide PEGA resin, peptide **P3** on Fmoc-Cys(Trt)-NovaSynPA500 resin, and peptide **P4** on Fmoc-Pro-NovaSynPA500 (Scheme 2), all from Novabiochem. The pyridinium salt of 3-tritylthiopropionic acid was obtained by the standard tritylation procedure and finally crystallized (ether/hexane); mp 175-177 °C. ¹H NMR (CDCl₃): δ 7.43-7.19 (m, 15H, arom.), 2.45 (t, 2H, $J = 7.4$ Hz, -CH₂-), 2.33 (t, 2H, $J = 7.4$ Hz, -CH₂-). The synthesis of all peptides was performed by a solid-phase method on a Milligen 9050 synthesizer. Standard protocols based on Fmoc/HBTU/TEA chemistry were used. 3-Tritylthiopropionic acid was introduced to the N-terminus of two peptides (**P2**, **P4**) directly on a synthesizer (HBTU/TEA condensation).

Oligonucleotide Synthesis. The oligonucleotide phosphorothioates were prepared on a solid support, bearing a disulfide linker (19). 2'-Deoxyribonucleoside 3'-phosphoramidites, fast-sulfurizing reagent, and fluorescein phosphoramidite were products of Glen Research. The solid-phase synthesis was performed on a PE Applied Biosystems 392 DNA synthesizer on a 1 μ M scale.

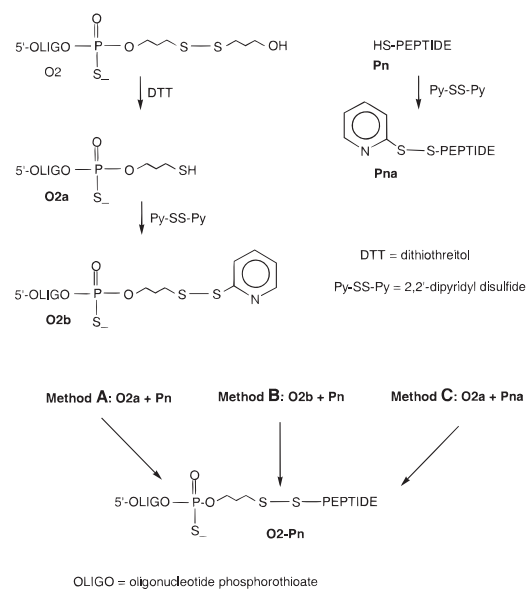
* To whom correspondence should be addressed. Phone: +358 17 162204. Fax: +358 17 162456. E-mail: Alex.Azhayev@uku.fi.

[†] Department of Pharmaceutical Chemistry.

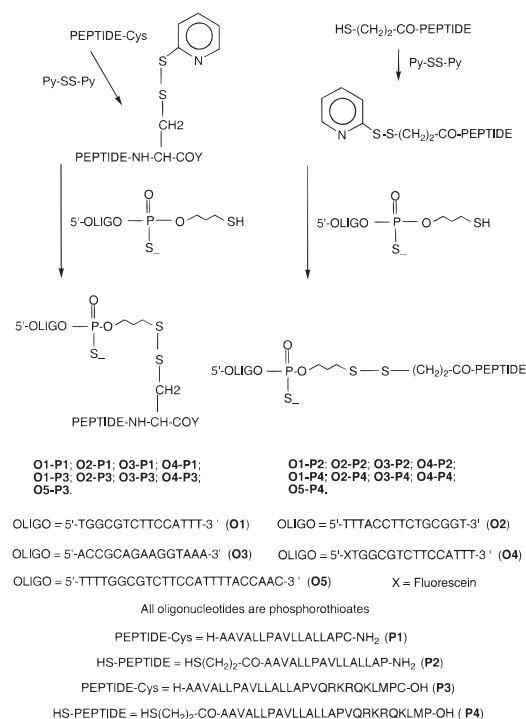
[‡] Department of Pharmaceutics.

[§] Department of Chemistry.

Scheme 1



Scheme 2



Cationic Lipid Formulations. Formulations with Cytfectin GS (Glen Research) were prepared following the manufacturer's procedure.

HPLC Techniques. The peptides and their 2-pyridylsulfide derivatives were analyzed and isolated by reversed-phase chromatography (RP) (column, Genesis C4, 300 Å, 4 μm, 4.0 × 150 mm, Jones Ltd.; buffer A, 0.05 M

triethylammonium acetate; buffer B, 0.05 M triethylammonium acetate in 80% MeCN; flow rate, 1.0 mL min⁻¹; a linear gradient from 40 to 100% B in 30 min was applied). The oligonucleotides containing disulfide tethers were analyzed and isolated by ion-exchange chromatography (IE) (column, PolyWax LP 300 Å, 4 μm, 4.6 × 100 mm, buffer A, 0.05 M KH₂PO₄ in 50% aqueous formamide, pH 6.7; buffer B, A + 1.5 M NaBr; flow rate, 1.0 mL min⁻¹; a linear gradient from 0 to 70% B in 30 min was applied) and RP [column, Genesis C18, 300 Å, 4 μm, 4.0 × 150 mm, Jones Ltd.; buffer A, 0.05 M triethylammonium acetate (TEAA); buffer B, 0.05 M TEAA in 80% MeCN; flow rate, 1.0 mL min⁻¹; a linear gradient from 0 to 50% B in 30 min was applied]. The conjugates were analyzed by IE as described for oligonucleotides. The final isolation and analysis of the conjugates were performed by RP HPLC similar to that described for oligonucleotides (a linear gradient from 0 to 100% B in 30 min was applied in this case).

Methods to Synthesize Disulfide Cross-Linked Conjugates. **Oligonucleotide O2a.** A 5% triethylamine (TEA) in ethanol (40 μL) was added to a solution of oligonucleotide O2 (20 OD) in 0.05 M TEAA buffer (1.5 mL). Dithiothreitol (3 mg) was then added, and the mixture was left for 3 h at rt and finally concentrated to a volume of 0.5 mL. The oligonucleotide bearing a free mercapto group was isolated by RP HPLC and used immediately.

Oligonucleotide O2b. Oligomer O2a (20 OD) in 0.05 M TEAA buffer (1.5 mL) was diluted with an equal volume of ethanol. 2,2'-Bis(dipyridyl)disulfide (3 mg) was then added, and the mixture was left to stand for 1 h at rt. The corresponding 2-pyridyl sulfide derivative O2b was then concentrated to a volume of 0.5 mL and separated from the excess of 2,2'-bis(dipyridyl)disulfide and other byproducts with RP.

Peptide P2a. Peptide (P2, 3 mg) was dissolved in a mixture of ethanol and formamide (1:1, 1 mL). 2,2'-Bis(dipyridyl)disulfide (5 mg) was then added to a solution and the mixture was left for 1 h at rt. The pyridyl sulfide derivative was purified by RP HPLC. The appropriate peak (1.5 mL) was collected and diluted with formamide to a volume of 30 mL, followed by addition of 5% TEA in ethanol (300 μL).

Method A. Oligomer O2a (2 OD) in 0.05 M TEAA buffer (0.15 mL) was added to a solution of peptide P2 (0.3 mg) in formamide-TEA (100:1, 3.03 mL) immediately after its separation. The mixture was kept overnight at rt and applied onto a DEAE-Toyopearl 650M column (10 × 80 mm, Br⁻), equilibrated with 50% formamide. The column was washed with 50% formamide (50 mL), and the conjugate was eluted with 1 M NaBr and 0.05 M potassium phosphate buffer in 50% formamide (pH 6.5). Crude conjugate was finally analyzed, purified by RP HPLC, and desalted.

Method B. Oligomer O2b (2 OD) in 0.05 M TEAA buffer (0.15 mL) was added to a solution of peptide P2 (0.3 mg) in formamide-TEA (100:1, 3.03 mL). The mixture was kept overnight at rt and the crude conjugate was analyzed and purified as in method A.

Method C. Oligomer O2a (2 OD) in 0.05 M TEAA buffer (0.15 mL) was added to a solution of peptide P2a (0.3 mg) in formamide-TEA (100:1, 3.03 mL). The mixture was kept overnight at rt and the crude conjugate was analyzed and purified as in method A.

Peptide-Oligonucleotide Phosphorothioate Conjugates. Each conjugate was synthesized according to method C, starting from 20 OD of initial oligonucleotide.

Electrospray Ionization Mass Spectrometry. Mass spectra were acquired using an LQC quadrupole ion trap mass spectrometer equipped with an electrospray ionization source (Finnigan MAT, San Jose, CA). The spray needle was set to -3 kV. The nitrogen sheath gas flow rate was set to 70. The stainless steel inlet capillary was heated to 200°C , and the capillary voltage was -39 V. The number of negative charges was maximized by calibrating the tube lens offset with a 15-mer oligonucleotide (data not shown). The value chosen was -10 V. The spectra were measured using 200 ms for collection of the ions in the trap, and 5–12 microscans were summed. The eluent consisted of 80% acetonitrile containing 25 mM TEA. The eluent flow rate was set to $10\ \mu\text{L}/\text{min}$, and 5 μL samples containing 1–20 pmol of conjugates were injected to the system. Positive ion mass spectra of the peptides were acquired by using 50% methanol as the eluent. The sample concentration was $10\ \mu\text{g}/\text{mL}$, and 5 μL was injected. The spray needle potential was set to 5 kV, capillary voltage 20 V, and tube lens 10 V. Other conditions were as in negative ion mode. The molecular weights of the compounds were calculated using computer program Gretas Carbos, created by Hines and Gibson (UCSF).

^{32}P -Labeling of Phosphorothioate Oligonucleotides and Oligonucleotide–Peptide Conjugates and Their Gel Electrophoresis. Oligonucleotides and conjugates were $5'$ - ^{32}P -labeled with T4 polynucleotide kinase (Pharmacia), purified on the OPS cartridge (PE-Applied Biosystems). A 15% PAGE was employed to analyze the oligonucleotides and conjugates.

Development of Stable Cell Lines Expressing Luciferase Activity. CHO-AA8-Luc cells expressing luciferase activity were purchased from Clontech Inc. (Palo Alto, CA). Stable cell lines expressing tetracycline-regulated luciferase mRNA and activity were developed by the method of Gossen and Bujard (20) according to the instructions and plasmids from Clontech Inc (Palo Alto, CA). Briefly, monkey kidney fibroblast CV1-P and human retinal pigmented epithelium D407 cell lines were transfected with pTet-Off with calcium phosphate transfection (21), and cells with stably integrated plasmid DNA were selected in the presence of 0.4 mg/mL G418 (Calbiochem, La Jolla, CA) and tested for the expression of tetracycline-sensitive regulator by transient transfection of pTRE-luc and pCMV-beta-galactosidase plasmids, culturing in the presence or absence of 2 mg/L tetracycline and luciferase assays. Those cell lines displaying tetracycline-repressible luciferase activity were expanded and transfected with pTRE-luc plus pTK-hyg plasmids. Cells with stably integrated luciferase cDNA were selected in the presence of both 0.4 mg/mL G418 and 0.1 mg/mL hygromycin B (Calbiochem) and screened again for tetracycline-repressible luciferase activity. This procedure yielded derivatives indistinguishable from their parent CV1-P and D407 with respect to cell morphology and growth characteristics. The CV1-P derivatives CV-11 and CV-19 and D407 derivative 6-2 were used in this study.

Uptake of ^{32}P -Labeled Oligonucleotides and Conjugates. CV1-P cells were plated in Dulbecco's modified Eagle's medium (DMEM, Gibco) with 10% fetal bovine serum (FBS, Gibco) in 96-well plates, 2×10^5 cells/well, and grown for 24 h in a humidified cell incubator with 5% CO_2 at 37°C . After washing the cells, medium was replaced with 180 μL of the serum-free medium containing a mixture of $5'$ -labeled (3.5×10^4 – 1.75×10^6 cpm) and unlabeled oligonucleotide or conjugate (0.1 – $5\ \mu\text{M}$). After 4 h of incubation at 37°C , cells were washed several

times with medium, phosphate buffer saline (PBS, Gibco), high salt-low pH buffer solution (0.4 M NaOAc, 1 M NaCl, pH 3.3), and finally with PBS (22, 23). The cells were solubilized in 1% sodium dodecyl sulfate (SDS, Sigma) solution and the radioactivity was measured in the same plates with Micro Beta counter (Wallac). Aliquots of 20 μL from each well were taken for protein measurement. Background estimation experiments were conducted in parallel in separate plates without cells, where the corresponding amounts of cold and labeled oligonucleotides or conjugates were added. Both protein content data and background estimation experiments were taken into consideration while presenting the results of cellular uptake experiments. The stability of the oligonucleotides and conjugates in the cellular uptake experiments was controlled by PAGE electrophoresis which did not reveal any substantial degradation of the compounds.

Antisense Activity of the Oligonucleotides and Oligonucleotide–Peptide Conjugates. The luciferase-expressing cells were plated in 24-well plates at a density of $(4$ – $5) \times 10^4$ cells/well and grown for 24 h to approximately 60–80% confluence. CV1-P cells were grown in DMEM with 10% of FBS, D 407 cells in DMEM with 5% of FBS, and CHO cells in α -modified Eagle's medium (α -MEM, Gibco) with 10% of FBS and medium before transfection was replaced by serum-free medium containing oligonucleotides, conjugates, or their Cytotectin GC formulation and incubated for 4 h. Cells were then grown in the normal medium for 12–20 h, washed with PBS, lysed, and tested for the luciferase activity as described earlier (24).

Luciferase Expression Assay. The influence of the compounds on the luciferase expression *in vitro* in the cell-free system was studied using TNT Coupled Wheat Germ Extract Systems kit (Promega) as described earlier (24).

RNase H Cleavage Experiments. Synthetic RNA fragment $5'$ -UACUGUUGGUA AAAAUGGAAGACGCCA-AAAACAUA-3' (M) was $5'$ labeled with ^{32}P using T4 polynucleotide kinase (Pharmacia). One picomole of labeled matrix was annealed to 1 pmol of oligonucleotides or conjugates by heating to 70°C and slowly decreasing the temperature to 25°C over 2 h. Annealed complexes were incubated with 1 unit of RNase H (USB–Amersham Pharmacia Biotech) in 20 mM Tris-HCl buffer, pH 7.5; containing 20 mM KCl, 10 mM MgCl_2 , 0.1 mM EDTA, and 0.1 mM cystamine for 30 min at 37°C . Products of the reaction were analyzed by 15% PAGE and subsequent autoradiography.

Confocal Fluorescence Microscopy. Luciferase-expressing cells were plated in glass Lab Tek 8-chamber slides (NUNC Inc.) at a density of $(6$ – $10) \times 10^4$ cells/well and cultured for 36 h. The culture medium was discarded and after washing replaced by the serum-free medium containing fluorescein-labeled oligonucleotides, oligonucleotide–peptide conjugates, or their Cytotectin GC formulation. Cells were incubated for 4 h and washed twice with the serum-free medium and three times with PBS. After washing, cells were fixed with 0.1% glutaric dialdehyde in PBS for 5 min, washed with PBS, and mounted in 90% glycerol in PBS. Cells were examined under the confocal laser scanning microscope (Leica).

RESULTS AND DISCUSSION

Comparison of Methods To Synthesize Disulfide Cross-Linked Peptide-Oligonucleotide Phosphorothioate Conjugates. It is obvious that the yield of any reaction leading to the disulfide cross-linked POPC strongly depends on the spatial structures of the peptide

and the oligonucleotide in question. To develop a method of cross-linking that is as independent as possible of the structures of the molecules to be linked together, the composition of the solvent mixture and concentrations of the reacting components were first optimized. A large number of preliminary experiments demonstrated that the best yields were obtained when the resulting conjugation mixture contained about 90% of a chaotropic solvent, formamide, the concentration of peptides being about 0.09 mg/mL and that of oligonucleotides about 0.6 OD/mL. In principle, there are at least three straightforward routes to generate a disulfide bond between an oligonucleotide phosphorothioate tethered with a linker, bearing a mercapto group, and a synthetic peptide also having a mercapto function. This function may reside either in peptide's C-terminal cysteine or in a mercaptopropionic acid residue, attached to the N-terminus. We have investigated the applicability of these possible alternative procedures by binding peptides **P1**–**P4** to oligonucleotide **O2**: method A, the reaction of a thiol containing peptide with an oligonucleotide bearing mercaptoalkyl group [analogous to the approach mentioned in the literature (17)]; method B, the reaction of a thiol containing peptide with an oligonucleotide possessing a pyridyl disulfide function, similar to procedure reported by Lebleu et al (8); and, finally, method C, the reaction of a pyridyl disulfide containing peptide with an oligonucleotide having a mercaptoalkyl group (Scheme 1).

The results of these experiments have demonstrated that the yield of isolated conjugate strongly depends on the method of coupling and the peptide's structure. Method A gave yields ranging from 0.4 to 23%. Testing of method B has also revealed relatively low yields from 7 to 24%. Method C, however, have demonstrated the highest yields, ranging from 36 to 88%.

An additional experiment, employing method C, was carried out in order to demonstrate the absence of coupling between the peptide, activated by a pyridyl disulfide function and the phosphorothioate groups of the oligonucleotide. In this experiment, a control oligonucleotide phosphorothioate had the same sequence as **O1**, but contained no 3'-mercaptoalkyl function. After 12 h at rt, IE HPLC has revealed no formation of any conjugated structure. Oligonucleotide phosphorothioate appeared to be intact. RP HPLC, in turn, has demonstrated the formation of only 3% of peptide dimer, with the rest of the activated peptide remaining stable in the reaction mixture.

Thus, method C appears to be the procedure of choice for preparation of the disulfide cross-linked peptide-oligonucleotide phosphorothioate conjugates.

Synthesis and Characterization of Peptide-Oligonucleotide Phosphorothioate Conjugates. Method C was employed to synthesize 18 POPCs (Scheme 2). In all of these conjugates, the oligonucleotide moiety is a 15-mer (**O1**–**O4**) or 25-mer (**O5**) phosphorothioate. The peptide moiety is either a modified 17-mer hydrophobic MPM (**P1**, **P2**) or a modified 27-mer sequence, containing the above-mentioned 17-mer sequence and a the basic 10-mer NLS (**P3**, **P4**). The disulfide bridge was formed between the 3'-ends of **O1**–**O5** oligonucleotides and either the C-termini (**P1**, **P3**) or N-termini (**P2**, **P4**) of peptides. The yields of conjugates synthesized were 35–60%, and purity, as assessed from RP HPLC was higher than 95%. The 15% denaturing PAGE (data not shown) revealed good purity for all conjugates synthesized. The migration rate of the conjugates of peptides **P1** and **P2** was about 0.73–0.75 times, and that of peptides **P3** and **P4** conjugates 0.63–0.65 times that of the parent oligo-

nucleotides. The final characterization of POPCs was achieved by electrospray ionization mass spectrometry (ESI-MS), which has proven to be a powerful method for the characterization of oligonucleotides (25, 26) as well as their peptide conjugates (27). In our study, the negative ion ESI mass spectra of the conjugates displayed a series of deprotonated molecules ($(M - nH)^{-}$ as major peaks, the charge states ranging from 4 to 9. Figure 1 demonstrates a typical ESI mass spectrum obtained after injection of 5 μ L of conjugate **O4**–**P3**. Mass deconvolution program can be used for reconstruction of the molecular weight of the conjugate using the m/z values of the multiply deprotonated molecules (Figure 2). The measured and theoretically calculated average molecular weights of compounds reported here were in excellent agreement. The difference between the calculated and measured molecular masses was always less than 3.1 mass units (0.05%).

Attempted Inhibition of Luciferase Gene Expression in Vivo in Living Cells by Peptide-Oligonucleotide Phosphorothioate Conjugates. The peptide moiety of conjugates reported here contains membrane translocation and nuclear localization motives which are supposed to assist the oligonucleotide in passing through the cell membrane and reaching the nucleus. The oligonucleotide moiety is expected to display its antisense effect in the cytoplasm and nucleus, inhibiting the target gene expression (28).

We have attempted to influence the luciferase gene expression in stably transfected CV1-P, CHO-AA8-Luc, or D-407 luciferase producing cells with our conjugates. As in **O1**, the oligonucleotide sequence in the tested conjugates **O1**–**Pn** was complementary to the initiation codon region of firefly luciferase mRNA and was reported earlier to work as an effective antisense compound (29). The rest of the conjugates were used as controls containing either a reversed (**O2**–**Pn**) or a sense (**O3**–**Pn**) stretches. More than 10 identical experiments were performed in which the influence of these compounds on the reporter gene expression was compared to the inhibition of expression by the cationic lipid formulation of **O1** or **O1**–**P3** with the Cytofectin GC. These experiments have demonstrated the inability of the conjugate **O1**–**P3** alone to display any serious antisense effect. We have obtained more or less similar results for conjugates **O1**–**P1**, **O1**–**P2**, and **O1**–**P4** and conjugates **O5**–**P3** and **O5**–**P4**, which contain a longer antisense oligonucleotide sequence **O5** in comparison to **O1**. It is noteworthy that a substantial inhibition of luciferase expression was observed in all experiments with the Cytofectin formulation of **O1** or **O1**–**P3**. It appears that unlike the case where cationic lipid formulation was used, our conjugates alone fail to display reproducible antisense action.

Nevertheless, it was still interesting to find out which part of these conjugates (oligonucleotide or peptide) failed to play the desired role.

Cellular Uptake Studies with 5'-[³²P]-Oligonucleotide Phosphorothioates and Peptide-5'-[³²P]-Oligonucleotide Phosphorothioate Conjugates. Our unsuccessful attempt to inhibit the luciferase gene expression in cells raised some points of substance. First, it was necessary to verify if any of our conjugates were taken up by these cells. If some conjugates entered living cells, then it would be interesting to find out whether they remain intact throughout our experiment. Figure 3 demonstrates a typical result of cellular uptake experiments. One can see a relatively strong association of conjugate **O2**–**P3** with CV1-P cells in comparison to conjugates **O2**–**P1** and **O2**–**P2** and oligonucleotide **O2**.

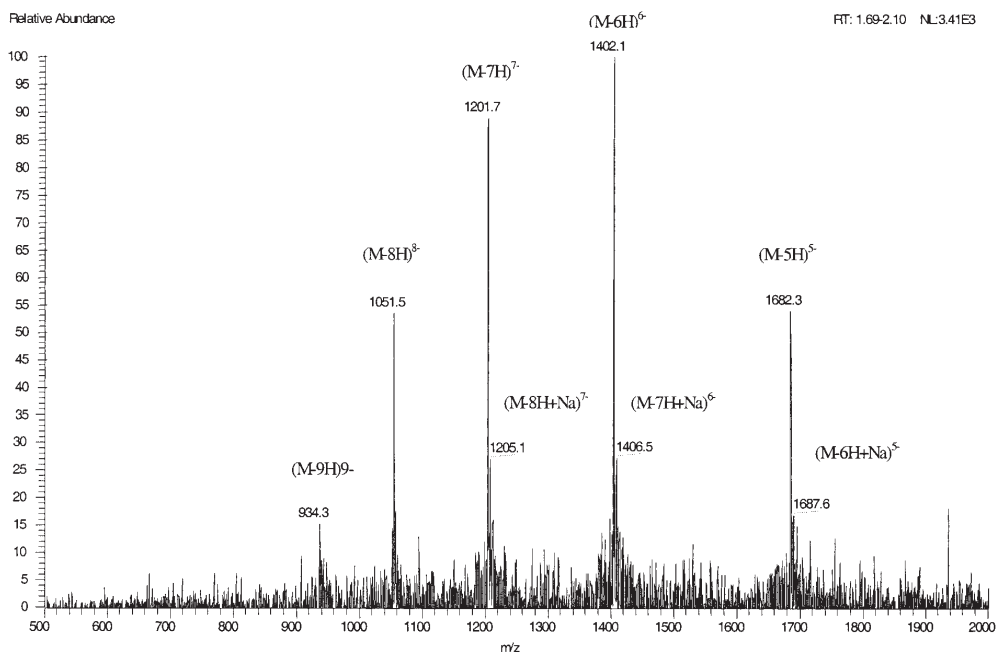


Figure 1. Negative ion ESI mass spectrum of conjugate **O4-P3**. The major multiply charged ions represent negative charge states from 5 to 9. Sample: 5 μ L of conjugate **O4-P3**. Eluent: 10 μ L/min of 80% acetonitrile with 25 mM triethylamine.

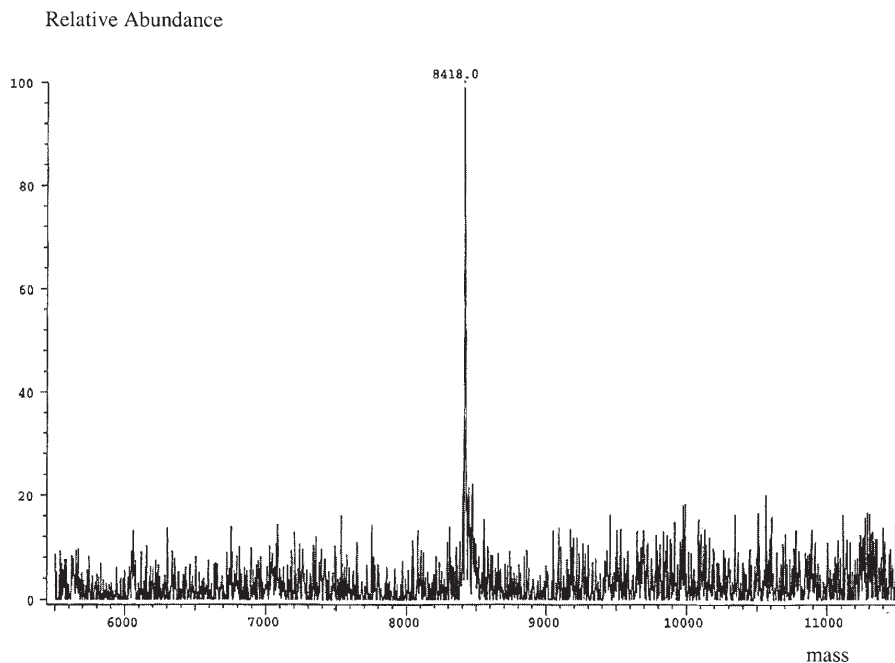


Figure 2. Reconstructed molecular weight spectrum of conjugate **O4-P3** (calculated mass 8418.1).

It is clear that the presence of the long 27-mer peptide with both membrane translocation and nuclear localization properties (**O2-P3**) is somehow responsible for this strong association, while the presence of mere membrane permeable motif (**O2-P1** and **O2-P2**) for some reason

retards association even as compared to oligonucleotide **O2**. This conclusion received additional support from the stability test. Figure 4 shows the autoradiography of PAGE of cell lysates after incubation with 32 P-labeled conjugates and careful washing—standard procedure,

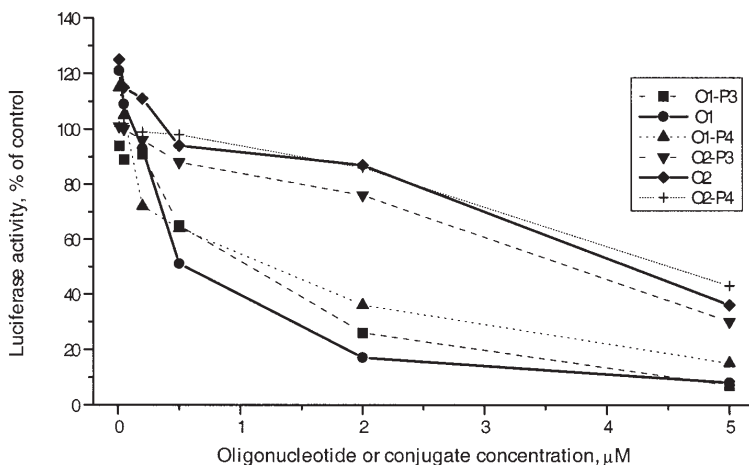


Figure 6. Influence of the antisense and control oligonucleotides and/or oligonucleotide-peptide conjugates on the luciferase reporter gene expression in cell-free system.

and **O1-P4** was noticeably smaller than that of **O1**. This fact may be attributed to the reduced binding affinity of oligonucleotide part of conjugates to the target RNA, when compared to that of oligonucleotide phosphorothioate **O1**.

As indicated above, our conjugates contained sequences complementary to the initiation codon region of the firefly luciferase mRNA, and therefore, it was reasonable to probe their antisense properties in a cell-free luciferase gene expression system which proved to be a rather useful tool in our previous studies (24). In fact, this type of experiment would mimic the testing with living cells better than the enzymatic assay with RNase H, and it would hence better elucidate the potency of our conjugates as antisense agents. Figure 6 shows that conjugates **O1-P3** or **O1-P4**, as well as oligonucleotide **O1**, all containing the antisense sequence, were able to decrease the luciferase activity by 60–80% at 2 μM concentration, while the control conjugates **O2-P3**, **O2-P4**, and control oligonucleotide **O2**, all containing reversed sequence, showed inhibition of only 10–20% under the same conditions. Hence, it became obvious that our conjugates are taken up by the cells and they are in principle capable of showing the antisense properties. Their failure to demonstrate these features in the experiments with cells should be attributed to their “incorrect” intracellular distribution, i.e., absence from the cytoplasm and/or nucleus, where they have to be present in order to display antisense properties.

Cellular Localization of Peptide-Oligonucleotide Phosphorothioate Conjugate. To gain insight into localization of our conjugates in cells, we treated CV1-P cells with 5'-fluorescein-labeled oligonucleotide **O4**, conjugate **O4-P3**, and finally with **O4-P3** as a cationic lipid formulation with the Cytofectin GC, and examined the cells with confocal microscopy. Figure 7A demonstrates that while most of the conjugate **O4-P3** associated with cells is localized in endosomes, there is only faint fluorescence in cytoplasm and nucleus. Even lower level of nuclear fluorescence was detected when CV1-P cells were incubated with oligonucleotide **O4** (Figure 7B) alone. The cytoplasmic fluorescence detected in this case was much weaker than with conjugate **O4-P3**, and it may in all likelihood be attributed to very low level of oligonucleotide phosphorothioate internalization. In con-

trast to that, when the conjugate **O4-P3** was employed as a cationic lipid formulation, a very strong fluorescence was found within the nucleus (Figure 7C), indicating a different type of intracellular distribution as compared to results with pure conjugate (Figure 7A). Taken together, the microscopy results clearly show that although our conjugates as such indeed possess a clear affinity to cells they are trapped in the endosomes unlike the liposomal formulation. Therefore, the access of POPCs to their target in cytoplasm and nucleus is limited.

CONCLUSION

We have optimized the preparation of disulfide cross-linked POPCs. According to our results, the most efficient procedure makes use of a disulfide exchange reaction between an oligonucleotide phosphorothioate tethered with a mercaptoalkyl group and a peptide bearing a pyridyl disulfide function in 90% formamide. Eighteen compounds were prepared in a yield of 35–60% and thoroughly characterized by electrospray ionization mass spectroscopy.

The present work demonstrates that our POPCs are capable of inhibiting the luciferase gene expression in a cell-free model transcription-translation system. When applied to the living cells, some of conjugates with MPM-NLS peptide display the efficient intracellular penetration properties but fail to show any serious antisense effect. Studies on the intracellular distribution of the fluorescein-labeled conjugates have revealed their endosomal localization, thus indicating a failure to reach the cytoplasm and/or nucleus and hence to produce the antisense effect. On the contrary, when used as a cationic lipid formulation with the Cytofectin GC, our conjugates achieved effective and selective antisense inhibition of the reporter gene expression. All these data taken together brings over the conclusion that the structure of the conjugates of oligonucleotide phosphorothioates with peptides, exhibiting membrane translocation and nuclear localization properties, yet has to contain some additional feature to avoid endosomal trapping. It appears that mere conjugation of antisense oligonucleotides and peptides possessing membrane penetration and nuclear localization properties does not necessarily result in a reliable delivery system which works well with a number of cell types. However, the chemical methodology devel-

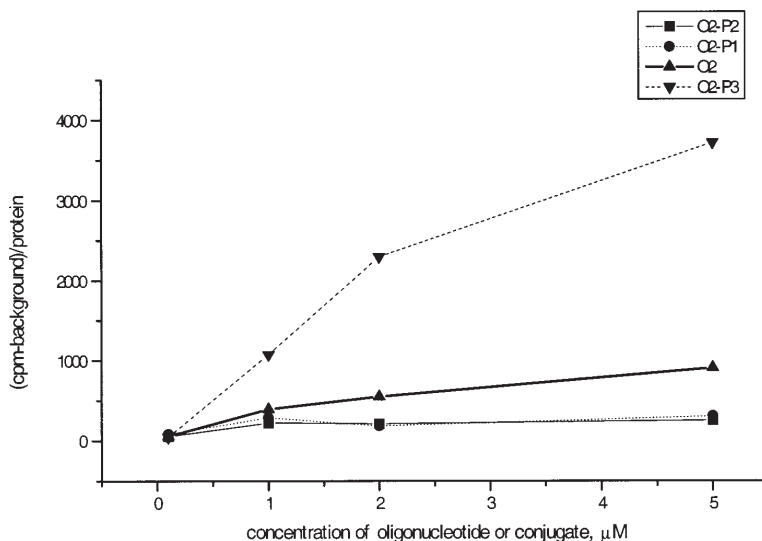


Figure 3. Uptake of the ^{32}P -labeled oligonucleotide and oligonucleotide-peptide conjugates by CV1-P cells. Dependence of cell associated radioactivity on the concentration of ^{32}P -labeled oligonucleotides and oligonucleotide-peptide conjugates in the incubation mixture. Cells were incubated with control substances for 4 h, washed and lysed as described in Experimental Procedures.

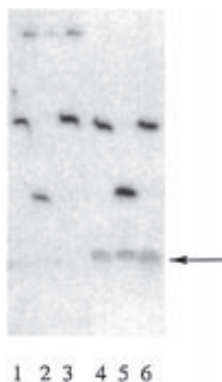


Figure 4. Stability of the oligonucleotide-peptide conjugates in the cells. Autoradiogram of 15% PAAG electrophoresis of the cell lysates and control ^{32}P -labeled conjugates: lines 1-3—cells incubated with mixtures of 5 μM unlabeled and 1.75×10^6 cpm of ^{32}P -labeled **O1-P3**, **O1-P1**, or **O2-P3** respectively; lines 4-6— ^{32}P -labeled **O1-P3**, **O1-P1**, or **O2-P3**. The migration position of **O1** is indicated with arrow.

removing the noninternalized conjugates and dead cells, capable of accumulating labeled compounds (22, 23). Very little if any degradation was detected, demonstrating sufficient stability of the peptide-oligonucleotide phosphorothioate conjugates throughout our experiments with cells.

RNase H Mediated Cleavage of Synthetic RNA-Conjugate Complexes and Inhibition of Luciferase Gene Expression in an in Vitro Transcription-Translation System. The next question was whether our conjugates were capable of triggering the RNase H mediated cleavage of the target RNA. The answer to this question appears to be of significant importance since this type of mRNA degradation is believed to be the most common mechanism of the antisense action (30). To investigate this subject, we synthesized a 34-mer oligori-

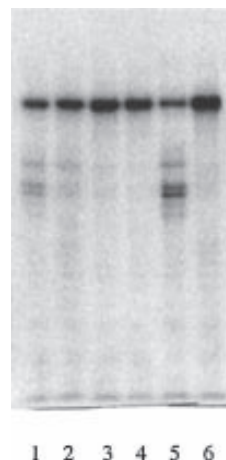


Figure 5. RNase H digestion of $^{[32]\text{P}}\text{M}$ in the presence of oligonucleotides and conjugates: line 1—in the presence of **O1-P3**; line 2—in the presence of **O1-P4**; line 3—in the presence of **O3-P3**; line 4—in the presence of **O3-P4**; line 5—in the presence of **O1**; line 6— $^{[32]\text{P}}\text{M}$.

bonucleotide (**M**), corresponding to the -13 to +21 fragment of the luciferase mRNA. This RNA fragment was 5'- ^{32}P -labeled and subjected to the action of RNase H in the presence of oligonucleotide **O1** and conjugate **O1-P3** or **O1-P4**, all containing the 15-mer complementary sequence. Conjugates **O3-P3** and **O3-P4** containing the sense sequences were used as controls. The autoradiography of PAGE referring to these experiments is shown in Figure 5. One can see that while conjugates **O1-P3** or **O1-P4**, as well as oligonucleotide **O1**, clearly triggered the RNase H activity (Figure 5, lines 1, 2, and 5), control conjugates **O3-P3** and **O3-P4** were unable to recruit the enzyme for the RNA fragment digestion (Figure 5, lines 3 and 4). The observed effect of **O1-P3**

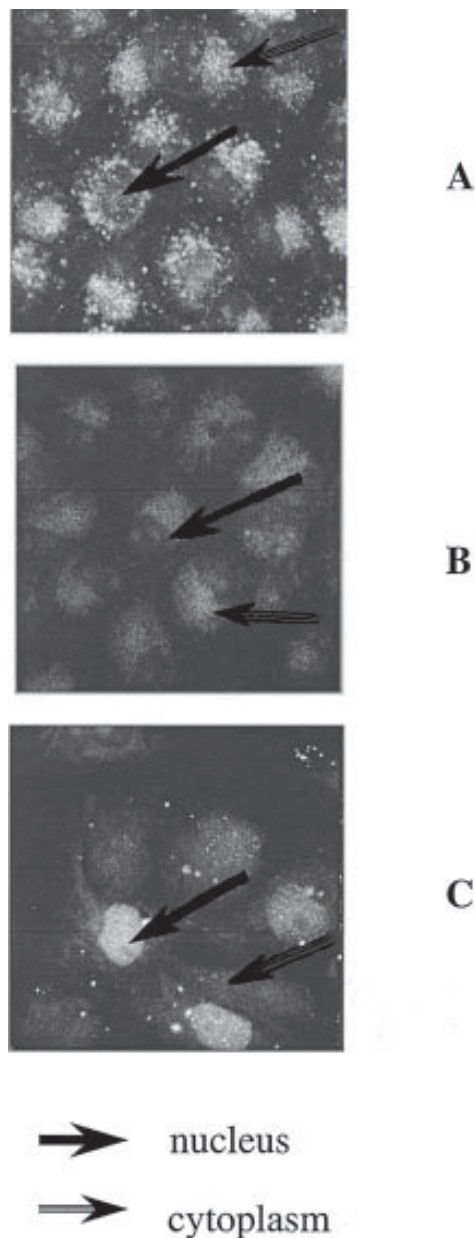


Figure 7. Confocal microscopy pictures of CV1-P cells after 4 h incubation with the fluoresceine-labeled antisense oligonucleotide and antisense oligonucleotide-peptide conjugate. Cells were incubated with (A) 0.5 μ M of O4-P3, (B) 0.5 μ M O4, (C) 0.5 μ M O4-P3 in the presence of 2.5 μ g/mL of cytofectin.

oped by us allows conjugation of oligonucleotides also to peptide sequences enhancing endosomal escape and hence antisense activity.

ACKNOWLEDGMENT

Financial support from the Ministry of Education and Technology Development Center of Finland is gratefully acknowledged.

LITERATURE CITED

- (1) Dokka, S., Toledo-Velasquez, D., Shi, X., Wang, L., and Rojanasakul, Y. (1997) Cellular delivery of oligonucleotides by synthetic import peptide carrier. *Pharm. Res.* *14*, 1759-1764.
- (2) Morris, M. C., Vidal, P., Chaloin, L., Heitz, F., and Divita, G. A. (1997) New peptide vector for efficient delivery of oligonucleotides into mammalian cells. *Nucleic Acids Res.* *25*, 2730-2736.
- (3) Eritja, R., Pons, A., Escarceller, M., Giralt, E., and Albericio, F. (1991) Synthesis of defined peptide-oligonucleotides hybrids containing a nuclear transport signal sequence. *Tetrahedron* *47*, 4113-4120.
- (4) Tung, C.-H., Rudolph, M. J., and Stein, S. (1991) Preparation of oligonucleotide-peptide conjugates. *Bioconjugate Chem.* *2*, 464-465.
- (5) Zhu, T., and Stein, S. (1994) Preparation of vitamin B₆-conjugated peptides at the amino terminus and of vitamin B₆-peptide-oligonucleotide conjugates. *Bioconjugate Chem.* *5*, 312-315.
- (6) Wei, Z., Tung, C.-H., Zhu, T., and Stein, S. (1994) Synthesis of oligoarginine-oligonucleotide conjugates and oligoarginine-bridged oligonucleotide pairs. *Bioconjugate Chem.* *5*, 468-474.
- (7) Edge, N. J., Tregear, G. W., and Haralambidis, J. (1994) Routine preparation of thiol oligonucleotides: application to the synthesis of oligonucleotide-peptide hybrids. *Bioconjugate Chem.* *5*, 373-378.
- (8) Bongartz, J.-P., Aubertin, A.-M., Milhaud, P. G., and Leblue, B. (1994) Improved biological activity of antisense oligonucleotides conjugated to a fusogenic peptide. *Nucleic Acids Res.* *22*, 4681-4688.
- (9) Robles, J., Pedroso, E., and Grandas, A. (1994) Stepwise solid-phase synthesis of the nucleopeptide Phac-Phe-Val-Ser-(p³ACT)-Gly-OH. *J. Org. Chem.* *59*, 2482-2486.
- (10) Soukchareun, S., Tregear, G. W., and Haralambidis, J. (1995) Preparation and characterization of antisense oligonucleotide-peptide hybrids containing viral fusion peptides. *Bioconjugate Chem.* *6*, 43-53.
- (11) Tung, C.-H., Wang, J., Leibowitz, M., and Stein, S. (1995) Dual-specificity interaction of HIV-1 TAR RNA with Tat peptide-oligonucleotide conjugates. *Bioconjugate Chem.* *6*, 292-295.
- (12) Robles, J., Pedroso, E., and Grandas, A. (1995) Solid-phase synthesis of a nucleopeptide from the linking site of adenovirus-2 nucleoprotein. -Ser(p³CATCAT)-Gly-Asp-. Convergent versus stepwise strategy. *Nucleic Acids Res.* *23*, 4151-4161.
- (13) Truffert, J.-C., Asseline, U., Brack, A., and Thuong, N. T. (1996) Synthesis, purification and characterization of two peptide-oligonucleotide conjugates as potential artificial nucleases. *Tetrahedron* *53*, 3005-3016.
- (14) Bruick, R. K., Dawson, P. E., Kent, S. B. H., Usman, N., and Joyce, G. F. (1996) Template-directed ligation of peptides to oligonucleotides. *Chem. Biol.* *3*, 49-56.
- (15) Robles, J., Maseda, M., Concernau, M., Pedroso, E., and Grandas, A. (1997) Synthesis and enzymatic stability of phosphodiester-linked peptide-oligonucleotide hybrids. *Bioconjugate Chem.* *8*, 785-788.
- (16) Rajur, S. B., Roth, C. M., Morgan, J. R., and Yarmush, M. L. (1997) Covalent protein-oligonucleotide conjugates for efficient delivery of antisense molecules. *Bioconjugate Chem.* *8*, 935-940.
- (17) Chaloin, L., Vidal, P., Lory, P., Mery, J., Lautredou, N., Divita, G., and Heitz, F. (1998) Design of carrier peptide-oligonucleotide conjugates with rapid membrane translocation and nuclear localization properties. *Biochem. Biophys. Res. Commun.* *243*, 601-608.
- (18) Lin, Y.-Z., Yao, S., Veach, R. A., Torgerso, T. R., and Hawiger, J. (1995) Inhibition of nuclear translocation of transcription factor NF- κ B by a synthetic peptide containing a cell membrane-permeable motif and nuclear localization sequence. *J. Biol. Chem.* *270*, 14255-14258.
- (19) Azhayeva, E., Azhayev, A., Guzaev, A., Hovinen, J., and Lönnberg, H. (1995) Looped oligonucleotides form stable

PEPTIDE-OLIGONUCLEOTIDE PHOSPHOROTHIOATE CONJUGATES WITH MEMBRANE
TRANSLOCATION AND NUCLEAR LOCALIZATION PROPERTIES*

606 *Bioconjugate Chem.*, Vol. 10, No. 4, 1999

Antopolsky et al.

- hybrid complexes with a single-stranded DNA. *Nucleic Acids Res.* 25, 4954–4961.
- (20) Gossen, M., and Bujard, H. (1992) Tight control of gene expression in mammalian cells by tetracycline responsive promoters. *Proc. Natl. Acad. Sci. U.S.A.* 89, 5547–5551.
- (21) Chen, C., and Okayama, H. (1987) High-efficiency transfection of mammalian cells by plasmid DNA. *Mol. Cell Biol.* 7, 2745–2752.
- (22) Basu, S., and Wickstrom, E. (1997) Synthesis and characterization of peptide nucleic acid conjugated to a D-peptide analogue of insulin-like growth factor 1 for increased cellular uptake. *Bioconjugate Chem* 8, 481–488.
- (23) Gray, G. D., Basu, S., and Wickstrom, E. (1997) Transformed and immortalized cellular uptake of oligonucleotide phosphorothioate conjugates, 3'-alkylamino oligonucleotides, 2'-O-methyl oligoribonucleotides, oligodeoxynucleotide methylphosphonates and peptide nucleic acids. *Biochem. Pharmacol.* 48, 1465–1476.
- (24) Azhayeva, E., Azhayev, A., Auriola, S., Tengvall, U., Urtili, A., and Lönnberg, H. (1997) Inhibitory properties of double helix forming circular oligonucleotides. *Nucleic Acids Res.* 25, 4954–4961.
- (25) Barry, J., Vouros P., Van Schepdael, A., and Law, S.-J. Mass and sequence verification of modified oligonucleotides using electrospray tandem mass spectrometry. (1995) *J. Mass Spectrom.* 30, 993–1006.
- (26) Bothner, B., Chatham, K., Sarkisian, M., and Siuzdak, G. (1995) Liquid chromatography mass spectrometry of antisense oligonucleotides. *Bioorg. Med. Chem. Lett.* 5, 2863–2868.
- (27) Jensen, O., Kulkarni, S., Aldrich, J., and Barofsky, D. (1996) Characterization of peptide-oligonucleotide heteroconjugates by mass spectrometry. *Nucleic Acids Res.* 24, 3866–3872.
- (28) Marcusson, E. G., Bhat, B., Manohoran, M., Bennett, C. F., and Dean, N. M. (1998) Phosphorothioate oligodeoxyribonucleotides dissociate from cationic lipids before entering the nucleus. *Nucleic Acids Res.* 26, 2016–2023.
- (29) Stull, R. A., Zon, G., and Szoka, F. C. (1996) An *in vitro* messenger RNA binding assay as tool for identifying hybridization-competent antisense oligonucleotides. *Antisense Nucleic Acid Drug Dev.* 6, 221–228.
- (30) Toulme, J.-J. (1992) Artificial regulation of gene expression by complementary oligonucleotides-an overview. In *Antisense RNA and DNA* (J. A. H. Murray, Ed.) pp 175–194, Wiley-Liss, Inc., New York.

BC980133Y

7 SELECTIVE CIRCULAR OLIGONUCLEOTIDE PROBES IMPROVE DETECTION OF POINT MUTATIONS IN DNA*

Abstract

The synthesis of disulfide-cross-linked circular oligonucleotides, employing two different approaches, was accomplished. Several circular oligomers, which bear a C(5)-aminoalkyl-tethered thymidine unit, were labeled with photoluminescent europium(III) chelates. All circular structures were thoroughly characterized with denaturing PAGE and electrospray ionization mass spectrometry. It was demonstrated that the disulfide cross-linking, resulting in circularization, considerably increases the enzymatic stability of phosphodiester oligonucleotides in biological media. In addition, UV melting experiments, followed, where possible, by extraction of thermodynamic parameters, revealed that several circular oligomers appear to be more selective towards their complementary targets than their corresponding linear precursors. Finally, the mixed-phase hybridization experiments have demonstrated that use of circular probes indeed improves the selectivity in the detection of DNA point mutations.

* Adapted from: Tennilä T, Ketomäki K, Penttinen P, Tengvall U, Azhayeva E, Auriola S, Lönnberg H, Azhayev A. 2004. Selective circular oligonucleotide probes improve detection of point mutations in DNA. *Chem Biodivers.* 1(4): 609–625. Reprinted with kind permission from John Wiley & Sons, Inc.



Available online at www.sciencedirect.com

SCIENCE @ DIRECT®

Journal of Pharmaceutical and Biomedical Analysis
32 (2003) 581–590

JOURNAL OF
PHARMACEUTICAL
AND BIOMEDICAL
ANALYSIS

www.elsevier.com/locate/jpba

Characterization of antisense oligonucleotide–peptide conjugates with negative ionization electrospray mass spectrometry and liquid chromatography–mass spectrometry

Unni Tengvall^a, Seppo Auriola^{a,*}, Maxim Antopolsky^a, Alex Azhayev^a,
Leo Biegelman^b

^a Department of Pharmaceutical Chemistry, University of Kuopio, P.O. Box 1627, FIN-70211 Kuopio, Finland

^b Ribozyme Pharmaceuticals Inc., 2950 Wilderness Place, Boulder, CO 80301, USA

Received 24 April 2002; received in revised form 4 November 2002; accepted 7 November 2002

Abstract

Covalent post-synthesis or solid-phase conjugation of peptides to oligonucleotides has been reported as a possible method of delivering antisense oligonucleotides into cells. While synthesis strategies for preparing these conjugates have been widely addressed, few detailed reports on their structural characterization have been published. This paper discusses the negative ion electrospray ionization mass spectrometric (ESI-MS) and liquid chromatography–mass spectrometric (LC–MS) analysis of various peptide–oligonucleotide conjugates ranging from small T₆-nucleopeptides to large peptide–oligonucleotide phosphorothioate conjugates and ribozyme–peptide hybrids (3–13 kDa). Molecular weight determination with mass errors of 0.1–3.1 amu were conducted, employing on-line IP-RP-HPLC and high *m/z* range mode to facilitate the analysis of large compounds and difficult modifications.

© 2003 Elsevier Science B.V. All rights reserved.

Keywords: Antisense oligonucleotides; Oligonucleotide–peptide conjugates; MS; LC–MS

1. Introduction

Antisense oligonucleotides are new potential drugs showing promise for the treatment of viral infections and cancer [1,2]. Their systemic therapeutic use is, however, hindered by their poor cellular uptake and inability to reach the nucleus.

Oligonucleotides have been found to be taken into cells by endocytosis, after which they remain entrapped in endosomal compartments [3]. Several strategies have been introduced to overcome this problem, including the attachment of lipophilic or cell receptor-binding molecules to oligonucleotides [4]. Peptides possessing various beneficial properties have been seen as a possible method of delivery [5]. Several studies have employed hydrophobic peptide sequences known to penetrate cellular membranes [6,7], nuclear localization sequences [8], or both of them combined [5,9]. Many

* Corresponding author. Tel.: +358-17-16-2469; fax: +358-17-16-2456.

E-mail address: seppo.auriola@uku.fi (S. Auriola).

Table 1
Oligonucleotide sequences

Name	Sequence
SAS1	5'-TGG CGT CTT CCA TTT-3'
LSAS1	5'-TTT TGG CGT CTT CCA TTT TAC CAA C-3'
SC1	5'-TTT ACC TTC TGC GGT-3'
SC2	5'-ACC GCA GAA GGT AAA-3'
Rz ^a	5'-g _s c _s a _s g _s ug gcc gaa agg Cga gUg aGG uCu agc uca B-3'

SAS1 and LSAS1, antisense inhibitors of firefly luciferase mRNA; SC1, reversed control; SC2, sense control; Rz, ribozyme "zinzyme".

^a Lower case, 2'-OMe; C, 2'-amino-C; U, c-allyl-U; G, ribo G; B, inverted abasic; s, phosphorothioate linkages.

of the conjugates have indeed exhibited enhanced cellular delivery and accumulation in the nucleus [6,9]. In addition, 3'-conjugation seems to stabilize phosphodiester oligonucleotides against nucleases [10], and no adverse effect on duplex formation has been observed [8,11]. The use of noncovalently complexed peptide–oligonucleotide hybrids has been reported [6,10], but the main interest has lately been on covalently attached conjugates. They can be synthesized either by post-synthetic coupling of pre-purified peptides and oligonucleotides [9,12] or by stepwise solid phase synthesis without intermediate purifications [11,13,14], the latter being more convenient for routine applications because of its speed and easiness.

Electrospray ionization mass spectrometric (ESI-MS) analysis of peptides and, increasingly,

of oligonucleotides can be considered a routine method. A number of peptide–oligonucleotide conjugates have been characterized by MALDI-MS [15,16], ion spray MS [11] or ESI-MS [7,9,13,14,17]. However, very few detailed articles can be found on the mass spectrometry of peptide–oligonucleotide conjugates. The successful ESI-MS of peptide–oligothymidylates has been reported on a triple–quadrupole system, including attempts to sequence these conjugates by tandem-MS [18].

In this study, negative ionization ion trap ESI-MS and LC-MS were used to characterize several peptide–oligonucleotide conjugates synthesized either by post-synthetic conjugation (convergent synthesis) or direct solid-phase assembly (stepwise synthesis).

2. Experimental

2.1. Reagents and chemicals

DNA synthesis reagents were obtained from Glen Research, except 2,6-lutidine (99%) and *N*-methylimidazole (99+%, redistilled) which were from Aldrich. The Fmoc-L-amino acids and resins for peptide synthesis were purchased from Bachem and Novabiochem. 2,2'-Bis-dipyridyl disulfide (98%, Aldrithiol™) and threo-1,4-dimercapto-2,3-butandiol (1,4-dithio-D,L-threitol; 98%) were from

Table 2
Peptide sequences

Name	Sequence
MPMc	H-AAVALLPAVLLALLAPC-NH ₂
MPMn	HS-(CH ₂) ₂ -CO-AAVALLPAVLLALLAP-NH ₂
NLS _c	H-VQRKRQKLMPC-OH
NLS _n	HS-(CH ₂) ₂ -CO-VQRKRQKLMPC-OH
MPM-NLS _c	H-AAVALLPAVLLALLAPVQRKRQKLMPC-OH
MPM-NLS _n	HS-(CH ₂) ₂ -CO-AAVALLPAVLLALLAPVQRKRQKLMPC-OH
TAT	H-GRKKRRQRRRPPQC-OH
ANT	H-RQIKIWFQNRRMKWKKC-OH

MPM, membrane permeable motif (hydrophobic region of a signal peptide sequence of the Kaposi fibroblast growth factor); NLS, nuclear localization sequence of transcription nuclear factor *kB*; TAT, truncated HIV-1 Tat protein basic domain; ANT, 43–58 homeodomain of *pAntennapedia*; c, thiol group at C-terminus; n, thiol group at N-terminus.

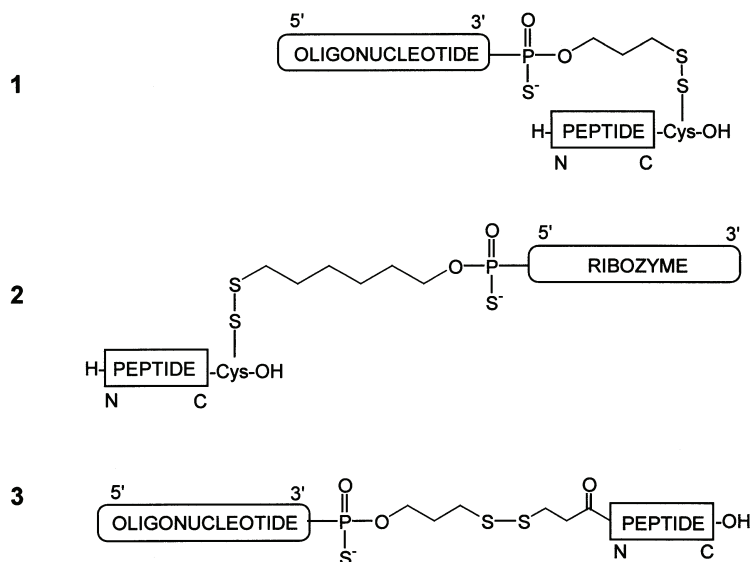


Fig. 1. Structures of the conjugates prepared by convergent synthesis: linked via (1) peptide C-terminus and oligonucleotide 3'-terminus, (2) peptide C-terminus and ribozyme 5'-terminus or (3) peptide N-terminus and oligonucleotide 3'-terminus.

Aldrich. Acetonitrile (ACN) and other solvents were HPLC grade.

LC-MS eluents containing triethylammonium acetate (TEAA) and dimethylhexylammonium formate (DMHA-F) were prepared by adjusting the pH of 25 mM triethylamine (TEA; puriss. p.a., for HPLC, >99.5%, Fluka) to 7 with acetic acid or by adjusting the pH of 20 mM *N,N*-dimethylhexylamine (DMHA; 98%, Aldrich) to 7 with formic acid. The pH was adjusted before adding ACN to any eluents. The eluents containing 1,1,1,3,3,3-hexafluoro-2-propanol (HFIP; puriss. p.a., for GC, ≥99.8%, Fluka) were prepared as described earlier [19].

2.2. Synthesis

2.2.1. Convergent synthesis

The oligonucleotides were synthesized on an Applied Biosystems 392 DNA/RNA synthesizer using standard methods, as described earlier [20], introducing a masked mercapto function at the 3'-

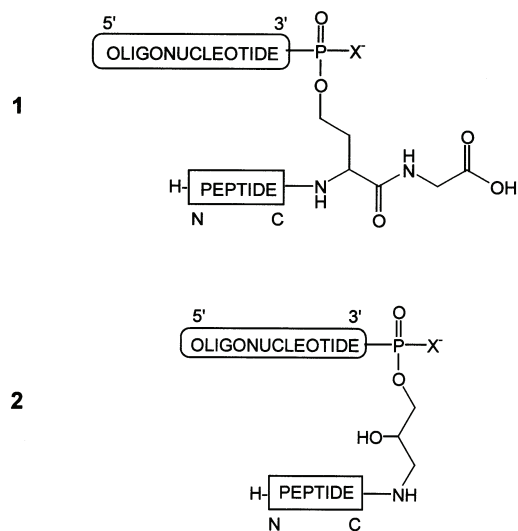


Fig. 2. Structures of the conjugates prepared by stepwise synthesis: (1) HseGly-linker, (2) APD-linker. X = O (phosphodiester T_δ) or S (phosphorothioate SAS1).

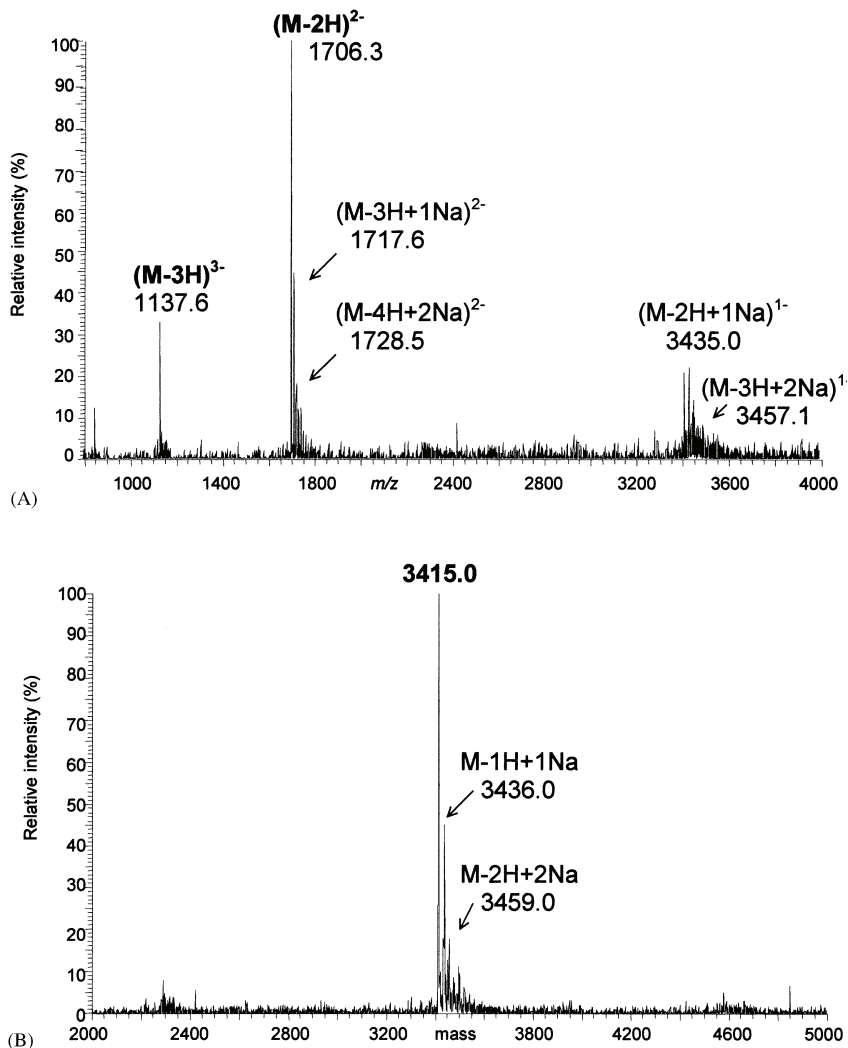


Fig. 3. Full scan (A) and reconstructed (B) negative ion ESI mass spectra of conjugate T_6 -(APD)-MPM (calculated MW 3412.2). Direct injection in 25 mM TEA/80% ACN.

terminus of each oligonucleotide. The sequences included 15- and 25-mer antisense inhibitors of firefly luciferase mRNA and 15-mer reversed and sense control sequences (Table 1). The 15-mer antisense oligonucleotide was also fluorescently labeled at the 5'-terminus by using fluorescein phosphoramidite during synthesis. In addition to

these, a 34-mer ribozyme bearing a C6-thiol linker at the 5'-terminus, synthesized at RPI (Ribozyme Pharmaceuticals, Inc.), was used for conjugation.

The peptides were synthesized on a Milligen 9050 peptide synthesizer, using Fmoc/HBTU/TEA chemistry [9]. The peptide sequences ranged from 10 to 27 amino acids and included a K-FGF

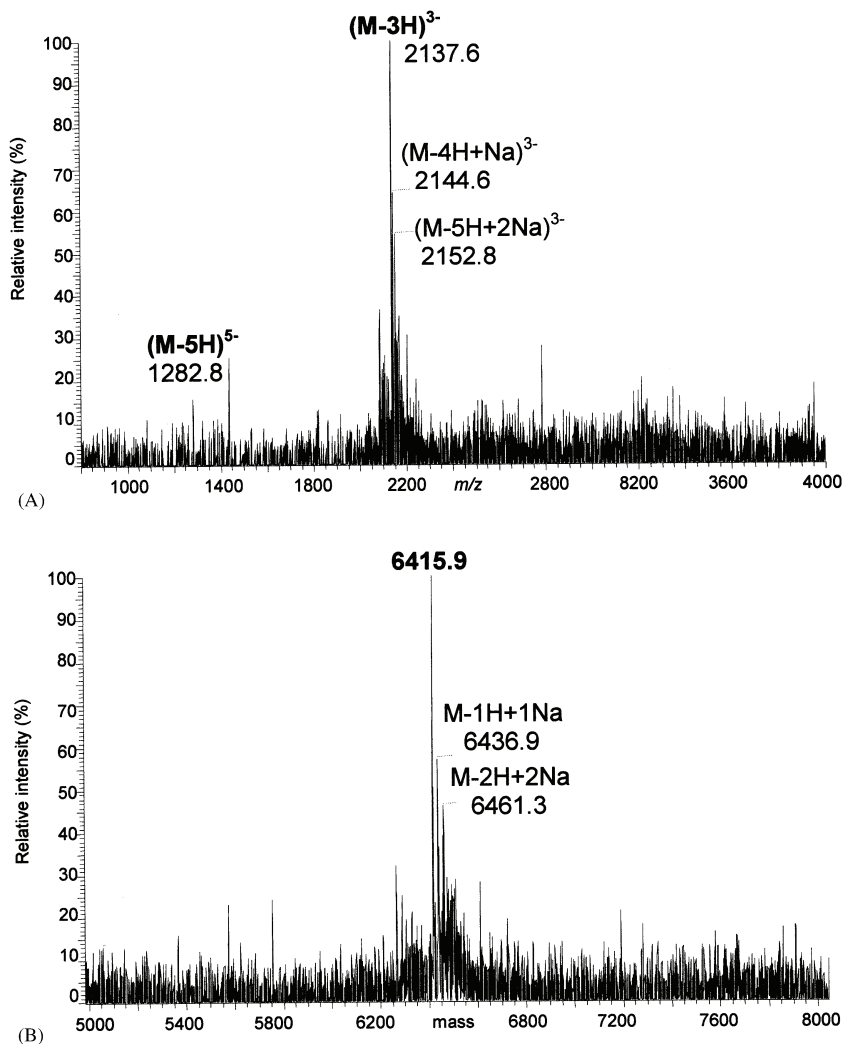


Fig. 4. Full scan (A) and reconstructed (B) negative ion ESI mass spectra of conjugate SASI-(APD)-MPM (calculated MW 6414.9). Direct injection in 25 mM TEA/80% ACN.

membrane permeable motif, NF- κ B nuclear localization signal, HIV-1 Tat basic domain and *Antennapedia* homeodomain (Table 2). 3-Tri-tylthiopropionic acid was attached to the N-termini of some of the peptides directly on the synthesizer.

The peptide–oligonucleotide conjugates were prepared by activating the free thiol group of the peptide with bis-2,2'-dipyridyl disulfide and reacting it with the free thiol group of the oligonucleotide. The masked thiol function of the oligonucleotide was first released by reducing it

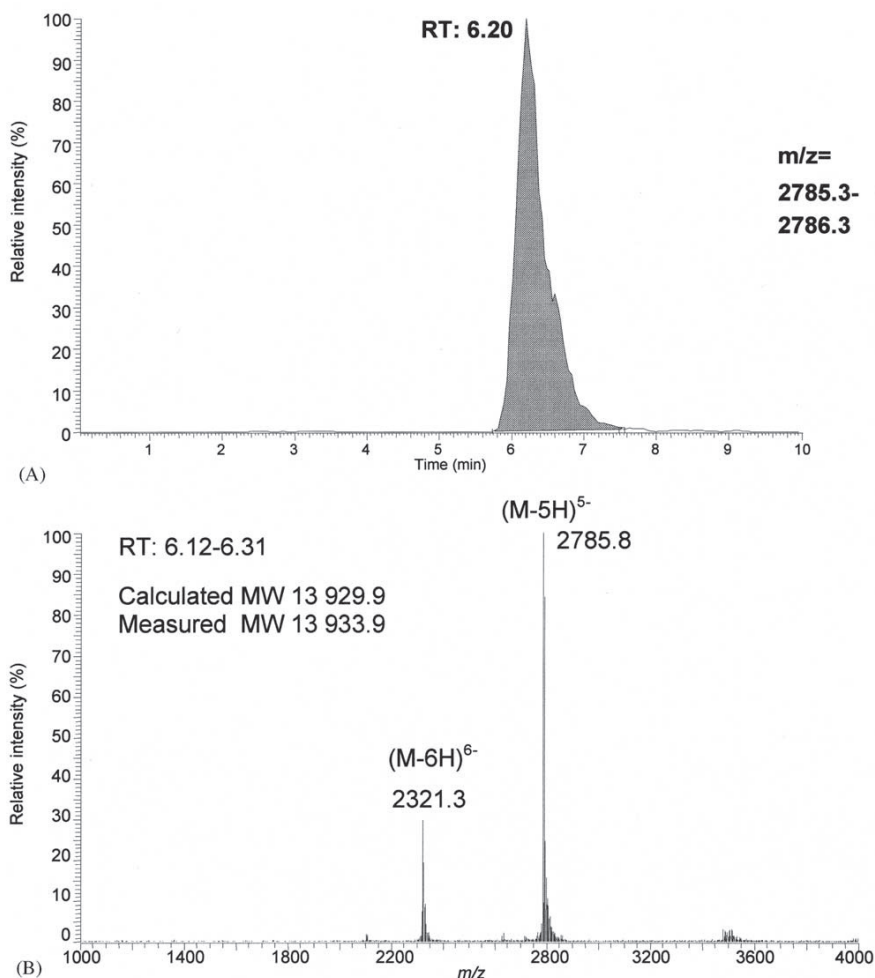


Fig. 5. Selected ion chromatogram (A) and full scan negative ion ESI mass spectrum (B) of ribozyme conjugate Rz-ANT. Injection of 30 pmol, (A), TEAA (pH 7; 25 mM), (B) TEAA (pH 7; 25 mM) in 75% ACN, gradient: 5–100% B, 5+1 min, 100 μ l/min, Luna C18 column (50 \times 2 mm i.d., Phenomenex).

with dithiothreitol [9]. The general structures of the conjugates are shown in Fig. 1.

2.2.2. Stepwise synthesis

In the stepwise solid-phase synthesis, the peptide MPM (see Table 2) was first assembled with the synthesizer mentioned above, employing standard Fmoc/TBTU/TEA chemistry and a solid support

bearing either a homoserine–glycine (HseGly) or 3-aminopropan-1,2-diol (APD) linker [17]. The oligonucleotide part, which was either phosphodiester T₆ or phosphorothioate SAS1 (see Table 1), was then synthesized with the synthesizer mentioned above, cleaved and deprotected using standard protocols. The general structures of the conjugates are shown in Fig. 2.

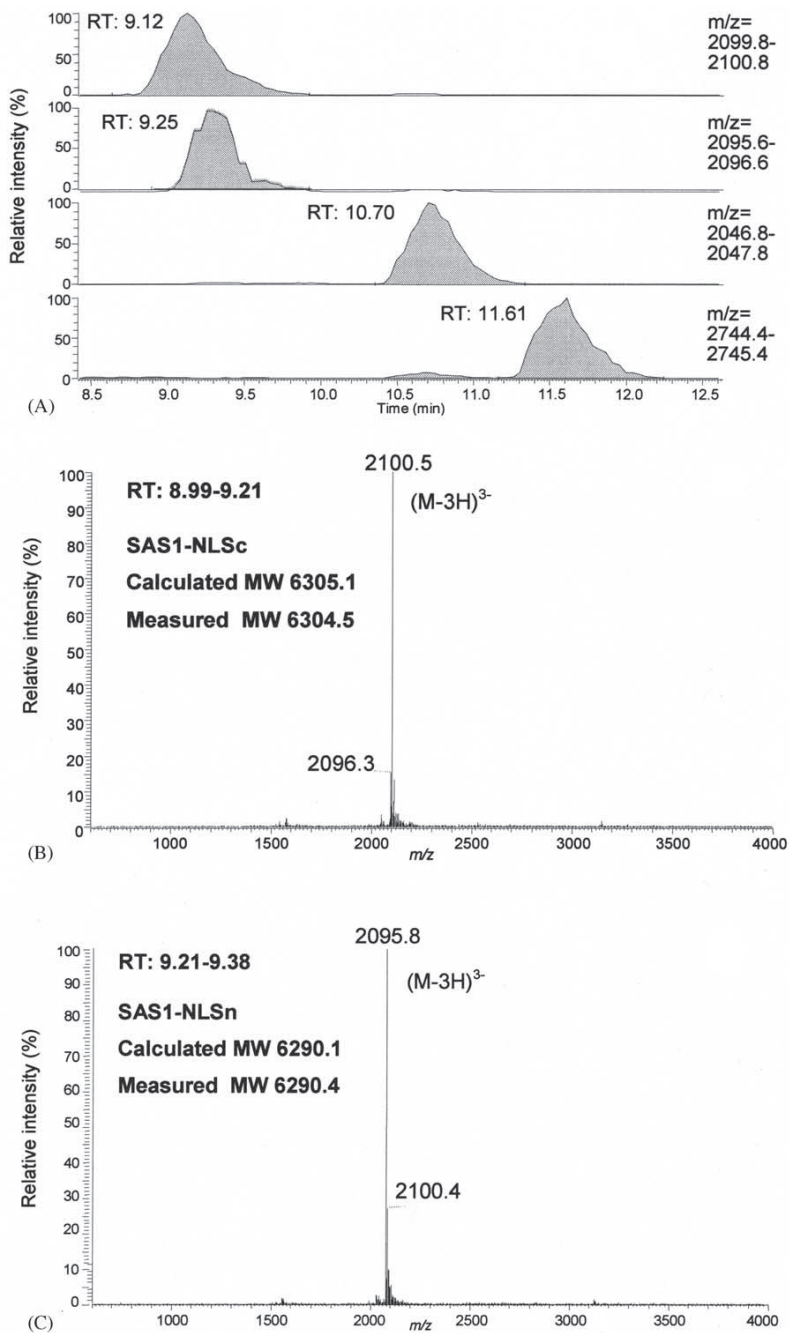
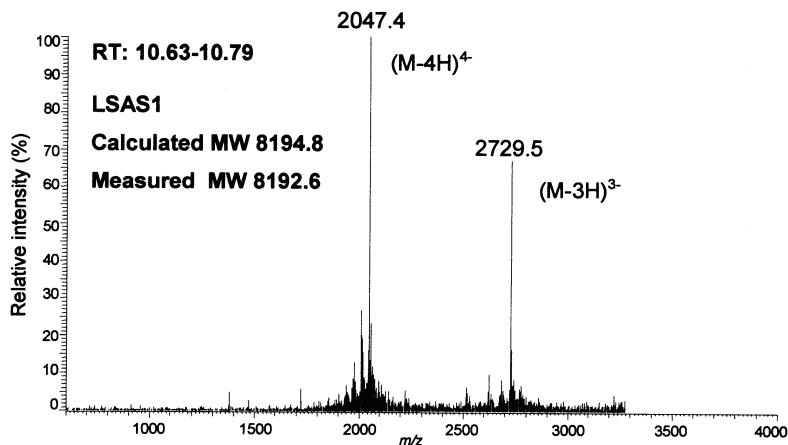
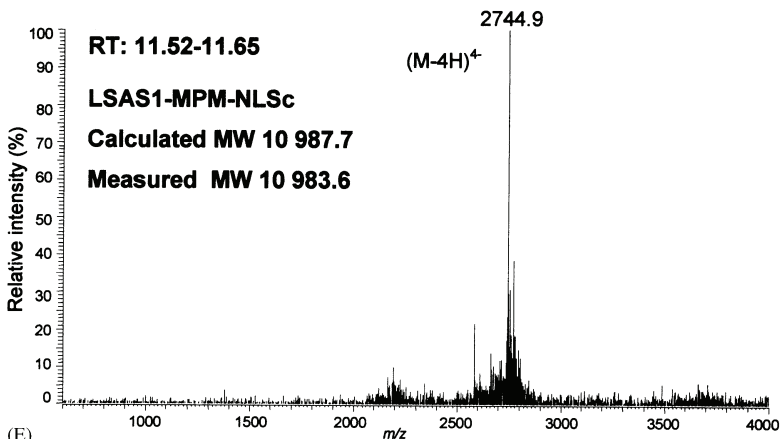


Fig. 6. Selected ion chromatograms (A) and full scan negative ion ESI mass spectra (B–E) of short conjugates SAS1-NLSc and SAS1-NLSn, long oligonucleotide LSAS1 and long conjugate LSAS1-MPM-NLSc, respectively. Injection of 20 pmol each, (A) DMHA-F (pH 7; 20 mM), (B) 90% ACN, gradient: 10–80% B, 20+3 min, 100 μ l/min, Genesis C4 column (50 \times 2 mm i.d.).



(D)



(E)

Fig. 6 (Continued)

2.3. ESI-MS

The conjugates were analyzed on an LCQ quadrupole ion trap ESI mass spectrometer (Finnigan MAT, San Jose, CA) in the negative ion mode. The compounds were diluted to 10–30 μM for direct injection and 1–10 μM for LC-MS analysis. Some of the measurements were done in the high mass-to-charge (m/z) range mode which

facilitates the analysis of large compounds by enabling the detection of lower charge states up to m/z 4000.

Most of the conjugates were analyzed using direct 5 μl injections to the mass spectrometer, the eluent consisting of 25 mM TEA in 80% ACN. The eluent flow rate was 5–10 $\mu\text{l}/\text{min}$. The spray needle was set to -3 kV, the nitrogen sheath gas flow rate to 70 and the tube lens offset to -10 V

Table 3
Measured and calculated molecular weights of conjugates

Conjugate	Calculated	Measured	Error (amu)
SAS1-MPMc	6536.4	6533.3	3.1
SAS1-MPMn	6521.4	6519.7	1.7
SAS1-NLSc ^{a,b}	6305.1	6304.5	0.6
SAS1-NLSn ^{a,b}	6290.1	6289.3	0.8
SAS1-MPM-NLSc	7803.0	7800.5	2.5
SAS1-MPM-NLSn	7788.0	7787.3	0.7
SAS1-TAT	6740.2	6739.0	1.2
SAS1-ANT ^{a,b}	7268.0	7268.1	0.1
FL-SAS1-MPMc	7151.5	7151.7	0.2
FL-SAS1-MPMn	7138.5	7137.2	1.3
FL-SAS1-MPM-NLSc	8418.1	8418.0	0.1
FL-SAS1-MPM-NLSn	8405.1	8403.2	1.9
LSAS1-MPM-NLSc ^{a,b}	10 987.7	10 986.5	1.2
LSAS1-MPM-NLSn	10 974.7	10 973.3	1.4
SC1-MPMc	6536.4	6534.5	1.9
SC1-MPMn	6521.4	6518.6	2.8
SC1-MPM-NLSc	7803.0	7801.8	1.2
SC1-MPM-NLSn	7788.0	7787.7	0.3
SC2-MPMc	6630.5	6627.5	3.0
SC2-MPMn	6615.5	6613.9	1.6
SC2-NLSc	6399.2	6398.5	0.7
SC2-NLSn	6384.2	6383.3	0.9
SC2-MPM-NLSc	7897.1	7896.9	0.2
SC2-MPM-NLSn	7881.5	7880.7	0.8
SC2-TAT	6833.4	6834.8	1.4
Rz-ANT ^{a,b}	13 929.9	13 933.9	0.4
T ₆ -HseGly-MPM ^{a,b,c}	3497.3	3498.0	0.7
T ₆ -(APD)-MPM ^{a,b,c}	3412.2	3413.8	1.6
SAS1-HseGly-MPM ^{a,b,c}	6500.0	6499.5	0.5
SAS1-(APD)-MPM ^{a,b,c}	6414.9	6415.9	1.0

^a Measured using the high m/z range mode.

^b Measured with LC–MS.

^c Prepared by stepwise solid-phase synthesis.

(–30 V for high m/z range). The stainless-steel inlet capillary was heated to 200 °C, and the capillary voltage was –39 V. The spectra were measured using 200 ms for collection of the ions in the trap, and 5–12 microscans were summed.

The LC–MS measurements were done in similar conditions, using narrowbore LC columns and flow rates of 100–200 $\mu\text{l}/\text{min}$. Typically, a 50 \times 2 mm C18 column was used with a gradient of 10–90% ACN or methanol and 15–25 mM TEAA or DMHA-F as the ion-pair reagent.

The mass spectra were deconvoluted, i.e. the molecular weights of the compounds were reconstructed from the spectra, either manually using

the formula $z_2 = (m/z_1 + 1)/(m/z_1 - m/z_2)$ or with computer programs (e.g. BIOMASS deconvolution).

3. Results and discussion

As reported earlier, the behavior of oligonucleotide–peptide conjugates in ESI-MS is mainly due to their oligonucleotide portion and negative ionization is suitable for their analysis, especially when the oligonucleotide contributes more to the conjugate mass than does the peptide [18]. As is the case for oligonucleotides, the mass spectra obtained here show a series of multiply deprotonated ions ($M - n\text{H}$)^{*n*–} as major ions [21]. The charge states range from 2 to 12 lost protons, depending on the size of the molecule, on the MS conditions during analysis and on the eluent used [22]. Some sodium adduct ions are also seen after direct injection ESI-MS of conjugates, although the samples were desalted and the eluent contained organic base. As can be seen from the spectra in Figs. 3 and 4, the degree of cation adduction increases with the length of the oligonucleotide and is more extensive with phosphorothioates than with phosphodiesteres [23].

The background noise is, however, significantly reduced by the use of LC–MS. The high m/z range further increases the signal-to-noise (S/N) ratio; it is especially useful when analyzing molecules larger than 10 kDa which often produce uninterpretable spectra below m/z 2000 (Fig. 5). Using LC–MS, a fair resolution of relatively similar compounds can be obtained. As can be seen from Fig. 6(A–C), the almost identical conjugates SAS1-NLSc and SAS1-NLSn are not completely resolved—the chromatogram peaks overlap and peaks corresponding to both compounds are seen on the spectra. Nevertheless, the spectra obtained are more than adequate for simple molecular weight confirmation. The longer oligonucleotide and its conjugate are well resolved (Fig. 6(D–E)). LC–MS eluents used for oligonucleotides contain organic bases such as TEA, tripropylamine (TPA) or diisopropylethylamine (DIPEA), while the acid component of the ion pair reagent is usually acetic acid, formic acid or carbonic acid [24–26]. Some

papers report also the advantages of using HFIP with TEA and a methanol gradient [19,27]. It was found during this study that at least TEAA and DMHA-F with ACN gradients seem to work well for the LC-MS of peptide-oligonucleotide conjugates (Figs. 5 and 6).

Altogether, 30 conjugates were successfully characterized. The measured molecular weights correlated well with the calculated values, the error being 3.1 amu or less in all cases (Table 3). While the ESI-MS of oligonucleotide-peptide conjugates is generally as straight-forward as that of oligonucleotides, some difficult modifications remain that cause problems during analysis. These include conjugates where the peptide part contains a large number of arginine and lysine residues which can bind various salts irreversibly during HPLC purifications, thus severely complicating the spectra, and conjugates assembled by stepwise solid-phase synthesis where no intermediate purifications are used to remove side products, yielding complex mixtures analyzable by HPLC but showing no MS peaks corresponding to the right mass. Hence, some synthesis products were encountered during this work which could not be successfully measured with the current MS methods (data not shown). Fortunately there were very few of these compounds, and the methods described here can be used as an efficient and rapid way to characterize novel peptide-oligonucleotide conjugates in most cases.

References

- [1] S.T. Crooke, *Annu. Rev. Pharmacol. Toxicol.* 32 (1992) 329–376.
- [2] C.F. Bennett, *Biochem. Pharmacol.* 55 (1998) 9–19.
- [3] J.F. Milligan, M.D. Matteucci, J.C. Martin, *J. Med. Chem.* 36 (1993) 1923–1937.
- [4] C.A. Stein, Y.-C. Cheng, *Science* 261 (1993) 1004–1012.
- [5] L. Chaloin, P. Vidal, P. Lory, J. Méry, N. Lautredou, G. Divita, F. Heitz, *Biochem. Biophys. Res. Commun.* 243 (1998) 601–608.
- [6] S. Dokka, D. Toledo-Velasquez, X. Shi, L. Wang, Y. Rojanasakul, *Pharm. Res.* 14 (1997) 1759–1764.
- [7] M. Antopolsky, A. Azhayev, *Tetrahedron Lett.* 41 (2000) 9113–9117.
- [8] R. Eritja, A. Pons, M. Escarceller, E. Giralt, F. Albericio, *Tetrahedron* 47 (1991) 4113–4120.
- [9] M. Antopolsky, E. Azhayeva, U. Tengvall, S. Auriola, I. Jääskeläinen, S. Rönkkö, P. Honkakoski, A. Urtili, H. Lönnberg, A. Azhayev, *Bioconj. Chem.* 10 (1999) 598–606.
- [10] M.C. Morris, P. Vidal, L. Chaloin, F. Heitz, G. Divita, *Nucleic Acids Res.* 25 (1997) 2730–2736.
- [11] S. Soukchareun, G.W. Tregear, J. Haralambidis, *Bioconj. Chem.* 6 (1995) 43–53.
- [12] N.J. Ede, G.W. Tregear, J. Haralambidis, *Bioconj. Chem.* 5 (1994) 373–378.
- [13] J. Robles, M. Maseda, M. Beltrán, M. Concernau, E. Pedroso, A. Grandas, *Bioconj. Chem.* 8 (1997) 785–788.
- [14] M. Antopolsky, E. Azhayeva, U. Tengvall, A. Azhayev, *Tetrahedron Lett.* 43 (2002) 527–530.
- [15] R.K. Bruick, P.E. Dawson, S.B.H. Kent, N. Usman, G.F. Joyce, *Chem. Biol.* 3 (1996) 49–56.
- [16] E.M. Zubin, E.A. Romanova, E.M. Volkov, V.N. Tashlitsky, G.A. Korshunova, Z.A. Shabarova, T.S. Oretskaya, *FEBS Lett.* 456 (1999) 59–62.
- [17] M. Antopolsky, A. Azhayev, *Helv. Chim. Acta* 82 (1999) 2130–2140.
- [18] O.N. Jensen, S. Kulkarni, J.V. Aldrich, D.F. Barofsky, *Nucleic Acids Res.* 24 (1996) 3866–3872.
- [19] A. Apffel, J.A. Chakel, S. Fischer, K. Lichtenwalter, W.S. Hancock, *J. Chromatogr. A* 777 (1997) 3–21.
- [20] E. Azhayeva, A. Azhayev, A. Guzaev, J. Hovinen, H. Lönnberg, *Nucleic Acids Res.* 25 (1995) 4954–4961.
- [21] C.R. Iden, R.A. Rieger, M.C. Torres, L.B. Martin, in: A.P. Snyder (Ed.), *Biochemical and Biotechnological Applications of Electrospray Ionization Mass Spectrometry*, American Chemical Society, Washington DC, 1995, pp. 281–293.
- [22] R.H. Griffey, H. Sasmor, M.J. Greig, *J. Am. Soc. Mass Spectrom.* 8 (1997) 155–160.
- [23] M. Greig, R.H. Griffey, *Rapid Commun. Mass Spectrom.* 9 (1995) 97–102.
- [24] C.G. Huber, A. Krajete, *Anal. Chem.* 71 (1999) 3730–3739.
- [25] H.J. Gaus, S.R. Owens, M. Winniman, S. Cooper, L.L. Cummins, *Anal. Chem.* 69 (1997) 313–319.
- [26] B. Bothner, K. Chatman, M. Sarkisian, G. Siuzdak, *Bioorg. Med. Chem. Lett.* 5 (1995) 2863–2868.
- [27] R.H. Griffey, M.J. Greig, H.J. Gaus, K. Liu, D. Monteith, M. Winniman, L.L. Cummins, *J. Mass Spectrom.* 32 (1997) 305–313.

7.1 Introduction

A number of assays based on multiplexed mixed-phase hybridization have been reported and used over the last decade. Such assays utilize either oligonucleotide arrays on solid supports (Lipshutz et al. 1999) or mixtures of categorized oligonucleotide-coated microparticles (Fulton et al. 1997; Hakala et al. 1998b). Although both approaches allow for a number of applications, some hurdles have yet to be overcome. For example, quantitative measurements with microparticles on a solid phase have shown that reliable detection of point mutations and deletions is still problematic, as the selectivity of hybridization is markedly changed when going from one sequence to another (Hakala et al. 1998a, 1998b). In addition, the distance between mismatch and site of immobilization within a probe (Ketomäki et al. 2002, 2003), the loading of oligonucleotide probes onto the particle, and, to a lesser extent, the homogeneity of probes all affect selectivity (Hakala et al. 1997a, 1997b, 1998a). Accordingly, detection of single-base alterations within certain sequences may still be difficult and even when possible, depends on time-consuming optimization of the probe length. Earlier, we reported the synthesis and highly selective binding of looped oligonucleotides to single-stranded DNA (Azhayeva et al. 1995a, 1995b) and also the interesting inhibitory properties of double-helix-forming circular oligomers (Azhayeva et al. 1997). More recently, we investigated the interaction of some double-helix-forming circular oligonucleotide probes with various DNA targets, employing thermodynamic analysis. Our preliminary results indicated that these circular oligonucleotides were capable of forming stable complexes with complementary target, and that the selectivity of circular probes appears to be superior to the selectivity of conventional linear probes in a number of cases.

These preliminary data resulted in the conclusion that restriction of the conformation of a hybridization probe may be associated with an increase in selectivity of target recognition. Circular probes may display additional advantages, as they are expected to be more stable towards enzymatic digestion, a common problem for oligonucleotides in biological matrices or cell growth media. In this report, we describe the synthesis of circular disulfide cross-linked oligonucleotides. The circular compounds, bearing both phosphodiester and phosphorothioate internucleotide linkages, were characterized by electrospray ionization mass spectrometry and liquid chromatography–mass spectrometry, and their enzymatic stability in serum and cellular extracts was assessed using solid-phase extraction sample pre-treatment coupled to ion-exchange HPLC analysis. The interactions of these double-helix-forming circular oligonucleotides with model DNA targets were examined by thermodynamic analysis, and the interactions of circular probes labeled with a photoluminescent lanthanide chelate with complementary and single-mismatch-containing DNA sequences were investigated by sandwich-type mixed-phase hybridization assays and compared with the data obtained from conventional linear probes.

7.2 Materials and methods

7.2.1 Oligonucleotide synthesis

The oligomers were prepared on a solid support **1** bearing a disulfide bond, or on commercially available nucleoside-bound solid supports (Glen Research, Sterling, VA, USA). Monomer **2**, bearing an ester function, was prepared as described by Hovinen et al. (1994a). Monomer **3**, which has a disulfide bond for its introduction on the 5'-termini of oligonucleotides (thiol-modifier C6 S-S; **Method B**), was also a commercial product (Glen Research). Conventional 2'-deoxyribonucleoside 3'-phosphoramidites and the amino-modifier C6 dT phosphoramidite **4** were also obtained from Glen Research. Oligonucleotides were assembled on an Applied Biosystems 392 DNA synthesizer on a 1- μ M scale. Introduction of the cystamine residue into assembled oligonucleotides bearing ester functions was achieved with 1 M cystamine as the free base (**Method A**). Generation of free thiol functions on the 5'- and 3'-termini of the oligomers, and the subsequent cross-linking by the disulfide-bond formation via oxidation, to give the corresponding circular oligonucleotide (**Methods A and B**), was performed as described by Azhayeva et al. (1995a, 1995b). A phosphorothioate oligonucleotide was also synthesized with standard methods, employing the Beaucage reagent for oxidation during DNA synthesis, and circularized with the same method (data not shown).

7.2.2 Labeling of oligonucleotides

Labeling of the circular oligonucleotides *co8-co10* and *co12-co14*, and two linear reference sequences, *o2* (5'-*TCA CCG CCC GGT ACA CC-3'; same sequence as *co8*) and *o3* (5'-*TTA TAA CCG AGA AGA GA-3'; same sequence as *co12*), was achieved with the isothiocyanate, *Eu-i*, and dichlorothiazin, *Eu-t*, activated terpyridine derived Eu(III) chelates (Mukkala et al. 1993) on the aliphatic amino group of a C(5)-amino-tethered thymidine unit **T**. The oligonucleotide (50 μ g, ca. 9 nmol) was dried in a small Eppendorf tube. Dichlorotriazine or the isothiocyanate-activated europium(III) terpyridine chelate (Mukkala et al. 1993) was added in 50 mM aq. NaHCO₃/Na₂CO₃, pH 9.5–10.0, in 10- to 20-fold excess, estimated on the basis of UV absorption (UV_{max} 320 nm, ϵ = 27 000 M⁻¹ cm⁻¹) in 10–20 μ l. The reaction was incubated overnight in the dark. The resulting mixture was initially passed through a NAP-5 gel filtration column with H₂O. The oligonucleotide fraction obtained was then purified with RP-HPLC on a ThermoHypersil C-18 column (4.6 mm \times 150 mm; buffer A: 0.1 M triethylammonium acetate (TEAA), buffer B: 0.1 M TEAA + 65% MeCN; linear gradient 0–40 min 0–40% B; t_R ca. 35 min) and desalted.

The identity of each labeled oligonucleotide was confirmed by ESI-TOF mass spectrometry (ABI Mariner System 5272).

7.2.3 Characterization

PAGE was carried out as described by Azhayeva et al. (1995a). Anion exchange by HPLC to purify and characterize oligonucleotides was performed on a PolyWAX LP (300 Å, 5 µm, 4.6 × 100 mm) column (PolyLC).

Electrospray ionization mass spectra of the non-labeled oligonucleotides were recorded on an LCQ quadrupole ion trap mass spectrometer (Finnigan MAT). The voltage at the spray needle was set to -2.5 kV, and the nitrogen sheath gas flow was 68. The stainless steel capillary was set at a temperature of 200°C and a voltage of -39 V. The tube lens offset was -10 V. The spectra were measured by collecting ions in the trap for 200 ms, summing 5–12 microscans and averaging 3–10 scans for each injection. For direct injection analyses, the eluent flow rate was 3 µl/min and injection volume 2–5 µl. The samples contained 1–20 pmol of oligonucleotide in 25 mM triethylamine–80% MeCN. For LC/MS analyses, we used narrowbore reversed-phase columns with 50 × 2 mm dimensions (*e.g.* XTerra C-18 and Genesis C-4), flow rates of 100–200 µl/min, and 5–20 min MeCN gradients. The ion-pair reagents used were triethylammonium acetate (TEAA, pH 7) and *N,N*-dimethylhexylammonium formate (DMHA-F, pH 7). The theoretical molecular weights of the compounds were calculated manually using average atomic weights.

7.2.4 Stability of circular oligonucleotides

Fetal bovine serum (FBS) was diluted in 0.05 M KH₂PO₄ (pH 7.4). CV-1 and D-407 cells were washed with phosphate buffered saline (PBS) several times and scraped in One-Phor-All Buffer (10 mM Tris-acetate, 10 mM magnesium acetate, 50 mM potassium acetate, pH 7.0). The cell suspension was sonicated several times to lyse the cells, and centrifuged at 4°C (13,000 rpm, 3 min). The supernatant was collected, stored at -70°C, and used undiluted for the incubations. A stock solution of each oligonucleotide was mixed with the medium to a final oligonucleotide concentration of 2 µM.

The circular phosphodiester oligonucleotides were incubated at 37°C for 10 h, and the phosphorothioates for 24–42 h. Several samples containing 170–300 pmol of oligonucleotide were taken during the incubation (linear and circular oligonucleotide, 6 samples; linear tethered precursor, 3 samples). Each sample was immediately diluted with 1 ml of H₂O and solid-phase extracted with a small DNA synthesis column (Empty Synthesis TWIST Style Column, Glen Research) packed with Toyopearl DEAE-650M anion-exchange resin (TosoHaas). After loading the sample, the column was washed with 5 ml of H₂O, proteins were removed with 5 ml of 75 mM NaCl, and the oligonucleotides were eluted with 5 ml of 0.75 M NaCl. For phosphorothioates, the NaCl concentrations were 150 mM and 1.5 M, respectively. The sample was then desalted with PolyPAK™ cartridges (Glen Research). The cartridge was first equilibrated with 2 ml of MeCN and 2 ml of 2 M TEAA. The sample was then loaded on the cartridge, the salts were washed out with 3 ml of 0.1 M TEAA, and the oligonucleotides were eluted with 1 ml of 50% MeCN. The solution was evaporated to 50–100 µl, depending on the initial volume of the sample.

The samples were then analyzed by ion-exchange HPLC, with a DNAPac PA-100 column (4 × 250 mm; Dionex Inc.). The column temperature was set to 30°C for both linear and circular oligomers to enhance the resolution, using a MetaTherm™ HPLC Column Temperature Control oven (MetaChem Technologies Inc.). Buffer A was 0.1 M sodium acetate (pH 8) in 20% MeCN, and buffer B was 0.4 M NaClO₄ in buffer A. The flow rate was 1 ml/min. Different two-stage gradients were selected for each oligonucleotide to ensure good resolution of metabolites and *t_R* values of 25–27 min for intact oligomer. The gradients used were: *i*) for linear phosphodiester oligonucleotides, 5–15%B (10 min) and 15–18%B (20 min); *ii*) for the circular phosphodiester oligonucleotide, 5–16%B (10 min) and 16–19%B (20 min); *iii*) for the linear phosphorothioate, 10–25%B (10 min) and 25–65%B (20 min); and *iv*) for the circular phosphorothioate, 10–30%B (10 min) and 30–70%B (20 min). The percentage of intact oligonucleotide left in each sample was calculated, relative to all peak areas in the chromatogram. The half-lives of each oligonucleotide in different media were estimated by fitting the data to semilogarithmic plots.

7.2.5 Melting experiments

UV spectra were recorded and melting experiments were performed on a Varian Cary 300 Bio UV/VIS spectrophotometer, equipped with Cary temperature controller and multicell Peltier block. The Cary Win UV thermal application software was used to increase temperature at a rate of 0.5°C/min, recording the melting curves at 260 nm. The oligomer concentrations were in the μM range in a buffer containing 10 mM Tris-HCl, pH 6.8; 0.1 M NaCl; 10 mM MgCl₂. Extinction coefficients of oligonucleotides were calculated by the nearest-neighbor method (Petersheim et al. 1983). The thermodynamic parameters for dissociation melting curves of complexes were extracted by employing the MeltWin software (a kind gift from Prof. Douglas H. Turner, University of Rochester, USA). Uncertainty in the Δ*G*_{37°}, Δ*H*°, and Δ*S*° values was estimated to be less than ±10% and *T_m* values less than ±0.3°C, based on triple repetition of each measurement.

7.2.6 Preparation of oligonucleotide-coated microparticles

The polymer particles (∅ = 50 μm) used to immobilize the oligonucleotide probes were made of glycidyl methacrylate (40%) and ethylene dimethylacrylate (60%) copolymer, then derivatized with diethylenetriamine, yielding a 1-mmol/g density of primary amino functions (SINTEF). A desired proportion (8–28 μmol/g) of the amino groups was acylated with [(4,4'-dimethoxytrityl)oxy]acetic acid, and the remaining groups were capped by repeated acetylations (Hovinen et al. 1994b). Two oligonucleotide probes, 3'-TTT AAG CTG TCG CTG CAC C-5' and 3'-TTT CGA CAG CTT CGC GAG C-5', were assembled on these supports *via* a normal phosphoramidite strategy, as described in detail by Ketomäki et al. (2003).

7.2.7 Hybridization assays

Hybridization assays were carried out in Tris buffer (50 mM, pH 7.5, containing 0.5 M NaCl and 0.01% Tween 20). Typically, 50 oligonucleotide-coated particles were shaken in 10 μ l of buffer containing the target oligonucleotide (*T3-T47*) and the fluorescent probe (*o2/Eu*, *o3/Eu*, *co8/Eu-co10/Eu*, *co12/Eu-co14/Eu*) at a concentration of 17 or 51 nM. The mixtures were shaken in sealed tubes with a rotamix (15 rpm) at 25°C overnight. The particles were then rapidly washed with buffer, and 10 of the particles were subjected to a time-resolved measurement of the fluorescence emission directly from the particle, one after another (Ketomäki et al. 2003). The standard deviation ranged from 5 to 20%. The emission signal was converted to the number of fluorescent probes attached to the particle with the aid of a calibration line obtained by determining the amount of Eu(III) ions released from the particle by the DELFIA protocol (Hemmilä et al. 1984), as described in more detail by Hakala et al. (1998a).

7.3 Results and discussion

7.3.1 Synthesis and characterization of circular oligonucleotides

We previously demonstrated the applicability of disulfide linkers for the cyclization of oligonucleotides (Azhayeva et al. 1995a, 1995b, 1997). In the present study, introduction of the disulfide functions at both the 5'- and 3'-termini of the oligomer was achieved as an initial and a final step in oligonucleotide assembly (**Method A, Scheme 1**, and **Method B, Scheme 2**). These disulfide bonds were subsequently cleaved by a reduction reaction, and the resulting oligomer contained two SH functional groups, which were allowed to cross-link by disulfide bond formation upon oxidation to give a circular oligonucleotide bearing the conjugated 5'- and 3'-termini. To synthesize various circular oligomers, solid support **1** and the 'active ester' monomeric block **2** (Method A, **Scheme 1**) or 'disulfide' monomeric block **3** (Method B, **Scheme 2**) were employed. In addition, a C(5)-amino-tethered thymine monomer block **4** was used for several sequences (Method B, **Scheme 2**). This modification allowed the straightforward labeling of oligonucleotides for mixed-phase hybridization experiments described below. Oligonucleotide sequences, comprised of linear precursors *lo1-lo14* and circular probes *co1-co14* (Schemes 1 and 2), are presented in **Table 1**.

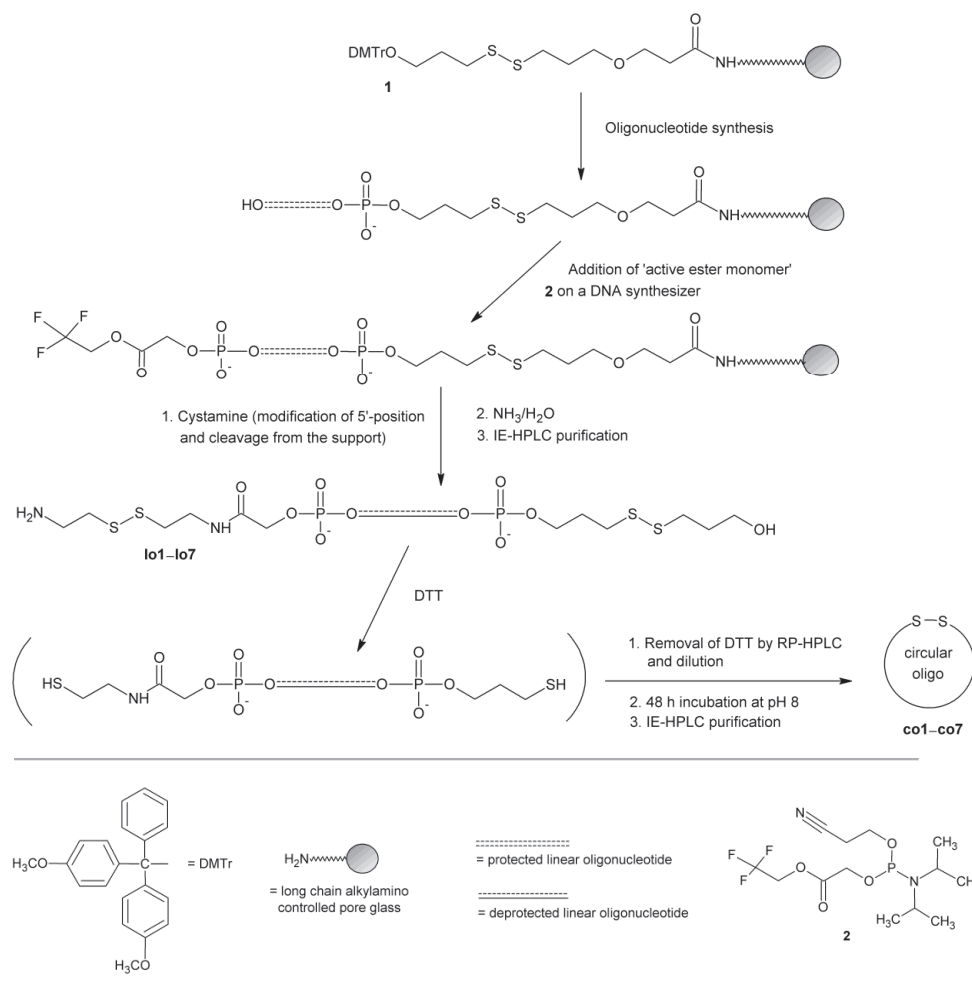
Labeling. Labeling of the circular oligonucleotides *co8-co10* and *co12-co14*, and two linear reference sequences, *o2* and *o3*, was achieved with the isothiocyanate, *Eu-i*, and dichlorothiazin, *Eu-t*, activated terpyridine derived Eu(III) chelates (Mukkala et al. 1993; structures shown in **Scheme 3**) on the aliphatic amino group of a C(5)-amino-tethered thymidine unit **1**, introduced by monomer **4**, resulting in the photoluminescent oligomers *co8/Eu-co10/Eu*, *co12/Eu-co14/Eu*, *o2/Eu*, and *o3/Eu*. The sequences of the labeled circular oligonucleotides were identical to those of the corresponding parent oligonucleotides.

Electrophoresis. The 15% denaturing PAGE showed reasonable purity for all of the synthesized compounds. All circular oligomers migrated differently than their

linear precursors or linear oligonucleotides with two terminal SH groups. These products were obtained by treating either the precursors *lo1-lo14* or circular oligomers *co1-co14* with dithiothreitol (DTT) in the presence of Et₃N, prior to the application on the gel. While circular structures shorter than 29-mer migrated faster than their linear counterparts, cyclic oligonucleotides longer than 30-mer always migrated slower than their linear precursors. Interestingly, the migration rates of the circular and linear 29-mer oligomers were nearly equivalent (data not shown).

HPLC. Anion-exchange HPLC also appears to be characteristic to the circular oligonucleotides, which displayed retention times longer by ca. 2 min than those of their linear precursors. RP-HPLC demonstrated that the purity of all circular oligonucleotides was >95% (data not shown).

Scheme 1 Synthesis of circular oligonucleotides (**Method A**).



Scheme 2 Synthesis of circular oligonucleotides (**Method B**).

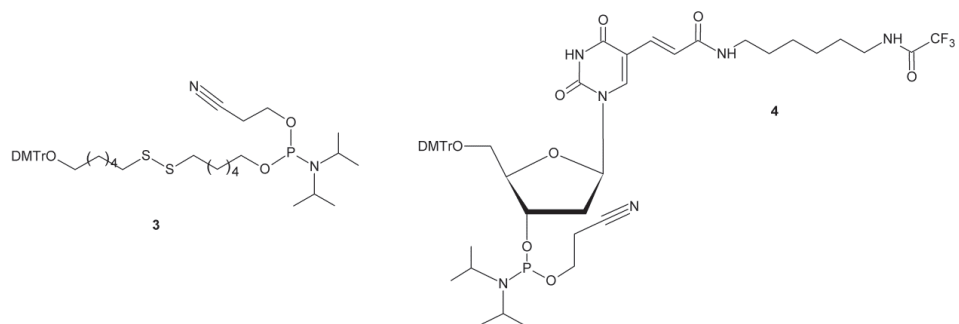
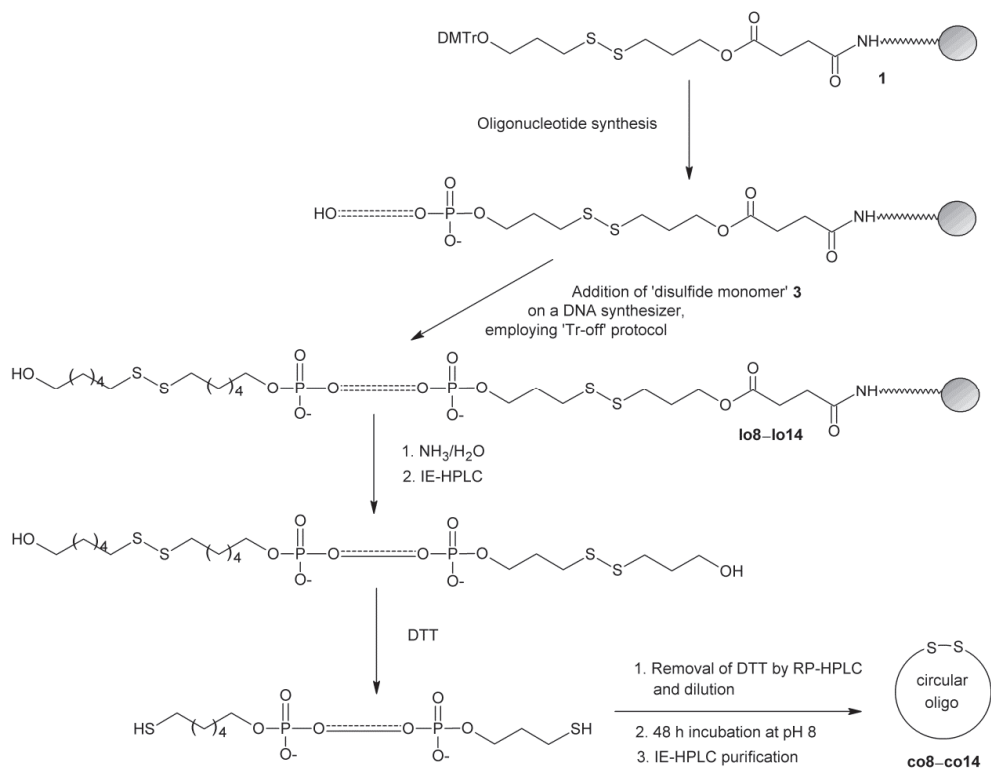
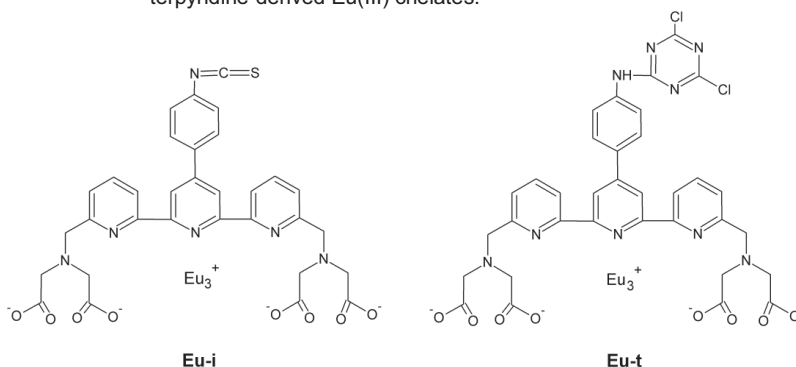


Table 1. Sequences comprising linear and circular oligonucleotides.

Oligomer	Sequence ¹
lo1, co1	5'-TTT TGG CGT CTT CCA TTT TAC CAA C-3'
lo2, co2	5'-CTT TTG GCG TCT TCC ATT TTA CCA ACC-3'
lo3, co3	5'-ACT TTT GGC GTC TTC CAT TTT ACC AAC CA-3'
lo4, co4	5'-ACT GTT TTG GCG TCT TCC ATT TTA CCA ACC A-3'
lo5, co5	5'-ACT GCG TTT TGG CGT CTT CCA TTT TAC CAA CCA-3'
lo6, co6	5'-ACT GCG TTT TTT GGC GTC TTC CAT TTT ACC AAC CA-3'
lo7, co7	5'-ACT GCG TTG TTT TTG GCG TCT TCC ATT TTA CCA ACC A-3'
lo8, co8	5'- <u>I</u> CA CCG CCC GGT ACA CC-3'
lo9, co9	5'-TT <u>I</u> CAC CGC CCG GTA CAC CCT T-3'
lo10, co10	5'-TTT TT <u>I</u> CAC CGC CCG GTA CAC CCT TTT T-3'
lo11, co11	5'-C <u>I</u> A TAA CCG AGA AGA GAT C-3'
lo12, co12	5'- <u>I</u> TA TAA CCG AGA AGA GA-3'
lo13, co13	5'-TT <u>I</u> TAT AAC CGA GAA GAG ACT T-3'
lo14, co13	5'-TTT TT <u>I</u> TAT AAC CGA GAA GAG ACT T-3'

¹ I = C(5)-amino-tethered thymidine used to attach Eu(III) label.

Scheme 3 Structures of the isothiocyanate (*Eu-i*) and dichlorothiazin (*Eu-t*) activated terpyridine-derived Eu(III) chelates.



Mass spectrometry. Electrospray ionization mass spectrometry is a sensitive method for the analysis of circular oligonucleotides (Azhayeva et al. 1997). The measured and theoretically calculated average molecular masses of the circular phosphodiester oligonucleotides are shown in **Table 2**, including those for the fluorescently labeled oligonucleotides *co8/Eu-co10/Eu* and *co12/Eu-co14/Eu*, which were measured by our collaborators elsewhere since we failed to succeed in measuring them with the ESI-quadrupole ion trap. For all other compounds, good quality ESI mass spectra were obtained by direct injection analysis, using 25 mM TEA in 80% MeCN as eluent, or, when necessary, by LC/MS using narrowbore RP columns and ion-pair reagents. The error between measured and calculated mass exceeds 0.03% only in one case, and none of the measurements exceed a mass error of 0.05%, which might be considered a threshold for failing results. Eight of the 14

compounds measured in our lab display a mass error of 0.01% or less, which is the highest accuracy routinely attainable with ESI–quadrupole ion trap MS.

Figure 1 shows the direct injection and LC/MS spectra of the 37-mer circular phosphodiester oligonucleotide *co7*, illustrating the usefulness of LC/MS in the analysis of large modified oligonucleotides. The direct injection ESI spectrum displays an extremely high degree of noise and cation adduction, despite using organic bases in the eluent. LC/MS of the same compound, in contrast, improves the spectral quality remarkably. In addition, similar spectra were measured for a 25-mer circular phosphorothioate oligonucleotide (**Figure 2**). While this compound is not as large, the phosphorothioate backbone attracts more contaminating species and is more difficult to purify than a phosphodiester of corresponding length. While the two main peaks are clearly visible even in the direct injection spectrum, LC/MS significantly enhances the signal-to-noise ratio.

Table 2. *Measured and theoretically calculated average molecular masses of the circular oligonucleotides.*

Oligonucleotide	Calculated mass	Measured mass	Mass error (%)
<i>co1</i>	7898.2	7897.2	0.01
<i>co2</i>	8476.6	8475.2	0.02
<i>co3</i>	9103.0	9101.8	0.01
<i>co4</i>	9736.4	9735.0	0.01
<i>co5</i>	10354.8	10352.3	0.02
<i>co6</i>	10963.2	10960.6	0.02
<i>co7</i>	11596.6	11600.7	0.04
<i>co8</i>	5579.8	5577.9	0.03
<i>co9</i>	7084.9	7085.2	<0.01
<i>co10</i>	8910.1	8910.0	<0.01
<i>co11</i>	6333.4	6333.0	<0.01
<i>co12</i>	5755.0	5753.1	0.03
<i>co13</i>	7260.0	7259.6	<0.01
<i>co14</i>	8172.6	8172.4	<0.01
<i>co8/Eu</i> ¹	6384.4	6385.3	0.01
<i>co9/Eu</i> ¹	7958.9	7959.8	0.01
<i>co10/Eu</i> ¹	9784.1	9783.6	<0.01
<i>co12/Eu</i> ¹	6629.0	6628.5	<0.01
<i>co13/Eu</i> ¹	8134.0	8134.5	<0.01
<i>co14/Eu</i> ¹	9046.6	9046.9	<0.01

¹ Measured with ESI-TOF MS.

SELECTIVE CIRCULAR OLIGONUCLEOTIDE PROBES IMPROVE DETECTION OF POINT MUTATIONS IN DNA*

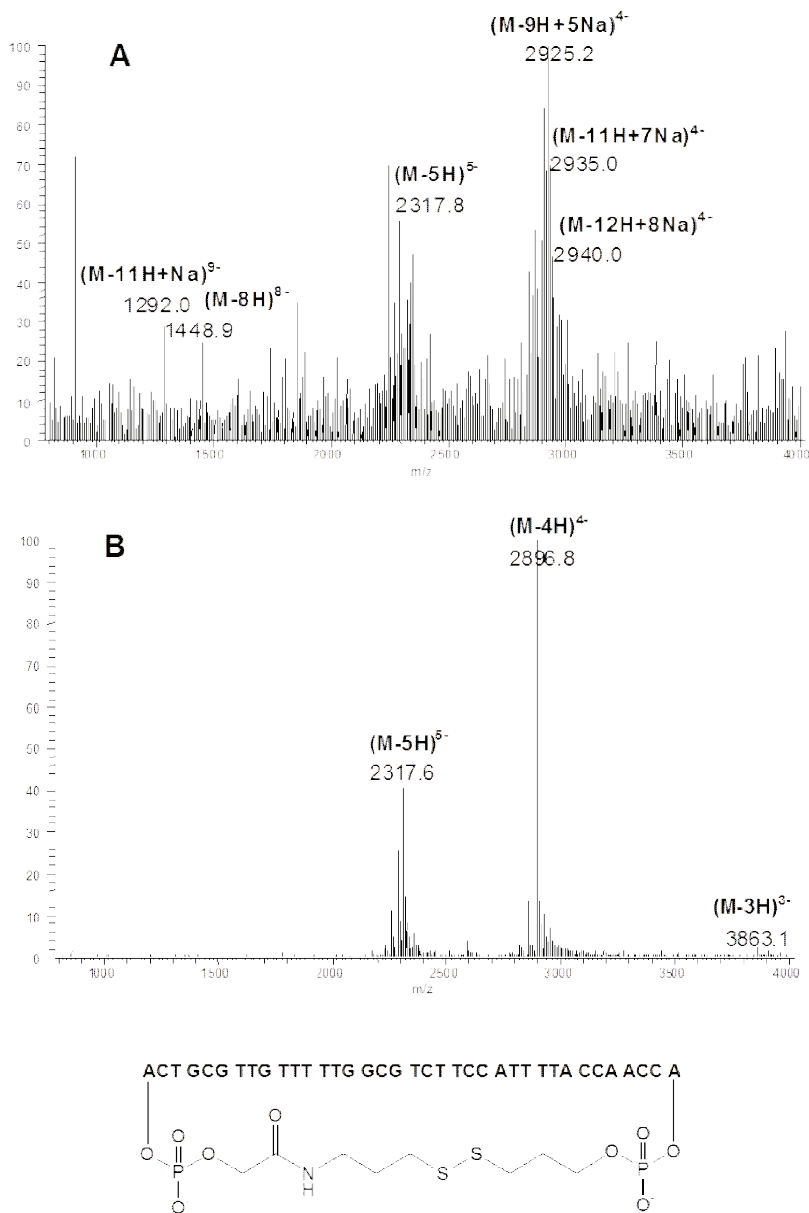


Figure 1 a) Direct injection ESI mass spectrum¹, b) ESI-LC/MS spectrum², and the structure of circular phosphodiester oligonucleotide *co7* (mol. weight = 11597). ¹Eluent: 25 mM triethylamine in 80% MeCN, flow rate: 10 μ l/min; ²Genesis C-4 column, 25 min MeCN gradient, DMHA-F (pH 7), flow rate: 100 μ l/min. [Previously unpublished.]

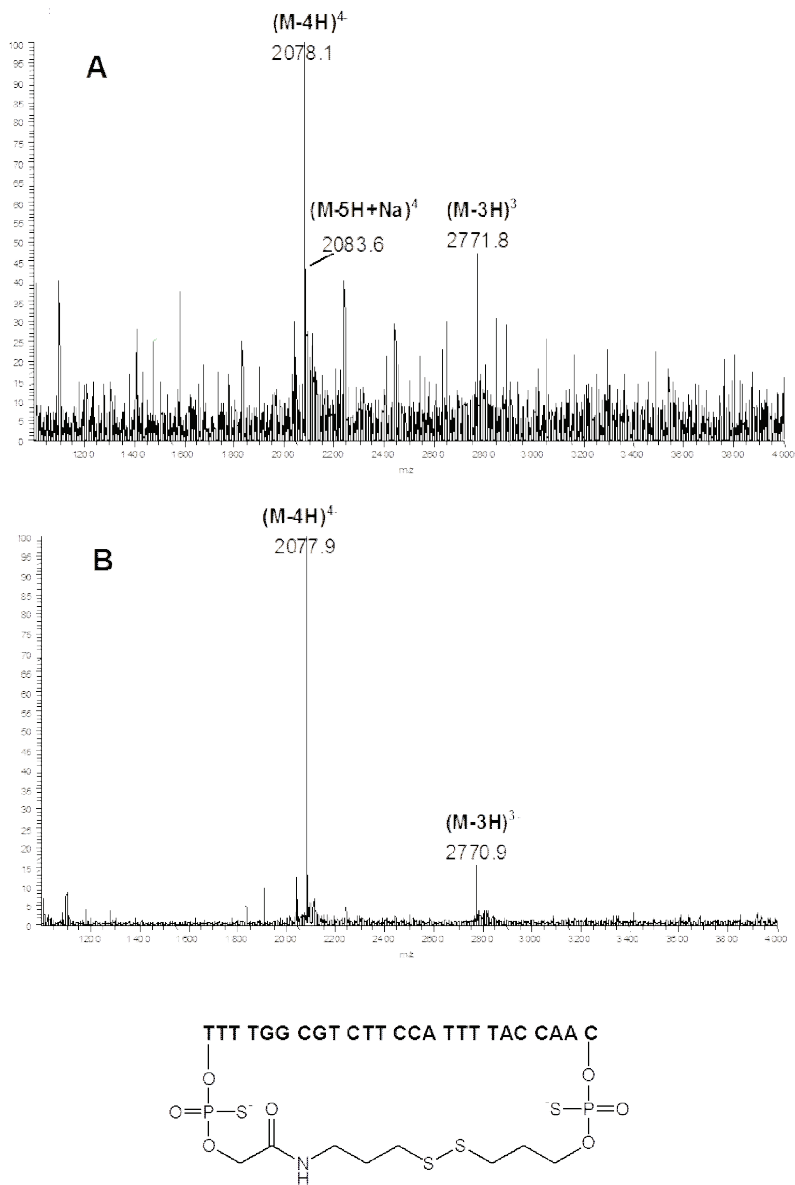


Figure 2 **a)** Direct injection ESI mass spectrum¹, **b)** ESI-LC/MS spectrum², and the structure of 25-mer circular phosphorothioate oligonucleotide *Sco1* (mol. weight = 8316). ¹Eluent: 25 mM triethylamine in 80% MeCN, flow rate: 20 μ l/min; ²XTerra C-18 column, 5 min MeCN gradient + TEAA (pH 7), flow rate: 200 μ l/min. [Previously unpublished.]

7.3.2 Stability of circular oligonucleotides

Unmodified oligodeoxyribonucleotides undergo rapid degradation by nuclease enzymes in serum and cells, with half-lives of *ca.* 30 min (Woolf et al. 1990). Since the primary degrading activity in biological media is due to 3'-exonucleases, it seemed possible to design phosphodiester oligonucleotides where only the 3'-terminus was protected from degradation. End-capping was achieved by replacing a few of the 3'-terminal nucleotides with nuclease-resistant modifications, *e.g.*, phosphorothioates, or by designing circular oligonucleotides that have no 5'- or 3'-termini. In some cases, 3'-capping had indeed conferred significant improvement towards the stability of phosphodiester oligonucleotides (Woolf et al. 1990; Crooke et al. 1995). The enzymatic stability of oligonucleotides has frequently been evaluated by purified nucleases, but more applicable results can be obtained by conducting these tests in biological systems that are commonly used in antisense-activity studies.

Methods for separating and quantitating the intact oligonucleotide and its metabolites include PAGE with autoradiography, CGE, HPLC, and ESI-LC/MS. While PAGE is limited by the inconvenience of using radiolabeled compounds (Shaw et al. 1991), the other methods often require extensive sample preparation such as phenol/CHCl₃ extractions, EtOH precipitation and desalting (Bourque and Cohen 1993; Gaus et al. 1997). To simplify sample preparation, Leeds et al. (1996) introduced a two-step solid-phase extraction (SPE) method by which proteins and lipids were first removed with a strong anion-exchange column, followed by desalting with a reversed-phase column. Anion-exchange HPLC is compatible with these SPE purifications, and good resolution of 25-mer and smaller oligomers has been achieved (Bourque and Cohen 1993).

In the present work, the metabolism of linear and circular oligonucleotides bearing either phosphodiester or phosphorothioate backbones was studied in three biological systems: 10% fetal bovine serum (FBS), African green monkey kidney fibroblast (CV-1) lysate, and human retina epithelial (D-407) cell lysate. Samples taken from the incubation mixture were purified by anion-exchange and reversed-phase SPE before analysis by ion-exchange HPLC. The recovery of oligonucleotides from SPE columns varied considerably, and, therefore, the amount of degradation in each sample was estimated by calculating the percentage of the peak area corresponding to the full-length oligonucleotide, relative to all peaks in the chromatogram.

An illustrative example of the HPLC chromatogram after incubating the linear phosphodiester 5'-TTT TGG CGT CTT CCA TTT TAC CAA C-3' (*o1*) in D-407 cell lysate is shown in **Figure 3a-c**. A progression of shorter metabolites appears in the chromatogram, indicating the usual mechanism of degradation by exonucleases. The results for the linear oligonucleotide *o1*, which has the same sequence as the 3'- and 5'-tethered linear precursor *lo1* and the circular *co1*, demonstrate that it was rapidly degraded in all media, with less than 10% of the parent compound intact after 2-4 hours of incubation (**Figure 4a-c**). As the linear precursor *lo1* contained modified 3'- and 5'-ends, it was expected to be approximately as stable as the circular *co1*. This was true in the case of CV-1 and D-407 cell lysates (**Figures 4b**

and **4c**), where *ca.* 20–30% of both parent compounds remained intact after 10 h. However, in 10% FBS, *lo1* was significantly less stable than *co1*, with remaining amounts at 10 h being 30% and 80%, respectively (**Figure 4a**). A longer incubation of 42 h with *co1* in 10% serum (data not shown) demonstrated that the amount of intact *co1* was *ca.* 50%. After fitting the obtained data to semilogarithmic plots, half-lives of the phosphodiester oligonucleotides were estimated (**Table 3**).

Interestingly, the circular compound *co1* had a much longer $t_{1/2}$ in 10% serum than in cell lysates. This could be due to the higher amounts of endonucleases in cells, in agreement with earlier studies (Bourque and Cohen 1993; Fisher et al. 1993; Crooke et al. 2000). Endonucleases are capable of degrading end-modified oligonucleotides. However, the same is not observed for the precursor *lo1*, suggesting that it may be susceptible to exonucleases despite the terminal modifications. The linear phosphorothioate oligonucleotide (*So1*) as well as the circular phosphorothioate (*Sco1*) were completely stable in all media for 42 h (data not shown). Therefore, concerning enzymatic stability, there is no additional advantage for circularizing phosphorothioates, as they are already stable enough.

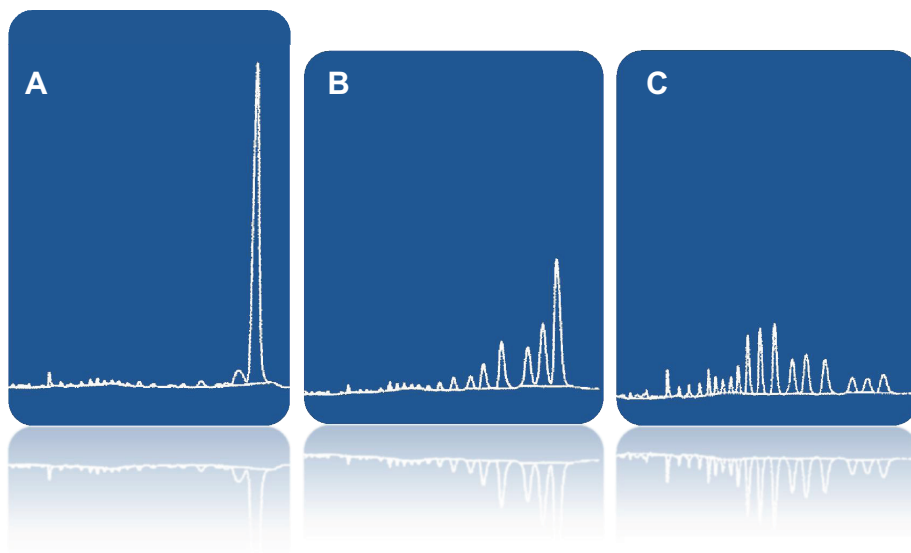


Figure 3 Ion-exchange HPLC chromatogram (absorbance at 260 nm vs. time in min) of the linear phosphodiester oligonucleotide *o1* after **a)** 0 minutes, **b)** 30 minutes, and **c)** 2 hours of incubation in human retina epithelial (D-407) cell lysate. **[A, C: Previously unpublished.]**

SELECTIVE CIRCULAR OLIGONUCLEOTIDE PROBES IMPROVE DETECTION OF POINT MUTATIONS IN DNA*

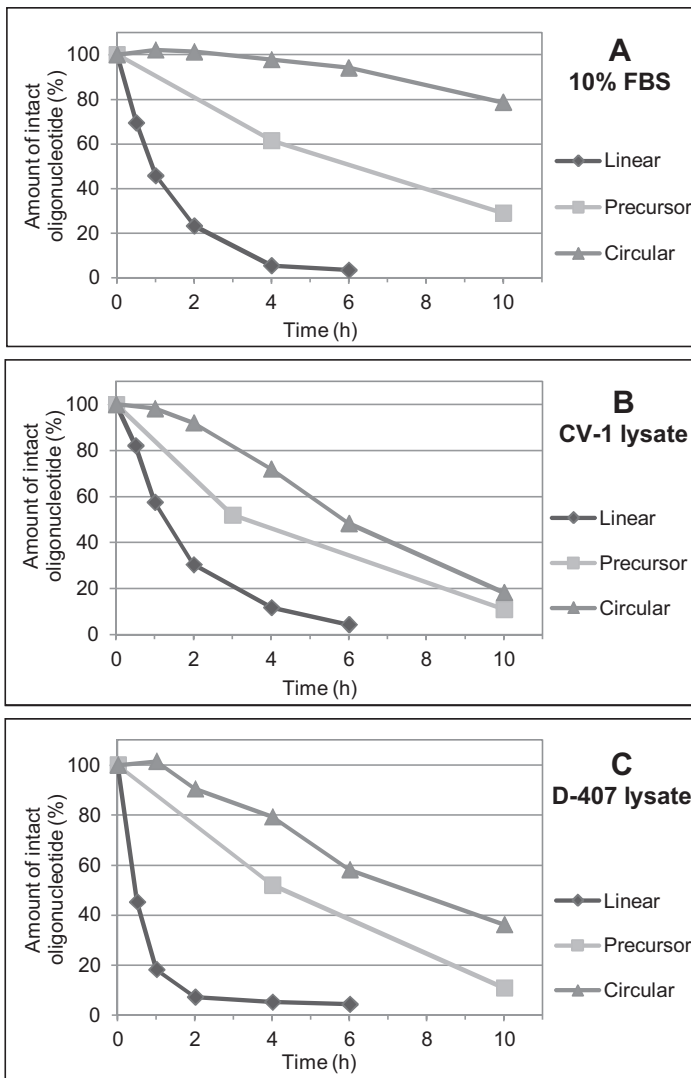


Figure 4 Amount of intact oligonucleotide (% of initial amount) in **a)** 10% fetal bovine serum, **b)** CV-1 cell lysate, and **c)** D-407 cell lysate.

Table 3. Calculated half-lives of the phosphodiester oligonucleotides.

Oligonucleotide	10% FBS	CV-1 lysate	D-407 lysate
<i>o1</i>	1.2 h	1.3 h	0.53 h
<i>lo1</i>	5.6 h	3.1 h	3.1 h
<i>co1</i>	28.1 h	4.0 h	6.5 h

7.3.3 Binding of circular oligonucleotides to complementary targets

Scheme 4 shows the structures of circular and linear oligomer complexes, *co1*–*co7* and *lo1*–*lo7*, respectively, with a fully complementary DNA sequence *T1* and a similar DNA stretch *T2*, containing a single mismatch in the middle of the sequence. To elucidate and compare the affinity and selectivity of circular and linear oligonucleotides, a number of melting experiments were performed. The T_m values and thermodynamic parameters for the dissociation were calculated, where possible, by applying a two-state model (Petersheim et al. 1983) with the MeltWin software, which uses a non-linear least-squares method; *i.e.*, the Marquardt–Levenberg fitting routine, A vs. T . The melting curves for complexes of *co1*, *co2*, and *co5* with *T1* are shown in **Figure 5** as an illustrative example. It can be seen that the curves referring to circular *co1* ($X = Z = 0$) and *co2* ($X = 5'$ -C-, $Z = -$ C-3'; **Scheme 4**), incorporating either no mismatching or a very short random mismatching sequence, appear to display only one transition, and they strongly resemble the melting curve of regular linear DNA fragments. The curve for *co5* ($X = 5'$ -ACTGCG-, $Z = -$ CA-3'; **Scheme 4**), incorporating eight totally random mismatched nucleoside units, shows two distinct transitions. This observation indicates a more complex type of association, and does not allow the application of a two-state model (Petersheim et al. 1983) and subsequent extraction of thermodynamic data from the melting curves. The situation was similar for melting curves of complexes *co3*, *co4*, *co6*, and *co7* with oligomer *T1* (data not shown).

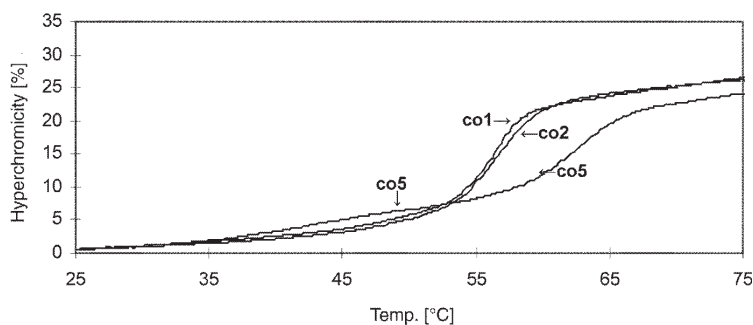


Figure 5 Melting curves for complexes of circular oligonucleotides *co1*, *co2*, or *co5* with a completely matching complementary DNA sequence *T1*.

In contrast to circular oligomers (*co3*–*co7*), the melting curves for the dissociation of all linear (*lo1*–*lo7*) and two circular (*co1* and *co2*) oligonucleotides resulted in only one transition. This allowed for the application of a two-state model in thermodynamic analysis. To elucidate the effect of a single mismatch on the efficiency of hybridization of circular oligonucleotides, *co1* and *co2*, compared to their linear precursors *lo1* and *lo2*, two sets of melting experiments were performed; *i*) the completely matching oligomer *T1* with *lo1*, *lo2*, *co1*, or *co2* (**Scheme 4**); and *ii*) the DNA stretch *T2*, containing a single mismatch in the middle of the sequence with *lo1*, *lo2*, *co1*, or *co2* (**Scheme 4**). **Figure 6** shows the melting curves for complexes of *T1* with *co1* (A) and *co2* (B), and *T2* with *co1* (C) and *co2* (D), and

Scheme 4 Structural complexes of linear and circular oligonucleotides with a completely matching complementary DNA sequence and a DNA stretch containing a single mismatch. (*lo1*, *co1*: X and Z = 0; *lo2*, *co2*: X = 5'-C-, Z = -C-3'; *lo3*, *co3*: X = 5'-AC-, Z = -CA-3'; *lo4*, *co4*: X = 5'-ACTG-, Z = -CA-3'; *lo5*, *co5*: X = 5'-ACTGCG-, Z = -CA-3'; *lo6*, *co6*: X = 5'-ACTGCGTT-, Z = -CA-3'; *lo7*, *co7*: X = 5'-ACTGCGTTGT-, Z = -CA-3'; ~SS~ = disulfide linker. Matching sequences are given in bold, and mismatching in plain fonts.)

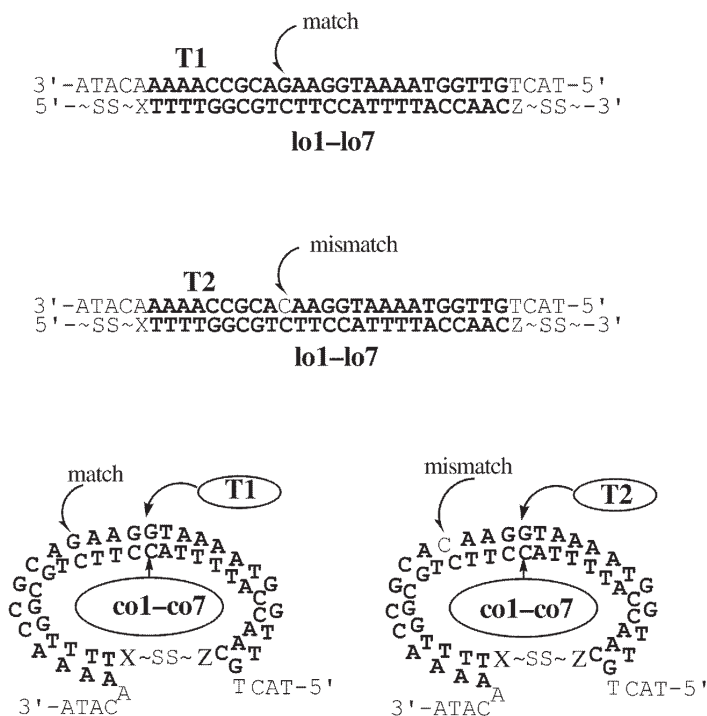


Table 4 summarizes the extracted T_m values and thermodynamic data. It can be seen that circular oligonucleotides are capable of forming stable complexes with a single-stranded complementary oligomer *T1* (**Scheme 4** and **Table 4**). These complexes appear to have T_m values lower by ca. 15°C and free energies of association (ΔG_{37°) 2.5–5.0 kcal/mol less negative than those of the corresponding complexes of *T1* and linear oligomers *lo1* and *lo2*. Interestingly, the introduction of a single mismatch into the complex leads to a substantial destabilization in the case of circular oligonucleotides ($Sel_{37^\circ} = 7.6$ kcal/mol for *co1* and $Sel_{37^\circ} = 4.6$ kcal/mol for *co2*), whereas the complexes of linear oligomers remain more stable ($Sel_{37^\circ} = 2.9$ kcal/mol for *lo1* and $Sel_{37^\circ} = 2.6$ kcal/mol for *lo2*). These results indicate that the cyclization (*i.e.*, restriction of the conformation) of a hybridization probe may be associated with a considerable increase in selectivity of target recognition. The increased selectivity appears to be of enthalpic origin, although the reliability of the breakdown of free energy to enthalpic and entropic contributions on the bases of a melting curve's shape may well be questioned. Unfortunately, no clear-cut conclusion may be drawn in most cases, due to the complex nature of the

association process for a single-stranded DNA target with five out of the seven circular oligonucleotides studied. Clearly, the melting experiments alone are not sufficient to answer the main questions; *i.e.*, are the circular oligonucleotide probes more selective in target recognition than conventional linear oligonucleotides, and can they serve to improve the fidelity of hybridization assays, in dealing with the detection of DNA point mutations?

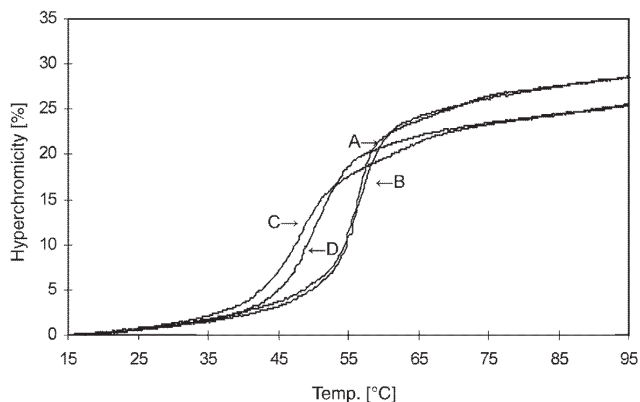


Figure 6 Melting curves for complexes of *co1/T1* (A), *co2/T1* (B), *co1/T2* (C), and *co2/T2* (D).

Table 4. Melting temperatures (T_m) and thermodynamic parameters for circular and linear oligonucleotides with fully complementary (T1) and mismatched (T2) DNA sequences. Thermodynamic data were calculated as mean values of three melting experiments.

Oligomer	Target	T_m (°C)	ΔT_m^1 (°C)	ΔH° (kcal/mol)	ΔS° (cal/K \times mol)	$\Delta G_{37^\circ}^\circ$ (kcal/mol)	$Sel_{37^\circ}^2$ (kcal/mol)
<i>co1</i>	T1	55.6		-194.3	-561	-20.4	
	T2	46.7	8.9	-111.9	-320	-12.8	-7.6
<i>co2</i>	T1	56.2		-155.6	-442	-18.4	
	T2	49.9	6.3	-109.78	-310	-13.8	-4.6
<i>lo1</i>	T1	70.4		-139.2	-375	-22.9	
	T2	62.7	7.7	-138.5	-382	-20.0	-2.9
<i>lo2</i>	T1	70.6		-143.7	-388	-23.4	
	T2	63.0	7.6	-147.9	-410	-20.8	-2.6

¹ $\Delta T_m = T_m$ (complex formed by completely matching sequences) - T_m (complex formed by sequences containing a single mismatch);

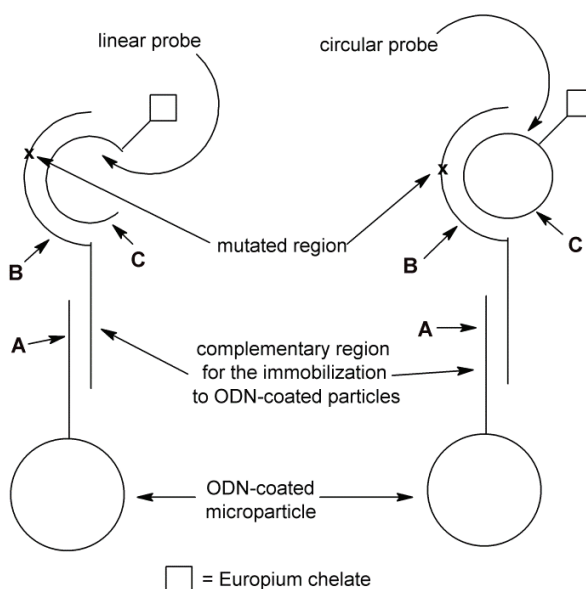
² $Sel_{37^\circ} = \Delta G_{37^\circ}$ (complex formed by completely matching sequences) - ΔG_{37° (complex formed by sequences containing a single mismatch).

7.3.4 Mixed-phase hybridization experiments

To find out whether the cyclization of an oligonucleotide probe really can increase the selectivity of hybridization, and, hence, the reliability in the screening of a single

nucleotide polymorphism suggested by the melting temperature, the effect of various single-base mutations on the hybridization efficiency of linear and circularized probes was examined by an independent method, *i.e.*, the sandwich-type mixed-phase hybridization assay described by Hakala et al. (1998a) and depicted schematically in **Scheme 5**. This assay is based on the time-resolved quantification of a fluorescent probe (**C**) directly on the surface of the microscopic polymer particle. In the present application, the complementary sequence between the particle-bound probe (**A**) and the sandwiched oligonucleotide (**B**) was kept sufficiently long (16 nucleotides) to ensure quantitative binding. Accordingly, the intensity of the fluorescence emission that is measured from a single particle is proportional to the amount of the fluorescently tagged probe (**C**), either circular or linear, that is bound to the sandwiched oligonucleotide (**B**). It should be noted that, when a lanthanide chelate is used as a reporter group, no concentration quenching occurs (Hakala et al. 1997b, 1998a). The length of the complementary region between the fluorescent (**C**) and sandwiched (**B**) probes varied from 10 to 17 nucleotides, according to the design of probe **B**, and one-base mismatches were generated similarly within this region.

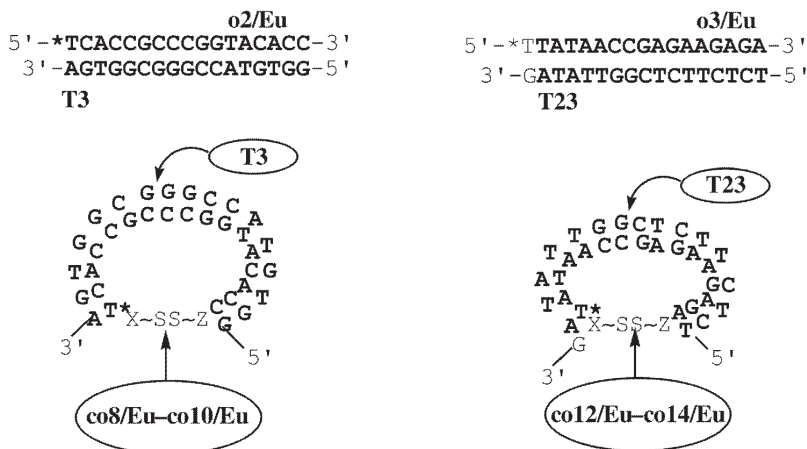
Scheme 5 Principle of the mixed-phase hybridization assays.



Two sets of experiments were performed. The first set was a comparative study on the hybridization of a linear, *o2/Eu*, and three circular oligonucleotides *co8/Eu-co10/Eu*, all incorporating the same sequence, 5'-TCA CCG CCC GGT ACA CC-3'. The circular oligomers differed from each other with respect to the ring size. The hybridization of these probes with sequences *T3*, *T7*, *T11*, *T15*, and *T19*, fully complementary with the probes over 17, 13, 12, 11, and 10 nucleotides in length,

respectively, was quantified. In addition, the effect of three different one-base mismatches (G→T, C→G, C→T) on the hybridization efficiency of these fully complementary targets was determined (**Scheme 6** and **Table 5**). The second set was, in principle, similar, but the linear (*o3/Eu*) and circular (*co12/Eu-co14/Eu*) probes incorporated the sequence 5'-TTA TAA CCG AGA AGA GA-3', and the length of the complementary region varied from 10 to 16 nucleotides (**Scheme 6** and **Table 6**). In brief, and concerning the oligonucleotides *o3/Eu* and *co13/Eu* (**Table 6**) in particular, the cyclization of the probe considerably improved selectivity. For example, a single-base mismatch close to the 3'-terminus of the probe (*o3/Eu-T23* vs. *o3/Eu-T24-T27*; **Table 6**) decreased the affinity of a linear oligonucleotide by only 20–50% when the concentration was 51 nM, and the complementary region consisted of 16 base pairs. By contrast, with a circular probe, the affinity decreased by more than 90% (*co13/Eu-T23* vs. *co13/Eu-T24-T27*, **Table 6**), hence allowing unequivocal detection of the mutation. Moreover, excellent selectivity remained when the length of the complementary region varied over a wide range; *i.e.* from 16 to 11 base pairs (*co13/Eu-T23* vs. *co13/Eu-T24-T27*, *co13/Eu-T28* vs. *co13/Eu-T29-T32*, *co13/Eu-T33* vs. *co13/Eu-T34-T37*, and *co13/Eu-T38* vs. *co13/Eu-T39-T42*; **Table 6**). With a linear probe, similar selectivity was achieved only at one particular length of the complementary region (11 base pairs; *o3/Eu-T38* vs. *o3/Eu-T39-T42*, **Table 6**). With oligonucleotides *o2/Eu* and *co9/Eu* (**Table 5**), the superiority of the circular probe was slightly less impressive.

Scheme 6 Structural complexes of linear (*o2/Eu*, *o3/Eu*) and circular (*co8/Eu-co10/Eu*, *co12/eu-co14/Eu*) oligonucleotides with sequences T3 and T23. (*co8/Eu*: X and Z = 0; *co9/Eu*: X = 5'-TT-, Z = -CTT-3'; *co10/Eu*: X = 5'-TTTTT-, Z = -CTTTTT-3'; *co12/Eu*: X = 5'-T-, Z = 0; *co13/Eu*: X = 5'-TTT-, Z = -CTT-3'; *co14/Eu*: X = 5'-TTTTT-, Z = -CTT-3'; *T = photoluminescent tagged thymidine unit; ~SS~ = disulfide linker. Matching sequences are given in bold and mismatching plain.)



Clearly, no reasonable detection was possible with a linear probe. The affinity of a linear probe in complexes *o2/Eu-T3* vs. *o2/Eu-T4-T6* (**Table 5**) decreased by only less than 5% when the concentration was 51 nM, and the complementary region consisted of 17 base pairs. On the contrary, the circular probe allowed for the detection of a single-base mismatch. For example, a single-base mismatch (*co9/Eu-T3* vs. *co9/Eu-T4-T6*, **Table 5**) decreased the affinity of a circular probe by 35–95% when the concentration was 51 nM, and the complementary region consisted of 17 base pairs. Comparison of the results of circular probes with different ring size (*co13/Eu* with *co12/Eu* or *co14/Eu*; **Table 5**) indicates that a ring size of 22 nucleotides is optimal. In general, the results obtained with a 17-mer (*co8/Eu*, *co12/Eu*) or 25–28-mer (*co14/Eu*, *co10/Eu*) circular oligonucleotides were parallel to those described for the 22-mers.

Table 5. Hybridization efficiencies of linear oligonucleotide *o2/Eu* and circular oligomers *co8/Eu*–*co10/Eu* with target sequences T3–T22.

Target sequence	Number of compl. bases	Hybridization, % of <i>o2/Eu</i> , 17 nM/51 nM	Hybridization, % of <i>co9/Eu</i> , 17 nM/51 nM	Hybridization, % of <i>co8/Eu</i> , 17 nM/51 nM	Hybridization, % of <i>co10/Eu</i> , 17 nM/51 nM
<i>T3</i>	17	28/32	29/27	8/15	26/47
<i>T4</i>		54/28	0/1	0/0	25/13
<i>T5</i>		35/31	8/18	1/6	14/33
<i>T6</i>		27/30	11/15	7/14	9/22
<i>T7</i>	13	26/35	4/6	1/1	7/17
<i>T8</i>		2/4	0/0	0/0	0/0
<i>T9</i>		30/32	0/1	0/0	2/8
<i>T10</i>		29/31	0/1	1/1	2/8
<i>T11</i>	12	31/33	1/1	0/1	2/7
<i>T12</i>		1/1	0/0	0/0	0/0
<i>T13</i>		32/29	0/0	0/0	0/1
<i>T14</i>		23/29	0/0	0/0	0/1
<i>T15</i>	11	26/44	1/2	0/0	2/9
<i>T16</i>		0/0	0/0	0/0	0/0
<i>T17</i>		0/2	0/0	0/0	0/0
<i>T18</i>		0/0	0/0	0/0	0/0
<i>T19</i>	10	1/3	0/0	0/1	0/0
<i>T20</i>		0/0	0/0	0/0	0/0
<i>T21</i>		0/0	0/0	0/0	0/0
<i>T22</i>		0/0	0/0	0/0	0/0

Table 6. *Hybridization efficiencies of linear oligonucleotide o3/Eu and circular oligomers co12/Eu–co14/Eu with target sequences T23–T47.*

Target sequence	Number of compl. bases	Hybridization, % of o3/Eu 17 nM/51 nM	Hybridization, % of co13/Eu 17 nM/51 nM	Hybridization, % of co14/Eu 17 nM/51 nM	Hybridization, % of co12/Eu 17 nM/51 nM
T23	16	11/56	2/62	84/100	2/6
T24		3/37	0/2	2/4	0/0
T25		3/49	1/6	4/8	1/1
T26		2/38	1/4	5/8	1/1
T27		2/30	0/2	3/5	0/1
T28	13	10/44	1/42	41/89	1/5
T29		2/10	0/1	2/2	0/0
T30		3/19	0/1	1/3	0/0
T31		2/21	0/1	2/3	0/1
T32		3/14	0/0	0/2	0/0
T33	12	7/43	1/30	17/40	1/2
T34		3/5	0/0	0/1	0/0
T35		4/5	0/0	0/1	0/0
T36		4/7	0/0	0/0	0/0
T37		6/6	0/0	0/0	0/0
T38	11	3/30	0/28	5/34	0/1
T39		1/0	0/0	0/0	0/0
T40		2/3	0/0	0/0	0/0
T41		1/4	0/0	0/0	0/0
T42		1/1	0/0	0/0	0/0
T43	10	3/15	0/2	0/4	0/2
T44		0/0	0/0	0/0	0/0
T45		0/0	0/0	0/0	0/0
T46		0/0	0/0	0/0	0/0
T47		0/0	0/0	0/0	0/0

7.4 Conclusions

The synthesis of circular oligonucleotides, their labeling with photoluminescent europium(III) chelates, and characterization by ESI-MS was achieved. The disulfide cross-linking, which resulted in circularization, apparently increased the enzymatic stability of phosphodiester oligonucleotides, especially in serum but also in cell extracts. This novel feature of circular probes may be very useful in tuning hybridization assays performed with biological samples and, in certain cases, may even be useful for some antisense experiments. In addition, the use of circular probes instead of conventional linear probes may considerably improve the detection selectivity of point mutations in DNA. In particular, cyclization of the probe may help in screening these frequently encountered point mutations, which, for some reason, do not markedly destabilize the duplex formation of linear oligonucleotides.

Acknowledgements

Financial support by the Technology Development Centre of Finland is gratefully acknowledged.

7.5 References

- Azhayeva E, Azhayev A, Auriola S, Tengvall U, Urtili A, Lönnberg H. 1997. Inhibitory properties of double helix forming circular oligonucleotides. *Nucleic Acids Res.* 25(24): 4954–4961.
- Azhayeva E, Azhayev A, Guzaev A, Hovinen J, Lönnberg H. 1995a. Looped oligonucleotides form stable hybrid complexes with a single-stranded DNA. *Nucleic Acids Res.* 23(7): 1170–1176.
- Azhayeva E, Azhayev A, Guzaev A, Lönnberg H. 1995b. Selective binding of looped oligonucleotides to a single-stranded DNA and its influence on replication *in vitro*. *Nucleic Acids Res.* 23(21): 4255–4261.
- Bourque AJ, Cohen AS. 1993. Quantitative analysis of phosphorothioate oligonucleotides in biological fluids using fast anion-exchange chromatography. *J Chromatogr.* 617(1): 43–49.
- Crooke RM, Graham MJ, Cooke ME, Crooke ST. 1995. *In vitro* pharmacokinetics of phosphorothioate antisense oligonucleotides. *J Pharmacol Exp Ther.* 275(1): 462–473.
- Fulton RJ, McDade RL, Smith PL, Kienker LJ, Kettman JR Jr. 1997. Advanced multiplexed analysis with the FlowMetrix system. *Clin Chem.* 43(9): 1749–1756.
- Gaus HJ, Owens SR, Winniman M, Cooper S, Cummins LL. 1997. On-line HPLC electrospray mass spectrometry of phosphorothioate oligonucleotide metabolites. *Anal Chem.* 69(3): 313–319.
- Hakala H, Heinonen P, Iitiä A, Lönnberg H. 1997a. Detection of oligonucleotide hybridization on a single microparticle by time-resolved fluorometry: hybridization assays on polymer particles obtained by direct solid phase assembly of the oligonucleotide probes. *Bioconjugate Chem.* 8(3): 378–384.
- Hakala H, Lönnberg H. 1997b. Time-resolved fluorescence detection of oligonucleotide hybridizations on a single microparticle: covalent immobilizations of oligonucleotides and quantification of a model system. *Bioconjugate Chem.* 8(2): 232–237.
- Hakala H, Mäki E, Lönnberg H. 1998a. Detection of oligonucleotide hybridization on a single microparticle by time-resolved fluorometry: quantification and optimization of a sandwich type assay. *Bioconjugate Chem.* 9(3): 316–321.
- Hakala H, Virta P, Salo H, Lönnberg H. 1998b. Simultaneous detection of several oligonucleotides by time-resolved fluorometry: the use of a mixture of categorized microparticles in a sandwich type mixed-phase hybridization assay. *Nucleic Acids Res.* 26(24): 5581–5588.
- Hemmilä I, Dakubu S, Mukkala VM, Siitari H, Lövgren T. 1984. Europium as a label in time-resolved immunofluorometric assays. *Anal Biochem.* 137(2): 335–343.
- Hovinen J, Guzaev A, Azhayev A, Lönnberg H. 1994a. Novel non-nucleosidic phosphoramidite building blocks for versatile functionalization of oligonucleotides at primary hydroxy groups. *J Chem Soc Perkin Trans 1.* (19): 2745–2749.
- Hovinen J, Guzaev A, Azhayev A, Lönnberg H. 1994b. Novel solid supports for the preparation of 3'-derivatized oligonucleotides: introduction of 3'-alkylphosphate tether groups bearing amino, carboxy, carboxamido, and mercapto functionalities. *Tetrahedron.* 50(24): 7203–7218.

- Ketomäki K, Hakala H, Kuronen O, Lönnberg H. 2003. Hybridization properties of support-bound oligonucleotides: the effect of the site of immobilization on the duplex stability and selectivity of duplex formation. *Bioconjugate Chem.* 14(4): 811–816.
- Ketomäki K, Hakala H, Lönnberg H. 2002. Mixed-phase hybridization of short oligodeoxyribonucleotides on microscopic polymer particles: effect of one-base mismatches on duplex stability. *Bioconjugate Chem.* 13(3): 542–547.
- Leeds JM, Graham MJ, Truong L, Cummins LL. 1996. Quantitation of phosphorothioate oligonucleotides in human plasma. *Anal Biochem.* 235(1): 36–43.
- Lipshutz RJ, Fodor SP, Gingeras TR, Lockhart DJ. 1999. High density synthetic oligonucleotide arrays. *Nature Genet.* 21(1 Suppl), 20–24.
- Mukkala VM, Helenius M, Hemmilä I, Kankare J, Takalo H. 1993. Development of luminescent europium(III) and terbium(III) chelates of 2,2':6',2''-terpyridine derivatives for protein labeling. *Helv Chim Acta.* 76(3): 1361–1378.
- Petersheim M, Turner DH. 1983. Base-stacking and base-pairing contributions to helix stability: thermodynamics of double-helix formation with CCGG, CCGGp, CCGGAp, ACCGGp, CCGGUp, and ACCGGUp. *Biochemistry.* 22(2): 256–263.
- Shaw JP, Kent K, Bird J, Fishback J, Froehler B. 1991. Modified deoxyoligonucleotides stable to exonuclease degradation in serum. *Nucleic Acids Res.* 19(4): 747–750.
- Woolf TM, Jennings CG, Rebagliati M, Melton DA. 1990. The stability, toxicity and effectiveness of unmodified and phosphorothioate antisense oligodeoxynucleotides in *Xenopus* oocytes and embryos. *Nucleic Acids Res.* 18(7): 1763–1769.

8 ONE-STEP PRODUCTION OF PEPTIDE-MODIFIED GOLD NANOPARTICLES FOR SIRNA DELIVERY*

Abstract

Oligonucleotides such as short interfering RNA (siRNA) comprise a promising group of therapeutics that suffers from inefficient cellular uptake and enzymatic degradation. To overcome these disadvantages, researchers have introduced numerous delivery vehicles. These vehicles include gold nanoparticles (GNPs), which can be surface-coated with cationic molecules to form a complex with siRNA. In addition, various cell-penetrating peptides (CPPs) are known to enhance the intracellular delivery of biomacromolecules and nanocarriers. However, few studies have examined cell-penetrating peptide-modified gold nanoparticles (CPP-GNPs) for siRNA delivery.

In this study we combined gold nanoparticles with cysteamine and a cationic analog of Tat₄₈₋₆₀, one of the most extensively investigated CPPs. The CPP-GNPs were prepared by a one-step procedure, characterized by microscopic and spectroscopic methods, and complexed with siRNA. The effect of the CPP-GNPs on cellular viability and gene silencing was then analyzed in a human retinal pigment epithelial cell line stably producing the reporter enzyme secreted alkaline phosphatase (SEAP-ARPE-19). Our results indicate that the CPP-GNPs form stable complexes with siRNA and are able to deliver siRNA into cells in an active form, causing a dose-dependent gene silencing of 49% or more. The complexes inhibited SEAP production in serum-containing growth medium as well, suggesting that the gold particles shield their cargo from enzymatic degradation. Although we found the peptide itself toxic at high concentrations, we observed no toxicity for the CPP-GNPs at any of the concentrations tested. Furthermore, the CPP-GNPs increased both the SEAP secretion and cell viability of SEAP-ARPE-19 cells above 100%, indicating a GNP-induced stimulation of cellular proliferation by an unknown mechanism.

* Adapted from: Tengvall U, Elizarova T, Takashima Y, Pietilä L, Reinisalo M, Laurén P, Urtti A, Antopolsky M, Yliperttula M. One-step production of peptide-modified gold nanoparticles for siRNA delivery. (In revision.)

8.1 Introduction

Short interfering RNA (siRNA) and other oligonucleotides show great potential against many genetic diseases currently lacking effective and non-toxic treatments (Bennett and Swayze 2010). However, this promising group of therapeutics is still not in clinical use because of its unfavorable pharmacokinetics. Oligonucleotides are extensively metabolized by serum nucleases and excreted by the kidneys *in vivo* (Juliano et al. 2009). Moreover, they exhibit poor permeability through cell membranes due to their negatively charged nature. Even when oligonucleotides do enter cells *via* endocytosis, they frequently remain trapped in endosomes, and do not gain access to their targets in the cytoplasm (Beltinger et al. 1995). A good delivery vehicle would thus protect the oligonucleotide against degradation and aid its endosomal escape or, alternatively, use non-endocytic pathways for cellular internalization. Most of the current methods of choice are lipid-containing formulations such as cationic lipids, which destabilize the endosomal membrane, thereby releasing the cargo into the cytoplasm (Zelphati and Szoka 1996). RNA interference (RNAi) was accomplished *in vivo* by covalently conjugating the sense strand of siRNA to cholesterol (Soutschek et al. 2004) and by complexing siRNA with stable nucleic acid lipid particles (SNALPs) (Zimmermann et al. 2006). The first successful systemic administration of siRNA in humans involved transferrin-mediated targeting to solid tumors by cyclodextrin-based nanoparticles (Davis et al. 2010), a good example of the current multifunctional approach employing a biocompatible nanoparticle core with various surface moieties for cellular uptake, nuclear targeting or avoiding recognition by phagocytes.

Another versatile nanocarrier candidate is colloidal gold, which is anticipated to be biocompatible due to its chemical inertness and has been widely investigated for diagnostic and therapeutic applications (Ghosh et al. 2008). Citrate-stabilized (Chithrani et al. 2006) and oligonucleotide-coated (Giljohann et al. 2007) gold nanoparticles (GNPs) enter cancer cells efficiently *via* endocytosis mediated by adsorbed serum proteins. GNPs have been used for the delivery of various biomacromolecules, including antisense oligonucleotides (Rosi et al. 2006). *In vitro* delivery was demonstrated for covalent siRNA–GNP conjugates prepared either by co-loading thiolated siRNA and thiolated poly(ethylene glycol) (PEG) (Oishi et al. 2006) or by attachment of siRNA to pre-loaded SH–PEG–NH₂ *via* a disulfide linker (Lee et al. 2009). RNAi *in vitro* was also achieved with non-covalent siRNA/GNP complexes, in which the GNPs were rendered positively charged by coating them with cations such as cysteamine (Lee et al. 2008), poly(ethylene imine) (PEI) (Song et al. 2010), or cationic lipids (Kong et al. 2012). The GNP core could also be functionalized with cell-penetrating peptides (CPPs), short cationic peptides that contain membrane translocation and/or nuclear localization sequences (Fonseca et al. 2009). CPPs are known to deliver molecules into cells, and several CPPs have been employed in siRNA delivery (Simeoni et al. 2003; Muratovska and Eccles 2004). One of the most promising and extensively studied CPPs is the Tat_{48–60} peptide, which comprises the basic region of the HIV-1 TAT protein responsible for its efficient cellular uptake and nuclear localization (Vivès et al. 1997). Tat_{48–60} has

been shown to enter cells *via* various, predominantly endocytic mechanisms, while rapid translocation leading to cytoplasmic distribution has also been seen at high concentrations and with smaller cargoes (Tünnemann et al. 2006; Duchardt et al. 2007). The key factor triggering CPP internalization by any of the mechanisms seems to be the ionic interaction with negatively charged glycosaminoglycans at the cell membrane (Richard et al. 2005; Nakase et al. 2007). A study comparing the cellular uptake of several Tat_{48–60} analogs, all bearing the same number of cationic amino acids, found no difference between the sequences, indicating that the ionic interaction is in fact crucial for the uptake to occur (Subrizi et al. 2012). According to that study, in contrast to earlier results, the absence of cell-surface glycosaminoglycans enhanced rather than diminished the uptake. The intracellular distribution suggested an endocytic cell entry and endosomal entrapment, which had also previously been found to preclude the antisense effect of oligonucleotide–CPP conjugates (Antopolsky et al. 1999). However, some CPPs can facilitate the endosomal escape of cargoes (Jääskeläinen et al. 2000). Effective siRNA delivery has been achieved by covalent conjugation of Tat to one of the siRNA strands (Chiu et al. 2004; Meng et al. 2009) and by complexing siRNA with Tat-derived peptides (Arthanari et al. 2010; Uchida et al. 2011). Multifunctional nanoparticles such as gold nanoshells (Braun et al. 2009), quantum dots (Jung et al. 2010), and poly(ϵ -caprolactone) block copolymer micelles (Kanazawa et al. 2012) have been linked to Tat for siRNA delivery. Gold nanospheres, in contrast, have so far only been conjugated with Tat peptide for nuclear targeting studies (de la Fuente and Berry 2005; Berry et al. 2007) but not for enhancing the cellular uptake of siRNA.

Here we describe the straightforward, reproducible one-step synthesis of positively charged gold nanoparticles (GNPs) surface-coated with cysteamine and a cationic CPP modified from the Tat_{48–60} sequence, the characterization of the particles with various methods, complex formation with siRNA and subsequent transfection of ARPE-19 cells stably producing the reporter protein secreted alkaline phosphatase (SEAP). Our purpose was to produce good quality peptide-modified GNPs by facile synthesis methods, characterize them thoroughly, and investigate their efficacy in the intracellular delivery of anti-SEAP siRNA as well as their effect on the growth and viability of SEAP-ARPE-19 cells.

8.2 Materials and methods

8.2.1 Peptide synthesis

Tat-related CPP (H-CGRKKRWWPQRWWRWWRPPQ-OH) (Subrizi et al. 2012) was synthesized with ACT-396 peptide synthesizer, using Wang resin, double coupling standard Fmoc-chemistry protocols, TBTU/HOBT as coupling reagent, 2% DBU/2% piperidine in NMP for Fmoc deprotection, and a mixture of phenol:H₂O:EDT:thioanisole:TFA (1.5:1:1:1:10) for 2 h at room temperature for final cleavage and deprotection. All coupling reagents, amino acid derivatives and resins were purchased from GL Biochem Ltd (Shanghai, China). After cleavage and deprotection, the crude peptide was precipitated with ice-cold diethyl ether, filtered,

dried and analyzed by RP-HPLC (HP 1050 series chromatography, Supelco Discovery C18 column, 15 cm × 4.6 mm, 5 μm, λ = 220 nm, linear gradient from 0 to 60% B in 40 min; A = 0.1% TFA; B = 0.1% TFA in 80% MeCN). Purification was performed by RP-HPLC (Supelco Ascentic™ C18 semi-preparative column, 15 cm × 10 mm, 5 μm). After purification the peptide was freeze-dried, its purity was analyzed by RP-HPLC (Supelco Discovery C18 column, 15 cm × 4.6 mm, 5 μm, λ = 220 nm, linear gradient from 0 to 50% B in 40 min; A = 0.05 M KH₂PO₄, pH 3.0; B = 0.05 M KH₂PO₄ in 70% MeCN, pH 3.0), and it was characterized by MALDI-TOF mass spectrometry. The peptide was stored frozen at -20°C.

8.2.2 Oligonucleotide synthesis

All siRNAs were synthesized with ASM-800 DNA/RNA synthesizer. Each strand was synthesized separately following standard RNA synthesis protocols, using TOM-protected monomers purchased from Glen Research (Sterling, VA, USA), and following standard protocols for cleavage and deprotection. The oligonucleotides were then purified by ion-exchange HPLC (TOSOH TSKgel DEAE-2SW column, 25 cm × 4.6 mm, λ = 280 nm, linear gradient from 0 to 50% B in 30 min; A = 0.1 M sodium acetate in 20% MeCN; B = A + 0.4 M sodium perchlorate), desalted either by gel permeation chromatography (Sephadex G-10 column, 10 × 150 mm, elution with RNase-free water at a flow rate of 0.5 ml/min) or by using PolyPak II cartridges (Glen Research) following standard protocol, and kept frozen in water solution at -70°C. The siRNAs were quantified by measuring the absorbance of each strand at 260 nm, assuming the generally accepted amount of single-stranded RNA per optical unit (1 OD = 40 μg/ml). The siRNA strands were annealed immediately prior to biological experiments following standard procedures in Dharmacon siRNA buffer (20 mM KCl, 6 mM HEPES, 0.2 mM MgCl₂ × 6H₂O, pH 7.5).

Model double-stranded oligodeoxyribonucleotide was synthesized with the same equipment using monomers purchased from Glen Research and following standard DNA coupling protocol. It was cleaved/deprotected, purified and characterized in the same manner as described above.

8.2.3 Synthesis of cell-penetrating peptide-modified gold nanoparticles

The cell-penetrating peptide-modified gold nanoparticles (CPP-GNPs) with a 40:1 ratio (mol/mol) of the surface stabilizing agent (cysteamine) and CPP, were prepared with the following method: 5 mg (14 μmol) of gold(III)chloride trihydrate (ACS Reagent; Sigma-Aldrich, St. Louis, MO, USA) was dissolved in 5 ml of deionized water and, while stirring, 2.4 mg (21.2 μmol) of cysteamine (98%, Fluka, Sigma-Aldrich) and 1.55 mg (0.53 μmol) of peptide co-dissolved in 4 ml of deionized water was added. After 5 min of stirring at room temperature, a solution of 0.02 mg of NaBH₄ (98.5%, Sigma-Aldrich) in 0.5 ml of deionized water was added dropwise within 20 min and the reaction mixture was left overnight under vigorous stirring. The reaction mixture was transferred into a dialysis tube (MWCO 12–14 kDa; Medicell International Ltd., London, UK) and dialyzed against deionized water for

48 h. The resulting colloidal solution of CPP–GNPs was kept in a glass flask at room temperature. All other CPP–GNPs were synthesized in a similar manner, varying only the ratio between CPP and cysteamine as mentioned in Table 1. The concentration of CPP–GNPs (mg/ml) was calculated from the amount of gold chloride added to the reaction solution, assuming 100% reduction, resulting in a CPP–GNP solution containing 0.5 mg/ml gold (5 mg of gold chloride in a total volume of 9.5 ml). After determining the diameter of the particles, the average amount of gold atoms per particle and the molar concentration of the solution were calculated using the formulae from Liu et al. (2007):

$$(1) \quad N = \frac{\pi \rho D^3}{6M} N_A,$$

where N = the average number of gold atoms per particle, ρ = density for fcc gold (19.3 g/cm³), D = particle diameter (cm), M = atomic weight of gold (197 g/mol), and N_A = Avogadro's constant, and

$$(2) \quad C = \frac{N_{total}}{NVN_A},$$

where N_{total} = total number of gold atoms (equivalent to the initial amount of gold salt added to the reaction solution) and V = the volume of the reaction solution (in liters). The molar concentration calculated for 20-nm CPP–GNPs was 10 nM.

8.2.4 Preparation of siRNA/gold nanoparticle complexes

The complexes were prepared 30 minutes prior to use by mixing the corresponding amounts of double-stranded siRNA in RNase-free water and CPP–GNP. Different siRNA:gold ratios (by mass) were prepared and tested for complex stability by electrophoresis, using a double-stranded oligodeoxyribonucleotide as a model for siRNA (see next section).

8.2.5 Characterization of gold nanoparticles and siRNA/gold nanoparticle complexes

Transmission electron microscopy. The CPP–GNPs were visualized with JEOL 1200-EX II transmission electron microscope on carbon-coated copper grids with magnifications from 100 K to 200 K. The particle diameters were measured manually with Scion Image 4.0.2 software (Scion Corporation, Frederick, MD, USA).

UV/VIS spectroscopy. Optical spectra from 200 to 800 nm of the CPP–GNPs and siRNA/CPP–GNP complexes were measured with Cary 100 Conc UV/VIS spectrophotometer (Varian, Agilent Technologies, Santa Clara, CA, USA).

Loading measurements. After the reaction of CPP-modified GNPs had been completed, an 1-ml aliquot of the reaction mixture was analyzed for the presence of free CPP by RP-HPLC as following. The CPP–GNPs were precipitated by adding 100

μ l of 2 M HCl and centrifuged. The amount of unattached peptide in the supernatant was analyzed by RP-HPLC as described for peptide synthesis and compared to a calibration curve obtained for peptide concentrations from 0.05 to 1.0 mg/ml.

Gel electrophoresis. A double-stranded oligodeoxynucleotide, bearing the same sequence as the active siRNA, was synthesized to serve as a model compound for siRNA/ CPP-GNP complex stability. Different oligonucleotide:peptide mass ratios were prepared and tested with 15% PAGE, using GeneRuler™ DNA ladder (Ultra low range, 10 bp; Fermentas, Thermo Scientific Life Sciences, Waltham, MA, USA) as MW standard, to see if the complexes were stable. Lability of the complexes would be seen as presence of free oligonucleotide on the gel.

8.2.6 Engineering of stable ARPE-19 cell lines expressing secreted alkaline phosphatase

To produce a cell line stably expressing secreted alkaline phosphatase (SEAP), human ARPE-19 retinal pigment epithelial cells (CRL-2302™; ATCC, Manassas, VA, USA) were seeded on 100 mm culture dishes (1×10^6 cells/dish). After overnight culture, the cells were transfected with 7 μ g of pCMV-SEAP2/neo reporter plasmid (Wikström et al. 2008) complexed with 25 kDa branched poly(ethylene imine) (PEI25; Sigma-Aldrich, St. Louis, MO, USA) at a charge ratio of +4. Cells were cultured in the presence of 0.8 mg/ml neomycin analog, G418 (Calbiochem, Merck KGaA, Darmstadt, Germany), as a selective agent. Formed cell colonies were trypsinized and expanded in 48-well plates with medium containing 0.6 mg/ml G418. The SEAP expression levels of the cells were quantified by using a chemiluminescent assay (The Great EscAPe SEAP Kit; Clontech, Mountain View, CA, USA). Several cell colonies displaying various SEAP expression levels and normal growth rate were chosen for future experiments.

8.2.7 Cell culture and transfection

SEAP-ARPE-19 cells (colony 12.7, P5–15) were cultured in DMEM/F-12 (Gibco, Life Technologies Corporation, Carlsbad, CA, USA) supplemented with 10% fetal bovine serum (FBS), 50 IU/ml penicillin, 50 μ g/ml streptomycin, 2 mM L-glutamine, and 0.4 μ g/ml G418 (Geneticin®, Gibco). The cells were grown at 37°C under a 7% CO₂ atmosphere and subcultured once a week. For transfection, the cells were seeded on 96-well plates (Nunc, ThermoFisher Scientific, Waltham, MA, USA) at a density of 10^4 cells per well in 100 μ l of growth medium. After 24 h of incubation, the cells were washed with PBS, and 100 μ l of transfection mixtures diluted either in Opti-MEM (Gibco) or DMEM/F-12 (supplemented as mentioned above but without G418) were added. The first experiment was conducted by washing the cells with PBS and adding 100 μ l of fresh DMEM/F-12 growth medium 3 h after transfection, followed by SEAP assay at 6, 24 and 48 hours after transfection to see how the expression changed over time and if it was affected by the CPP–GNPs. In other experiments, the cells were tested for SEAP production and/or cell viability either 24 h or 48 h after transfection. In the latter case, fresh medium was added to the cells 24 h post-transfection. In one experiment, the effect of CPP–GNPs on the

proliferation of cells was studied by transfecting the cells with CPP–GNPs and counting the amount of transfected and non-transfected cells at 24 and 48 h after transfection. The cells were counted manually using erythrosine dye and a Bürker counting chamber.

8.2.8 Cell viability assay

The viability of transfected cells was tested using the MTT assay. First, a 5 mg/ml solution of MTT (thiazolyl blue tetrazolium bromide, BioReagent, ≥97.5%, Sigma-Aldrich, St. Louis, MO, USA) was prepared in PBS and filtered through a 0.2 µm membrane. After transfection and either 24 or 48 hours of incubation, the cells were washed with PBS, and 100 µl of a mixture of DMEM/F-12 and the MTT solution (10:1, v/v) was added to each well, including negative control wells without cells and positive control wells with non-transfected cells. The cells were incubated for 2 h at 37°C and 7% CO₂. After this the medium was removed and 100 µl of DMSO (BioReagent, ≥99.9%, Sigma-Aldrich) was added to dissolve the formazan crystals formed by intact cells. Absorbance at 570 nm was then measured with VarioSkan Flash multimode reader (ThermoFisher Scientific, Waltham, MA, USA). Cell viability was expressed as percentage of positive control after subtracting the negative control from all values. To ensure that the gold did not interfere with the absorbance measurement, cells transfected with high concentrations of CPP–GNPs were tested using a modified assay where only growth medium was added to the cells instead of the medium–MTT mixture.

8.2.9 SEAP expression assay

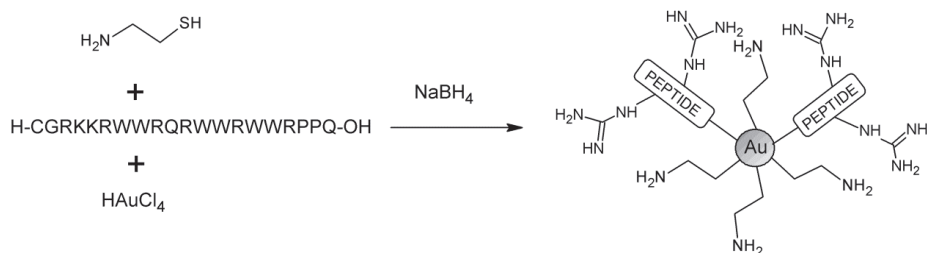
The SEAP production of the cells was analyzed using the Great EscAPe SEAP Chemiluminescence Kit 2.0 (Clontech, Mountain View, CA, USA). A typical assay was performed in the following way: After transfection and incubation, 60-µl samples were taken from the growth medium. The samples were centrifuged at 12,000 rpm for 1 min, the supernatants were transferred to new tubes, and stored at –20°C until assaying. The thawed samples were then diluted 20 times in conditioned growth medium, 15 µl aliquots were transferred to a 96-well plate (white IsoPlate or Optiplate; PerkinElmer Inc., Waltham, MA, USA), and 45 µl of 1x Dilution Buffer from the kit was added. The sealed plate was incubated at 65°C for 30 min, the samples were cooled on ice for 2–3 min, and equilibrated to room temperature. SEAP substrate solution (60 µl) was then added, the samples were incubated at room temperature for 60 min, and the SEAP signal was detected using either Microbeta 1450 luminometer/liquid scintillation counter (Wallac, PerkinElmer Inc.) or VarioSkan Flash multimode reader (ThermoFisher Scientific, Waltham, MA, USA).

8.3 Results and discussion

8.3.1 Synthesis and characterization

The synthesis of CPP–GNPs is a modified version of the Brust–Schiffrin reaction (Brust et al. 1994), using NaBH_4 as reductive agent, and its more recent water-soluble variant yielding 30-nm cysteamine-coated cationic GNPs (Niidome et al. 2004). Our reaction introduces the cysteamine and the CPP in one step (**Scheme 1**), resulting in a mixed monolayer of cysteamine moieties and two to three CPP residues per nanoparticle, as determined by assaying unattached peptide from the reaction mixture. The most favorable cysteamine:CPP ratio was found to be 40:1 (mol/mol), as it produced the most stable nanoparticles (data not shown). TEM analysis revealed spherical GNPs with a diameter of 22.1 ± 4.5 nm (mean \pm SD; $n = 23$) (**Figure 1a**), while two other batches gave diameters of 20.9 ± 3.5 nm ($n = 50$) and 13.4 ± 2.0 nm ($n = 50$). The UV/VIS spectrum of CPP–GNPs showed a surface plasmon resonance band at about 520 nm (**Figure 1b**), characteristic for gold nanospheres of this size range (Link and El-Sayed 1999; Jain et al. 2006). The absorbance of siRNA/CPP–GNP complexes was strongly red-shifted and broadened. This may reflect some degree of interparticle aggregation into larger clusters due to charge neutralization, as was seen previously for siRNA/cysteamine-coated GNP complexes (Lee et al. 2008).

Scheme 1 Synthesis of cell-penetrating peptide-modified gold nanoparticles (CPP–GNPs).



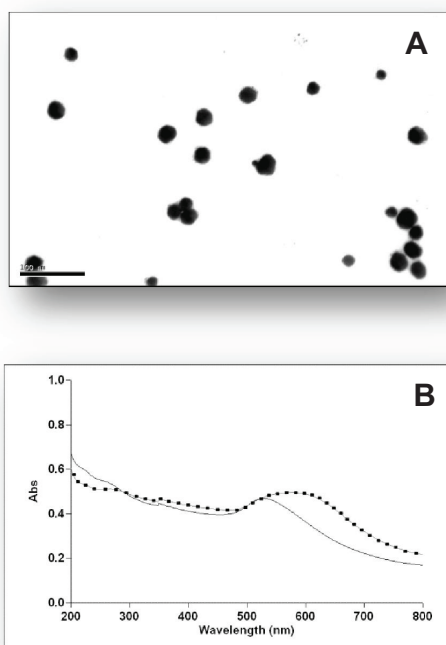


Figure 1 (a) TEM image of cell-penetrating peptide-modified gold nanoparticles (CPP-GNPs; magnification 300 K). (b) UV/VIS spectra of CPP-GNPs (*straight line*) and their complexes with anti-SEAP siRNA-1795 (siRNA/CPP-GNPs, 1:40 by mass) (*dotted line*).

8.3.2 Complex formation with siRNA

The stability of siRNA/CPP-GNP complexes was studied by gel electrophoresis using a model oligonucleotide instead of siRNA (**Figure 2**). Complexes with a 1:40 ratio of oligonucleotide to gold (w/w) exhibited higher stability than complexes with ratios 1:10 to 1:30, as assessed from the absence of free oligonucleotide on the gel, and were therefore used in the biological experiments. A weight excess of gold was also desired to maintain the complexes sufficiently cationic for cell adhesion. In 1:40 (w/w) complexes, the corresponding molar ratio remains in favor to siRNA (about 100:1 siRNA:gold). However, Lee et al. (2008) found that a single cysteamine-coated 15-nm GNP may have over 5000 primary amine groups on its surface, which would in our case translate into an N/P ratio of approximately 1.25. Moreover, Niidome et al. (2004) successfully transfected HeLa cells with plasmid DNA:cysteamine-coated GNP complexes with a weight ratio of 1:17, even though plasmid DNA is significantly larger and contains more negative charges than siRNA. Thus the cationic charge of our complexes should be more than enough to allow for cellular uptake.

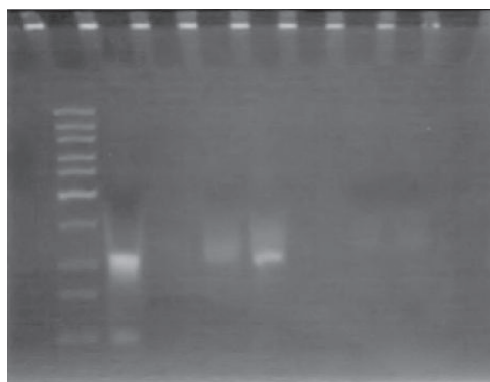


Figure 2 Gel electrophoresis (15% PAGE) of complexes of model oligonucleotide and cell-penetrating peptide-modified gold nanoparticles (CPP–GNPs). Lane 1, 10 bp DNA ladder; lane 2, free oligonucleotide; lane 3, empty; lane 4, complex 1:10 (oligonucleotide: gold m/m); lane 5, complex 1:20; lane 6, complex 1:30; lane 7, complex 1:40; lane 8, complex 1:80. The absence of free oligonucleotide indicates stable complexes that are retained in the wells.

8.3.3 Cell viability

Gold nanoparticles with different sizes and surface modifications have been shown to be non-toxic in various cell lines (Connor et al. 2005; Shukla et al. 2005; Arnida et al. 2010). Since Lee et al. (2008) found no cytotoxicity for their cationic cysteamine-coated GNPs similar to our particles, it can be hypothesized that any toxicity caused by our particles would probably be due to the peptide. The native Tat peptide has been found to be relatively non-toxic in various cell lines at concentrations up to 100 μM (Cardozo et al. 2007; Sugita et al. 2008). Our modified Tat peptide was previously found non-toxic in ARPE-19 cells at 2 μM , corresponding to 0.6 μg in 100 μl (Subrizi et al. 2012). Here the CPP concentration might be even lower if the CPP–GNPs contained only GNP-bound peptide; however, it cannot be overlooked that the solution may contain free unbound peptide even after dialysis. Hence, to obtain full toxicity profile for the CPP, we tested the cell viability over a range of concentrations from 2 μM up to 153 μM , which exceeds the theoretical maximum concentration estimated from the amount of peptide added to the CPP–GNP synthesis reaction, 0.16 mg/ml. **Table 1** shows the toxicity (as decrease in cell viability compared to positive control cells) of different CPP concentrations found by MTT assay. First we tested the toxicity 24 hours after transfection in a reduced-serum medium (Opti-MEM). Pure peptide at the theoretical maximum concentrations was compared to the corresponding amounts of CPP–GNPs and siRNA/CPP–GNP complexes at siRNA doses of 0.3 to 1.0 μg (**Figure 3**). The peptide was non-toxic up to 15 μM (4 μg) and exhibited 50% toxicity at 30 μM (9 μg) and 90% toxicity at 45 μM (13 μg). Remarkably, the CPP–GNPs and siRNA/CPP–GNP complexes show a cell viability of more than 100% compared to untreated positive control cells. The fact that the gold nanoparticles increased the amount of formazan produced in the MTT assay to almost 200% is indicative of increased

cellular proliferation and is discussed in more detail in section 7.3.4. These results seem to provide additional proof to the well-known fact that CPPs lose their toxicity when they are bound to nanoparticles (M. Antopolsky, personal communication). However, since the MTT assay only measures the extent of proliferation and does not analyze its causes, it is difficult to assess if the GNP-stimulated proliferation is covering any toxic effects in our case.

Table 1. Cell-penetrating peptide (CPP)-associated toxicity in SEAP-ARPE-19 cells.

Concentration of CPP (μM)	Amount of CPP (μg)	24-hour toxicity (Opti-MEM)	48-hour toxicity (Opti-MEM)	48-hour toxicity (DMEM/F-12)
2	0.6	non-toxic	–	–
15	4.4	non-toxic	non-toxic	25%
30	8.8	50%	–	–
45	13.2	90%	non-toxic	non-toxic
95	28	–	80%	70%
153	45	–	98%	94%

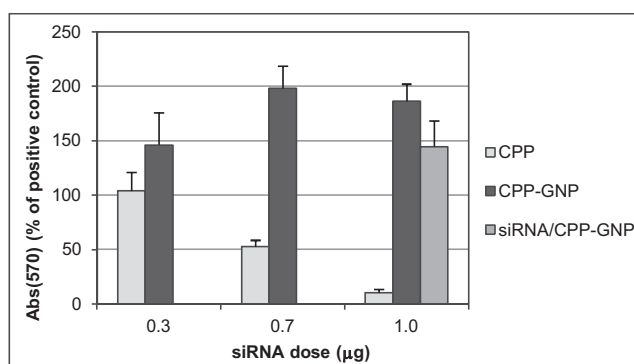


Figure 3 SEAP-ARPE-19 cell viability (mean \pm SEM; $n = 3$) 24 h after transfection with cell-penetrating peptides (CPP), CPP-modified gold nanoparticles (CPP–GNPs), and their complexes with anti-SEAP siRNA-1795 (siRNA/CPP–GNPs; 1:40 by mass) in reduced-serum medium (Opti-MEM). [For siRNA doses of 0.3 μg , 0.7 μg , and 1.0 μg , the corresponding amounts of CPP are 4 μg , 9 μg , and 13 μg (15 μM , 30 μM , and μM), respectively.]

Unexpectedly, when we performed the MTT assay 48 hours after transfection, the peptide appeared significantly less toxic; it did not show 90% toxicity until at 153 μM (45 μg ; data not shown) and was non-toxic up to 41 μM (12 μg) (**Figure 4**). This initial plummet in cell viability at 24 h post-transfection raises a question whether it results from an early shock after membrane perturbation by the CPP, followed by gradual recovery of cellular proliferation. The study by Subrizi et al. (2012), however, found no evidence of non-endocytic cell entry for this peptide, although it had interacted with a model membrane more strongly than the native Tat peptide.

However, their study used relatively low peptide concentrations (2 μM), while Duchardt et al. (2007) had observed concentration-dependence in Tat uptake, rapid non-endocytic uptake occurring at concentrations exceeding 10 μM . In any case, it might be worthwhile to do additional toxicity testing with methods that measure cell membrane integrity such as the LDH (lactate dehydrogenase) release assay; this would also provide a more mechanistic insight into the apparent stimulation of proliferation caused by CPP–GNPs. Repeated 48-hour MTT assays confirmed that significant toxicity, exceeding that of Lipofectamine 2000, starts at 95 μM (28 μg), which is beyond the theoretical maximum CPP concentration in the CPP–GNP solution (**Figure 4**). It must be noted that in this experiment the CPP was tested at higher concentrations, which are directly comparable to CPP–GNP but do not represent the amounts present in the CPP–GNP solution. Expectedly, the gold nanoparticles showed no toxicity at any of the concentrations studied. However, here we did not observe the increased cellular proliferation which was seen in the 24-hour assay. A transfection in a medium containing 10% fetal bovine serum (DMEM/F-12) gave similar results, except that the cell viability was again increased by CPP–GNPs in some cases and Lipofectamine 2000 was less toxic than in serum-free medium (**Figure 5**). Naked siRNA showed no significant toxicity (data not shown), and the complexes of siRNA with CPP and CPP–GNPs at a 1:40 (w/w) ratio showed no difference to naked CPP and CPP–GNPs, respectively (**Figures 3–5**).

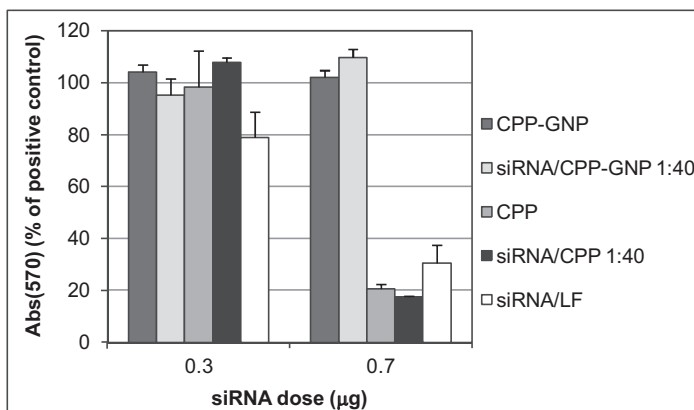


Figure 4 SEAP-ARPE-19 cell viability (mean \pm SEM; $n=3$) 48 h after transfection with cell-penetrating peptide-modified gold nanoparticles (CPP–GNP), anti-SEAP siRNA-1795 complexes with CPP–GNPs (siRNA/CPP–GNP, 1:40 by mass), cell-penetrating peptide (CPP; 12 μg and 28 μg), siRNA-1795 complexes with CPP (siRNA/CPP, 1:40 by mass), and siRNA-1795 complexes with Lipofectamine 2000 (siRNA/LF; 3.57 μl LF per μg siRNA) in reduced-serum medium (Opti-MEM).

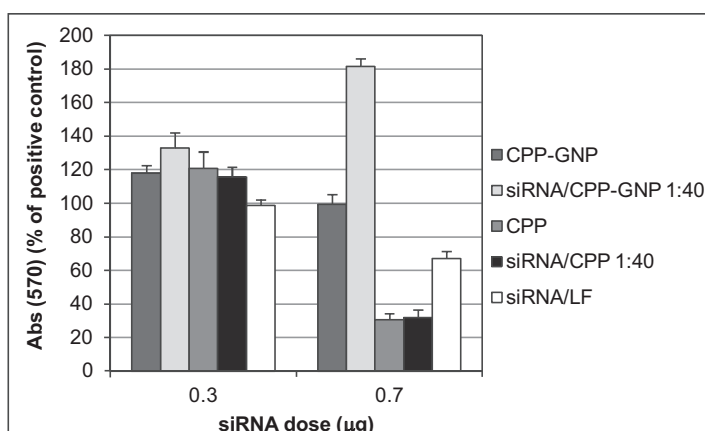


Figure 5 SEAP-ARPE-19 cell viability (mean \pm SEM; n=3) 48 h after transfection with cell-penetrating peptide-modified gold nanoparticles (CPP-GNP), anti-SEAP siRNA-1795 complexes with CPP-GNPs (siRNA/CPP-GNP, 1:40 by mass), cell-penetrating peptide (CPP; 12 μ g and 28 μ g), siRNA-1795 complexes with CPP (siRNA/CPP, 1:40 by mass), and siRNA-1795 complexes with Lipofectamine 2000 (siRNA/LF; 3.57 μ l LF per μ g siRNA) in serum-containing medium (DMEM/F-12).

8.3.4 Effect of gold nanoparticles on SEAP secretion

In the first experiment, we aimed to establish an understanding on how the SEAP secretion of SEAP-ARPE-19 cells develops over time. We found the SEAP secretion to be at its greatest at 24 h after transfection with CPP-GNPs (48 h after seeding on 96-well plate) in untreated cells (**Figure 6**). Surprisingly, the CPP-GNPs were found to increase the SEAP secretion compared to untreated cells. The increase seemed dose-dependent and close to linear at 6 h and 24 h after transfection; however, the effect was lost and even slightly reversed at 48 h. In accordance with these findings, our studies indicated a corresponding increase in the number of cells after incubating with CPP-GNPs (data not shown) as well as a cell viability of more than 100% in the MTT assay (*vide ultra*). The reason for this unexpected phenomenon is not known but might be related to the fact that 30-nm GNPs have been shown to stimulate the proliferation of human prostate cancer cells (Arnida et al. 2010). The authors speculated that this stimulation might arise from the previously demonstrated ability of GNPs to reduce the amount of reactive oxygen species in macrophages (Shukla et al. 2005). Smaller GNPs with a diameter of 5 nm, in contrast, have been found to inhibit the proliferation of multiple myeloma cells (Bhattacharya et al. 2007). It is noteworthy that the GNP sizes, the surface chemistries and the cell types are different in these studies, which may affect the GNP-cell interactions significantly. Due to the large extent and the almost linear nature of the increase in SEAP signal, we decided to take it into account in the gene silencing results and to use it as a reference control in addition to untreated cells.

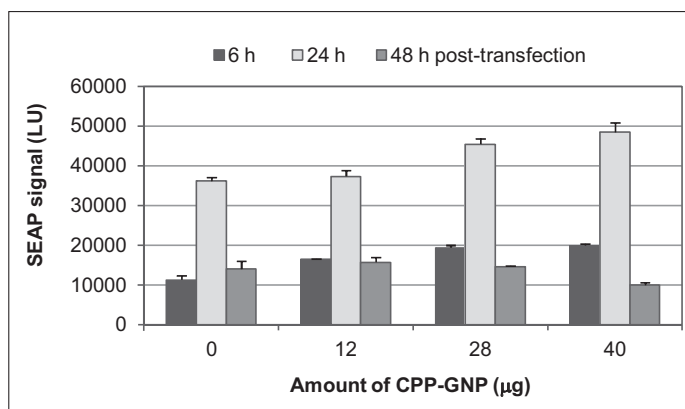


Figure 6 SEAP production of SEAP-ARPE-19 cells (mean \pm SEM, n = 3) 6 h, 24 h and 48 h after transfection with cell-penetrating peptide-modified gold nanoparticles (CPP-GNPs) in reduced-serum medium (Opti-MEM).

8.3.5 Gene silencing

The first transfections were performed using the previously reported (Khvorova et al. 2003) anti-SEAP siRNA 2217 (antisense strand: 5'-UGA CAA CGG GCA ACA ACU CdTdT-3'), but no effect was seen below a dose of 0.7 μ g (data not shown). Sequence 1795 (5'-UGA CAA CGG GCA ACA ACU CdTdT-3') (Khvorova et al. 2003), in turn, was found active at a dose of 0.5 μ g when used as a complex with CPP-GNPs (**Figure 7**) but not as naked siRNA. At a dose of 0.7 μ g, it caused a 49% gene knockdown compared to untreated cells, measured 24 h after transfection. Furthermore, when compared to the elevated SEAP levels caused by the CPP-GNPs (*vide ultra*), termed from this point forward as 'expected SEAP', the gene silencing effect was as high as 75%. Similar results were obtained in serum-containing medium (DMEM/F-12), where the same dose of siRNA/CPP-GNPs caused a gene knockdown of 85% compared to untreated cells and 93% compared to expected SEAP, although the results were obscured by the fact that even naked siRNA caused a 59% knockdown (**Figure 8**). Transfected in DMEM/F-12 and measured 48 hours after transfection, the CPP-GNPs decrease rather than increase the SEAP secretion (**Figure 9**), as was seen in section 7.3.4 (**Figure 6**). Hence the 92% knockdown caused by siRNA/CPP-GNPs is reduced to 84% when compared to expected SEAP instead of untreated cells. In this experiment, naked siRNA was not active, but an unexplained increase in SEAP secretion by naked siRNA and lower concentration of siRNA/CPP-GNPs were seen. These discrepancies warrant further studies to confirm a true specific RNA interference mechanism by mRNA expression studies and new experiments with additional controls. Nevertheless, these preliminary results indicate that the CPP-GNPs are indeed able to carry siRNA into cells in an active form. Furthermore, the anti-SEAP siRNA remains active in the presence of 10% FBS, indicating that it is protected against serum nucleases by the gold particles.

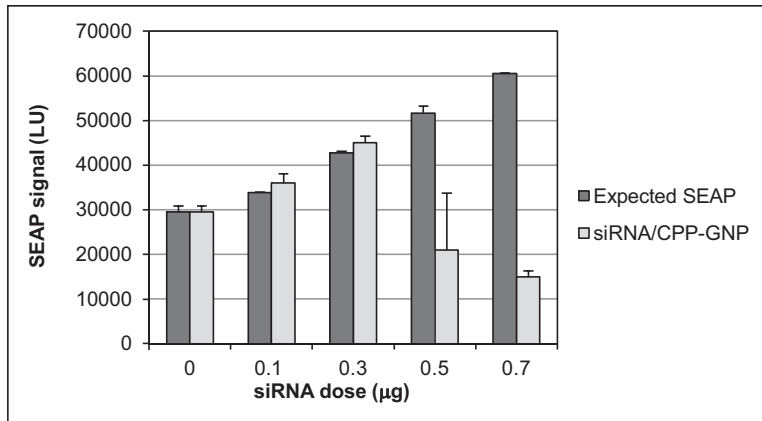


Figure 7 SEAP secretion of SEAP-ARPE-19 cells (mean \pm SEM; n=2) 24 h after transfection with cell-penetrating peptide-modified gold nanoparticles (CPP-GNPs) ('expected SEAP') or their complexes with anti-SEAP siRNA-1795 (siRNA/CPP-GNPs, 1:40 by mass) in reduced-serum medium (Opti-MEM).

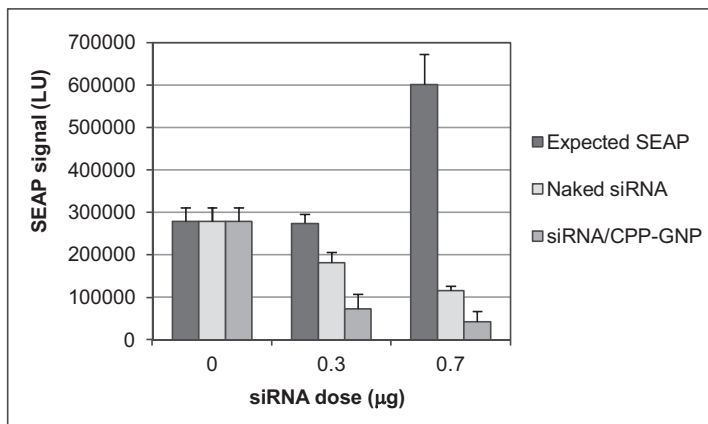


Figure 8 SEAP secretion of SEAP-ARPE-19 cells (mean \pm SEM; n=3) 24 h after transfection with cell-penetrating peptide-modified gold nanoparticles (CPP-GNPs) ('expected SEAP'), naked anti-SEAP siRNA-1795, or siRNA-1795 complexes with CPP-GNPs (siRNA/CPP-GNPs, 1:40 by mass) in serum-containing medium (DMEM/F-12).

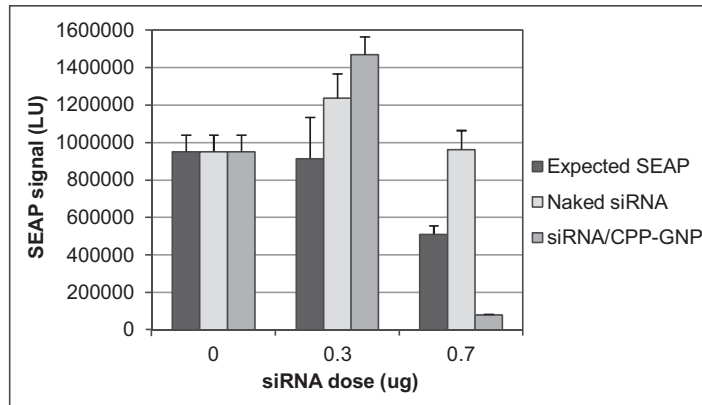


Figure 9 SEAP secretion of SEAP-ARPE-19 cells (mean \pm SEM; $n=3$) 48 h after transfection with cell-penetrating peptide-modified gold nanoparticles (CPP-GNPs) ('expected SEAP'), naked anti-SEAP siRNA-1795, or siRNA-1795 complexes with CPP-GNPs (siRNA/CPP-GNPs, 1:40 by mass) in serum-containing medium (DMEM/F-12).

8.4 Conclusions

Herein we developed a straightforward, reproducible one-step method to synthesize positively charged gold nanoparticles surface-modified with a mixed monolayer of cysteamine and a Tat-derived cell-penetrating peptide sequence. The peptide-modified gold nanoparticles proved non-toxic at all concentrations studied, while the peptide itself was toxic at high concentrations. Anti-SEAP siRNA as complex with the gold particles caused a significant and dose-dependent gene silencing effect. This effect was not lost in the presence of serum, indicating that siRNA is protected from enzymatic degradation. Furthermore, our studies revealed an unexpected phenomenon where the gold particles increased both the cell viability and SEAP secretion above those of control cells, possibly due to gold nanoparticle-induced stimulation of cellular proliferation.

Acknowledgements

We would like to thank Ms. Juliette Leguevaques, Erasmus exchange student from University of Nice Sophia Antipolis, for helping with the experiments. We thank the Electron Microscopy Unit of the Institute of Biotechnology for providing laboratory facilities. Academy of Finland grant NapGen (project number 128105) and Tekes PrinCell project are acknowledged for providing financial support.

8.5 References

Antopolsky M, Azhayeva E, Tengvall U, Auriola S, Jääskeläinen I, Rönkkö S, Honkakoski P, Urtti A, Lönnberg H, Azhayev A. 1999. Peptide-oligonucleotide phosphorothioate

- conjugates with membrane translocation and nuclear localization properties. *Bioconjugate Chem.* 10(4): 598–606.
- Arnida, Malugin A, Ghandehari H. 2010. Cellular uptake and toxicity of gold nanoparticles in prostate cancer cells: a comparative study of rods and spheres. *J Appl Toxicol.* 30(3): 212–217.
- Arthanari Y, Pluen A, Rajendran R, Aojula H, Demonacos C. 2010. Delivery of therapeutic shRNA and siRNA by Tat fusion peptide targeting BCR-ABL fusion gene in chronic myeloid leukemia cells. *J Control Release.* 145(3): 272–280.
- Beltinger C, Saragovi HU, Smith RM, LeSauteur L, Shah N, DeDionisio L, Christensen L, Raible A, Jarett L, Gewirtz AM. 1995. Binding, uptake, and intracellular trafficking of phosphorothioate-modified oligodeoxynucleotides. *J Clin Invest.* 95(4): 1814–1823.
- Bennett CF, Swayze EE. 2010. RNA targeting therapeutics: molecular mechanisms of antisense oligonucleotides as a therapeutic platform. *Annu Rev Pharmacol Toxicol.* 50: 259–293.
- Berry CC, de la Fuente JM, Mullin M, Chu SW, Curtis AS. 2007. Nuclear localization of HIV-1 tat functionalized gold nanoparticles. *IEEE Trans Nanobioscience.* 6(4): 262–269.
- Bhattacharya R, Patra CR, Verma R, Kumar S, Greipp PR, Mukherjee P. 2007. Gold nanoparticles inhibit the proliferation of multiple myeloma cells. *Adv Mater.* 19(5): 711–716.
- Braun GB, Pallaoro A, Wu G, Missirlis D, Zasadzinski JA, Tirrell M, Reich NO. 2009. Laser-activated gene silencing *via* gold nanoshell–siRNA conjugates. *ACS Nano.* 3(7): 2007–2015.
- Brust M, Walker M, Bethell D, Schiffrin DJ, Whyman R. 1994. Synthesis of thiol-derivatised gold nanoparticles in a two-phase liquid–liquid system. *J Chem Soc, Chem Commun.* 1994(7): 801–802.
- Cardozo AK, Buchillier V, Mathieu M, Chen J, Ortis F, Ladrière L, Allaman-Pillet N, Poirot O, Kellenberger S, Beckmann JS, et al. 2007. Cell-permeable peptides induce dose- and length-dependent cytotoxic effects. *Biochim Biophys Acta.* 1768(9): 2222–2234.
- Chithrani BD, Ghazani AA, Chan WC. 2006. Determining the size and shape dependence of gold nanoparticle uptake into mammalian cells. *Nano Lett.* 6(4): 662–668.
- Chiu YL, Ali A, Chu CY, Cao H, Rana TM. 2004. Visualizing a correlation between siRNA localization, cellular uptake, and RNAi in living cells. *Chem Biol.* 11(8): 1165–1175.
- Connor EE, Mwamuka J, Gole A, Murphy CJ, Wyatt MD. 2005. Gold nanoparticles are taken up by human cells but do not cause acute cytotoxicity. *Small.* 1(3): 325–327.
- Davis ME, Zuckerman JE, Choi CH, Seligson D, Tolcher A, Alabi CA, Yen Y, Heidel JD, Ribas A. 2010. Evidence of RNAi in humans from systemically administered siRNA via targeted nanoparticles. *Nature.* 464(7291): 1067–1070.
- de la Fuente JM, Berry CC. 2005. Tat peptide as an efficient molecule to translocate gold nanoparticles into the cell nucleus. *Bioconjugate Chem.* 16(5): 1176–1180.
- Duchardt F, Fotin-Mleczek M, Schwarz H, Fischer R, Brock R. 2007. A comprehensive model for the cellular uptake of cationic cell-penetrating peptides. *Traffic.* 8(7): 848–866.
- Fonseca SB, Pereira MP, Kelley SO. 2009. Recent advances in the use of cell-penetrating peptides for medical and biological applications. *Adv Drug Deliv Rev.* 61(11): 953–964.
- Ghosh P, Han G, De M, Kim CK, Rotello VM. 2008. Gold nanoparticles in delivery applications. *Adv Drug Deliv Rev.* 60(11): 1307–1315.
- Giljohann DA, Seferos DS, Patel PC, Millstone JE, Rosi NL, Mirkin CA. 2007. Oligonucleotide loading determines the cellular uptake of DNA-modified gold nanoparticles. *Nano Lett.* 7(12): 3818–3821.
- Jääskeläinen I, Peltola S, Honkakoski P, Mönkkönen J, Urtti A. 2000. A lipid carrier with a membrane active component and a small complex size are required for efficient cellular

- delivery of anti-sense phosphorothioate oligonucleotides. *Eur J Pharm Sci.* 10(3): 187–193.
- Jain PK, Lee KS, El-Sayed IH, El-Sayed MA. 2006. Calculated absorption and scattering properties of gold nanoparticles of different size, shape, and composition: applications in biological imaging and biomedicine. *J Phys Chem B.* 110(14): 7238–7248.
- Juliano R, Bauman J, Kang H, Ming X. 2009. Biological barriers to therapy with antisense and siRNA oligonucleotides. *Mol Pharm.* 6(3): 686–695.
- Jung J, Solanki A, Memoli KA, Kamei K, Kim H, Drahl MA, Williams LJ, Tseng HR, Lee K. 2010. Selective inhibition of human brain tumor cells through multifunctional quantum-dot-based siRNA delivery. *Angew Chem Int Ed Engl.* 49(1): 103–107.
- Kanazawa T, Sugawara K, Tanaka K, Horiuchi S, Takashima Y, Okada H. 2012. Suppression of tumor growth by systemic delivery of anti-VEGF siRNA with cell-penetrating peptide-modified MPEG–PCL nanomicelles. *Eur J Pharm Biopharm.* 81(3): 470–477.
- Khvorova A, Reynolds A, Jayasena SD. 2003. Functional siRNAs and miRNAs exhibit strand bias. *Cell.* 115(2): 209–216.
- Kong WH, Bae KH, Jo SD, Kim JS, Park TG. 2012. Cationic lipid-coated gold nanoparticles as efficient and non-cytotoxic intracellular siRNA delivery vehicles. *Pharm Res.* 29(2): 362–374.
- Lee JS, Green JJ, Love KT, Sunshine J, Langer R, Anderson DG. 2009. Gold, poly(β -amino ester) nanoparticles for small interfering RNA delivery. *Nano Lett.* 9(6): 2402–2406.
- Lee SH, Bae KH, Kim SH, Lee KR, Park TG. 2008. Amine-functionalized gold nanoparticles as non-cytotoxic and efficient intracellular siRNA delivery carriers. *Int J Pharm.* 364(1): 94–101.
- Link S, El-Sayed MA. 1999. Spectral properties and relaxation dynamics of surface plasmon electronic oscillations in gold and silver nanodots and nanorods. *J Phys Chem B.* 103(40): 8410–8426.
- Liu X, Atwater M, Wang J, Huo Q. 2007. Extinction coefficient of gold nanoparticles with different sizes and different capping ligands. *Colloids Surf B Biointerfaces.* 58(1): 3–7.
- Meng S, Wei B, Xu R, Zhang K, Wang L, Zhang R, Li J. 2009. TAT peptides mediated small interfering RNA delivery to Huh-7 cells and efficiently inhibited hepatitis C virus RNA replication. *Intervirology.* 52(3): 135–140.
- Muratovska A, Eccles MR. 2004. Conjugate for efficient delivery of short interfering RNA (siRNA) into mammalian cells. *FEBS Lett.* 558(1–3): 63–68.
- Nakase I, Tadokoro A, Kawabata N, Takeuchi T, Katoh H, Hiramoto K, Negishi M, Nomizu M, Sugiura Y, Futaki S. 2007. Interaction of arginine-rich peptides with membrane-associated proteoglycans is crucial for induction of actin organization and macropinocytosis. *Biochemistry.* 46(2): 492–501.
- Niidome T, Nakashima K, Takahashi H, Niidome Y. 2004. Preparation of primary amine-modified gold nanoparticles and their transfection ability into cultivated cells. *Chem Commun (Camb).* (17): 1978–1979.
- Oishi M, Nakaogami J, Ishii T, Nagasaki Y. 2006. Smart PEGylated gold nanoparticles for the cytoplasmic delivery of siRNA to induce enhanced gene silencing. *Chem Lett.* 35(9): 1046–1047.
- Richard JP, Melikov K, Brooks H, Prevot P, Lebleu B, Chernomordik LV. 2005. Cellular uptake of unconjugated TAT peptide involves clathrin-dependent endocytosis and heparan sulfate receptors. *J Biol Chem.* 280(15): 15300–15306.
- Rosi NL, Giljohann DA, Thaxton CS, Lytton-Jean AK, Han MS, Mirkin CA. 2006. Oligonucleotide-modified gold nanoparticles for intracellular gene regulation. *Science.* 312(5776): 1027–1047.
- Shukla R, Bansal V, Chaudhary M, Basu A, Bhonde RR, Sastry M. 2005. Biocompatibility of gold nanoparticles and their endocytotic fate inside the cellular compartment: a microscopic overview. *Langmuir.* 21(23): 10644–10654.

- Simeoni F, Morris MC, Heitz F, Divita G. 2003. Insight into the mechanism of the peptide-based gene delivery system MPG: implications for delivery of siRNA into mammalian cells. *Nucleic Acids Res.* 31(11): 2717–2724.
- Song WJ, Du JZ, Sun TM, Zhang PZ, Wang J. 2010. Gold nanoparticles capped with polyethyleneimine for enhanced siRNA delivery. *Small.* 6(2): 239–246.
- Soutschek J, Akinc A, Bramlage B, Charisse K, Constien R, Donoghue M, Elbashir S, Geick A, Hadwiger P, Harborth J, et al. 2004. Therapeutic silencing of an endogenous gene by systemic administration of modified siRNAs. *Nature.* 432(7014): 173–178.
- Subrizi A, Tuominen E, Bunker A, Róg T, Antopolsky M, Urtti A. 2012. Tat(48-60) peptide amino acid sequence is not unique in its cell penetrating properties and cell-surface glycosaminoglycans inhibit its cellular uptake. *J Control Release.* 158(2): 277–285.
- Sugita T, Yoshikawa T, Mukai Y, Yamanada N, Imai S, Nagano K, Yoshida Y, Shibata H, Yoshioka Y, Nakagawa S, et al. 2008. Comparative study on transduction and toxicity of protein transduction domains. *Br J Pharmacol.* 153(6): 1143–1152.
- Tünnemann G, Martin RM, Haupt S, Patsch C, Edenhofer F, Cardoso MC. 2006. Cargo-dependent mode of uptake and bioavailability of TAT-containing proteins and peptides in living cells. *FASEB J.* 20(11): 1775–1784.
- Uchida T, Kanazawa T, Takashima Y, Okada H. 2011. Development of an efficient transdermal delivery system of small interfering RNA using functional peptides, Tat and AT-1002. *Chem Pharm Bull (Tokyo).* 59(2): 196–201.
- Vivès E, Brodin P, Lebleu B. 1997. A truncated HIV-1 Tat protein basic domain rapidly translocates through the plasma membrane and accumulates in the cell nucleus. *J Biol Chem.* 272(25): 16010–16017.
- Wikström J, Elomaa M, Syväjärvi H, Kuokkanen J, Yliperttula M, Honkakoski P, Urtti A. 2008. Alginate-based microencapsulation of retinal pigment epithelial cell line for cell therapy. *Biomaterials.* 29(7): 869–876.
- Zelphati O, Szoka FC Jr. 1996. Mechanism of oligonucleotide release from cationic liposomes. *Proc Natl Acad Sci USA.* 93(21): 11493–11498.
- Zimmermann TS, Lee AC, Akinc AC, Bramlage A, Bumcrot D, Fedoruk MN, Harborth J, Heyes JA, Jeffs LB, John M, et al. 2006. RNAi-mediated gene silencing in non-human primates. *Nature.* 441(7089): 111–114.

9 GENERAL DISCUSSION AND FUTURE PERSPECTIVES

Although oligonucleotide (ON) drugs have encountered more problems than expected, they are steadily progressing towards the clinic. Most of the advanced applications employ topical or *ex vivo* administration, allowing the accumulation of large amounts of ONs at the site of action. After systemic injections, in contrast, unmodified ONs are rapidly excreted by the kidneys. Therefore, systemic ON therapies frequently employ nanosize carriers which accumulate mainly in the liver and in solid tumors due to their size, unless they are actively targeted to specific tissues. Since modified ONs exhibit different *in vivo* pharmacokinetics than phosphodiester ONs, *e.g.* the high plasma protein binding of phosphorothioate ONs delaying their excretion, they may also be injected as such or conjugated to smaller cellular uptake enhancers such as cell-penetrating peptides (CPPs). Especially the non-ionic ON analogs used for splice correction, phosphorodiamidate morpholino oligomers (PMOs) and peptide nucleic acids (PNAs), have been found to benefit from CPP-mediated delivery. However, CPPs are not the only alternative; numerous lipid-based, polymeric, and gold nanoparticles with or without targeting moieties have been investigated to improve ON delivery. We aspired to contribute to this research area by developing modifications and carriers to enhance ON delivery *in vitro*. During this process we optimized various synthetic and analytical methods. Finally, we tested the biological consequences of these modifications and carriers *in vitro*, using cell-free methods and reporter gene-expressing cell lines.

Optimization of analytical methods (I–III). Electrospray ionization mass spectrometry (ESI-MS) is a sensitive and reproducible method, ideal for the molecular weight verification of biomacromolecules. In ESI, the analyte ions are formed spontaneously in the eluent, and are simply brought to the gas phase *via* evaporation of the eluent upon spraying through a heated high-voltage capillary. ESI does not cause fragmentation of the ions, which might complicate the spectra of large molecules. Moreover, ONs are generally always negatively charged in solution. The ESI spectra of ONs exhibit a series of multiply charged ions, enabling the analysis of large molecules on a low mass range equipment. Peptides, in contrast, usually exhibit singly charged positive ions in ESI-MS.

We optimized an ESI-quadrupole ion trap system for ON analysis, tuning parameters such as the tube lens offset to affect the charge states of the ONs. Volatile organic bases (*e.g.* triethylamine) are key components in the eluent; they affect the charge state and the amount of non-volatile cation adduct ions which can complicate the spectra. Direct injection analysis is usually adequate for normal size ONs, including phosphorothioates (PS), although PS-ONs attract more sodium adducts than phosphodiesters do (**Figure 9**, p. 37; previously unpublished). For low signal-to-noise samples such as large ONs, complicated modifications, or analogs synthesized *via* unconventional methods, liquid chromatography–mass spectrometry (LC/MS) using narrowbore RP-HPLC columns with ion-pair reagents is a valuable tool to improve the quality of spectra. We characterized 14 circular

phosphodiester ONs and a circular PS-ON by ESI-MS with mass errors ranging from <0.01 to 0.04%, employing LC/MS when necessary (III). **Figures 1 and 2** (pp. 72–73; previously unpublished) illustrate the significance of LC/MS in improving the spectral quality for a 37-mer circular phosphodiester ON and a 25-mer circular PS-ON, respectively: the direct injection spectra are complicated by high background noise, although they were purified by HPLC after circularization, while LC/MS spectra exhibit excellent signal-to-noise ratio. For unknown reasons, we failed to obtain decent spectra of europium-labeled ONs, and they were analyzed in their original laboratory by ESI-TOF MS.

In covalent peptide–ON conjugates (POCs), each part of the molecule displays different properties: the hydrophilic, polyanionic ON with a molecular weight typically of 5–8 kDa and the peptide exhibiting sequence-dependent size, lipophilicity, and number of positive charges. We have synthesized POCs employing both convergent (I) and stepwise solid-phase synthesis (Antopolsky and Azhayevev 1999; Antopolsky and Azhayevev 2000; Antopolsky et al. 2002) strategies. The convergent strategy comprises the post-synthetic conjugation of purified ONs, bearing a free thiol group, with purified peptides containing a terminal cysteine or other thiol, which is activated by 2,2'-bis(dipyridyl)disulfide. Stepwise solid-phase synthesis of POCs does not entail intermediate purifications, and the products may contain impurities despite the final purification step. A high level of background noise could possibly decrease the accuracy of measurement, especially when using mass reconstruction software which may mistake adduct peaks for real ones.

We successfully characterized 30 POCs, four of which were prepared by stepwise synthesis and the rest by the convergent method, by ESI-MS or ESI-LC/MS with mass errors less than 0.05% (<0.03% in 25 cases) (II). The POCs were measurable by negative ion ESI but not on the positive side, in agreement with previous observations that the ON part governs the behavior of the conjugates in ESI-MS (Jensen et al. 1996). The accuracy of measurement was not significantly affected either by the stepwise synthesis method or by large size of the POCs (up to 14 kDa). In addition, we analyzed six more POCs prepared by new stepwise strategies, introducing a method for arginine-containing peptides (Antopolsky and Azhayevev 2000) and a novel solid support (Antopolsky et al. 2002), with mass errors less than 0.04% and 0.03%, respectively.

To study the enzymatic stability of linear and circular ONs in biological fluids, we optimized an assay comprising a two-step sample pre-treatment and subsequent analysis of metabolites by ion-exchange HPLC (III). Good resolution of 25-mer and smaller PS-ONs had earlier been achieved by strong anion-exchange HPLC using preanalytical liquid–liquid extractions, elution by halides, and elevated column temperatures (Bourque and Cohen 1993). Leeds et al. (1996) developed a two-step solid-phase extraction method with ion-exchange and reversed-phase column, requiring a second desalting step by dialysis to render the samples compatible with capillary gel electrophoresis. We adapted a similar sample pre-treatment method, requiring no additional desalting, for ion-exchange HPLC analysis of circular phosphodiester ONs from biological matrices. Baseline resolution of the full-length ON and its metabolites was achieved using perchlorate elution and elevated column

temperature. However, our method is semiquantitative at best, since we did not use an internal standard and, since the recovery from extractions was found to be poorly reproducible, we calculated the amount of intact ON as percentage relative to all peaks in the chromatogram. The latter calculation may not yield completely accurate results, as it was previously found that shorter ONs do not exhibit equal recoveries in the extractions (Leeds et al. 1996). Nevertheless, the method confers valuable information on the metabolism of ONs and can be further optimized.

Chemical modification of oligonucleotides *via* cyclization (III). Circularized ONs display many advantages: they can form triple helices with high affinity and selectivity, resist nucleolytic degradation, act as templates for rolling circle RNA/DNA synthesis (reviewed in Kool 1996a), form double helices (Azhayeva et al. 1997), and mimic double-stranded nucleic acids (reviewed in Gambari 2004). Cyclization can be achieved enzymatically or *via* activation of a terminal phosphate, the latter requiring template-directed alignment of the ON termini in order to succeed for larger ONs (reviewed in Kool 1996a). Kool emphasized in his review that non-templated approaches had never succeeded in ligating larger than 14-nucleotide ONs. However, Azhayeva et al. (1995) had indeed circularized a 31-nucleotide ON by disulfide cross-linking in 65% yield, although the yield had been improved to 76% by the use of a template. We circularized 14 phosphodiester ONs of 17 to 37 nucleotides in length and one 25-mer PS-ON with the same method (III). The circular ONs were characterized by gel electrophoresis and ESI-MS.

We demonstrated, using the stability assay described above, that the half-life in 10% serum of a 25-mer phosphodiester was increased from *ca.* 1 h to 30 h by circularization. This finding is in agreement with earlier studies incubating 34-mer circular phosphodiester ONs in 100% human serum (Rumney and Kool 1992, cited in Kool 1996a). The stabilization of our circular ON was not as pronounced in CV-1 and D-407 cell lysates, where the circular ON exhibited half-lives of 4 to 6 h, probably because of the endonucleases present in cells (Fisher et al. 1993) but not in serum, where the main source of degradation is due to 3'-exonucleases (Shaw et al. 1991). This is in line with the observation that the linear precursor ON, bearing tether groups at the 5'- and 3'-termini, also displayed somewhat prolonged half-lives of 5 h in serum and 3 h in cellular extracts, compared to linear ON without any 5'- or 3'-end modifications. However, its half-life in serum was not nearly as long as for the circular ON, indicating that it may be susceptible to exonucleolytic degradation despite the terminal modifications.

Melting experiments showed that the melting points of circular ON-target DNA complexes were *ca.* 15°C lower than those of linear ONs. More importantly, a single mismatch in the target DNA sequence significantly destabilized the complex for circular ONs, while their linear precursors showed less destabilization. These results were confirmed using a sandwich-type mixed-phase hybridization assay (Hakala et al. 1998) employing complementary and mismatched target sequences hybridized to a microparticle-bound probe. The hybridization of fluorescently labeled circular ONs was destabilized much more by single-base mismatches than that of the linear counterparts, *e.g.* 90% vs. 20–50%, respectively.

Thus, we concluded that circular ONs are significantly more selective towards complementary targets than linear ONs, making them very attractive candidates as detection probes for *e.g.* single-nucleotide polymorphisms. In addition, they exhibit increased nuclease stability in biological media, allowing their use in diagnostic assays and therapeutic strategies such as the antisense, antigene, or decoy approach. Surprisingly few articles can be found on circular ONs, especially as therapeutics, despite of their versatile properties. We previously showed that cyclization does not adversely affect the RNase H-mediated antisense activity of phosphodiester ONs (Azhayeva et al. 1997). Circular dumbbell ONs exhibit a stabilized double-stranded structure and have been employed in the decoy approach to inhibit DNA-binding proteins *in vivo* (Kim et al. 2010). Recently, Tang et al. (2010) developed ‘caged’ antisense ONs circularized *via* a photolabile linker, exhibiting light-triggered antisense inhibition *in vitro*.

Covalent conjugation of oligonucleotides to cell-penetrating peptides (I).

We attempted to deliver 15- and 25-mer antisense PS-ONs with a chimeric CPP containing a hydrophobic membrane permeable motif (MPM) derived from Kaposi fibroblast growth factor and a cationic nuclear localization sequence (NLS) from NF- κ B (I). Using the synthesis route producing the highest yields, ONs carrying a free mercapto group were covalently conjugated with thiol-containing CPPs activated with a 2-pyridylsulfide group, either *via* the N- or C-termini of the peptides. The resulting disulfide-linked conjugates exhibited >95% purity and yields of 35–60%, and were characterized using HPLC and ESI-MS. However, the conjugates failed to show any significant antisense effect in luciferase-expressing cell lines, unless delivered with cationic lipids. Cellular uptake studies using 32 P-labeled ONs showed that the conjugates were strongly associated with cells and remained intact in the process. Furthermore, the NLS part was necessary for cellular association, as the MPM part alone showed even less uptake than the ON. The conjugates were found capable of inhibiting luciferase expression and of activating RNase H in cell-free systems. Examination of conjugate-treated cells by confocal microscopy revealed that the conjugates were entrapped in endosomes after being internalized. Thus the conjugates were able to exert pharmacodynamic effect and enter cells, but were not able to reach the site of action in the cytoplasm or nucleus.

Dokka et al. (1997) showed efficient PS-ON delivery as complex with this MPM coupled to the cationic homopolypeptide poly-(L-lysine) by measuring the fluorescence of treated A549 cells. Their results seem reliable since they treated the cells with trypsin prior to measurements in order to remove any surface-bound compounds. In contrast to our study, they found a nuclear non-punctate fluorescence pattern, indicative of a non-endocytic internalization mechanism, supported also by temperature-independence, but they did not perform any biological activity measurements to confirm delivery to the site of action. The ineffectiveness of the MPM without the cationic part was observed previously by Arzumanov et al. (2003) in HeLa cells. We aspired to employ a more effective NLS part, which indeed proved necessary for cellular association but failed to deliver the ONs to the nucleus; perhaps it could be augmented or replaced with an endosomolytic sequence. The hydrophobic MPM had been shown to interact with lipid

bilayers (Lin et al. 1995), suggesting capability for membrane fusion; however, interaction with lipid models does not always correlate with the extent of cellular uptake (Subrizi et al. 2012). Had we chosen a more efficient CPP, the results might have been different, as some CPPs seem to display non-endocytic uptake or enhanced endosomal release. Also, when dealing with ionic ON analogs, one must assess whether it would be more effective and/or straightforward to employ non-covalent complexes. Meade and Dowdy (2008) argued that the excess of cationic CPP in ON/CPP complexes might enhance their cell-surface association and subsequent internalization, and provide additional protection from enzymatic degradation. *In vivo*, however, maintaining such excess would only be possible after local administration to closed compartments. Moreover, high concentrations of positively charged CPPs might give rise to toxic effects *via* interaction with proteins and other biomolecules.

Delivery of siRNA by cell-penetrating peptide-modified gold nanoparticles (IV). In the case of siRNA, the ON backbone cannot be uniformly modified, and naked siRNA is useful mainly for local administration or renal diseases. Systemic siRNA therapies usually employ delivery vehicles such as stable nucleic acid lipid particles (SNALPs) or other nanoparticles, which are frequently PEGylated to increase the plasma circulation half-life. *In vivo* siRNA delivery, accompanied by gene silencing effect, has also been achieved by endosomolytic CPPs such as Chol-MPG-8 (Crombez et al. 2009) and PepFect6 (El Andaloussi et al. 2011). One of the most interesting siRNA delivery vehicles are gold nanoparticles (GNPs), which have been extensively investigated *in vitro* both as covalent conjugates and electrostatic complexes (reviewed in Lytton-Jean et al. 2011). However, only three papers have been published so far on the *in vivo* siRNA delivery by GNPs, which exhibited photothermal targeted delivery (Lu et al. 2010), pH-responsive release (Han et al. 2012), and multifunctionality (Conde et al. 2012). Even fewer studies have described the combination of CPPs with GNPs for siRNA delivery. Tat-lipid-coated siRNA/PEG-gold nanoshells were successfully used for laser-activated gene silencing *in vitro* (Braun et al. 2009). In their study comparing different functionalities on GNPs, Conde et al. (2012) also examined the effect of Tat on GNP-mediated siRNA delivery, and found that rather than augmenting gene knockdown, Tat actually diminished the effect.

We investigated the *in vitro* delivery of siRNA by electrostatically bound cationic GNPs (IV). The GNPs were rendered cationic *via* stabilization with cysteamine, as described by Lee et al. (2008). In contrast to that study, our GNPs did not contain PEG, and were further surface-modified with a Tat-derived CPP analog in a one-step synthesis. The CPP was expected to enhance cellular translocation because of its previously observed interaction with model membranes, even though that had not translated into cellular uptake (Subrizi et al. 2012). The siRNA/CPP-GNP complexes were found to elicit a reporter gene knockdown of 49% or more, both in serum-free and serum-containing media, and did not affect cell viability of SEAP-ARPE-19 cells. The peptide alone, in contrast, decreased the cell viability at high concentrations. In addition, the GNPs seemed to stimulate cellular proliferation. These results, while very promising, warrant further investigations confirming the

role of the CPP by control experiments using non-peptide-modified GNPs, elucidating the toxic effects by membrane integrity assays, and certifying the RNA interference mechanism with additional controls and/or mRNA expression tests.

Future perspectives. ONs have been found to modulate gene expression *via* numerous mechanisms, offering platforms for various therapeutic strategies. One systemic antisense ON has been granted marketing authorization for the treatment of severe hypercholesterolemia. This represents a major step forward for ON drugs, albeit that its use is limited due to toxic effects. Before this, two locally injected ONs for ophthalmic diseases had reached the market, and topical formulations are still very abundant in clinical trials. Modified, systemically administered ONs are being evaluated against severe conditions, *e.g.* cancers and genetic muscular dystrophies, which could be effectively treated by inhibiting oncogenes or by correcting splicing defects, respectively. One nuclease-resistant antisense ON is even being studied as an oral formulation against *myasthenia gravis*. The chemical structure of siRNAs, on the other hand, cannot be uniformly modified and remains vulnerable to nucleases. As unmodified ONs are rapidly excreted via the kidneys, naked siRNAs are being investigated against renal diseases such as graft failure. Nanoparticle carriers, in contrast, usually accumulate in the liver because of their size which does not allow their filtration in the glomeruli. They may also accumulate in solid tumors, either by passive targeting due to the enhanced permeability and retention (EPR) effect, or by active targeting ligands, known to be overexpressed in tumors, attached to the nanoparticle surface. Cancers, and especially hepatic cancer, therefore represent an ideal target for nanocarrier-bound siRNAs. In addition to these applications, which have already advanced to the clinical level, preclinical studies are being conducted for numerous conditions which remain without cure, *e.g.* Huntington's disease, rabies infections, and cystic fibrosis.

In summary, an efficient method for *in vivo* ON delivery must protect the ON from enzymatic degradation and facilitate its cellular uptake and/or endosomal escape (**Figure 10**). The main strategies include:

(1) Chemical modification of the oligonucleotide backbone, *e.g.* 2'-O-(2-methoxyethyl)/phosphorothioate (2'-MOE/PS) or phosphorodiamidate morpholino (PMO), to confer *(i)* nuclease resistance and *(ii)* favorable *in vivo* pharmacokinetic properties, enabling unassisted delivery to the site of action.

(2) Use of non-toxic multifunctional nanocarriers to afford: *(i)* spatial protection from enzymes; *(ii)* avoidance of phagocytes by PEGylation, leading to extended circulation half-lives; *(iii)* active targeting to a specific cell type, allowing accumulation at the appropriate site; *(iv)* enhanced endosomal escape mediated by *e.g.* fusogenic peptides; *(v)* triggered release from the carrier and/or from the endosome by external stimuli, *e.g.* pH change or light, affording a high efficacy/toxicity ratio.

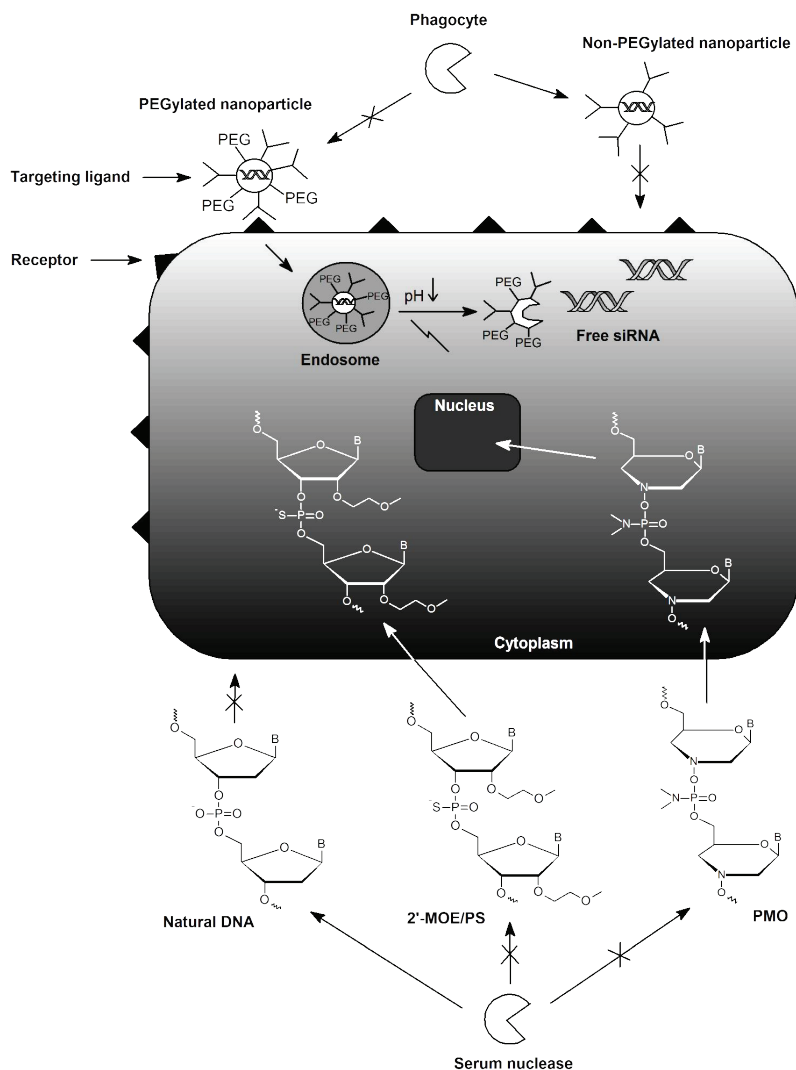


Figure 10 Delivery strategies for oligonucleotides. **Above:** An ideal nanocarrier for oligonucleotides such as short interfering RNA (siRNA) protects its cargo from degradation and may exhibit various functions: targeting to specific cell type; avoidance of phagocytes by PEGylation; and release of the cargo triggered by external stimuli such as pH change or light. **Below:** Unmodified oligonucleotides are readily degraded by nuclease enzymes, whereas chemically modified oligonucleotides [e.g. 2'-O-(2-methoxyethyl) phosphorothioates (2'-MOE/PS) or phosphorodiamidate morpholino oligomers (PMO)] are highly nuclease resistant and may even be delivered unassisted to their cellular site of action.

10 CONCLUSIONS

Antisense technology has existed for more than three decades, during which time an enormous amount of knowledge has accumulated on its principles, defects and possibilities. While many methodological breakthroughs have been made in the past, new discoveries continue to emerge. The main objective of this study was to design chemically modified and nanocarrier-bound oligonucleotides to overcome the pharmacokinetic limitations of oligonucleotide therapeutics, *i.e.* extensive enzymatic degradation and poor cellular uptake. The main conclusions of this thesis are the following:

- 1) Electrospray ionization mass spectrometry offers an extremely useful platform for characterizing oligonucleotides and peptide–oligonucleotide conjugates. Liquid chromatography–mass spectrometry, in particular, enables the analysis of samples with an inherently low signal-to-noise ratio such as large molecules, difficult modifications, or peptide–oligonucleotide conjugates prepared by stepwise solid-phase synthesis without intermediate purifications. In addition, a two-step solid-phase extraction pretreatment enables the analysis of metabolites of modified oligonucleotide analogs in biological samples.
- 2) Circular phosphodiester oligonucleotides exhibit a significantly enhanced enzymatic stability, compared to their linear counterparts, in serum and cell lysates. In the latter media, the effect is not as pronounced, probably due to endonucleases present in cells. Moreover, circular oligonucleotides display improved selectivity towards complementary targets, which makes them excellent candidates for the detection of single-nucleotide polymorphisms.
- 3) Peptide–oligonucleotide conjugates, where phosphorothioate antisense oligonucleotides and a chimeric cell-penetrating peptide are connected *via* bioreducible disulfide cross-links, are taken up by cells but remain entrapped in endosomes, which explains the lack of antisense effect in cells despite their observed anti-luciferase activity in cell-free systems.
- 4) Cationic gold nanoparticles surface-modified with cysteamine and a Tat-peptide analog form stable non-covalent complexes with siRNA, deliver siRNA into cells in an active form in serum-free and serum-containing media, and do not affect cell viability. Furthermore, the gold nanoparticles seem to have a stimulating effect on cellular proliferation.

In conclusion, we have optimized chemical methods to synthesize and analyze various oligonucleotide analogs and carriers. Many of these methods are easily applicable to different oligonucleotide chemistries, therapeutic targets, and mechanisms of action. We have also tested the effect of these modifications using biological methods such as reporter gene-expressing cell lines.

11 REFERENCES

- Abe T, Takai K, Nakada S, Yokota T, Takaku H. 1998. Specific inhibition of influenza virus RNA polymerase and nucleoprotein gene expression by circular dumbbell RNA/DNA chimeric oligonucleotides containing antisense phosphodiester oligonucleotides. *FEBS Lett.* 425(1): 91–96.
- Abes R, Moulton HM, Clair P, Yang ST, Abes S, Melikov K, Prevot P, Youngblood DS, Iversen PL, Chernomordik LV, et al. 2008. Delivery of steric block morpholino oligomers by (R-X-R)₄ peptides: structure-activity studies. *Nucleic Acids Res.* 36(20): 6343–6354.
- Abes S, Turner JJ, Ivanova GD, Owen D, Williams D, Arzumanov A, Clair P, Gait MJ, Lebleu B. 2007. Efficient splicing correction by PNA conjugation to an R₆-Penetratin delivery peptide. *Nucleic Acids Res.* 35(13): 4495–4502.
- Agrawal S. 1999. Importance of nucleotide sequence and chemical modifications of antisense oligonucleotides. *Biochim Biophys Acta.* 1489(1): 53–68.
- Agrawal S, Goodchild J, Civeira MP, Thornton AH, Sarin PS, Zamecnik PC. 1988. Oligodeoxynucleoside phosphoramidates and phosphorothioates as inhibitors of human immunodeficiency virus. *Proc Natl Acad Sci USA.* 85(19): 7079–7083.
- Agrawal S, Jiang Z, Zhao Q, Shaw D, Cai Q, Roskey A, Channavajjala L, Saxinger C, Zhang R. 1997. Mixed-backbone oligonucleotides as second generation antisense oligonucleotides: *In vitro* and *in vivo* studies. *Proc Natl Acad Sci USA.* 94(6): 2620–2625.
- Agrawal S, Temsamani J, Tang JY. 1991. Pharmacokinetics, biodistribution, and stability of oligodeoxynucleotide phosphorothioates in mice. *Proc Natl Acad Sci USA.* 88(17): 7595–7599.
- Akhtar S, Kole R, Juliano RL. 1991. Stability of antisense DNA oligodeoxynucleotide analogs in cellular extracts and sera. *Life Sci.* 49(24): 1793–1801.
- Akita H, Kogure K, Moriguchi R, Nakamura Y, Higashi T, Nakamura T, Serada S, Fujimoto M, Naka T, Futaki S, et al. 2010. Nanoparticles for *ex vivo* siRNA delivery to dendritic cells for cancer vaccines: programmed endosomal escape and dissociation. *J Control Release.* 143(3): 311–317.
- Amantana A, Iversen PL. 2005. Pharmacokinetics and biodistribution of phosphorodiamidate morpholino antisense oligomers. *Curr Opin Pharmacol.* 5(5): 550–555.
- Antopolsky M. 2002. Synthesis of peptide–oligonucleotide conjugates [dissertation]. [Kuopio, Finland]: University of Kuopio. ISBN 951-781-156-X.
- Antopolsky M, Azhayev A. 1999. Stepwise solid-phase synthesis of peptide–oligonucleotide conjugates on new solid supports. *Helv Chim Acta.* 82(12): 2130–2140.
- Antopolsky M, Azhayev A. 2000. Stepwise solid-phase synthesis of peptide–oligonucleotide phosphorothioate conjugates employing Fmoc peptide chemistry. *Tetrahedron Lett.* 41(47): 9113–9117.
- Antopolsky M, Azhayeva E, Tengvall U, Azhayev A. 1999. General method to synthesize disulfide cross-linked peptide–oligonucleotide phosphorothioate conjugates. In: Holý A, Hocek M, editors. Chemistry of nucleic acid components. XIth symposium; 1999 Sep 4–9; Spindleruv Mlýn, Czech Republic. Prague: Institute of organic chemistry and biochemistry. p. 294–297.
- Antopolsky M, Azhayeva E, Tengvall U, Azhayev A. 2002. Towards a general method for the stepwise solid-phase synthesis of peptide–oligonucleotide conjugates. *Tetrahedron Lett.* 43(3): 527–530.
- Apffel A, Chakel JA, Fischer S, Lichtenwalter K, Hancock WS. 1997. New procedure for the use of high-performance liquid chromatography–electrospray ionization mass spectrometry for the analysis of nucleotides and oligonucleotides. *J Chromatogr A.* 777(1): 3–21.

REFERENCES

- Arita M, Bianchini F, Aliberti J, Sher A, Chiang N, Hong S, Yang R, Petasis NA, Serhan CN. 2005. Stereochemical assignment, anti-inflammatory properties, and receptor for the omega-3 lipid mediator resolvin E1. *J Exp Med.* 201(5): 713–722.
- Arzumanov A, Stestenko DA, Malakhov AD, Reichelt S, Sørensen MD, Babu BR, Wengel J, Gait MJ. 2003. A structure-activity study of the inhibition of HIV-1 Tat-dependent *trans*-activation by mixmer 2'-*O*-methyl oligoribonucleotides containing locked nucleic acid (LNA), α -L-LNA, or 2'-thio-LNA residues. *Oligonucleotides.* 13(6): 435–453.
- Astriab-Fisher A, Sergueev D, Fisher M, Shaw BR, Juliano RL. 2002. Conjugates of antisense oligonucleotides with the Tat and antennapedia cell-penetrating peptides: effects on cellular uptake, binding to target sequences, and biologic actions. *Pharm Res.* 19(6): 744–754.
- Azhayeva E, Azhayev A, Auriola S, Tengvall U, Urtili A, Lönnberg H. 1997. Inhibitory properties of double helix forming circular oligonucleotides. *Nucleic Acids Res.* 25(24): 4954–4961.
- Azhayeva E, Azhayev A, Guzaev A, Hovinen J, Lönnberg H. 1995. Looped oligonucleotides form stable hybrid complexes with a single-stranded DNA. *Nucleic Acids Res.* 23(7): 1170–1176.
- Barry JP, Vouros P, Van Schepdael A, Law S. 1995. Mass and sequence verification of modified oligonucleotides using electrospray tandem mass spectrometry. *J Mass Spectrom.* 30(7): 993–1006.
- Bartlett MG, McCloskey JA, Manalili S, Griffey RH. 1996. The effect of backbone charge on the collision-induced dissociation of oligonucleotides. *J Mass Spectrom.* 31(11): 1277–1283.
- Bartz R, Fan H, Zhang J, Innocent N, Cherrin C, Beck SC, Pei Y, Momose A, Jadhav J, Tellers DM, et al. 2011. Effective siRNA delivery and target mRNA degradation using an amphipathic peptide to facilitate pH-dependent endosomal escape. *Biochem J.* 435(2): 475–487.
- Behlke MA. 2008. Chemical modification of siRNAs for *in vivo* use. *Oligonucleotides.* 18(4): 305–319.
- Beisner J, Dong M, Taetz S, Nafee N, Griese EU, Schaefer U, Lehr CM, Klotz U, Mürdter TE. 2010. Nanoparticle mediated delivery of 2'-*O*-methyl-RNA leads to efficient telomerase inhibition and telomere shortening in human lung cancer cells. *Lung Cancer.* 68(3): 346–354.
- Bellon L, Barascut JL, Maury G, Divita G, Goody R, Imbach JL. 1993. 4'-Thio-oligo- β -D-ribonucleotides: synthesis of β -4'-thio-oligouridylates, nuclease resistance, base pairing properties, and interaction with HIV-1 reverse transcriptase. *Nucleic Acids Res.* 21(7): 1587–1593.
- Beltinger C, Saragovi HU, Smith RM, LeSauteur L, Shah N, DeDionisio L, Christensen L, Raible A, Jarett L, Gewirtz AM. 1995. Binding, uptake, and intracellular trafficking of phosphorothioate-modified oligodeoxynucleotides. *J Clin Invest.* 95(4): 1814–1823.
- Bennett CF, Chiang MY, Chan H, Shoemaker JE, Mirabelli CK. 1992. Cationic lipids enhance cellular uptake and activity of phosphorothioate antisense oligonucleotides. *Mol Pharmacol.* 41(6): 1023–1033.
- Bennett CF, Swayze EE. 2010. RNA targeting therapeutics: molecular mechanisms of antisense oligonucleotides as a therapeutic platform. *Annu Rev Pharmacol Toxicol.* 50: 259–293.
- Berezhna SY, Supekova L, Supek F, Schultz PG, Deniz AA. 2006. siRNA in human cells selectively localizes to target RNA sites. *Proc Natl Acad Sci USA.* 103(20): 7682–7687.
- Berry CC, de la Fuente JM, Mullin M, Chu SWL, Curtis ASG. 2007. Nuclear localization of HIV-1 Tat functionalized gold nanoparticles. *IEEE Trans Nanobiosci.* 6(4): 262–269.
- Beverly M, Hartsough K, Macherer L. 2005. Liquid chromatography/electrospray mass spectrometric analysis of metabolites from an inhibitory RNA duplex. *Rapid Commun Mass Spectrom.* 19(12): 1675–1682.
- Bielinska A, Shivdasani RA, Zhang LQ, Nabel GJ. 1990. Regulation of gene expression with double-stranded phosphorothioate oligonucleotides. *Science.* 250(4983): 997–1000.

- Billen LP, Li Y. 2004. Synthesis and characterization of topologically linked single-stranded DNA rings. *Bioorg Chem.* 32(6): 582–598.
- Bonoiu AC, Mahajan SD, Ding H, Roy I, Yong KT, Kumar R, Hu R, Bergey EJ, Schwartz SA, Prasad PN. 2009. Nanotechnology approach for drug addiction therapy: gene silencing using gold nanorod–siRNA nanoplex in dopaminergic neurons. *Proc Natl Acad Sci USA.* 106(14): 5546–5550.
- Boschenok J, Sheil MM. 1996. Electrospray tandem mass spectrometry of nucleotides. *Rapid Commun Mass Spectrom.* 10(1): 144–149.
- Bothner B, Chatman K, Sarkisian M, Siuzdak G. 1995. Liquid chromatography mass spectrometry of antisense oligonucleotides. *Bioorg Med Chem Lett.* 5(23): 2863–2868.
- Bourque AJ, Cohen AS. 1993. Quantitative analysis of phosphorothioate oligonucleotides in biological fluids using fast anion-exchange chromatography. *J Chromatogr.* 617(1): 43–49.
- Boussif O, Lezoualc'h F, Zanta MA, Mergny MD, Scherman D, Demeneix B, Behr JP. 1995. A versatile vector for gene and oligonucleotide transfer into cells in culture and *in vivo*: polyethylenimine. *Proc Natl Acad Sci USA.* 92(16): 7297–7301.
- Braun GB, Pallaoro A, Wu G, Missirlis D, Zasadzinski JA, Tirrell M, Reich NO. 2009. Laser-activated gene silencing *via* gold nanoshell–siRNA conjugates. *ACS Nano.* 3(7): 2007–2015.
- Breaker RR, Joyce GF. 1994. A DNA enzyme that cleaves RNA. *Chem Biol.* 1(4): 223–229.
- Bruick RK, Dawson PE, Kent SB, Usman N, Joyce GF. 1996. Template-directed ligation of peptides to oligonucleotides. *Chem Biol.* 3(1): 49–56.
- Bumcrot D, Manoharan M, Koteliansky V, Sah DW. 2006. RNAi therapeutics: a potential new class of pharmaceutical drugs. *Nat Chem Biol.* 2(12): 711–719.
- Burnett JC, Rossi JJ. 2012. RNA-based therapeutics: current progress and future prospects. *Chem Biol.* 19(1): 60–71.
- Burrer R, Neuman BW, Ting JP, Stein DA, Moulton HM, Iversen PL, Kuhn P, Buchmeier MJ. 2007. Antiviral effects of antisense morpholino oligomers in murine coronavirus infection models. *J Virol.* 81(11): 5637–5648.
- Campbell JM, Bacon TA, Wickstrom E. 1990. Oligodeoxynucleoside phosphorothioate stability in subcellular extracts, culture media, sera and cerebrospinal fluid. *J Biochem Biophys Methods.* 20(3): 259–267.
- Carriero S, Damha MJ. 2003. Inhibition of pre-mRNA splicing by synthetic branched nucleic acids. *Nucleic Acids Res.* 31(21): 6157–6167.
- Cech TR, Zaug AJ, Grabowski PJ. 1981. *In vitro* splicing of the ribosomal RNA precursor of Tetrahymena: involvement of a guanosine nucleotide in the excision of the intervening sequence. *Cell.* 27(3 Pt 2): 487–496.
- Chaudhuri NC, Kool ET. 1995. Very high affinity DNA recognition by bicyclic and cross-linked oligonucleotides. *J Am Chem Soc.* 117(42): 10434–10442.
- Chiu YL, Ali A, Chu CY, Cao H, Rana TM. 2004. Visualizing a correlation between siRNA localization, cellular uptake, and RNAi in living cells. *Chem Biol.* 11(8): 1165–1175.
- Chu BC, Orgel LE. 1992. The stability of different forms of double-stranded decoy DNA in serum and nuclear extracts. *Nucleic Acids Res.* 20(21): 5857–5858.
- Cirak S, Arechavala-Gomez V, Guglieri M, Feng L, Torelli S, Anthony K, Abbs S, Garralda ME, Bourke J, Wells DJ, et al. 2011. Exon skipping and dystrophin restoration in patients with Duchenne muscular dystrophy after systemic phosphorodiamidate morpholino oligomer treatment: an open-label, phase 2, dose-escalation study. *Lancet.* 378(9791): 595–605.
- Clusel C, Ugarte E, Enjolras N, Vasseur M, Blumenfeld M. 1993. *Ex vivo* regulation of specific gene expression by nanomolar concentration of double-stranded dumbbell oligonucleotides. *Nucleic Acids Res.* 21(15): 3405–3411.
- Conde J, Ambrosone A, Sanz V, Hernandez Y, Marchesano V, Tian F, Child H, Berry CC, Ibarra MR, Baptista PV, et al. 2012. Design of multifunctional gold nanoparticles for *in vitro* and *in vivo* gene silencing. *ACS Nano.* 6(9): 8316–8324.

REFERENCES

- Console S, Marty C, Garcia-Echeverria C, Schwendener R, Ballmer-Hofer K. 2003. Antennapedia and HIV transactivator of transcription (TAT) 'protein transduction domains' promote endocytosis of high molecular weight cargo upon binding to cell surface glycosaminoglycans. *J Biol Chem.* 278(37): 35109–35114.
- Coursindel T, Järver P, Gait MJ. 2012. Peptide-based *in vivo* delivery agents for oligonucleotides and siRNA. *Nucleic Acid Ther.* 22(2): 71–76.
- Covey TR, Bonner RF, Shushan BI, Henion J. 1988. The determination of protein, oligonucleotide and peptide molecular weights by ion-spray mass spectrometry. *Rapid Commun Mass Spectrom.* 2(11): 249–256.
- Crick F. 1970. Central dogma of molecular biology. *Nature.* 227(5258): 561–563.
- Crombez L, Morris MC, Dufort S, Aldrian-Herrada G, Nguyen Q, McMaster G, Coll JL, Heitz F, Divita G. 2009. Targeting cyclin B1 through peptide-based delivery of siRNA prevents tumour growth. *Nucleic Acids Res.* 37(14): 4559–4569.
- Crooke RM, Graham MJ, Martin MJ, Lemonidis KM, Wyrzykiewicz T, Cummins LL. 2000. Metabolism of antisense oligonucleotides in rat liver homogenates. *J Pharmacol Exp Ther.* 292(1): 140–149.
- Crooke ST, Geary RS. 2012. Clinical pharmacological properties of mipomersen (Kynamro), a second generation antisense inhibitor of apolipoprotein B. *Br J Clin Pharmacol* [published online ahead of print 2012 Sep 26]. [cited 2013 Jan 14]. Available from: doi:10.1111/j.1365-2125.2012.x.
- Crooke ST, Graham MJ, Zuckerman JE, Brooks D, Conklin BS, Cummins LL, Greig MJ, Guinasso CJ, Kornbrust D, Manoharan M, et al. 1996. Pharmacokinetic properties of several novel oligonucleotide analogs in mice. *J Pharmacol Exp Ther.* 277(2): 923–937.
- Cummins LL, Owens SR, Risen LM, Lesnik EA, Freier SM, McGee D, Guinasso CJ, Cook PD. 1995. Characterization of fully 2'-modified oligoribonucleotide hetero- and homoduplex hybridization and nuclease sensitivity. *Nucleic Acids Res.* 23(11): 2019–2024.
- Damha MJ, Wilds CJ, Noronha A, Brukner I, Borkow G, Arion D, Parniak MA. 1998. Hybrids of RNA and arabinonucleic acids (ANA and 2'-ANA) are substrates of ribonuclease H. *J Am Chem Soc.* 120(49): 12976–12977.
- Dande P, Prakash TP, Sioufi N, Gaus H, Jarres R, Berdeja A, Swayze EE, Griffey RH, Bhat B. 2006. Improving RNA interference in mammalian cells by 4'-thio-modified small interfering RNA (siRNA): effect on siRNA activity and nuclease stability when used in combination with 2'-O-alkyl modifications. *J Med Chem.* 49(5): 1624–1634.
- Daubendiek SL, Kool ET. 1997. Generation of catalytic RNAs by rolling transcription of synthetic DNA nanocircles. *Nat Biotechnol.* 15(3): 273–277.
- Daubendiek SL, Ryan K, Kool ET. 1995. Rolling-circle RNA synthesis: circular oligonucleotides as efficient substrates for T7 RNA polymerase. *J Am Chem Soc.* 117(29): 7818–7819.
- Davidson TJ, Harel S, Arboleda VA, Prunell GF, Shelanski ML, Greene LA, Troy CM. 2004. Highly efficient small interfering RNA delivery to primary mammalian neurons induces microRNA-like effects before mRNA degradation. *J Neurosci.* 24(45): 10040–10046.
- Davis ME, Zuckerman JE, Choi CH, Seligson D, Tolcher A, Alabi CA, Yen Y, Heidel JD, Ribas A. 2010. Evidence of RNAi in humans from systemically administered siRNA via targeted nanoparticles. *Nature.* 464(7291): 1067–1070.
- de Smet MD, Meenken CJ, van den Horn GJ. 1999. Fomivirsen – a phosphorothioate oligonucleotide for the treatment of CMV retinitis. *Ocul Immunol Inflamm.* 7(3–4): 189–198.
- Deas TS, Bennett CJ, Jones SA, Tilgner M, Ren P, Behr MJ, Stein DA, Iversen PL, Kramer LD, Bernard KA, et al. 2007. *In vitro* resistance selection and *in vivo* efficacy of morpholino oligomers against West Nile virus. *Antimicrob Agents Chemother.* 51(7): 2470–2482.
- Derossi D, Chassaing G, Prochiantz A. 1998. Trojan peptides: the penetratin system for intracellular delivery. *Trends Cell Biol.* 8(2): 84–87.

- Derossi D, Joliot AH, Chassaing G, Prochiantz A. 1994. The third helix of the Antennapedia homeodomain translocates through biological membranes. *J Biol Chem.* 269(14): 10444–10450.
- Deroussent A, Le Caer JP, Rossier J, Gouyette A. 1995. Electrospray mass spectrometry for the characterization of the purity of natural and modified oligodeoxynucleotides. *Rapid Commun Mass Spectrom.* 9(1): 1–4.
- Deshayes S, Gerbal-Chaloin S, Morris MC, Aldrian-Herrada G, Charnet P, Divita G, Heitz F. 2004a. On the mechanism of non-endosomal peptide-mediated cellular delivery of nucleic acids. *Biochim Biophys Acta.* 1667(2): 141–147.
- Deshayes S, Heitz A, Morris MC, Charnet P, Divita G, Heitz F. 2004b. Insight into the mechanism of internalization of the cell-penetrating carrier peptide Pep-1 through conformational analysis. *Biochemistry.* 43(6): 1449–1457.
- Deshayes S, Plénat T, Aldrian-Herrada G, Divita G, Le Grimellec C, Heitz F. 2004c. Primary amphipathic cell-penetrating peptides: structural requirements and interactions with model membranes. *Biochemistry.* 43(24): 7698–7706.
- Deshayes S, Morris M, Heitz F, Divita G. 2008. Delivery of proteins and nucleic acids using a non-covalent peptide-based strategy. *Adv Drug Deliv Rev.* 60(4–5): 537–547.
- DeVincenzo J, Cehelsky JE, Alvarez R, Elbashir S, Harborth J, Toudjarska I, Nechev L, Murugaiah V, Van Vliet A, Vaishnav AK, et al. 2008. Evaluation of the safety, tolerability and pharmacokinetics of ALN-RSV01, a novel RNAi antiviral therapeutic directed against respiratory syncytial virus (RSV). *Antiviral Res.* 77(3): 225–231.
- Dheur S, Dias N, van Aerschot A, Herdewijn P, Bettinger T, Rémy JS, Hélène C, Saison-Behmoaras ET. 1999. Polyethylenimine but not cationic lipid improves antisense activity of 3'-capped phosphodiester oligonucleotides. *Antisense Nucleic Acid Drug Dev.* 9(6): 515–525.
- Dokka S, Toledo-Velasquez D, Shi X, Wang L, Rojanasakul Y. 1997. Cellular delivery of oligonucleotides by synthetic import peptide carrier. *Pharm Res.* 14(12): 1759–1764.
- Duchardt F, Fotin-Mleczek M, Schwarz H, Fischer R, Brock R. 2007. A comprehensive model for the cellular uptake of cationic cell-penetrating peptides. *Traffic.* 8(7): 848–866.
- Efimov V, Choob M, Buryakova A, Phelan D, Chakhmakcheva O. 2001. PNA-related oligonucleotide mimics and their evaluation for nucleic acid hybridization studies and analysis. *Nucleosides Nucleotides Nucleic Acids.* 20(4–7): 419–428.
- El-Andaloussi S, Johansson H, Magnusdottir A, Järver P, Lundberg P, Langel Ü. 2005. TP10, a delivery vector for decoy oligonucleotides targeting the Myc protein. *J Control Release.* 110(1): 189–201.
- El Andaloussi S, Lehto T, Mäger I, Rosenthal-Aizman K, Oprea II, Simonson OE, Sork H, Ezzat K, Copolovici DM, Kurrikoff K, et al. 2011. Design of a peptide-based vector, PepFect6, for efficient delivery of siRNA in cell culture and systemically *in vivo*. *Nucleic Acids Res.* 39(9): 3972–3987.
- Elbashir SM, Harborth J, Lendeckel W, Yalcin A, Weber K, Tuschl T. 2001. Duplexes of 21-nucleotide RNAs mediate RNA interference in cultured mammalian cells. *Nature.* 411(6836): 494–498.
- Elmén J, Lindow M, Schütz S, Lawrence M, Petri A, Obad S, Lindholm M, Hedtjärn M, Hansen HF, Berger U, et al. 2008. LNA-mediated microRNA silencing in non-human primates. *Nature.* 452(7189): 896–899.
- EMA. 2012. Refusal of the marketing authorization for Kynamro (mipomersen) [Internet]. [cited 2013 Mar 24]. Available from: http://www.ema.europa.eu/docs/en_GB/document_library/Summary_of_opinion_-_Initial_authorisation/human/002429/WC500136279.pdf.
- Endoh T, Ohtsuki T. 2009. Cellular siRNA delivery using cell-penetrating peptides modified for endosomal escape. *Adv Drug Deliv Rev.* 61(9): 704–709.
- Eyetechn Inc. 2008. Macugen® prescribing information [Internet]. [cited 2012 Oct 31]. Available from: <http://www.macugen.com/macugenUSPI.pdf>.

REFERENCES

- Fattal E, Couvreur P, Dubernet C. 2004. "Smart" delivery of antisense oligonucleotides by anionic pH-sensitive liposomes. *Adv Drug Deliv Rev.* 56(7): 931–946.
- Felgner PL, Gadek TR, Holm M, Roman R, Chan HW, Wenz M, Northrop JP, Ringold GM, Danielsen M. 1987. Lipofection: a highly efficient, lipid-mediated DNA-transfection procedure. *Proc Natl Acad Sci USA.* 84(21): 7413–7417.
- Fire A, Xu S, Montgomery MK, Kostas SA, Driver SE, Mello CC. 1998. Potent and specific genetic interference by double-stranded RNA in *Caenorhabditis elegans*. *Nature.* 391(6669): 806–811.
- Fischer D, Li Y, Ahlemeyer B, Krieglstein J, Kissel T. 2003. In vitro cytotoxicity testing of polycations: influence of polymer structure on cell viability and hemolysis. *Biomaterials.* 24(7): 1121–1131.
- Fisher L, Soomets U, Cortés Toro V, Chilton L, Jiang Y, Langel Ü, Iverfeldt K. 2004. Cellular delivery of a double-stranded oligonucleotide NF κ B decoy by hybridization to complementary PNA linked to a cell-penetrating peptide. *Gene Ther.* 11(16): 1264–1272.
- Fisher TL, Terhorst T, Cao X, Wagner RW. 1993. Intracellular disposition and metabolism of fluorescently-labeled unmodified and modified oligonucleotides microinjected into mammalian cells. *Nucleic Acids Res.* 21(16): 3857–3865.
- Fonseca SB, Pereira MP, Kelley SO. 2009. Recent advances in the use of cell-penetrating peptides for medical and biological applications. *Adv Drug Deliv Rev.* 61(11): 953–964.
- Freier SM, Altmann KH. 1997. The ups and downs of nucleic acid duplex stability: structure-stability studies on chemically-modified DNA:RNA duplexes. *Nucleic Acids Res.* 25(22): 4429–4443.
- Froehler B, Ng P, Matteucci M. 1988. Phosphoramidate analogues of DNA: synthesis and thermal stability of heteroduplexes. *Nucleic Acids Res.* 16(11): 4831–4839.
- Gambari R. 2004. New trends in the development of transcription factor decoy (TFD) pharmacotherapy. *Curr Drug Targets.* 5(5): 419–430.
- Gao H, Liu Y, Rumley M, Yuan H, Mao B. 2009. Sequence confirmation of chemically modified RNAs using exonuclease digestion and matrix-assisted laser desorption/ionization time-of-flight mass spectrometry. *Rapid Commun Mass Spectrom.* 23(21): 3423–3430.
- Gaus HJ, Owens SR, Winniman M, Cooper S, Cummins LL. 1997. On-line HPLC electrospray mass spectrometry of phosphorothioate oligonucleotide metabolites. *Anal Chem.* 69(3): 313–319.
- Geary RS, Leeds JM, Fitchett J, Burckin T, Truong L, Spainhour C, Creek M, Levin AA. 1997. Pharmacokinetics and metabolism in mice of a phosphorothioate oligonucleotide antisense inhibitor of *C-raf-1* kinase expression. *Drug Metab Dispos.* 25(11): 1272–1281.
- Gehring WJ. 1987. Homeo boxes in the study of development. *Science.* 236(4806): 1245–52.
- Geisbert TW, Hensley LE, Kagan E, Yu EZ, Geisbert JB, Daddario-DiCaprio K, Fritz EA, Jahrling PB, McClintock K, Phelps JR, et al. 2006. Postexposure protection of guinea pigs against a lethal ebola virus challenge is conferred by RNA interference. *J Infect Dis.* 193(12): 1650–1657.
- Genzyme Corporation. 2013. KYNAMRO™ prescribing information [Internet]. [cited 2013 Mar 24]. Available from: <http://www.kynamro.com/~media/Kynamro/Files/KYNAMRO-PI.pdf>.
- Gilar M, Belenky A, Budman Y, Smisek DL, Cohen AS. 1998. Study of phosphorothioate-modified oligonucleotide resistance to 3'-exonuclease using capillary electrophoresis. *J Chromatogr B Biomed Sci Appl.* 714(1): 13–20.
- Giovannangeli C, Montenay-Garestier T, Rougée M, Chassignol M, Thuong NT, Hélène C. 1991. Single-stranded DNA as a target for triple helix formation. *J Am Chem Soc.* 113(20): 7775–7777.
- Goemans NM, Tulinus M, van den Akker JT, Burm BE, Ekhardt PF, Heuvelmans N, Holling T, Janson AA, Platenburg GJ, Sipkens JA, et al. 2011. Systemic administration of PRO051 in Duchenne's muscular dystrophy. *N Engl J Med.* 364(16): 1513–1522.
- Gogoi K, Mane MV, Kunte SS, Kumar VA. 2007. A versatile method for the preparation of conjugates of peptides with DNA/PNA/analog by employing chemo-selective click

- reaction in water. *Nucleic Acids Res* [Internet]. [cited 2012 Nov 15]; 35(21): e139. Available from: doi:10.1093/nar/gkm935.
- Goracznik R, Behlke MA, Gunderson SI. 2009. Gene silencing by synthetic U1 adaptors. *Nat Biotechnol.* 27(3): 257–263.
- Graham MJ, Crooke ST, Lemonidis KM, Gaus HJ, Templin MV, Crooke RM. 2001. Hepatic distribution of a phosphorothioate oligodeoxynucleotide within rodents following intravenous administration. *Biochem Pharmacol.* 62(3): 297–306.
- Greig M, Griffey RH. 1995. Utility of organic bases for improved electrospray mass spectrometry of oligonucleotides. *Rapid Commun Mass Spectrom.* 9(1): 97–102.
- Griffey RH, Greig MJ, Gaus HJ, Liu K, Monteith D, Winniman M, Cummins LL. 1997a. Characterization of oligonucleotide metabolism *in vivo* via liquid chromatography/electrospray tandem mass spectrometry with a quadrupole ion trap mass spectrometer. *J Mass Spectrom.* 32(3): 305–313.
- Griffey RH, Sasmor H, Greig MJ. 1997b. Oligonucleotide charge states in negative ionization electrospray-mass spectrometry are a function of solution ammonium ion concentration. *J Am Soc Mass Spectrom.* 8(2): 155–160.
- Grijalvo S, Terrazas M, Aviñó A, Eritja R. 2010. Stepwise synthesis of oligonucleotide-peptide conjugates containing guanidium and lipophilic groups in their 3'-termini. *Bioorg Med Chem Lett.* 20(7): 2144–2147.
- Gryaznov S, Chen J. 1994. Oligodeoxyribonucleotide N3'→P5' phosphoramidates: synthesis and hybridization properties. *J Am Chem Soc.* 116(7): 3143–3144.
- Gryaznov S, Skorski T, Cucco C, Nieborowska-Skorska M, Chiu CY, Lloyd D, Chen JK, Koziolkiewicz M, Calabretta B. 1996. Oligonucleotide N3'→P5' phosphoramidates as antisense agents. *Nucleic Acids Res.* 24(8): 1508–1514.
- Gryaznov SM. 2010. Oligonucleotide N3'→P5' phosphoramidates and thio-phosphoramidates as potential therapeutic agents. *Chem Biodivers.* 7(3): 477–493.
- Gryaznov SM, Lloyd DH, Chen JK, Schultz RG, DeDionisio LA, Ratmeyer L, Wilson WD. 1995. Oligonucleotide N3'→P5' phosphoramidates. *Proc Natl Acad Sci USA.* 92(13): 5798–5802.
- Hakala H, Mäki E, Lönnberg H. 1998. Detection of oligonucleotide hybridization on a single microparticle by time-resolved fluorometry: quantification and optimization of a sandwich type assay. *Bioconjugate Chem.* 9(3): 316–321.
- Han L, Zhao J, Zhang X, Cao W, Hu X, Zou G, Duan X, Liang XJ. 2012. Enhanced siRNA delivery and silencing gold-chitosan nanosystem with surface-charge reversal polymer assembly and good biocompatibility. *ACS Nano.* 6(8): 7340–7351.
- Heidel JD, Yu Z, Liu JYC, Rele SM, Liang Y, Zeidan RK, Kornbrust DJ, Davis ME. Administration in non-human primates of escalating doses of targeted nanoparticles containing ribonucleotide reductase subunit M2 siRNA. *Proc Natl Acad Sci USA.* 104(14): 5715–5721.
- Herbert BS, Pongracz K, Shay JW, Gryaznov SM. 2002. Oligonucleotide N3'→P5' phosphoramidates as efficient telomerase inhibitors. *Oncogene.* 21(4): 638–642.
- Herdewijn P. 2010. Nucleic acids with a six-membered 'carbohydrate' mimic in the backbone. *Chem Biodivers.* 7(1): 1–59.
- Hornung V, Guenther-Biller M, Bourquin C, Ablasser A, Schlee M, Uematsu S, Noronha A, Manoharan M, Akira S, de Fougères A, et al. 2005. Sequence-specific potent induction of IFN- α by short interfering RNA in plasmacytoid dendritic cells through TLR7. *Nat Med.* 11(3): 263–270.
- Hoshika S, Minakawa N, Matsuda A. 2004. Synthesis and physical and physiological properties of 4'-thioRNA: application to post-modification of RNA aptamer toward NF- κ B. *Nucleic Acids Res.* 32(13): 3815–3825.
- Hu J, Matsui M, Gagnon KT, Schwartz JC, Gabillet S, Arar K, Wu J, Bezprozvanny I, Corey DR. 2009. Allele-specific silencing of mutant huntingtin and ataxin-3 genes by targeting expanded CAG repeats in mRNAs. *Nat Biotechnol.* 27(5): 478–484.

REFERENCES

- Hua Y, Sahashi K, Rigo J, Hung G, Horev G, Bennett CF, Krainer AR. 2011. Peripheral SMN restoration is essential for long-term rescue of a severe spinal muscular atrophy mouse model. *Nature*. 478(7367): 123–126.
- Huang TY, Kharlamova A, McLuckey SA. 2010. Ion trap collision-induced dissociation of locked nucleic acids. *J Am Soc Mass Spectrom*. 21(1): 144–153.
- Huber CG, Krajete A. 1999. Analysis of nucleic acids by capillary ion-pair reversed-phase HPLC coupled to negative-ion electrospray ionization mass spectrometry. *Anal Chem*. 71(17): 3730–3739.
- Hudziak RM, Barofsky E, Barofsky DF, Weller DL, Huang SB, Weller DD. 1996. Resistance of morpholino phosphorodiamidate oligomers to enzymatic degradation. *Antisense Nucleic Acid Drug Dev*. 6(4): 267–272.
- Inoue H, Hayase Y, Imura A, Iwai S, Miura K, Ohtsuka E. 1987. Synthesis and hybridization studies on two complementary nona(2'-O-methyl)ribonucleotides. *Nucleic Acids Res*. 15(15): 6131–6148.
- Jääskeläinen I, Peltola S, Honkakoski P, Mönkkönen J, Urtti A. 2000. A lipid carrier with a membrane active component and a small complex size are required for efficient cellular delivery of anti-sense phosphorothioate oligonucleotides. *Eur J Pharm Sci*. 10(3): 187–193.
- Jackson AL, Burchard J, Leake D, Reynolds A, Shelter J, Guo J, Johnson JM, Lim L, Karpilow J, Nichols K, et al. 2006. Position-specific chemical modification of siRNAs reduces “off-target” transcript silencing. *RNA*. 12(7): 1197–1205.
- Jakobsen MR, Haasnoot J, Wengel J, Berkhout B, Kjems J. 2007. Efficient inhibition of HIV-1 expression by LNA modified antisense oligonucleotides and DNazymes targeted to functionally selected binding sites. *Retrovirology* [Internet]. [cited 2012 Nov 8]; 4 (Art. 29). Available from: <http://www.retrovirology.com/content/4/1/29>.
- Jayaraman K, McParland K, Miller P, Ts'O PO. 1981. Selective inhibition of *Escherichia coli* protein synthesis and growth by nonionic oligonucleotides complementary to the 3' end of 16S rRNA. *Proc Natl Acad Sci USA*. 78(3): 1537–1541.
- Jefferies LB, Palmer LR, Ambegia EG, Giesbrecht C, Ewanick S, MacLachlan I. 2005. A scalable, extrusion-free method for efficient liposomal encapsulation of plasmid DNA. *Pharm Res*. 22(3): 362–372.
- Jensen ON, Kulkarni S, Aldrich JV, Barofsky DF. 1996. Characterization of peptide–oligonucleotide heteroconjugates by mass spectrometry. *Nucleic Acids Res*. 24(19): 3866–3872.
- Joliet A, Pernelle C, Deagostini-Bazin H, Prochiantz A. 1991. Antennapedia homeobox peptide regulates neural morphogenesis. *Proc Natl Acad Sci USA*. 88(5): 1864–1868.
- Judge AD, Bola G, Lee AC, MacLachlan I. 2006. Design of noninflammatory synthetic siRNA mediating potent gene silencing *in vivo*. *Mol Ther*. 13(3): 494–505.
- Juliano R, Bauman J, Kang H, Ming X. 2009. Biological barriers to therapy with antisense and siRNA oligonucleotides. *Mol Pharm*. 6(3): 686–695.
- Jung J, Solanki A, Memoli KA, Kamei K, Kim H, Drahl MA, Williams LJ, Tseng HR, Lee K. 2010. Selective inhibition of human brain tumor cells through multifunctional quantum-dot-based siRNA delivery. *Angew Chem Int Ed Engl*. 49(1): 103–107.
- Kale AA, Torchilin VP. 2007. Enhanced transfection of tumor cells *in vivo* using ‘Smart’ pH-sensitive TAT-modified pegylated liposomes. *J Drug Target*. 15(7–8): 538–545.
- Kanazawa T, Sugawara K, Tanaka K, Horiuchi S, Takashima Y, Okada H. 2012. Suppression of tumor growth by systemic delivery of anti-VEGF siRNA with cell-penetrating peptide-modified MPEG–PCL nanomicelles. *Eur J Pharm Biopharm*. 81(3): 470–477.
- Kang H, Fisher MH, Xu D, Miyamoto YJ, Marchand A, Van Aerschot A, Herdewijn P, Juliano RL. 2004. Inhibition of MDR1 gene expression by chimeric HNA antisense oligonucleotides. *Nucleic Acids Res*. 32(14): 4411–4419.
- Kang SH, Cho MJ, Kole R. 1998. Up-regulation of the luciferase gene expression with antisense oligonucleotides: implications and applications in functional assay development. *Biochemistry* 37(18): 6235–6239.

- Kawasaki AM, Casper MD, Freier SM, Lesnik EA, Zounes MC, Cummins LL, Gonzalez C, Cook PD. 1993. Uniformly modified 2'-deoxy-2'-fluoro phosphorothioate oligonucleotides as nuclease-resistant antisense compounds with high affinity and specificity for RNA targets. *J Med Chem.* 36(7): 831–841.
- Kim KH, Lee ES, Cha SH, Park JH, Park JS, Chang YC, Park KK. 2009. Transcriptional regulation of NF- κ B by ring type decoy oligodeoxynucleotide in an animal model of nephropathy. *Exp Mol Pathol.* 86(2): 114–120.
- Kim SJ, Park JH, Kim KH, Lee WR, Lee S, Kwon OC, Kim KS, Park KK. 2010. Effect of NF- κ B decoy oligodeoxynucleotide on LPS/high-fat diet-induced atherosclerosis in an animal model. *Basic Clin Pharmacol Toxicol.* 107(6): 925–930.
- Kipshidze N, Iversen P, Overlie P, Dunlap T, Titus B, Lee D, Moses J, O'Hanley P, Lauer M, Leon MB. 2007. First human experience with local delivery of novel antisense AVI-4126 with Infiltrator catheter in de novo native and restenotic coronary arteries: 6-month clinical and angiographic follow-up from AVAIL study. *Cardiovasc Revasc Med.* 8(4): 230–235.
- Kobayashi H, Eckhardt SG, Lockridge JA, Rothenberg ML, Sandler AB, O'Bryant CL, Cooper W, Holden SN, Aitchison RD, Usman N, et al. 2005. Safety and pharmacokinetic study of RPI.4610 (ANGIOZYME), an anti-VEGFR-1 ribozyme, in combination with carboplatin and paclitaxel in patients with advanced solid tumors. *Cancer Chemother Pharmacol.* 56(4): 329–336.
- Koizumi M. 2004. 2'-O,4'-C-ethylene-bridged nucleic acids (ENATM) as next-generation antisense and antigene agents. *Biol Pharm Bull.* 27(4): 453–456.
- Koizumi M, Morita K, Daigo M, Tsutsumi S, Abe K, Obika S, Imanishi T. 2003. Triplex formation with 2'-O,4'-C-ethylene-bridged nucleic acids (ENA) having C3'-endo conformation at physiological pH. *Nucleic Acids Res.* 31(12): 3267–3273.
- Kool ET. 1991. Molecular recognition by circular oligonucleotides: increasing the selectivity of DNA binding. *J Am Chem Soc.* 113(16): 6265–6266.
- Kool ET. 1996a. Circular oligonucleotides: new concepts in oligonucleotide design. *Annu Rev Biophys Biomol Struct.* 25: 1–28.
- Kool ET. 1996b. Topological modification of oligonucleotides for potential inhibition of gene expression. *Perspect Drug Discov.* 4(1): 61–75.
- Koren E, Apte A, Jani A, Torchilin VP. 2012. Multifunctional PEGylated 2C5-immunoliposomes containing pH-sensitive bonds and TAT peptide for enhanced tumor cell internalization and cytotoxicity. *J Control Release.* 160(2): 264–273.
- Koshkin AA, Rajwanshi VK, Wengel J. 1998. Novel convenient syntheses of LNA [2.2.1]bicyclo nucleosides. *Tetrahedron Lett.* 39(24): 4381–4384.
- Krieg AM, Tonkinson J, Matson S, Zhao Q, Saxon M, Zhang LM, Bhanja U, Yakubov L, Stein CA. 1993. Modification of antisense phosphodiester oligodeoxynucleotides by a 5' cholesteryl moiety increases cellular association and improves efficacy. *Proc Natl Acad Sci USA.* 90(3): 1048–1052.
- Krützfeldt J, Rajewsky N, Braich R, Rajeev KG, Tuschl T, Manoharan M, Stoffel M. 2005. Silencing of microRNAs *in vivo* with 'antagomirs'. *Nature.* 438(7068): 685–689.
- Kurreck J. 2003. Antisense technologies. Improvement through novel chemical modifications. *Eur J Biochem.* 270(8): 1628–1644.
- Kurreck J, Wyszko E, Gillen C, Erdmann VA. 2002. Design of antisense oligonucleotides stabilized by locked nucleic acids. *Nucleic Acids Res.* 30(9): 1911–1918.
- Langel Ü, Pooga M, Kairane C, Zilmer M, Bartfai T. 1996. A galanin–mastoparan chimeric peptide activates the Na⁺,K⁺-ATPase and reverses its inhibition by ouabain. *Regul Pept.* 62(1): 47–52.
- Lebars I, Richard T, Di Primo C, Toulmé J. 2007. LNA derivatives of a kissing aptamer targeted to the trans-activating responsive RNA element of HIV-1. *Blood Cells Mol Dis.* 38(3): 204–209.
- Lebleu B, Moulton HM, Abes R, Ivanova GD, Abes S, Stein DA, Iversen PL, Arzumanov AA, Gait MJ. 2008. Cell penetrating peptide conjugates of steric block oligonucleotides. *Adv Drug Deliv Rev.* 60(4–5): 517–529.

REFERENCES

- Lee MY, Park SJ, Park K, Kim KS, Lee H, Hahn SK. 2011a. Target-specific gene silencing of layer-by-layer assembled gold–cysteamine/siRNA/PEI/HA nanocomplex. *ACS Nano*. 5(8): 6138–6147.
- Lee SH, Bae KH, Kim SH, Lee KR, Park TG. 2008. Amine-functionalized gold nanoparticles as non-cytotoxic and efficient intracellular siRNA delivery carriers. *Int J Pharm*. 364(1): 94–101.
- Lee Y, Lee SH, Kim JS, Maruyama A, Chen X, Park TG. 2011b. Controlled synthesis of PEI-coated gold nanoparticles using reductive catechol chemistry for siRNA delivery. *J Control Release*. 155(1): 3–10.
- Leeds JM, Graham MJ, Truong L, Cummins LL. 1996. Quantitation of phosphorothioate oligonucleotides in human plasma. *Anal Biochem*. 235(1): 36–43.
- Lehto T, Abes R, Oskolkov N, Suhorutšenko J, Copolovici D, Mäger I, Viola JR, Simonson OE, Ezzat K, Guterstam P, et al. 2010. Delivery of nucleic acids with a stearylated (R_xR)₄ peptide using a non-covalent co-incubation strategy. *J Control Release*. 141(1): 42–51.
- Leonetti JP, Mechti N, Degols G, Gagnor C, Lebleu B. 1991. Intracellular distribution of microinjected antisense oligonucleotides. *Proc Natl Acad Sci USA*. 88(7): 2702–2706.
- Letsinger RL, Bach SA, Eadie JS. 1986. Effects of pendant groups at phosphorus on binding properties of d-ApA analogs. *Nucleic Acids Res*. 14(8): 3487–3499.
- Li W, Szoka FC Jr. 2007. Lipid-based nanoparticles for nucleic acid delivery. *Pharm Res*. 24(3): 438–449.
- Li X, Tao Ng MT, Wang Y, Liu X, Li T. 2007. Dumbbell-shaped circular oligonucleotides as inhibitors of human topoisomerase I. *Bioorg Med Chem Lett*. 17(17): 4967–4971.
- Lin YZ, Yao SY, Veach RA, Torgerson TR, Hawiger J. 1995. Inhibition of nuclear translocation of transcription factor NF- κ B by a synthetic peptide containing a cell membrane-permeable motif and nuclear localization sequence. *J Biol Chem*. 270(24): 14255–14258.
- Lindgren M, Hällbrink M, Prochiantz A, Langel Ü. 2000. Cell-penetrating peptides. *Trends Pharmacol Sci*. 21(3): 99–103.
- Lindgren M, Langel Ü. 2011. Classes and prediction of cell-penetrating peptides. *Methods Mol Biol* 683: 3–19.
- Liu C, Wu Q, Harms AC, Smith RD. 1996. On-line microdialysis sample cleanup for electrospray ionization mass spectrometry of nucleic acid samples. *Anal Chem*. 68(18): 3295–3299.
- Lonkar P, Kim KH, Kuan JY, Chin JY, Rogers FA, Knauert MP, Kole R, Nielsen PE, Glazer PM. 2009. Targeted correction of a thalassemia-associated β -globin mutation induced by pseudo-complementary peptide nucleic acids. *Nucleic Acids Res*. 37(11): 3635–3644.
- Lotz R, Gerster M, Bayer E. 1998. Sequence verification of oligodeoxynucleotides and oligophosphorothioates using electrospray ionization (tandem) mass spectrometry. *Rapid Commun Mass Spectrom*. 12(7): 389–397.
- Lu W, Zhang G, Zhang R, Flores LG 2nd, Huang Q, Gelovani JG, Li C. 2010. Tumor site-specific silencing of *NF- κ B p65* by targeted hollow gold nanosphere-mediated photothermal transfection. *Cancer Res*. 70(8): 3177–3188.
- Lundberg M, Johansson M. 2001. Is VP22 nuclear homing an artifact? *Nat Biotechnol*. 19(8): 713–714.
- Lundberg P, El-Andaloussi S, Sütli T, Johansson H, Langel Ü. 2007. Delivery of short interfering RNA using endosomolytic cell-penetrating peptides. *FASEB J*. 21(11): 2664–2671.
- Lundin P, Johansson Henrik, Guterstam P, Holm T, Hansen M, Langel Ü, El Andaloussi S. 2008. Distinct uptake routes of cell-penetrating peptide conjugates. *Bioconjugate Chem*. 19(12): 2535–2542.
- Lytton-Jean AKR, Langer R, Anderson DG. Five years of siRNA delivery: spotlight on gold nanoparticles. *Small*. 7(14): 1932–1937.

- Madani F, Lindberg S, Langel Ü, Futaki S, Gräslund A. 2011. Mechanisms of cellular uptake of cell-penetrating peptides. *J Biophys [Internet]*. [cited 2012 Nov 12]; 2011 (Art. 414729). Available from: doi:10.1155/2011/414729.
- Mäe M, El Andaloussi S, Lundin P, Oskolkov N, Johansson HJ, Guterstam P, Langel Ü. 2009. A stearylated CPP for delivery of splice correcting oligonucleotides using a non-covalent co-incubation strategy. *J Control Release*. 134(3): 221–227.
- Magzoub M, Eriksson LEG, Gräslund A. 2003. Comparison of the interaction, positioning, structure induction and membrane perturbation of cell-penetrating peptides and non-translocating variants with phospholipid vesicles. *Biophys Chem*. 103(3): 271–288.
- Mann DA, Frankel AD. 1991. Endocytosis and targeting of exogenous HIV-1 Tat protein. *EMBO J*. 10(7): 1733–1739.
- Manoharan M. 1999. 2'-Carbohydrate modifications in antisense oligonucleotide therapy: importance of conformation, configuration and conjugation. *Biochim Biophys Acta*. 1489(1): 117–130.
- Marian CO, Cho SK, McEllin BM, Maher EA, Hatanpaa KJ, Madden CJ, Mickey BE, Wright WE, Shay JW, Bachoo RM. 2010. The telomerase antagonist, imetelstat, efficiently targets glioblastoma tumor-initiating cells leading to decreased proliferation and tumor growth. *Clin Cancer Res*. 16(1): 154–163.
- Matsukura M, Shinozuka K, Zon G, Mitsuya H, Reitz M, Cohen JS, Broder S. 1987. Phosphorothioate analogs of oligodeoxynucleotides: inhibitors of replication and cytopathic effects of human immunodeficiency virus. *Proc Natl Acad Sci USA*. 84(21): 7706–7710.
- McCarthy SM, Gilar M, Gebler J. 2009. Reversed-phase ion-pair liquid chromatography analysis and purification of small interfering RNA. *Anal Biochem*. 390(2): 181–188.
- McLuckey SA, Habibi-Goudarzi S. 1993. Decompositions of multiply charged oligonucleotide anions. *J Am Chem Soc*. 115(25): 12085–12095.
- Meade BR, Dowdy SF. 2007. Exogenous siRNA delivery using peptide transduction domains/cell penetrating peptides. *Adv Drug Deliv Rev*. 59(2–3): 134–140.
- Meade BR, Dowdy SF. 2008. Enhancing the cellular uptake of siRNA following noncovalent packaging with protein transduction domain peptides. *Adv Drug Deliv Rev*. 60(4–5): 530–536.
- Milligan JF, Matteucci MD, Martin JC. 1993. Current concepts in antisense drug design. *J Med Chem*. 36(14): 1923–1937.
- Mitchell DJ, Kim DT, Steinman L, Fathman CG, Rothbard JB. 2000. Polyarginine enters cells more efficiently than other polycationic homopolymers. *J Pept Res*. 56(5): 318–325.
- Mook OR, Baas F, de Wissel MB, Fluiters K. 2007. Evaluation of locked nucleic acid-modified small interfering RNA *in vitro* and *in vivo*. *Mol Cancer Ther*. 6(3): 833–843.
- Morita K, Hasegawa C, Kaneko M, Tsutsumi S, Sone J, Ishikawa T, Imanishi T, Koizumi M. 2002a. 2'-O,4'-C-ethylene-bridged nucleic acids (ENA): highly nuclease-resistant and thermodynamically stable oligonucleotides for antisense drug. *Bioorg Med Chem Lett*. 12(1): 73–76.
- Morita K, Yamate K, Kurakata S, Abe K, Imanishi T, Koizumi M. 2002b. Down-regulation of VEGF mRNA expression by 2'-O,4'-C-ethylene-bridged nucleic acid (ENA) antisense oligonucleotides and investigation of non-target gene expression. *Nucleic Acids Res Suppl*. (2): 99–100.
- Morris KV, Chan SW, Jacobsen SE, Looney DJ. 2004a. Small interfering RNA-induced transcriptional gene silencing in human cells. *Science*. 305(5688): 1289–1292.
- Morris MC, Chaloin L, Choob M, Archdeacon J, Heitz F, Divita G. 2004b. Combination of a new generation of PNAs with a peptide-based carrier enables efficient targeting of cell cycle progression. *Gene Ther*. 11(9): 757–764.
- Morris MC, Depollier J, Mery J, Heitz F, Divita G. 2001. A peptide carrier for the delivery of biologically active proteins into mammalian cells. *Nat Biotechnol*. 19(12): 1173–1176.
- Morris MC, Gros E, Aldrian-Herrada G, Choob M, Archdeacon J, Heitz F, Divita G. 2007. A non-covalent peptide-based carrier for *in vivo* delivery of DNA mimics. *Nucleic Acids*

REFERENCES

- Res [Internet]. [cited 2012 Nov 8]; 35(7): e49. Available from: <http://nar.oxfordjournals.org/content/35/7/e49.full>.
- Morris MC, Vidal P, Chaloin L, Heitz F, Divita G. 1997. A new peptide vector for efficient delivery of oligonucleotides into mammalian cells. *Nucleic Acids Res.* 25(14): 2730–2736.
- Morvan F, Porumb H, Degols G, Lefebvre I, Pompon A, Sproat BS, Rayner B, Malvy C, Lebleu B, Imbach JL. 1993. Comparative evaluation of seven oligonucleotide analogs as potential antisense agents. *J Med Chem.* 36(2): 280–287.
- Moschos SA, Jones SW, Perry MM, Williams AE, Erjefalt JS, Turner JJ, Barnes PJ, Sproat BS, Gait MJ, Lindsay MA. 2007. Lung delivery studies using siRNA conjugated to TAT(48–60) and penetratin reveal peptide induced reduction in gene expression and induction of innate immunity. *Bioconjug Chem.* 18(5): 1450–1459.
- Moser HE, Dervan PB. 1987. Sequence-specific cleavage of double helical DNA by triple helix formation. *Science.* 238(4827): 645–650.
- Muddiman DC, Cheng X, Udseth HR, Smith RD. 1996. Charge-state reduction with improved signal intensity of oligonucleotides in electrospray ionization mass spectrometry. *J Am Soc Mass Spectrom.* 7(8): 697–706.
- Muhonen P, Tennilä T, Azhayaeva E, Parthasarathy RN, Janckila AJ, Väänänen HK, Azhayaeva A, Laitala-Leinonen T. 2007. RNA interference tolerates 2'-fluoro modifications at the Argonaute2 cleavage site. *Chem Biodivers.* 4(5): 858–873.
- Muratovska A, Eccles MR. 2004. Conjugate for efficient delivery of short interfering RNA (siRNA) into mammalian cells. *FEBS Lett.* 558(1–3): 63–68.
- Nauwelaerts K, Fisher M, Froeyen M, Lescrinier E, Aerschot AV, Xu D, DeLong R, Kang H, Juliano RL, Herdewijn P. 2007. Structural characterization and biological evaluation of small interfering RNAs containing cyclohexenyl nucleosides. *J Am Chem Soc.* 129(30): 9340–9348.
- Neu M, Fischer D, Kissel T. 2005. Recent advances in rational gene transfer vector design based on poly(ethylene imine) and its derivatives. *J Gene Med.* 7(8): 992–1009.
- Ng EW, Shima DT, Calias P, Cunningham ET Jr, Guyer DR, Adamis AP. 2006. Pegaptanib, a targeted anti-VEGF aptamer for ocular vascular disease. *Nat Rev Drug Discov.* 5(2): 123–132.
- Nielsen P, Dreißøe LH, Wengel J. 1995. Synthesis and evaluation of oligodeoxynucleotides containing acyclic nucleosides: introduction of three novel analogs and a summary. *Bioorg Med Chem.* 3(1): 19–28.
- Nielsen PE. 2010. Peptide nucleic acids (PNA) in chemical biology and drug discovery. *Chem Biodivers.* 7(4): 786–804.
- Nielsen PE, Egholm M, Berg RH, Buchardt O. 1991. Sequence-selective recognition of DNA by strand displacement with a thymine-substituted polyamide. *Science.* 254(5037): 1497–1500.
- Noronha A, Damha MJ. 1998. Triple helices containing arabinonucleotides in the third (Hoogsteen) strand: effects of inverted stereochemistry at the 2'-position of the sugar moiety. *Nucleic Acids Res.* 26(11): 2665–2671.
- Norton JC, Piatyszek MA, Wright WE, Shay JW, Corey DR. 1996. Inhibition of human telomerase activity by peptide nucleic acids. *Nat Biotechnol.* 14(5): 615–619.
- Obika S, Nanbu D, Hari Y, Andoh J, Morio K, Doi T, Imanishi T. 1998. Stability and structural features of the duplexes containing nucleoside analogs with a fixed N-type conformation, 2'-O,4'-C-methyleneribonucleosides. *Tetrahedron Lett.* 39(30): 5401–5404.
- Obika S, Nanbu D, Hari Y, Morio K, In Y, Ishida T, Imanishi T. 1997. Synthesis of 2'-O,4'-C-methyleneuridine and -cytidine. Novel bicyclic nucleosides having a fixed C₃, -endo sugar pucker. *Tetrahedron Lett.* 38(50): 8735–8738.
- Oehlke J, Birth P, Klauschenz E, Wiesner B, Beyermann M, Oksche A, Bienert M. 2002. Cellular uptake of antisense oligonucleotides after complexing or conjugation with cell-penetrating model peptides. *Eur J Biochem.* 269(16): 4025–4032.

- Oehlke J, Scheller A, Wiesner B, Krause E, Beyermann M, Klauschenz E, Melzig M, Bienert M. 1998. Cellular uptake of an α -helical amphipathic model peptide with the potential to deliver polar compounds into the cell interior non-endocytically. *Biochim Biophys Acta*. 1414(1-2): 127-139.
- Oehlke J, Wallukat G, Wolf Y, Ehrlich A, Wiesner B, Berger H, Bienert M. 2004. Enhancement of intracellular concentration and biological activity of PNA after conjugation with a cell-penetrating synthetic model peptide. *Eur J Biochem*. 271(14): 3043-3049.
- O'Rourke JR, Swanson MS. 2009. Mechanisms of RNA-mediated disease. *J Biol Chem*. 284(12): 7419-7423.
- Oyelere AK, Chen PC, Huang X, El-Sayed IH, El-Sayed MA. 2007. Peptide-conjugated gold nanorods for nuclear targeting. *Bioconjugate Chem*. 18(5): 1490-1497.
- Papahadjopoulos D, Allen TM, Gabizon A, Mayhew E, Matthay K, Huang SK, Lee KD, Woodle MC, Lasic DD, Redemann C, et al. 1991. Sterically stabilized liposomes: improvements in pharmacokinetics and antitumor therapeutic efficacy. *Proc Natl Acad Sci USA*. 88(24): 11460-11464.
- Pasternak A, Wengel J. 2011. Unlocked nucleic acid – an RNA modification with broad potential. *Org Biomol Chem*. 9(10): 3591-3597.
- Patel LN, Zaro JL, Shen WC. 2007. Cell penetrating peptides: intracellular pathways and pharmaceutical perspectives. *Pharm Res*. 24(11): 1977-1992.
- Pongracz K, Gryaznov S. 1999. Oligonucleotide N3'→P5' thiophosphoramidates: synthesis and properties. *Tetrahedron Lett*. 40(43): 7661-7664.
- Pooga M, Hällbrink M, Zorko M, Langel Ü. 1998. Cell penetration by transportan. *FASEB J*. 12(1): 67-77.
- Potier N, Van Dorsselaer A, Cordier Y, Roch O, Bischoff R. 1994. Negative electrospray ionization mass spectrometry of synthetic and chemically modified oligonucleotides. *Nucleic Acids Res*. 22(19): 3895-3903.
- Pourshahian S, Limbach PA. 2008. Application of fractional mass for the identification of peptide-oligonucleotide cross-links by mass spectrometry. *J Mass Spectrom*. 43(8): 1081-1088.
- Prakash TP, Allerson CR, Dande P, Vickers TA, Sioufi N, Jarres R, Baker BF, Swayze EE, Griffey RH, Bhat B. 2005. Positional effect of chemical modifications on short interference RNA activity in mammalian cells. *J Med Chem*. 48(13): 4247-4253.
- Resina S, Abes S, Turner JJ, Prevot P, Travo A, Clair P, Gait MJ, Thierry AR, Lebleu B. 2007. Lipoplex and peptide-based strategies for the delivery of steric-block oligonucleotides. *Int J Pharm*. 344(1-2): 96-102.
- Richard JP, Melikov K, Vivès E, Ramos C, Verbeure B, Gait MJ, Chernomordik LV, Lebleu B. 2003. Cell-penetrating peptides. A reevaluation of the mechanism of cellular uptake. *J Biol Chem*. 278(1): 585-590.
- Robles J, Maseda M, Beltran M, Concernau M, Pedroso E, Grandas A. 1997. Synthesis and enzymatic stability of phosphodiester-linked peptide-oligonucleotide hybrids. *Bioconjug Chem*. 8(6): 785-788.
- Robles J, Pedroso E, Grandas A. 1994. Stepwise solid-phase synthesis of the nucleopeptide Phac-Phe-Val-Ser(p3'ACT)-Gly-OH. *J Org Chem*. 59(9): 2482-2486.
- Rosi NL, Giljohann DA, Thaxton CS, Lytton-Jean AK, Han MS, Mirkin CA. 2006. Oligonucleotide-modified gold nanoparticles for intracellular gene regulation. *Science*. 312(5776): 1027-1030.
- Ruben S, Perkins A, Purcell R, Joung K, Sia R, Burghoff R, Haseltine VA, Rosen CA. 1989. Structural and functional characterization of human immunodeficiency virus tat protein. *J Virol*. 63(1): 1-8.
- Sands H, Gorey-Feret LJ, Ho SP, Bao Y, Cocuzza AJ, Chidester D, Hobbs FW. 1995. Biodistribution and metabolism of internally ^3H -labeled oligonucleotides. II. 3'.5'-Blocked oligonucleotides. *Mol Pharmacol*. 47(3): 636-646.

REFERENCES

- Schechter PJ, Martin RR. 1998. Safety and tolerance of phosphorothioates in humans. In: Crooke ST, editor. Antisense research and application. Springer Berlin Heidelberg. p. 233–241.
- Seidl CI, Ryan K. 2011. Circular single-stranded synthetic DNA delivery vectors for microRNA. PLoS One [Internet]. [cited 2012 Nov 8]; 6(2): e16925. Available from: doi:10.1371/journal.pone.0016925.
- Shaw JP, Kent K, Bird J, Fishback J, Froehler B. 1991. Modified deoxyoligonucleotides stable to exonuclease degradation in serum. Nucleic Acids Res. 19(4): 747–750.
- Shukla S, Sumaria CS, Pradeepkumar PI. 2010. Exploring chemical modifications for siRNA therapeutics: a structural and functional outlook. ChemMedChem. 5(3): 328–349.
- Sierakowska H, Sambade MJ, Agrawal S, Kole R. 1996. Repair of thalassemic human β -globin mRNA in mammalian cells by antisense oligonucleotides. Proc Natl Acad Sci USA. 93(23): 12840–12844.
- Simeoni F, Morris MC, Heitz F, Divita G. 2003. Insight into the mechanism of the peptide-based gene delivery system MPG: implications for delivery of siRNA into mammalian cells. Nucleic Acids Res. 31(11): 2717–2724.
- Siuzdak G. 1994. The emergence of mass spectrometry in biochemical research. Proc Natl Acad Sci USA. 91(24): 11290–11297.
- Sodroski J, Rosen C, Wong-Staal F, Salahuddin SZ, Popovic M, Arya S, Gallo RC, Haseltine WA. 1985. *Trans*-acting transcriptional regulation of human T-cell leukemia virus type III long terminal repeat. Science. 227(4683): 171–173.
- Soomets U, Lindgren M, Gallet X, Hällbrink M, Elmquist A, Balaspiri L, Zorko M, Pooga M, Brasseur R, Langel Ü. 2000. Deletion analogs of transportan. Biochim Biophys Acta. 1467(1): 165–176.
- Soukchareun S, Tregear GW, Haralambidis J. 1995. Preparation and characterization of antisense oligonucleotide–peptide hybrids containing viral fusion peptides. Bioconjug Chem. 6(1): 43–53.
- Soutschek J, Akinc A, Bramlage B, Charisse K, Constien R, Donoghue M, Elbashir S, Geick A, Hadwiger P, Harborth J, et al. 2004. Therapeutic silencing of an endogenous gene by systemic administration of modified siRNAs. Nature. 432(7014): 173–178.
- Spagnou S, Miller AD, Keller M. 2004. Lipidic carriers of siRNA: differences in the formulation, cellular uptake, and delivery with plasmid DNA. Biochemistry. 43(42): 13348–13356.
- Sproat BS, Lamond AI, Beijer B, Neuner P, Ryder U. 1989. Highly efficient chemical synthesis of 2'-*O*-methyloligoribonucleotides and tetrabiotinylated derivatives; novel probes that are resistant to degradation by RNA or DNA specific nucleases. Nucleic Acids Res. 17(9): 3373–3386.
- Stirchak EP, Summerton JE, Weller DD. 1989. Uncharged stereoregular nucleic acid analogs: 2. Morpholino nucleoside oligomers with carbamate internucleoside linkages. Nucleic Acids Res. 17(15): 6129–6141.
- Subrizi A, Tuominen E, Bunker A, Róg T, Antopolsky M, Urtti A. 2012. Tat(48–60) peptide amino acid sequence is not unique in its cell penetrating properties and cell-surface glycosaminoglycans inhibit its cellular uptake. J Control Release. 158(2): 277–285.
- Sun L, Liu D, Wang Z. 2008. Functional gold nanoparticle–peptide complexes as cell-targeting agents. Langmuir. 24(18): 10293–10297.
- Sussman JD, Argov Z, McKee D, Hazum E, Brawer S, Soreq H. 2008. Antisense treatment for myasthenia gravis: experience with monarsen. Ann NY Acad Sci. 1132: 283–90.
- Tan XX, Actor JK, Chen Y. 2005. Peptide nucleic acid antisense oligomer as a therapeutic strategy against bacterial infection: proof of principle using mouse intraperitoneal infection. Antimicrob Agents Chemother. 49(8): 3203–3207.
- Tang XJ, Su M, Yu LL, Lv C, Wang J, Li ZJ. 2010. Photomodulating RNA cleavage using photolabile circular antisense oligodeoxynucleotides. Nucleic Acids Res [Internet]. [cited 2013 Mar 27]; 38(11). Available from: doi:10.1093/nar/gkq079.

- Temsamani J, Tang JY, Agrawal S. 1992. Capped oligodeoxynucleotide phosphorothioates. Pharmacokinetics and stability in mice. *Ann NY Acad Sci.* 660: 318–320.
- Thibaudeau C, Plavec J, Garg N, Papchikhin A, Chattopadhyaya J. 1994. How does the electronegativity of the substituent dictate the strength of the gauche effect? *J Am Chem Soc.* 116(9): 4038–4043.
- Thompson JD, Kornbrust DJ, Foy JW, Solano EC, Schneider DJ, Feinstein E, Molitoris BA, Erlich S. 2012. Toxicological and pharmacokinetic properties of chemically modified siRNAs targeting p53 RNA following intravenous administration. *Nucleic Acid Ther* [Internet]. [cited 2012 Nov 19]; 22(4): 255–264. Available from: doi:10.1089/nat.2012.0371.
- Tkachenko AG, Xie H, Liu Y, Coleman D, Ryan J, Glomm WR, Shipton MK, Franzen S, Feldheim DL. 2004. Cellular trajectories of peptide-modified gold particle complexes: comparison of nuclear localization signals and peptide transduction domains. *Bioconjugate Chem.* 15(3): 482–490.
- Torchilin VP. 2008. Tat peptide-mediated intracellular delivery of pharmaceutical nanocarriers. *Adv Drug Deliv Rev.* 60(4–5): 548–558.
- Torchilin VP, Levchenko TS, Rammohan R, Volodina N, Papahadjopoulos-Sternberg B, D'Souza GG. 2003. Cell transfection *in vitro* and *in vivo* with nontoxic TAT peptide–liposome–DNA complexes. *Proc Natl Acad Sci USA.* 100(4): 1972–1977.
- Tripathi S, Chaubey B, Barton BE, Pandey VN. 2007. Anti HIV-1 virucidal activity of polyamide nucleic acid–membrane transducing peptide conjugates targeted to primer binding site of HIV-1 genome. *Virology.* 363(1): 91–103.
- Tuerk C, Gold L. 1990. Systematic evolution of ligands by exponential enrichment: RNA ligands to bacteriophage T4 DNA polymerase. *Science.* 249(4968): 505–510.
- Tung CH, Stein S. 2000. Preparation and applications of peptide–oligonucleotide conjugates. *Bioconjug Chem.* 11(5): 605–618.
- Tünnemann G, Martin RM, Haupt S, Patsch C, Edenhofer F, Cardoso MC. 2006. Cargo-dependent mode of uptake and bioavailability of TAT-containing proteins and peptides in living cells. *FASEB J.* 20(11): 1775–1784.
- Turner JJ, Jones S, Fabani MM, Ivanova G, Arzumano AA, Gait MJ. 2007. RNA targeting with peptide conjugates of oligonucleotides, siRNA and PNA. *Blood Cells Mol Diseases* 38(1): 1–7.
- Urban-Klein B, Werth S, Abuharbeid S, Czubayko F, Aigner A. 2005. RNAi-mediated gene-targeting through systemic application of polyethylenimine (PEI)-complexed siRNA *in vivo*. *Gene Ther.* 12(5): 461–466.
- Vaishnav AK, Cervantes A, Alsina M, Tabernero J, Infante JR, LoRusso P, Shapiro GI, Paz-Ares L, Schwartz G, Weiss G, et al. 2011. RNAi in humans: phase I dose-escalation study of ALN-VSP02, a novel RNAi therapeutic for solid tumors with liver involvement. *Nucleic Acid Ther* [Internet; poster abstract]. [cited 2012 Nov 19]; 21(5): A44. Available from: doi:10.1089/nat.2011.1502.
- Veedu RN, Wengel J. 2010. Locked nucleic acids: promising nucleic acid analogs for therapeutic applications. *Chem Biodivers.* 7(3): 536–542.
- Veldhoen S, Laufer SD, Trampe A, Restle T. 2006. Cellular delivery of small interfering RNA by a non-covalently attached cell-penetrating peptide: quantitative analysis of uptake and biological effect. *Nucleic Acids Res.* 34(22): 6561–6573.
- Verbeure B, Lescrinier E, Wang J, Herdewijn P. 2001. RNase H mediated cleavage of RNA by cyclohexene nucleic acid (CeNA). *Nucleic Acids Res.* 29(24): 4941–4947.
- Verheggen I, Van Aerschot A, Toppet S, Snoeck R, Janssen G, Balzarini J, De Clercq E, Herdewijn P. 1993. Synthesis and antiherpes virus activity of 1,5-anhydrohexitol nucleosides. *J Med Chem.* 36(14): 2033–2040.
- Vivès E, Brodin P, Lebleu B. 1997. A truncated HIV-1 Tat protein basic domain rapidly translocates through the plasma membrane and accumulates in the cell nucleus. *J Biol Chem.* 272(25): 16010–16017.
- Vivès E, Schmidt J, Pèlerin A. 2008. Cell-penetrating and cell-targeting peptides in drug delivery. *Biochim Biophys Acta.* 1786(2): 126–138.

REFERENCES

- Wallace TL, Bazemore SA, Kornbrust DJ, Cossum PA. 1996. Single-dose hemodynamic toxicity and pharmacokinetics of a partial phosphorothioate anti-HIV oligonucleotide (AR177) after intravenous infusion to cynomolgus monkeys. *J Pharmacol Exp Ther.* 278(3): 1306–1312.
- Wang J, Verbeure B, Luyten I, Lescrinier E, Froeyen M, Hendrix C, Rosemeyer H, Seela F, Van Aerschot A, Herdewijn P. 2000. Cyclohexene nucleic acids (CeNA): serum stable oligonucleotides that activate RNase H and increase duplex stability with complementary RNA. *J Am Chem Soc.* 122(36): 8595–8602.
- Wang Y, Wu L, Wang P, Lv C, Yang Z, Tang X. 2012. Manipulation of gene expression in zebrafish using caged circular morpholino oligomers. *Nucleic Acids Res [Internet]*. [cited 2013 Mar 27]; 40(21): 11155–11162. Available from: doi: 10.1093/nar/gks840.
- Whitehead KA, Langer R, Anderson DG. 2009. Knocking down barriers: advances in siRNA delivery. *Nat Rev Drug Discov.* 8(2): 129–138.
- Williams JH, Schray RC, Patterson CA, Ayitey SO, Tallent MK, Lutz GJ. 2009. Oligonucleotide-mediated survival of motor neuron protein expression in CNS improves phenotype in a mouse model of spinal muscular atrophy. *J Neurosci.* 29(24): 7633–7638.
- Wolf Y, Pritz S, Abes S, Bienert M, Lebleu B, Oehlke J. 2006. Structural requirements for cellular uptake and antisense activity of peptide nucleic acids conjugated with various peptides. *Biochemistry.* 45(50): 14944–14954.
- Wu L, Wang Y, Wu J, Lv C, Wang J, Tang X. 2012. Caged circular antisense oligonucleotides for photomodulation of RNA digestion and gene expression in cells. *Nucleic Acids Res [Internet]*. [cited 2013 Mar 27]; 41(1): 677–686. Available from: doi: 10.1093/nar/gks996.
- Yagi M, Takeshima Y, Surono A, Takagi M, Koizumi M, Matsuo M. 2004. Chimeric RNA and 2'-O,4'-C-ethylene-bridged nucleic acids have stronger activity than phosphorothioate oligodeoxynucleotides in induction of exon 19 skipping in dystrophin mRNA. *Oligonucleotides.* 14(1): 33–40.
- Yin H, Lu Q, Wood M. 2008. Effective exon skipping and restoration of dystrophin expression by peptide nucleic acid antisense oligonucleotides in *mdx* mice. *Mol Ther.* 16(1): 38–45.
- Yoshizawa T, Hattori Y, Hakoshima M, Koga K, Maitani Y. 2008. Folate-linked lipid-based nanoparticles for synthetic siRNA delivery in KB tumor xenografts. *Eur J Pharm Biopharm.* 70(3): 718–725.
- Zamecnik PC, Stephenson ML. 1978. Inhibition of Rous sarcoma virus replication and cell transformation by a specific oligodeoxynucleotide. *Proc Natl Acad Sci USA.* 75(1): 280–284.
- Zelphati O, Szoka FC Jr. 1996. Mechanism of oligonucleotide release from cationic liposomes. *Proc Natl Acad Sci USA.* 93(21): 11493–11498.
- Zhang C, Tang N, Liu X, Liang W, Xu W, Torchilin VP. 2006. siRNA-containing liposomes modified with polyarginine effectively silence the targeted gene. *J Control Release.* 112(2): 229–239.
- Zhang R, Iyer RP, Yu D, Tan W, Zhang X, Lu Z, Zhao H, Agrawal S. 1996. Pharmacokinetics and tissue disposition of a chimeric oligodeoxynucleoside phosphorothioate in rats after intravenous administration. *J Pharmacol Exp Ther.* 278(2): 971–979.
- Zielinski R, Chi KN. 2012. Custirsen (OGX-011): a second-generation antisense inhibitor of clusterin in development for the treatment of prostate cancer. *Future Oncol.* 8(10): 1239–1251.
- Zubin EM, Romanova EA, Volkov EM, Tashlitsky VN, Korshunova GA, Shabarova ZA. 1999. Oligonucleotide-peptide conjugates as potential antisense agents. *FEBS Lett.* 456(1): 59–62.